

# CPIMS 13

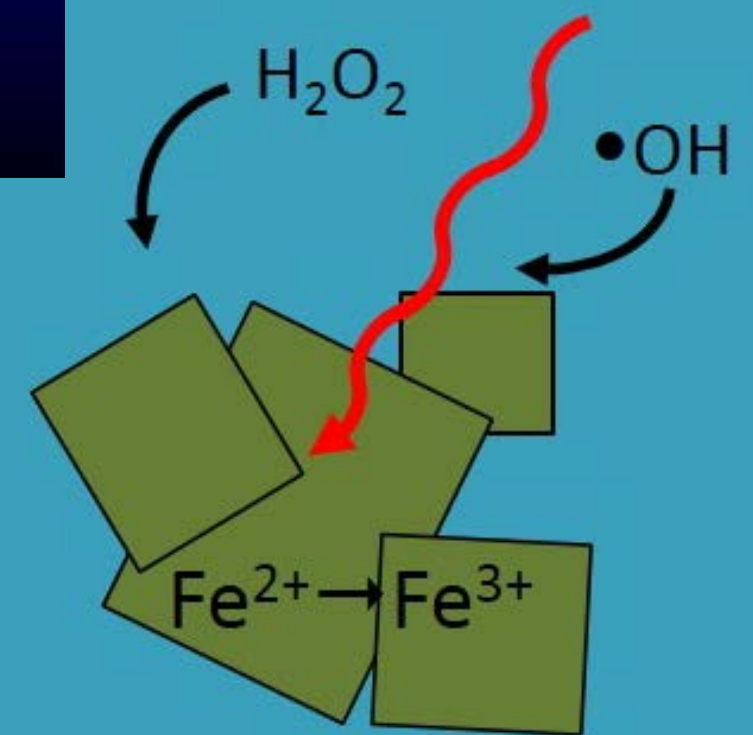
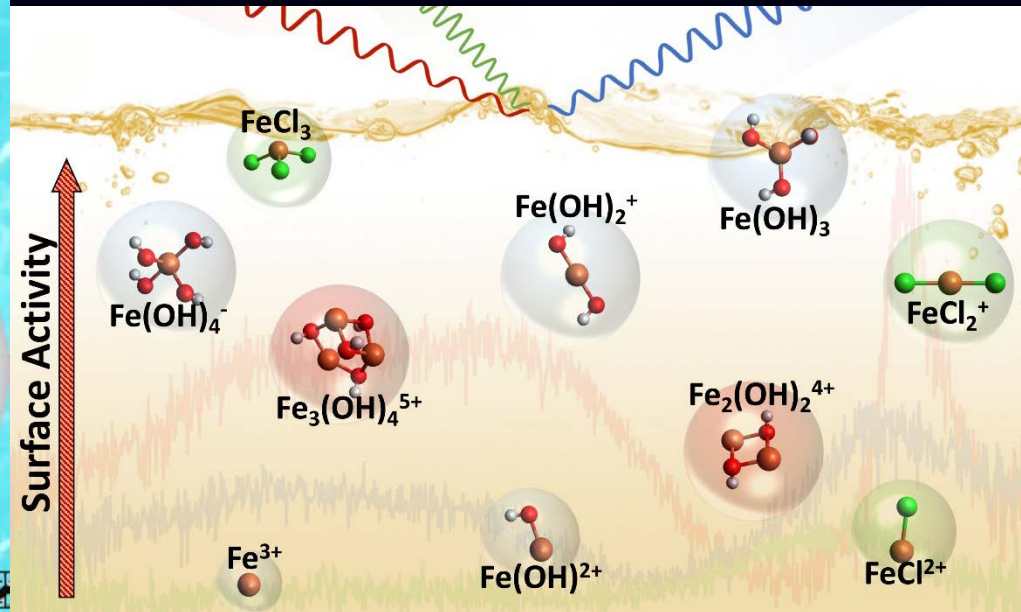
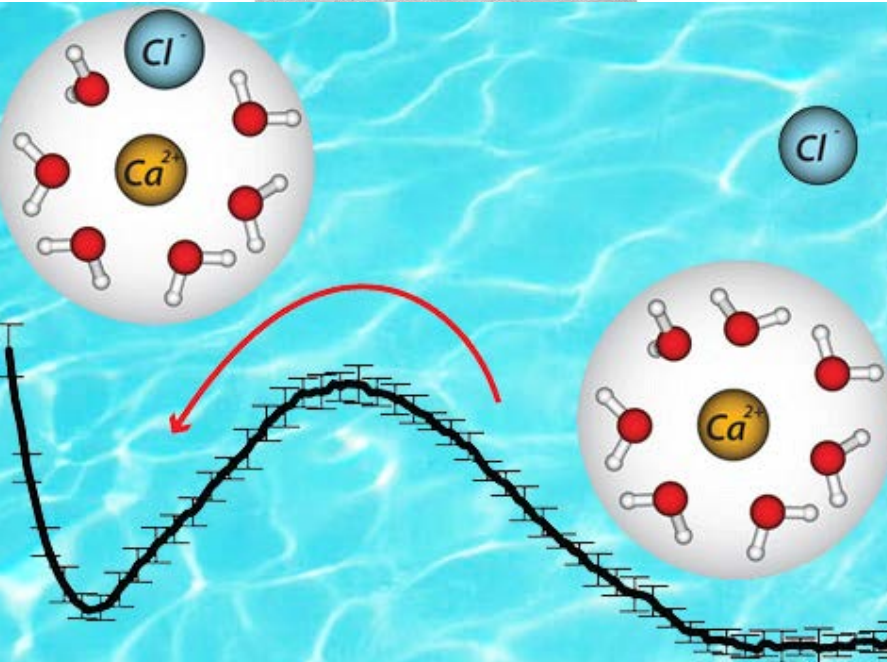
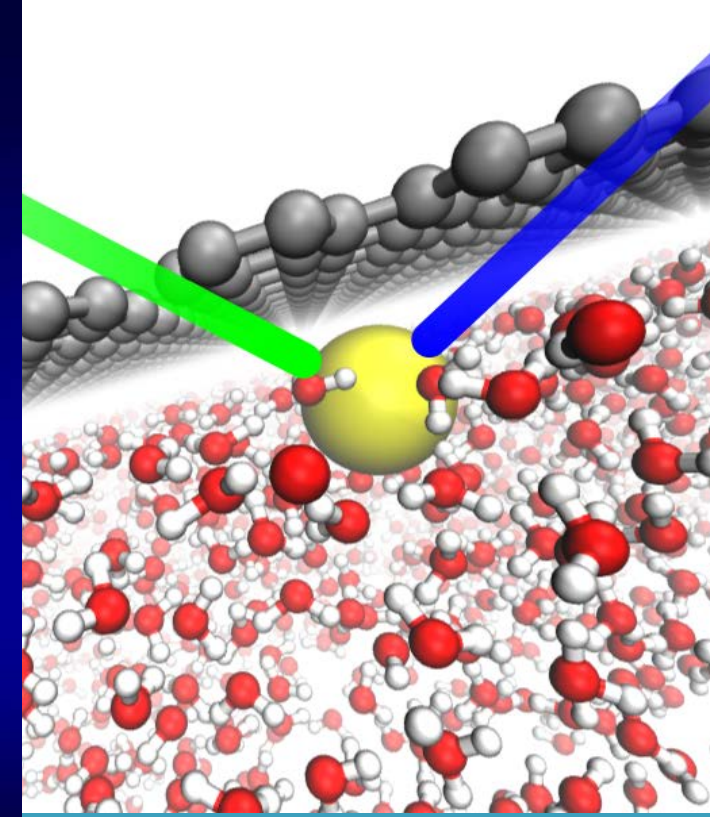
Thirteenth Condensed Phase and Interfacial Molecular Science (CPIMS) Research Meeting

Gaithersburg Marriot  
Washingtonian Center  
Gaithersburg, MD  
October 15-18, 2017



U.S. DEPARTMENT OF  
**ENERGY**

Office of  
Science



# CPIMS 13

## ABOUT THE COVER GRAPHICS

**Submitted by Greg Kimmel and Bruce Kay (Pacific Northwest National Laboratory)**

For more information, see Y. Xu, N.G. Petrik, R.S. Smith, B.D. Kay and G.A. Kimmel, "Growth rate of crystalline ice and the diffusivity of supercooled water from 126 to 262 K," *Proceedings of the National Academy of Sciences* **113**, 14921 (2016). DOI:

10.1073/pnas.1611395114

Abstract begins on page 62

**Submitted by Christopher Mundy (Pacific Northwest National Laboratory)**

For more information, see M. D. Baer and C. J. Mundy, "Local aqueous solvation structure around  $\text{Ca}^{2+}$  during  $\text{Ca}_2^{+}\text{-Cl}^-$  pair formation" *Journal of Physical Chemistry B* **120**, 1885, (2016). DOI: 10.1021/acs.jpcc.5b09579

Additional information can be found at T. T. Duignan M. D. Baer, and C. J. Mundy "Ions Interacting in Solution: Moving from Intrinsic to Collective Properties." *Current Opinion in Colloid & Interface Science* **23**, 58 (2016). DOI: 10.1016/j.cocis.2016.05.009

Abstract begins on page 86

**Submitted by Geraldine Richmond (University of Oregon)**

For more information, see J.K. Hensel, A.P. Carpenter, R.K. Ciszewski, B.K. Schabes, C.T. Kittredge, F.G. Moore and G.L. Richmond, "Molecular Characterization of Water and Surfactant AOT at Nanoemulsion Surfaces", *Proceedings of the National Academy of Sciences*, July 31, 2017 Early Edition. DOI: 10.1073/pnas.1700099114

Abstract begins on page 97

**Submitted by Heather Allen (Ohio State University)**

Sum frequency generation (SFG) measurements reveal surface solvation effects of  $\text{FeCl}_3$  (aq) aqueous solutions. Polyatomic ferric species are likely to have high surface activity owed to a relatively low surface charge density and large hydration sphere. SFG data suggests time-dependent formation of polymeric iron species that may differ from the aqueous bulk.

Abstract begins on page 6

**Submitted by Richard Saykally and Phill Geissler (University of California, Berkeley and Lawrence Berkeley National Laboratory)**

For more information, see D. L. McCaffrey, S. C. Nguyen, S. J. Cox, H. Weller, A. P. Alivisatos, P. L. Geissler, R. J. Saykally, "Mechanism of ion adsorption to aqueous interfaces: Graphene/water vs. air/water", *Proceedings of the National Academy of Sciences*, July 31, 2017 Early Edition. DOI: 10.1073/pnas.1702760114

Abstract begins on page 104

**Submitted by Jay LaVerne (Notre Dame Radiation Laboratory)**

For more information, see S.C. Reiff and J.A. LaVerne, "Radiation-Induced Chemical Changes to Iron Oxides" *Journal of Physical Chemistry B* **119**, 7358 (2015). DOI: 10.1021/jp510943j

Abstract begins on page 156

Program and Abstracts for

# CPIMS 13

Thirteenth Research Meeting of the  
Condensed Phase and Interfacial Molecular  
Science (CPIMS) Program

Gaithersburg Marriott Washingtonian Center  
Gaithersburg, Maryland  
October 16-18, 2017



U.S. DEPARTMENT OF

**ENERGY**

Office of  
Science

Office of Basic Energy Sciences

Chemical Sciences, Geosciences & Biosciences Division

The research grants and contracts described in this document are supported by the U.S. DOE Office of Science, Office of Basic Energy Sciences, Chemical Sciences, Geosciences and Biosciences Division.

# FOREWORD

This volume summarizes the scientific content of the Thirteenth Research Meeting on Condensed Phase and Interfacial Molecular Science (CPIMS) sponsored by the U. S. Department of Energy (DOE), Office of Basic Energy Sciences (BES). The research meeting is held for the DOE laboratory and university principal investigators within the BES CPIMS Program to facilitate scientific interchange among the PIs and to promote a sense of program awareness and identity.

This year's speakers are gratefully acknowledged for their investment of time and for their willingness to share their ideas with the meeting participants.

The abstracts in this book represent progress reports for each of the projects that receive support from the CPIMS program. Therefore, the book represents a snapshot in time of the scope of CPIMS-supported research. The CPIMS 13 agenda also features one speaker who receives support for his research from the BES Computational and Theoretical Chemistry (CTC) Program: Xiaosong Li, whose presentation will take place on Monday, October 16, and whose abstract is contained in the special, CTC section of this book. Moreover, several investigators receive co-funding for their work from both the CPIMS and CTC programs, including Thomas Markland (who speaks on Monday, October 16). Aurora Clark (who is also jointly supported by CPIMS/CTC) will speak on Monday afternoon about the IDREAM EFRC, and Sotiris Xantheas will speak about the new Center for Scalable, Predictive methods for Excitation and Correlated phenomena (SPEC). Finally, since the inception of the CPIMS meeting series, participants who work in the field of radiation chemistry (and receive support from the Solar Photochemistry program) have attended; the CPIMS 13 agenda includes presentations on Tuesday, October 17 from two speakers in this area: James Wishart and Irek Janik; their abstracts are contained in the Solar Photochemistry section of the abstract book.

A recent tradition is the use of the cover of this book to display research highlights from CPIMS investigators. This year, we have included six research highlights on the cover. These images were selected from highlights and abstracts submitted by CPIMS investigators during the past two years. We thank the investigators for allowing us to place their images on the cover of this book, and we thank all CPIMS investigators who submitted research highlights. CPIMS Investigators are encouraged to continue to submit highlights of their results; we will continue to receive these stories of success with great pride.

We are deeply indebted to the members of the scientific community who have contributed valuable time toward the review of proposals and programs. These thorough and thoughtful reviews are central to the continued vitality of the CPIMS Program. We appreciate the privilege of serving in the management of this research program. In carrying out these tasks, we learn from the achievements and share the excitement of the research of the many sponsored scientists and students whose work is summarized in the abstracts published on the following pages.

Special thanks are reserved for the staff of the Oak Ridge Institute for Science and Education, in particular, Connie Lansdon and Tim Ledford. We also thank Diane Marceau and Gwen Johnson in the Chemical Sciences, Geosciences, and Biosciences Division for their indispensable behind-the-scenes efforts in support of the CPIMS program. Finally, we welcome Bruce Garrett, who started as the new Director for the Chemical Sciences, Geosciences, and Biosciences Division approximately 11 months ago; Bruce will kick off the meeting on Monday morning with news from our Division.

Gregory J. Fiechtner, Mark R. Pederson, and Jeffrey L. Krause  
Chemical Sciences, Geosciences and Biosciences Division  
Office of Basic Energy Sciences

# *Agenda*



# CPIMS 13



U.S. DEPARTMENT OF  
**ENERGY**

Office of  
Science

Office of Basic Energy Sciences  
Chemical Sciences, Geosciences & Biosciences Division

## Thirteenth Condensed Phase and Interfacial Molecular Science (CPIMS) Research Meeting Gaithersburg Marriott Washingtonian Center, Gaithersburg, Maryland

---

### Sunday, October 15

- 3:00-6:00 pm \*\*\*\* Registration (Salon C-E) \*\*\*\*  
6:00 pm \*\*\*\* Reception (No Host, Lobby Lounge) \*\*\*\*  
6:30 pm \*\*\*\* Dinner (on your own) \*\*\*\*

### Monday, October 16

- 7:30 am \*\*\*\* Breakfast (Salon A-B) \*\*\*\*

#### All Presentations Held in Salon C-E

- 8:30 am *Update from BES Chemical Sciences, Geosciences, and Biosciences Division*  
**Bruce Garrett**, DOE Basic Energy Sciences
- 8:45 am *Introductory Remarks and Program Update*  
**Gregory Fiechtner**, DOE Basic Energy Sciences
- Session I** Chair: **Munira Khalil**, University of Washington
- 9:00 am *The Dynamics of Protons in Liquid Water Viewed through Ultrafast IR Spectroscopy*  
**Andrei Tokmakoff**, University of Chicago
- 9:30 am *Mulling over Emulsions: Molecular Structure and Assembly at Nanoemulsion Surfaces"*  
**Geraldine Richmond**, University of Oregon
- 10:00 am *Improving the Feasibility of 2D IR Microscopy to Probe Energy Technologies*  
**Amber Krummel**, Colorado State University
- 10:30 am \*\*\*\* Break \*\*\*\*
- Session II** Chair: **Benjamin Schwartz**, University of California, Los Angeles
- 11:00 am *Iron speciation at the air-aqueous interface: Insights into surface hydration*  
**Heather Allen**, Ohio State University
- 11:30 am *When is water a dielectric continuum with a structured interface?*  
**Phillip Geissler**, Lawrence Berkeley National Laboratory
- 12:00 pm *Quantum Dynamics Approaches for Modelling Charge and Energy Transfer in Solution*  
**Thomas Markland**, Stanford University
- 12:30 pm \*\*\*\* Lunch (Salon A-B) \*\*\*\*

1:30 pm–2:30 pm Free/Discussion Time

**Session III** Chair: **Musa Ahmed**, Lawrence Berkeley National Laboratory

2:30 pm *Overview of the IDREAM EFRC: Interfacial Dynamics in Radiation Environments and Materials*

**Aurora Clark**, Washington State University

3:00 pm *Overview of the Center for Scalable, Predictive methods for Excitation and Correlated phenomena (SPEC)*

**Sotiris Xantheas**, Pacific Northwest National Laboratory

3:10 pm *Overviews of New Grants*

**Miriam Freedman**, Pennsylvania State University

**Neeraj Rai**, Mississippi State University

**Benjamin Schwartz**, University of California, Los Angeles

**Adam Willard**, Massachusetts Institute of Technology

3:50 pm \*\*\*\*\* Break \*\*\*\*\*

**Session IV** Chair: **John Fulton**, Pacific Northwest National Laboratory

4:00 pm *Current Developments of Computational Spectroscopies*

**Xiaosong Li**, University of Washington

4:30 pm *Elucidating Surface Electron Dynamics in Metal Oxide Catalysts Using Ultrafast XUV Spectroscopy*

**L. Robert Baker**, Ohio State University

5:00 pm *Aqueous interface chemistry investigated by vibrational and core level spectroscopy*

**Hendrik Bluhm**, Lawrence Berkeley National Laboratory

5:30 pm \*\*\*\*\* Reception (No Host, Lobby Lounge) \*\*\*\*\*

6:00 pm \*\*\*\*\* Dinner (Salon A-B) \*\*\*\*\*

## Tuesday, October 17

7:30 am \*\*\*\*\* Breakfast (Salon A-B) \*\*\*\*\*

**Session V** Chair: **Greg Kimmel**, Pacific Northwest National Laboratory

8:30 am *Real-Time Density Functional Tight Binding: A New Computational Tool for Probing Optoelectronic Properties of Large Chemical Systems*

**Bryan Wong**, University of California, Riverside

9:00 am *Probing charge density and surface chemistry of nanostructured electrodes using single-particle spectro-electrochemistry*

**Stephan Link**, Rice University

9:30 am *Optical Parametric Imaging and Nonequilibrium Dynamics in Nanocrystal Arrays*

**Will Tisdale**, Massachusetts Institute of Technology

10:00 am *Nanoscale Imaging of Plasmon-Enhanced Electric Fields Using Photoelectrons and Raman Scattering*  
**Wayne Hess**, Pacific Northwest National Laboratory

10:30 am \*\*\*\*\* Break \*\*\*\*\*

**Session VI** Chair: **Ian Carmichael**, Notre Dame Radiation Laboratory

11:00 am *Ionic Liquids: Radiation Chemistry, Solvation Dynamics and Reactivity Patterns*  
**James Wishart**, Brookhaven National Laboratory

11:30 am *Vibrational characterization, kinetics and thermochemistry of hemibonded reaction intermediates*  
**Irek Janik**, Notre Dame Radiation Laboratory

12:00 pm \*\*\*\*\* Lunch (Salon A-B) \*\*\*\*\*

1:00 pm–4:00 pm Free/Discussion Time

**Session VII** Chair: **Adam Willard**, Massachusetts Institute of Technology

4:00 pm *Solvation at small and large length scales in trajectory space mediated by dynamical phase transitions*  
**Kranthi Mandadapu**, Lawrence Berkeley National Laboratory

4:30 pm *Rate Theory of Ion Pairing at the Liquid Interfaces*  
**Liem Dang**, Pacific Northwest National Laboratory

5:00 pm *Reaction coordinates in ion pairing and nucleation*  
**Greg Schenter**, Pacific Northwest National Laboratory

5:30 pm \*\*\*\*\* Reception (No Host, Lobby Lounge) \*\*\*\*\*

6:00 pm \*\*\*\*\* Dinner (on your own) \*\*\*\*\*

## Wednesday, October 18

7:30 am \*\*\*\*\* Breakfast (Salon A-B) \*\*\*\*\*

**Session VIII** Chair: **Kevin Wilson**, Lawrence Berkeley National Laboratory

8:30 am *New insights into the molecular scale interactions governing H<sub>2</sub> production from water over metal oxide and sulfide catalysts.*

**Caroline Chick Jarrold and Krishnan Raghavachari**, Indiana University

9:15 am *Accelerated Droplet-based Reaction Discovery: Toward Rational Design of Photocatalytic Methods for Aerobic Oxidation of N-heterocycles*

**Abraham Badu-Tawiah**, Ohio State University

9:45 am *New Progress in Electrospray Ionization Photoelectron Spectroscopy: From Multiply-Charged Anions, Transition State Spectroscopy to Aerosol Related Clusters*

**Xue-Bin Wang**, Pacific Northwest National Laboratory

10:15 am           \*\*\*\* Break \*\*\*\*

**Session IX**      Chair: **Neeraj Rai**, Mississippi State University

10:30 am      *Ab-initio analysis of molecular interactions in clusters and bulk systems*

**Marat Valiev**, Pacific Northwest National Laboratory

11:00 am      *The Role of Interfaces for Water and Binary Systems under Confinement*

**Teresa Head-Gordon**, Lawrence Berkeley National Laboratory

11:30 am      *Closing Remarks*

**Gregory Fichtner**, DOE Basic Energy Sciences

12:00 noon      \*\*\*\* Meeting Adjourns \*\*\*\*

***Table of Contents***



# TABLE OF CONTENTS

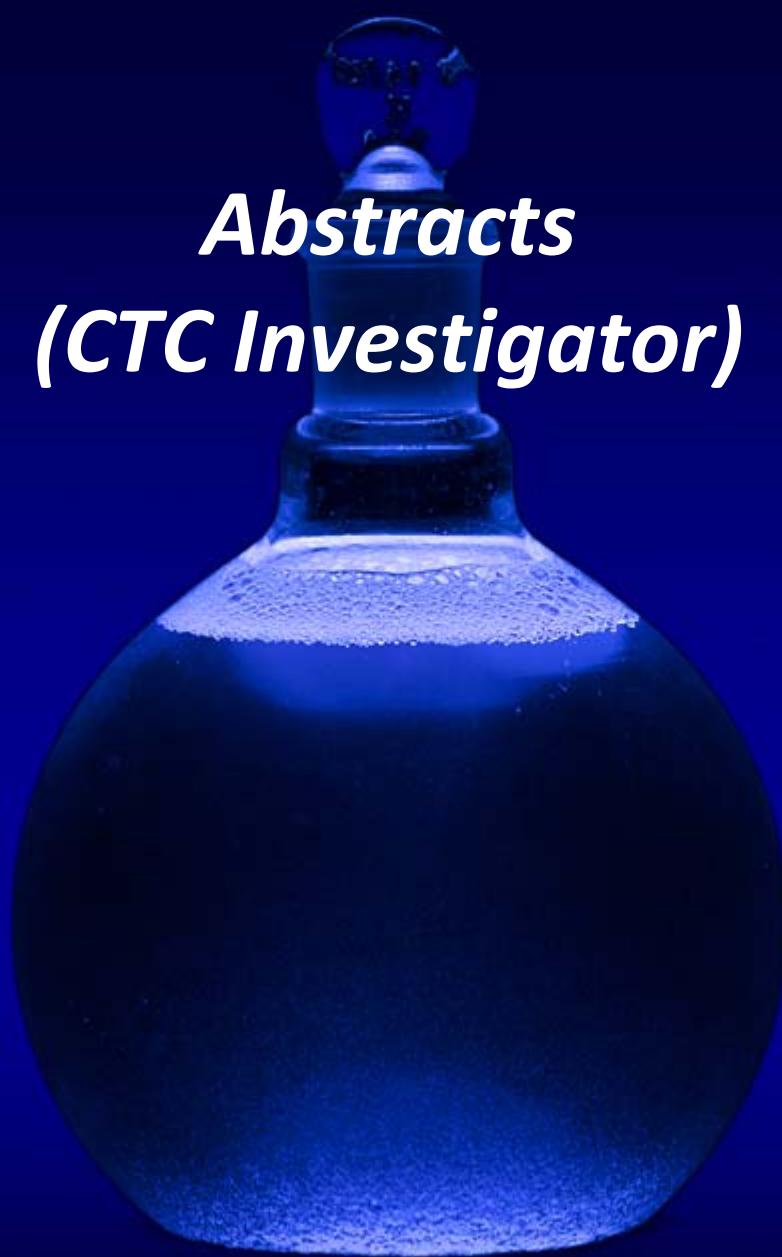
FOREWORD.....	ii
AGENDA .....	iii
TABLE OF CONTENTS .....	vii
ABSTRACTS .....	1
<b><u>CTC (Computational and Theoretical Chemistry) Principal Investigator Abstract</u></b>	
<i>Recent Developments in Computational Spectroscopy</i>	
Xiaosong Li (University of Washington) .....	1
<b><u>CPIMS Principal Investigator Abstracts</u></b>	
<i>Chemical Transformations in Bulk Aqueous Solutions and Near Interfaces</i>	
Musahid Ahmed, Hendrik Bluhm, Tanja Cuk, Teresa Head-Gordon, Richard Saykally and Kevin Wilson (Lawrence Berkeley National Laboratory) .....	2
<i>Controlling Aqueous Interfacial Phenomena of Redox-Active Ions with External Electric Fields</i>	
Heather C. Allen (The Ohio State University) .....	6
<i>Visible Light Photo-Catalysis in Charged Micro-Droplets</i>	
Abraham Badu-Tawiah (The Ohio State University) .....	10
<i>Probing Ion Solvation and Charge Transfer at Electrochemical Interfaces Using Nonlinear Soft X Ray Spectroscopy</i>	
L. Robert Baker (The Ohio State University) .....	14
<i>Development of Approaches to Model Excited State Charge and Energy Transfer in Solution</i>	
Aurora Clark (Washington State University), Christine Isborn (University of California Merced) and Thomas Markland (Stanford University).....	18
<i>Rate Theory of Ion Pairing at Liquid Interfaces</i>	
Liem X. Dang (Pacific Northwest National Laboratory) .....	20
<i>Nanoporous Materials and Ionic Liquids: Dynamics, Structure, and Interactions</i>	
Michael D. Fayer (Stanford University).....	24
<i>Size Dependence of Liquid-Liquid Phase Separation in Aerosol Particles</i>	
Miriam A. Freedman (Pacific Northwest National Laboratory) .....	28
<i>Fundamentals of Solvation under Extreme Conditions</i>	
John L. Fulton (Pacific Northwest National Laboratory).....	30
<i>Probing Chromophore Energetics and Couplings for Singlet Fission in Solar Cell Applications</i>	
Etienne Garand (University of Wisconsin) .....	34

<i>Methods for Addressing Strongly Heterogeneous and Far-From-Equilibrium Systems</i> Phillip L. Geissler, Teresa Head-Gordon, Kranthi Mandadapu and Kevin Wilson (Lawrence Berkeley National Laboratory) .....	38
<i>Laser Induced Reactions in Solids and at Surfaces</i> Wayne P. Hess (PI) Alan G. Joly and Patrick Z. El-Khoury (Pacific Northwest National Laboratory) .....	42
<i>Development of Approaches to Model Excited State Charge and Energy Transfer in Solution: Modeling Excited States in the Condensed Phase</i> Christine Isborn (University of California Merced), Aurora Clark (Washington State University) and Thomas Markland (Stanford University).....	46
<i>Probing Catalytic Activity in Defect Sites in Transition Metal Oxides and Sulfides using Cluster Models: A Combined Experimental and Theoretical Approach</i> Caroline Chick Jarrold and Krishnan Raghavachari (Indiana University) .....	50
<i>Unmasking the Mechanics of Proton Defect Accommodation and Transport in Water through Rational Control of Water Cluster Scaffolds</i> Kenneth D. Jordan (University of Pittsburgh) and Mark A. Johnson (Yale University) .....	54
<i>Nucleation Chemical Physics</i> Shawn M. Kathmann (Pacific Northwest National Laboratory) .....	58
<i>Structure and Reactivity of Ices, Oxides, and Amorphous Materials</i> Bruce D. Kay, R. Scott Smith, and Zdenek Dohnálek (Pacific Northwest National Laboratory) .....	62
<i>Probing Ultrafast Electron (De)localization Dynamics in Mixed Valence Complexes Using Femtosecond X-ray Spectroscopy</i> Munira Khalil (University of Washington, Seattle), Niranjan Govind (Pacific Northwest National Laboratory), Shaul Mukamel (University of California, Irvine) and Robert Schoenlein (SLAC National Accelerator Laboratory) .....	66
<i>Non-Thermal Reactions at Surfaces and Interfaces</i> Greg A. Kimmel and Nikolay G. Petrik (Pacific Northwest National Laboratory) .....	70
<i>2D IR Microscopy—Technology for Visualizing Chemical Dynamics in Heterogeneous Environments</i> Amber T. Krummel (Colorado State University) .....	74
<i>Probing Charge Density and Surface Chemistry of Nanostructured Electrodes using Single-Particle Spectro-Electrochemistry</i> Christy F. Landes and Stephan Link (Rice University) .....	78
<i>Development of Approaches to Model Excited State Charge and Energy Transfer in Solution: Quantum Dynamics Approaches for Modelling Charge and Energy Transfer in Solution</i> Thomas Markland (Stanford University)	

Christine Isborn (University of California Merced) and Aurora Clark (Washington State University).....	82
<i>Intrinsic to Collective Properties of Ions in Solution</i>	
Christopher J. Mundy (Pacific Northwest National Laboratory) .....	86
<i>Studies of Surface Adsorbate Electronic Structure and Femtochemistry at the Fundamental Length and Time Scales</i>	
Hrvoje Petek (University of Pittsburgh) .....	90
<i>Probing Condensed-Phase Structure and Dynamics in Hierarchical Zeolites and Nanosheets for Catalytic Upgradation of Biomass</i>	
Neeraj Rai (Mississippi State University) .....	94
<i>Molecular Structure, Bonding and Assembly at Nanoemulsion and Liposome Surfaces</i>	
Geraldine Richmond (University of Oregon) .....	97
<i>Enhancing Rare Events Sampling in Molecular Simulations of Complex Systems</i>	
Sapna Sarupria (Clemson University).....	101
<i>Equilibrium Structure and Dynamics of Aqueous Solutions and Interfaces</i>	
Richard Saykally, Musahid Ahmed, Phillip L. Geissler, Kranthi Mandadapu and Teresa Head-Gordon (Lawrence Berkeley National Laboratory) .....	104
<i>Molecular Theory and Modeling</i>	
Gregory K. Schenter (Pacific Northwest National Laboratory).....	108
<i>Understanding Chemical Bond Dynamics in Liquids Using Mixed Quantum/Classical Molecular Dynamics Simulation</i>	
Benjamin J. Schwartz (University of California, Los Angeles) .....	111
<i>An Atomic-scale Approach for Understanding and Controlling Chemical Reactivity and Selectivity on Metal Alloys</i>	
E. Charles H. Sykes (Tufts University) .....	115
<i>Imaging Interfacial Electric Fields on Ultrafast Timescales</i>	
William A. Tisdale (Massachusetts Institute of Technology) .....	119
<i>Structural Dynamics in Complex Liquids Studied with Multidimensional Vibrational Spectroscopy</i>	
Andrei Tokmakoff (University of Chicago) .....	123
<i>Ab-initio Analysis of Molecular Interactions in Clusters and Bulk Systems</i>	
Marat Valiev (Pacific Northwest National Laboratory).....	126
<i>Cluster Model Investigation of Condensed Phase Phenomena</i>	
Xue-Bin Wang (Pacific Northwest National Laboratory) .....	128
<i>Nonequilibrium Properties of Driven Electrochemical Interfaces</i>	
Adam P. Willard (Massachusetts Institute of Technology).....	132
<i>Free Radical Reactions of Hydrocarbons at Aqueous Interfaces</i>	
Kevin R. Wilson (Lawrence Berkeley National Laboratory) .....	136

<i>Non-Empirical and Self-Interaction Corrections for DFTB: Towards Accurate Quantum Simulations for Large Mesoscale Systems</i> Bryan M. Wong (University of California-Riverside).....	140
<i>Intermolecular Interactions in the Gas and Condensed Phases</i> Sotiris S. Xantheas (Pacific Northwest National Laboratory) .....	144
<b><u>Solar Photochemistry Principal Investigator Abstracts</u></b>	
<i>Fundamental Advances in Radiation Chemistry</i> David M. Bartels, Ian Carmichael, Ireneusz Janik, Jay A. LaVerne, and Sylwia Ptasińska (Notre Dame Radiation Laboratory) .....	148
<i>Pulse Radiolysis used to Study Conjugation, Entropy, and Charge Escapes</i> Andrew R. Cook, Matthew J. Bird and John R. Miller (Brookhaven National Laboratory) .....	152
<i>Radiation Chemical Impacts on Nuclear Power</i> Jay A. LaVerne and David M. Bartels (Notre Dame Radiation Laboratory) .....	162
<i>Solution Reactivity and Mechanisms through Pulse Radiolysis</i> Sergei V. Lymar (Brookhaven National Laboratory) .....	160
<i>Ionic Liquids: Radiation Chemistry, Solvation Dynamics and Reactivity Patterns</i> James F. Wishart (Brookhaven National Laboratory).....	164
<b>LIST OF PARTICIPANTS</b> .....	167

***Abstracts  
(CTC Investigator)***



# Recent Developments in Computational Spectroscopy

Xiaosong Li, University of Washington

**Abstract:** Spectroscopy techniques are indispensable tools for investigating photo-chemical processes of all kinds. A complete picture of the chemical dynamics and reaction mechanisms encoded in these spectra cannot be achieved without a full theoretical description of the underlying electronic configuration and structural relaxation on the excited state, including their explicit time-dependence and coherence far from the equilibrium. Towards this end, we have developed several *ab initio* computational spectroscopy techniques for studies of excited state transient vibration (Fig. 1), X-ray absorption (K-edge and L-edge), circular dichroism (Fig. 2), Faraday rotation and electronic coherence (Fig. 3). Prototypical photo-active molecules are used as test cases, showing the capabilities of these new computational methods. These theoretical method developments provide a direct route to reveal the physical underpinnings of (photo-)dynamics observed in experimental spectroscopies.

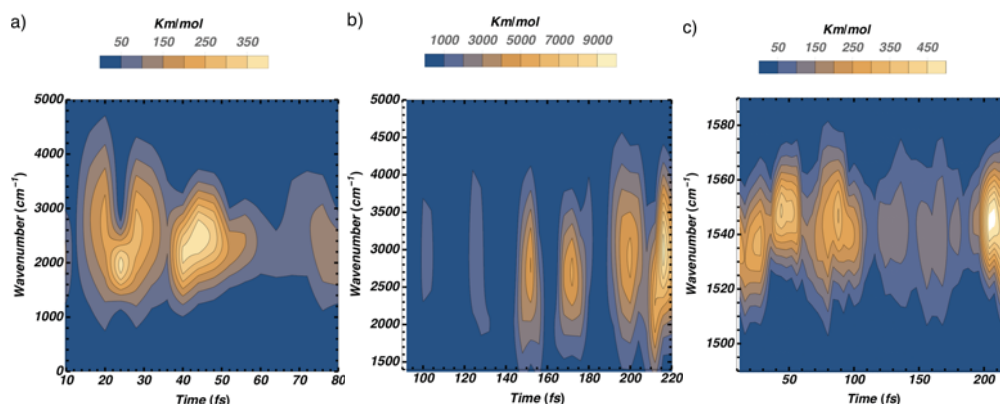


Figure 1. Transient vibrational spectra of (a) OH, (b) NH, and (c) backbone stretching modes following photoexcitation of the 2-(2'-hydroxyphenyl)-benzothiazole molecule from  $S_0$  to  $S_1$  state.

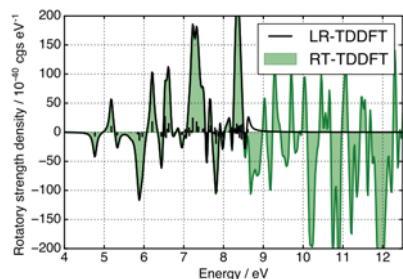


Figure 2. Computed electronic circular dichroism spectrum of  $\alpha$ -1,3-(R,R)-pinene. The vertical lines correspond to analogous LR-TDDFT results in cgs for the first 100 states. An artificial Lorentzian damping was applied to give the RT-TDDFT peaks a natural line width of 0.1 eV.

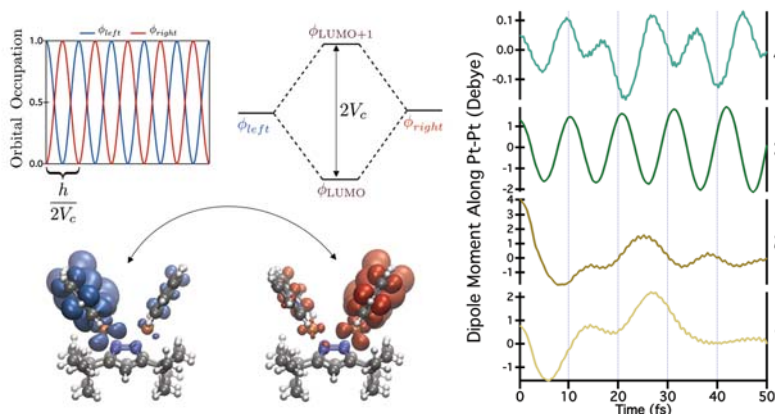
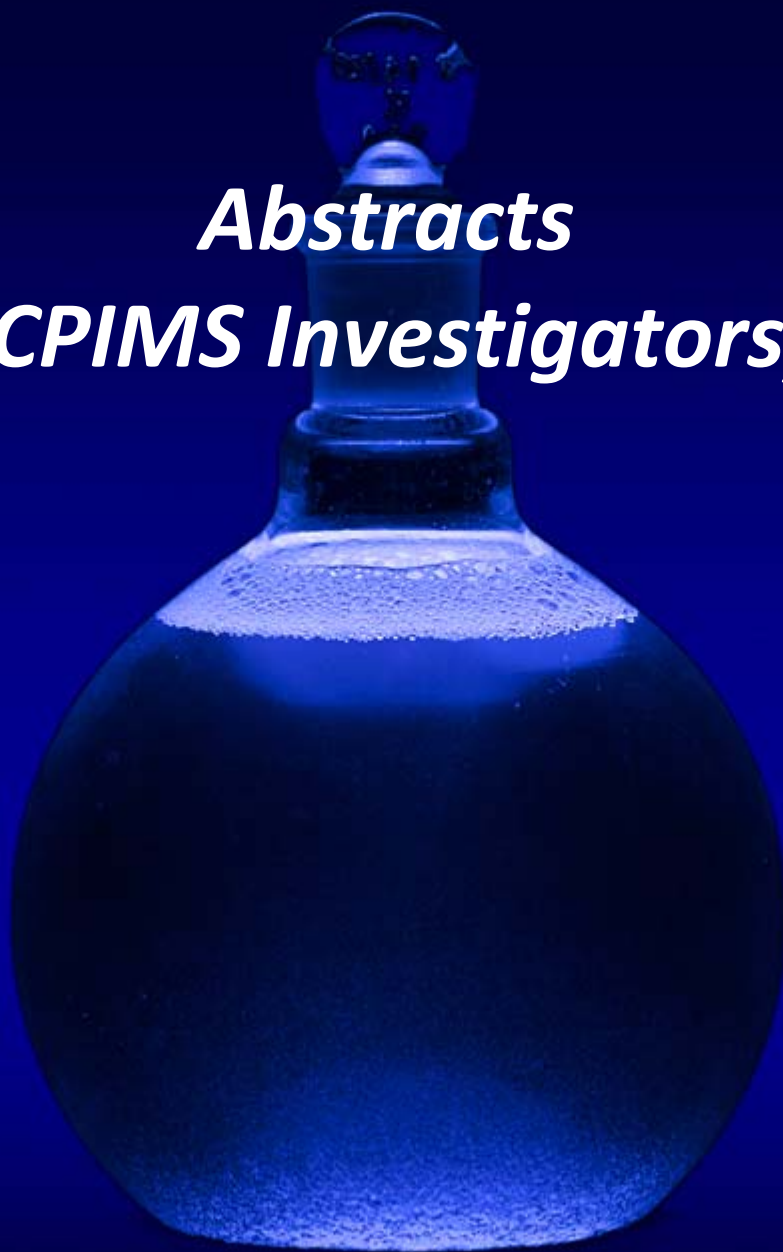


Figure 3. Left: Schematic of excited state coherence. The in-phase ( $\phi_{LUMO}$ ) and out-of-phase  $\phi_{LUMO+1}$  orbitals are formed from orbitals localized on either side of the system ( $\phi_{left}$  and  $\phi_{right}$ ). The coherent electron transfer can be analyzed in terms of the contribution of these localized orbitals to the time evolving density and dipole moment (Right).

***Abstracts***  
***(CPIMS Investigators)***



## Chemical Transformations in Bulk Aqueous Solutions and Near Interfaces

Musa Ahmed (mahmed@lbl.gov), Hendrik Bluhm (hbluhm@lbl.gov), Tanja Cuk (tanjacuk@berkeley.edu), Teresa Head-Gordon (thg@berkeley.edu), Richard Saykally (saykally@berkeley.edu), Kevin Wilson (krwilson@lbl.gov)  
*Lawrence Berkeley National Laboratory, Chemical Sciences Division,  
1 Cyclotron Road, Berkeley, CA 94720*

**Program Scope:** Chemical reactions in aqueous solutions, at interfaces and in confined geometries govern important phenomena in the environment and in numerous energy technology applications. The goal of project is to elucidate the principles that control reactivity in liquids and in heterogeneous environments through the development and application of state-of-the-art experimental and theoretical methods.

**Progress Report:** Cuk, Bluhm, and coworkers continue to investigate of the interaction of water vapor with metal oxides, with relevance to photocatalysis. The interface plays a crucial role in the photocatalytic process, yet its specific chemical composition is still not fully understood. We have used ambient pressure X-ray photoelectron spectroscopy (APXPS) in conjunction with density functional theory (DFT) to investigate the hydroxylation and water adsorption on the surface of TiO<sub>2</sub>-terminated, undoped SrTiO<sub>3</sub>(STO). The STO surface is hydroxylated at a relative humidity of as low as  $1 \times 10^{-6}$  %, with an onset of water adsorption at  $\sim 1 \times 10^{-3}$  %. The close agreement between theory and experiment for the coverage of hydroxyl and water on STO provides a pathway for a detailed description of the reaction of water vapor with other metal oxide surfaces, which is critical for an understanding of the structure-activity relationship in water oxidation reactions.

The dissolution of carbon dioxide in aqueous solutions and the ensuing hydrolysis reactions, are of profound importance for the understanding of the behavior and control of carbon, both in the terrestrial environment and in physiological systems. Essential aspects of this chemical transformation remain poorly understood, particularly those involving aqueous carbonic acid. Saykally and coworkers, using newly developed liquid microjet mixing technology, have obtained the first X-ray absorption spectra of aqueous carbonates, including the short-lived carbonic acid species itself. Spectra were measured as a function of pH to characterize the evolution of the electronic and hydration structure of carbonate, bicarbonate, carbonic acid and the dissolved CO<sub>2</sub> molecule. Using depth-dependent APXPS, Bluhm and Saykally have observed the relative locations of these species at the liquid/vapor interface. It was observed, surprisingly, that the doubly charged carbonate ion is closer to the vapor phase than the singly charged bicarbonate ion.

The interaction of a gas phase molecule with a liquid surface is a key process underlying many multiphase transformations. Evaporation the simplest example of this transformation. However, there remains considerable uncertainty in the underlying quantitative description of this process. Saykally and coworkers use microjets to examine evaporation, an approach that minimizes the obfuscating effects of condensation that have plagued previous studies. The most important practical result of our work is the quantification of the water evaporation coefficient (0.6), which has been highly controversial, and is a critical parameter in models of climate and cloud dynamics. The strongest influence on the evaporation coefficient was observed for HCl, where a 1.0 M HCl exhibits a 60% decrease relative to pure water, while 0.1 M HCl exhibits a  $\sim 45\%$  increase relative to pure water. These results suggest a large perturbation in the surface structure induced by either hydronium ions adsorbing to the water surface or by the presence of a Cl $\cdots$ H<sub>3</sub>O<sup>+</sup> ion-pair moiety in the interfacial region.

In anticipation of our group tackling more complex multiphase transformations new technical approaches are being developed by Bluhm and coworkers to examine a wide range of interfaces under operating conditions. This instrumentation combines infrared spectroscopy with APXPS thus allowing the simultaneous acquisition of vibrational and core level spectra from a sample at elevated gas pressures. The complementary information from the two techniques has enabled the unambiguous identification a rarely observed CO species in a top site on Pd(100). We plan to expand the combined IR/APXPS studies to other interfaces and systems, such as reactions at liquid/vapor interfaces.

Ahmed and coworkers examined the multiphase reactivity at liquid-nanoparticle interfaces. Electrospray ionization mass spectrometry coupled with micro-droplet based X-ray spectroscopy was used to probe the chlorination and oxidation of cobalt nanocrystals in the liquid phase. A novel mechanistic route was identified that leads to the formation of high valent cobalt complexes with decreasing particle size. Site specific proton transfer in aqueous arginine nanoparticles and phase changes in super-cooled water nanoparticles were recorded with Velocity Map Imaging X-ray photoelectron spectroscopy. In addition, the dynamics of laser-induced formation and self-assembly of Ag nanoparticle gratings on mesostructured and amorphous titania substrate were probed by synchrotron X-ray absorption spectroscopy and imaging mass spectrometry.

In anticipation of modeling chemical transformations in confined liquid environments, Head-Gordon has characterized water properties using *ab initio* molecular dynamics (AIMD) with two meta-generalized gradient approximation (meta-GGA) functionals, M06-L-D3 and B97M-rV, and compared their performance against a standard GGA corrected for dispersion, revPBE-D3, at ambient conditions (298 K, and 1 g/cm<sup>3</sup> or 1 atm). Simulations of the equilibrium density, radial distribution functions, self-diffusivity, the infrared spectrum, liquid dipole moments, and characterizations of the hydrogen bond network show that all three functionals have overcome the problem of the early AIMD simulations that erroneously found ambient water to be highly structured, but they differ substantially among themselves in agreement with experiment on this range of water properties. We show directly using water cluster data up through the hexamer that revPBE-D3 benefits from a cancellation of error by running classical trajectories, whereas the meta-GGA functionals are demonstrably more accurate and would require the simulation of nuclear quantum effects to realize better agreement with all cluster and condensed phase properties.

#### **Future Plans:**

***Condensed Phase Reactions.*** Saykally and coworkers will further improve microjet-based mixing system for generating short lived species, e.g. carbonic acid, in liquid microjets for study by X-ray spectroscopy, using both XAS and XPS. We will apply this technology to the study of hydration and hydrolysis of carbon dioxide, nitrogen oxides, and sulfur oxides, including temperature dependence. We will study the properties of aqueous carbonic acid, and its interactions with Ca<sup>2+</sup> and Mg<sup>2+</sup> ions to nucleate solid carbonate phases. Fundamental insights gained from these studies are expected to facilitate the development of CO<sub>2</sub> sequestering schemes based on saline aquifer burial. Similar investigations of nitrogen and sulfur oxides will be explored. Planar liquid jet technology will continue to be perfected for use on our nonlinear optics studies of interfaces, specifically addressing the interesting reversed fractionation of carbonates observed in XPS experiments.

***Reactions in confined geometries.*** Ahmed will investigate the chemical kinetics and dynamics of molecules in confined geometries, e.g., in nano-porous materials, nanoscale cracks in minerals, and in complex interphase regions. Ahmed seeks to use mass spectrometry, IR, Raman and X-Ray

spectroscopies coupled to novel reactors to probe model systems which are amenable to theoretical study. Ionic liquids apart from being useful as a green solvent, an electrolyte in chemical storage and transformations, and a template for soft functional material synthesis are also model systems to study self-assembly and molecular growth processes. We will probe non-covalent interactions (hydrogen bonding, electrostatic interactions) in ionic liquids upon solvation and chemical reactions that can lead to novel chemical dynamics.

Theoretical efforts of Head-Gordon will focus on *ab-initio* ring polymer contraction (AI-RPC) which will be evaluated with how water properties are changed with the inclusion of nuclear quantum effects in DFT using the meta-GGA B97M-rV functional. These *ab initio* models and techniques will then be used to explore the utilization of the altered solvent properties between confining interfaces to direct new reactive chemistry, e.g. in the Diels-Alder reactions in water, in bulk, at the liquid-vapor interface, and under nanoconfinement, for both the 1,4-naphthoquinone and the methyl vinyl ketone where we expect steric effects under strong confinement to substantially affect the reaction mechanisms and activation barrier.

Additional theory effort by Head-Gordon will be dedicated to exploring fundamental aspects of catalytic design. State-of-the-art methods use an active site construct derived from QM and subsequent empirical energy optimization to create a catalyst that often shows little activity, with most improvement coming from the subsequent set of mutations introduced through laboratory directed evolution (LDE). We propose to take a designed Kemp Eliminase, which has had no LDE applied to it, and to propose computational optimization of electric fields that are projected onto the substrate bonds to increase transition state stabilization. We will generalize this approach to characterize the role of electric field stabilization on the alkyl-alkyl reductive elimination within new confining environments such as nanocages. The combination of the two theory efforts will also be used to characterize the role of electric field stabilization on the alkyl-alkyl reductive elimination within nanocages.

***Heterogeneous Transformations.*** Saykally and coworkers plan to complete a detailed comparative study of water evaporation rates as a function of pH, comparing solutions of HCl, HBr, and NaOH, as a means of further addressing the highly controversial interfacial behavior of hydrated protons and hydroxide, respectively.

New approaches will be developed to investigate the role heterogeneous reactions at liquid/vapor interfaces. Bluhm with Wilson will combine vibrational (IR) and core-level spectroscopy (XAS, XPS) with a Langmuir trough to examine how interfacial packing of organic molecules control multiphase reaction pathways in aqueous solutions. This approach targets reactivity in 2D monolayer systems. First experiments will address the influence of the how surface molecular density and structure alter reaction pathways initiated by a reactive collision of a gas phase molecule. The long-term goal of this effort is the detailed characterization of the heterogeneous chemistry at aqueous solution/vapor interfaces as a function of trace gas species and partial pressure, molecular orientation and density, as well as the influence of ions at the interface.

We anticipate introducing new efforts to examine the multiphase reaction pathways at aqueous interfaces. Wilson will use levitated droplet arrays, to probe free radical reactions at the aqueous interfaces. Reaction rate and product distributions will be quantified by single droplet atmospheric pressure mass spectrometry. In parallel, Bluhm and Wilson will employ ambient pressure X-ray photoelectron spectroscopy (APXPS) to examine depth resolved reactions at droplets surfaces. Unlike the experiments described above using a 2D monolayers created in a Langmuir Trough,

this effort will examine the full array of coupling between surface and bulk phases to better elucidate the molecular coupling of water, diffusion and reaction in bimolecular and unimolecular free radical reactions.

### **Publications Acknowledging DOE BES CSBG Support:**

- S. Alayoglu, D. Rosenberg, M. Ahmed, Dalton Trans. **45**, 9932-9941 (2016). DOI: 10.1039/C6DT00204H
- A. Bhowmick, S. Sharma, T. Head-Gordon, J. Am. Chem. Soc. **139**, 5793-5800 (2017). DOI: 10.1021/jacs.6b12265
- A. Bhowmick, S. Sharma, T. Head-Gordon, Phys. Chem. Chem. Phys. **18**, 19386-19396 (2016). DOI: 10.1039/C6CP03622H
- X. Chen, D. Aschaffenburg, T. Cuk, Chem. Comm. **53**, 7254-7257 (2017). DOI: 10.1039/C7CC03061D
- X. Chen, D. Aschaffenburg, T. Cuk, J. Mat. Chem. A **5**, 11410-11417 (2017). DOI:10.1039/C7TA02240A
- X. Chen, S. Choing, D. Aschaffenburg, C.D. Pemmaraju, D. Prendergast T. Cuk, J. Am. Chem. Soc. **139**, 1830-1841 (2017). DOI: 10.1021/jacs.6b09550
- C.B. Gopal, S.C. Lee, M. Garcia-Melchor, Y. Shi, M. Monti, Z. Guan, R. Sinclair, H. Bluhm, A. Vojvodic, W.C. Chueh, Nat. Comm. **8**, 15360 (2017). DOI 10.1038/ncomms15360
- A.R. Head, O. Karslioglu, Y. Yu, T. Gerber, L. Trotochaud, J. Raso, Ph. Kerger, H. Bluhm, Surf. Sci. **665**, 51-55 (2017). DOI 10.1016/j.susc.2017.08.009
- O. Karslioglu, H. Bluhm, In: "Operando Studies in Heterogeneous Catalysis", Springer Series in Chemical Physics, Vol. XIV, Eds.: I.M.N. de Groot, J.W.M. Frenken, pp. 31-57 (2017). DOI 10.1007/978-3-319-44439-0\_2
- O. Kostko, B. Xu, M.I. Jacobs, M. Ahmed, J. Chem. Phys. **147**, 013931 (2017). DOI: 10.1063/1.4982822
- R.K. Lam, A.H. England, J.W. Smith, A.M. Rizzuto, O. Shih, D. Prendergast, R.J. Saykally, Chem. Phys. Lett. **633**, 214-217 (2015). DOI.org/10.1016/j.cplett.2015.05.039
- R.K. Lam, Z. Gamlieli, S.J. Harris, R.J. Saykally, Chem. Phys. Lett. **640**, 172-174 (2015). DOI:10.1016/j.cplett.2015.10.027
- R.K. Lam, J.W. Smith, A.M. Rizzuto, O. Karslioglu, H. Bluhm, R.J. Saykally, J. Chem. Phys. **146**, 094703 (2017). DOI 10.1063/1.4977046
- N. Mardirossian, L. Ruiz Pestana, J. C. Womack, C.-K. Skylaris, T. Head-Gordon, M. Head-Gordon, J. Phys. Chem. Lett. **8**, 35-40 (2017). DOI: 10.1021/acs.jpcclett.6b02527
- K. Pollock, H. Q. Doan, C. Stanton, T. Cuk, J. Phys. Chem. Lett. **8**, 922-928 (2017). DOI: 10.1021/acs.jpcclett.6b02835
- A.M. Rizzuto, E.S. Cheng, R.K. Lam, R.J. Saykally, J. Phys. Chem. C **121**, 4420-4425 (2017). DOI: 10.1021/acs.jpcc.6b12851
- L. Ruiz Pestana, N. Mardirossian, M. Head-Gordon, T. Head-Gordon, Chem. Sci. **8**, 3554 - 3565 (2017). DOI:10.1039/C6SC04711D
- N. Schwierz, R.K. Lam, Z. Gamlieli, J.J. Tills, A. Leung, P.L. Geissler, R.J. Saykally, J. Phys. Chem. C **120**, 14513-14521 (2016). DOI:10.1021/acs.jpcc.6b03788 ...
- L. Trotochaud, A.R. Head, O. Karslioglu, L. Kyhl, H. Bluhm, J. Phys.: Cond. Matt. **29**, 053002 (2017). DOI 10.1088/1361-648X/29/5/053002
- C.H. Wu, B. Eren, H. Bluhm, M.B. Salmeron, ACS Catalysis **7**, 1150-1157 (2017). DOI 10.1021/acscatal.6b02835
- B. Xu, M.I. Jacobs, O. Kostko, M. Ahmed, Chem. Phys. Chem. **18**, 1503-1506 (2017). DOI 10.1002/cphc.201700197
- J. Yao, D. Lao, X. Sui, Y. Zhou, S. K. Nune, X. Ma, T. P. Troy, M. Ahmed, Z. Zhu, D. J. Heldebrant, X-Y Yu, Phys. Chem. Chem. Phys. **19**, 22627-22632 (2017). DOI: 10.1039/C7CP03754F

**DOE-BES CPIMS****Condensed Phase and Interfacial Molecular Science****PI Heather C. Allen****Ohio State University**

Dept. of Chemistry and Biochemistry

100 W 18<sup>th</sup> Ave

Columbus OH 43210

**Program Scope**

***Controlling Aqueous Interfacial Phenomena of Redox-Active Ions with External Electric Fields.*** Ion hydration properties and interfacial water organization at the air/aqueous interface of redox active ions is of importance across a multitude of research areas and real life applications. Iron, in the 2+ and 3+ oxidation states, plays a pivotal role in many natural processes from corrosion to weathering of rocks to biogeochemical processing. Hydration, hydrolysis, carbonation, and oxidation/reduction are a subset of processes that are involved. Given these pervasive progressions and their common occurrences in nature, and in materials and their aqueous surface stability or lack thereof, makes understanding the mechanisms of such beyond curiosity sake. How can we predict the value or stability of a material if we do not understand its interaction with water for example? Water, although ubiquitous in water bodies such as the oceans, rivers, lakes, and in clouds, is also a major gas phase component in our atmosphere, existing in highly variable percentages, in the high parts per million with high dependence on temperature. Iron speciation is particularly intriguing and complex. In a FeCl<sub>3</sub> aqueous solution, it might seem that speciation is simple, yet the hydrolysis and chloro-hydro species with varying complexation charge state and polynuclear nanoparticle formation is by far - not simple. Both thermodynamics and kinetics must be considered. Iron speciation has however been studied for many decades (Stumm, Morgan 1981), yet aqueous surface speciation at a molecular scale has yet to be revealed. In our first year of DOE-BES CPIMS research, we have explored these complex processes and developed methods to understand the surface hydration of iron complexes at the air-aqueous interface. We have also made significant advances in instrument development, both in surface potential and in vibrational spectroscopic methodologies.

Our long term goal for the proposed DOE-BES research is to show proof of concept experiments, and understanding, for the organization of redox ions Fe(II) and Fe(III) at aqueous surfaces, and a deep understanding of how we can control these redox ions in externally applied electric fields at the hydrophobic air/water interface. Our investigations of acidity, co-anion, ionic strength, electric field strength, hydration, and organization of these redox ions and their associated complexes are part of this research plan. Method development continues and substantial progress has been made in the first 12 months of our grant cycle. Here, progress in understanding speciation and instrument development is presented.

**Recent Progress**

FeCl<sub>3</sub> speciation with regard to both chloro and hydro complexation has been studied utilizing several experimental approaches. We forge forward in revealing differences and similarities between aqueous surface and bulk aqueous behavior. The speciation of bulk Fe(III) complexes can be discussed in terms of hydrolysis reactions and polymer or polynuclear compound formation. (Collins et al. 2016; Dousma et al., 1976, 1978, 1979) Analysis via UV/vis spectroscopy provides a picture of speciation and the associated

kinetics. Yet, there is much to be learned beyond this viewpoint. At the surface of aqueous solutions, questions that commonly arise are: Which of the ion species are surface active, or not? What are the driving forces for surface speciation? A newer question that has arisen is: Is it true that the surface favors neutral species at the air/water interface? There is an ongoing debate as to whether the surface of water is acidic or basic, and yet when we discuss speciation of solutes in water, neutralized forms of electrolytes have been shown to be favored.

Thus, as a first step in thinking about surface speciation, an obvious approach is to measure the surface tension of the Fe salts. In Figure 1, we observe that  $\text{FeCl}_3$  increases the surface tension of water, and when compared to literature values of other salts in solution, there is a window of consistency albeit a hint of variation of a higher surface tension, even though Fe is an acid (Jarvis and Scheiman 1968; Li et al., 1999). From the literature, it is well known that the surface tension of simple acids decreases the surface tension of water. This is not the case for this metal acid in which at 1, 2, and 3 molal, the pH ranges from 0 to 1. The surface tension of  $\text{FeCl}_3$  appears to decrease in time (data not shown), yet it does stabilize to a value that is within 0.5 mN/m. This measurement is indicative of an overall depletion of ion or ionic complexes at the surface. Note that although this is a traditional interpretation, it is also clear from literature and out prior work that an increase in surface tension does NOT rule out prevalence of surface active ions. Rather, it is more common now to show proof of surface activity of some of the ions and surface depletion of others, giving rise to a change in surface potential and alignment of water due to these changing ion concentrations in the interfacial region.

Following this macroscopic measurement of surface free energy, it is an obvious next step to probe the surface with a surface selective spectroscopy such as vibrational sum frequency generation (VSFG). Thus, if Figure 2, the surface structure of water is presented for the 1 M  $\text{FeCl}_3$  solution (1M ~ 1m at room temperature). Here the top spectrum is that from neat water at room temperature revealing the unique, and well accepted, spectral shape for the hydrogen bonded and dangling OH stretching region of neat water. The three to four coordinate OH species are observed in the region below  $3600\text{ cm}^{-1}$  and the dangling OH is observed at  $\sim 3700\text{ cm}^{-1}$ . A second solution surface is measured, that of the 1M  $\text{FeCl}_3$  aqueous solution. Either with or without

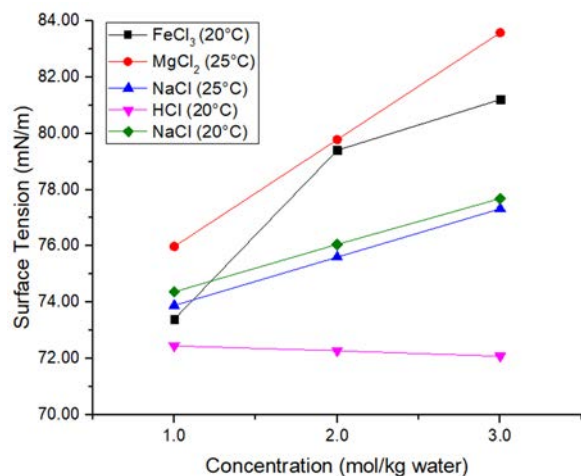


Figure 1. Surface tension of  $\text{FeCl}_3$  compared to other salts and HCl. Note that iron is an acid, yet it increases the surface tension of water similar to non-acids.

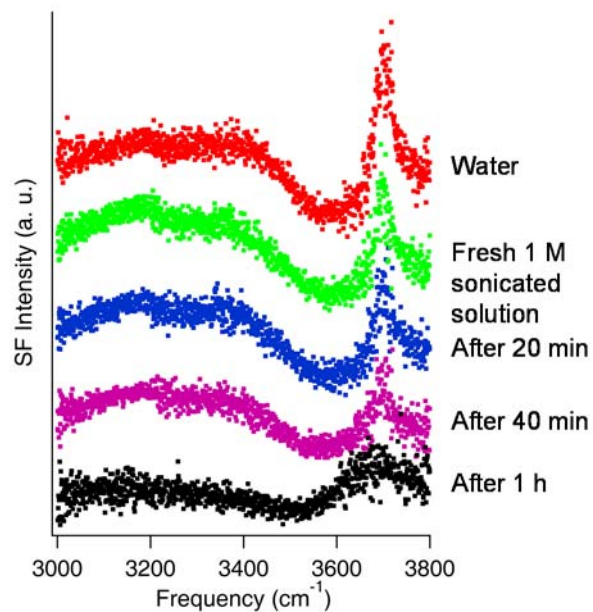


Figure 2. VSFG spectra of aqueous  $\text{FeCl}_3$  solution surfaces revealing time evolution of surface hydrolysis and water structures.

sonication produces similar spectra, although using sonication to ensure dissolution decreases the time to observe the dramatic restructuring of the OH stretch spectrum. For the sonicated solution, within 1 hour, the lower spectral region is highly suppressed as is the dangling OH band. However, interestingly,

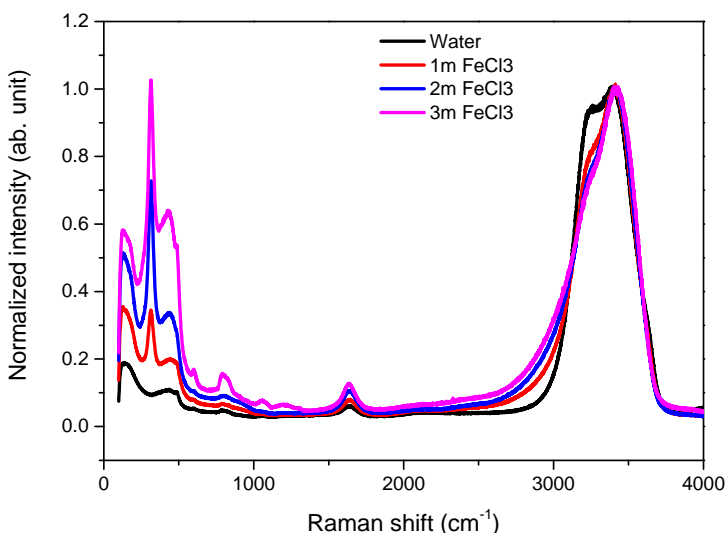


Figure 3. Unpolarized Raman spectra of bulk solutions revealing hydrogen bond network perturbation and iron speciation.

the OH dangling band appears to broaden and shift closer to  $3650\text{ cm}^{-1}$  indicative of complexation. We expect complexation in the bulk, yet at the surface it was not predicted. This direct measure of water reorganization leads us now to investigate the bulk speciation further, and as a function of preparation methods. We have also acquired both infrared (in transmission and attenuated total reflection data) and Raman spectra to report on the bulk hydrogen bonding environment and to access the Fe hydro-chloro complexation signatures in the lower spectral regions. Figure 3 shows the confocal Raman spectrum giving insight into this speciation (spectra shown are tethered to the  $3450\text{ cm}^{-1}$  band height). Fe-Cl complexation is evident as are the hydro speciation, although this needs further clarification and assignments. It is also clear that a proton continuum below  $3000\text{ cm}^{-1}$  exists, indicative of the acid strength of Fe(III). Analysis of these data and that of IR data obtained, reveals a nonlinear behavior to the speciation. Comparison to the surface spectra and deconvolution of the speciation kinetics at the surface versus the bulk is a next step. Moreover, the hydration structure and the evaluation of the surface active complexes present in the interfacial region and how these complexes evolve in time and are potentially stabilized or destabilized by different factors at the surface is to be completed.

### Future Plans

We are working on several fronts to advance our knowledge of hydration and complexation of redox species at aqueous surfaces and have plans to investigate aqueous  $\text{Fe}(\text{ClO}_4)_3$  and nitrate and sulfate species in an attempt to decipher the iron - chloro speciation, to focus on hydro speciation, and comparison studies with nanoparticle production, respectively. Interest continues to be in the hydration and the underpinnings of hydrolysis. Yet, measurement of the surface potential is next on the agenda, followed closely with applying kV electric fields across the interface to control speciation and complexation.

the OH dangling band appears to broaden and shift closer to  $3650\text{ cm}^{-1}$  indicative of complexation. We expect complexation in the bulk, yet at the surface it was not predicted. This direct measure of water reorganization leads us now to investigate the bulk speciation further, and as a function of preparation methods. We have also acquired both infrared (in transmission and attenuated total reflection data) and Raman spectra to report on the bulk hydrogen bonding environment and to access the Fe hydro-chloro complexation signatures in the lower spectral regions. Figure 3 shows the confocal Raman spectrum giving insight

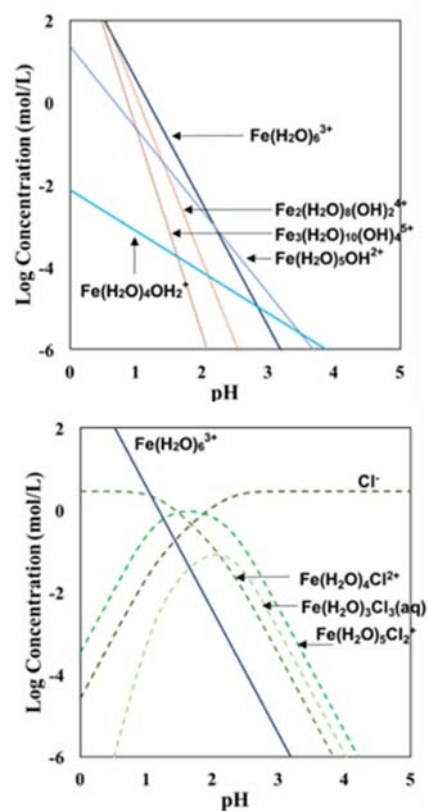


Figure 4. Calculated iron(III) speciation in bulk aqueous solution.

In regards to instrumentation, we have made significant progress on our Americium surface potential instrument to obtain inherent surface electric field information. Data has been obtained over the last several months from other salt solutions and charged lipids for instrument calibration and design improvements. There continues to be issues with determining the sign of the aqueous solution surface potential, and this may be due to the elusive absolute surface potential of neat water. We are moving forward on more advanced methods to improve and trouble shoot these issues. Incorporation of a surface height tracking device and major improvements in grounding our Faraday cage have occurred. We are also making substantial progress on our second harmonic measurements of surface potential by incorporating a reference line on a nonlinear BBO crystal to simultaneously measure both the aqueous sample surface and that of the nonlinear crystal and to capture both intensities simultaneously on different parts of the CCD chip. This work is ongoing and calibration salts and lipids are also the next step. In addition, in January we plan to begin implementing our design for applying the kV electric field across the air/aqueous interface.

Bulk [ ] Ranking	1 m Iron Species	Surface [ ] Ranking
	$\text{Fe}(\text{H}_2\text{O})_3\text{OH}_3(\text{aq})$ $\text{FeCl}_3(\text{aq})$	1
3	$\text{Fe}(\text{H}_2\text{O})_5\text{Cl}_2^+$ $\text{Fe}(\text{H}_2\text{O})_4\text{OH}_2^+$ $\text{Fe}(\text{H}_2\text{O})_2\text{OH}_4^-$	2
2	$\text{Fe}_2(\text{H}_2\text{O})_8(\text{OH})_2^{4+}$	3
4	$\text{Fe}_3(\text{H}_2\text{O})_{10}(\text{OH})_4^{5+}$	4
	$\text{Fe}(\text{H}_2\text{O})_5\text{OH}^{2+}$ $\text{Fe}(\text{H}_2\text{O})_4\text{Cl}^{2+}$	5
1	$\text{Fe}(\text{H}_2\text{O})_6^{3+}$ $\text{Cl}^-$	6 7

Table 1. Bulk speciation versus predicted surface speciation to be tested in future work.

Stumm, W. and Morgan, J. Aquatic Chemistry: An Introduction Emphasizing Chemical Equilibria in Natural Waters, 2nd ed. John Wiley & Sons, Inc. New York. **1981**

Dousma, J.; Debruyn, P. L., Hydrolysis-Precipitation Studies of Iron Solutions. 1. Model for Hydrolysis and Precipitation from Fe(III) Nitrate Solutions. *J Colloid Interf Sci* **1976**, *56* (3), 527-539.

Dousma, J.; Debruyn, P. L., Hydrolysis-Precipitation Studies of Iron Solutions. 2. Aging Studies and Model for Precipitation from Fe(III) Nitrate Solutions. *J Colloid Interf Sci* **1978**, *64* (1), 154-170.

Dousma, J.; Debruyn, P. L., Hydrolysis-Precipitation Studies of Iron Solutions. 3. Application of Growth-Models to the Formation of Colloidal Alpha-FeOOH from Acid-Solutions. *J Colloid Interf Sci* **1979**, *72* (2), 314-320.

Collins, R. N.; Rosso, K. M.; Rose, A. L.; Glover, C. J.; Waite, T. D., An in situ XAS study of ferric iron hydrolysis and precipitation in the presence of perchlorate, nitrate, chloride and sulfate. *Geochim Cosmochim Ac* **2016**, *177*, 150-169.

Li, Z.B., Li, Y.G., Lu, J.F. **1999**. *Industrial & engineering chemistry research* 38, no. 3: 1133-1139.

Jarvis, N.L., Scheiman, M.A., **1968**. *J. Phys. Chem.*, 72(1), pp.74-78.

Publications. None. (Grant start date: 09/01/2016)

## Visible light photo-catalysis in charged micro-droplets

DE-SC0016044

Abraham Badu-Tawiah

Department of Chemistry and Biochemistry, The Ohio State University. Columbus, OH 43210

badu-tawiah.1@osu.edu

### Program Scope

This research program seeks to establish the use of charged micro-droplet environment as a medium for studying photochemical reactions. The confined droplet environment has capacity to accelerate chemical reactions using only picomoles ( $10^{-12}$  mol) of reactants. The hypothesis is that the effect of electric fields used during charged droplet generation, the effect of concentration achieved by solvent evaporation from the resultant charged droplets, and the effect of droplet exposure to a highly intense and coherent visible laser source will enable the production of unique, reactive photo-chemical species for novel pathways that might be difficult to access in traditional bulk, condensed-phase conditions. Unlike traditional gas-phase reactions conducted under reduced pressure, the ionic environment of the charged droplets exists at the interface of solution-phase and the gas-phase, yielding information that is directly transferrable to large scale chemical synthesis. The main focus of our work has been the development of novel devices for charged droplet manipulation and real-time product detection by mass spectrometry (MS). Chemical systems of interest involve the study of interfacial oxidation of amines.

### Recent Progress

We have developed a novel contained-electrospray (ES) ionization device (Figure 1A) that is capable of (i) reactant confinement in charged droplets, and (ii) manipulation of the droplet reaction environment with a variety of stimuli (photons, electrical discharge, and heat). Progress is reported on the effects of photons and electrical energy on electrosprayed charged droplet reactivity. Experiments were performed using a simplified device (Figure 1B and 1C) involving nano-electrospray ionization (nESI) that mimicked only the outlet portion of the contained-ES apparatus. By coupling a portable laser source with nESI MS, we have established the first MS-based picomole-scale real-time photoreaction screening platform.

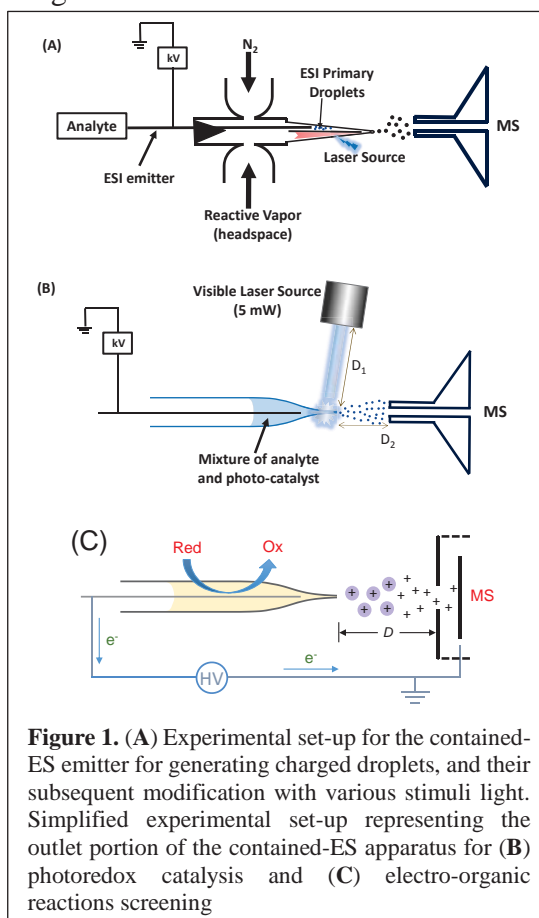
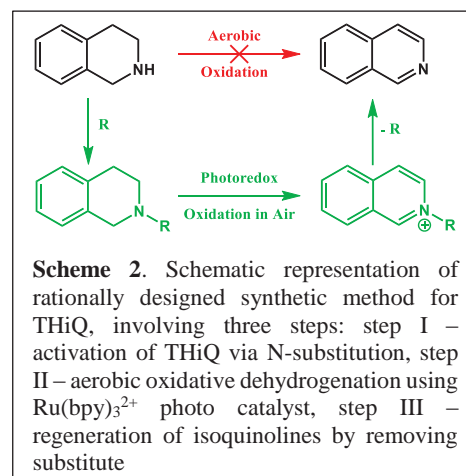
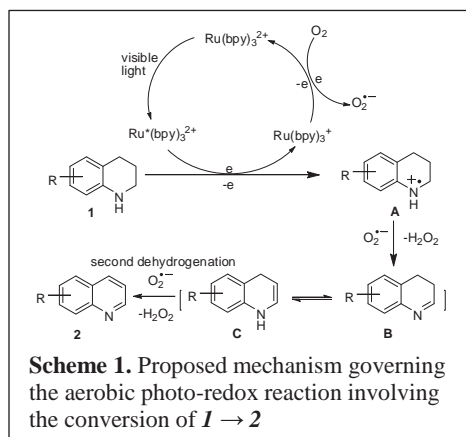


**Figure 1.** (A) Experimental set-up for the contained-ES emitter for generating charged droplets, and their subsequent modification with various stimuli light. Simplified experimental set-up representing the outlet portion of the contained-ES apparatus for (B) photoredox catalysis and (C) electro-organic reactions screening

The same setup can be adopted as a two-electrode electrochemical cell for picomole-scale real-time electro-organic reaction screening. These platforms can be used for direct and rapid screening of chemical transformations, and results are available within seconds of reaction initiation. With this approach, we discovered an effective photocatalytic pathway involving the dehydrogenation of 1,2,3,4-tetrahydroquinolines (THQ) to the corresponding quinolines. The reaction was catalyzed by the common visible-light-harvesting complex  $[\text{Ru}(\text{bpy})_3]\text{Cl}_2$  ( $\text{bpy}=2,2'$ -bipyridine) under ambient conditions. Detailed mechanistic studies revealed that the main active species in the electro-spray reaction environment is the superoxide anions ( $\text{O}_2^{\cdot-}$ ) produced during the process of photo-catalyst regeneration (Scheme 1), and that electrochemical effect on reaction yield is minimal. The droplet experimental condition was successfully transferred to bulk-phase conditions. For tetrahydroquinolines, the fully dehydrogenated quinolines were formed in >86% yield under sunlight for 2 h at 35 °C. Similar experiment was performed using tetrahydroisoquinoline (THiQ) but in this case, the dihydroisoquinoline intermediate was detected irrespective of visible light exposure time. This result is consistent with previous reports in which aerobic oxidative dehydrogenation of THiQ have always ended in the formation of the corresponding imine and not the fully dehydrogenated product. Surprisingly, the reasons for this inconsistent THQ/THiQ dehydrogenation are unknown until now. Detailed mechanistic investigation using DFT calculation and real-time reaction screening revealed a high-speed electronic interconversion bottleneck caused by hyperconjugation. By tuning the electron density, a new synthetic pathway was discovered that allows the production of isoquinolines from THiQ in three simple steps (Scheme 2): (i) N-substitution of a suitable auxiliary to reduce hyper-conjugation, (ii) photoredox oxidation of N-substituted THiQ using off-the-shelf, visible light harvesting  $\text{Ru}(\text{bpy})_3\text{Cl}_2$  complex under ambient conditions, and (ii) removal of N-substituted auxiliary to generate isoquinoline. Here too, the droplet reaction condition directly translates into bulk solution-phase allowing milligram quantities of isoquinoline to be synthesized using sun energy and atmospheric oxygen (71% yield).



## Future Plans

The focus of our work will remain (i) the development and refinement of methodologies to “process” ions at atmospheric pressure, where processing includes ion formation, ion stimulation, ion reaction, and product collection, and (ii) attempts to advance understanding of the fundamentals of photo-redox catalysis, and ion chemistry at interfaces and atmospheric pressure, using these new methodologies. Of particular interests are the elucidation of the complete

mechanism governing the photo-redox reaction to enable the creation of new pathways for other substrates.

Selection of appropriate electrode for the electrospray process utilized for droplet generation has been found to enable real-time screening of electro-organic reactions. For example, without photocatalyst, we discovered that dehydrogenation of THQ can be achieved using Pt electrode, as illustrated in Figure 1C. For the first time, the non-volatile reaction products and intermediates ensuing from the two-electrode electrochemical cell can be detected and characterized using only picomolar quantities of reagents. This discovery is exciting, and will likely lead to the development of device for studying interfacial reaction mechanism at electrode surfaces.

Detailed experiments are also needed to fully characterize the source of the  $O_2^{\cdot-}$  reactive species in droplet-based photochemistry, and the effect of nascent oxide formation during electrosprayed-based electro-organic reactions. To be certain of this reaction directions, we will first study the effect that radical scavengers (e.g., benzoquinone) have on the amine oxidation when using  $[Ru(bpy)_3]^{2+}$  with blue visible light. Benzoquinone can trap superoxide anions by an electron transfer mechanism and reduced reaction yield is expected. We will also employ 5,5-Dimethyl-1-Pyrroline-N-Oxide (DMPO) as a spin trapping reagent. In this case, DMPO is expected to react with O- and N- centered radicals present in the reaction system to form stable adducts that can be detected and characterized by MS. These experiments will provide both molecular and kinetic information. This result will encourage the development of novel electrospray-based methods that impose electrical discharge on illumination. The combined effect should make it possible to utilize highly abundant first row transition metal (e.g., copper and iron) complexes as catalyst for amine oxidation.

In particular, we are interested in *in-situ* preparation of active catalysts from simple salts (e.g.,  $CuBr_2$ ) and free ligands (e.g., 2,2'-bipyridine). For example, a previous report on a systematic investigation of the effect of different components in the Cu salt/bpy catalytic system showed better performance under basic (e.g., N-methylimidazole (NMI)) and stable radical (e.g., 2,2,6,6-tetramethylpiperidinyloxy (TEMPO)) conditions.<sup>[82]</sup> Spectroscopic investigation suggested the presence of  $[Cu(bpy)(NMI)O_2]^+$  and oxygen-bound dimer,  $[Cu(bpy)(NMI)(O_2)Cu(bpy)(NMI)]^{2+}$ , all indicating the importance of reactive oxygen species. Through negative mode electrospray, we will simplify the compositional complexity of this catalytic system. Solvent effects will be studied systematically on-line using the contained-ES apparatus. That novel and highly reactive chemical species can be generated under the charged micro-droplet environment motivates us to screen other first row transition metal salts including those of Ni and Fe. We have unique opportunity to vary a multitude of reaction conditions within a short time period. For this, we will electrospray various selected halides from different solvent compositions. Effects from confinement, photon and electrical discharge is expected to generate different micro-solvated  $[ML_n]^{n+}$  species (L = halide,  $H_2O$ ,  $CH_3CN$ ,  $OCH_3$ ,  $OHCH_3$ , etc.) with various oxidation states, some of which will be expected to have catalytic activities. Intermediate detection and characterization will be achieved by using

a novel transmission-mode desorption electrospray (TM-DESI) ion source, which enables rapidly moving charged droplets, of microseconds lifetimes, to be analyzed by MS.

By selecting appropriate photo-catalyst we will be able to explore the entire visible spectrum. We are particularly interested in the development of metal-free photo-catalytic strategies for dehydrogenation. We will test several off-the-shelf organic dyes to assess their susceptibility toward amine oxidation. Given the major limitations of organic dyes as photo-catalysts (including thermal instabilities, poor efficiencies, and slow reaction rates), we expect the droplet environment to facilitate their reactivity. Evaporative cooling and reagent concentration that results after pure solvent evaporation from the charged droplets are expected to accelerate organic dye photo-catalysis. In principle, excited organic dye can interact directly with amine reactant through an electron transfer reaction. Alternative pathways will include electron transfer reactions involving either water or oxygen molecules to generate oxidized products such as  $\text{OH}^-$ ,  $\text{O}_2^-$ , and  $^1\text{O}_2$ . We recognized that, just like electrical discharge, organic dyes can be combined with organometallic photo-catalysts to provide a cooperative photo-redox pathway through which elusive chemical reactions can be realized. Herein, we will study the effect of each photo-catalyst (organic versus organometallic) on our contained-ES apparatus, and the TM-DESI setup will be used to detect reactive intermediates when using the organic and organometallic photo-catalysts in combination.

### Recent Publications

1. Suming Chen, Qiongqiong Wan and Abraham K. Badu-Tawiah “Picomole-Scale Real-Time Photoreaction Screening: Discovery of the Visible-Light-Promoted Dehydrogenation of Tetrahydroquinolines under Ambient Conditions” *Angew. Chem. Int. Ed.* **2016**, 55, 9345
2. Kathryn M. Davis and Abraham K. Badu-Tawiah “Direct and Efficient Dehydrogenation of Tetrahydroquinolines and Primary Amines using Ionic Wind Generated on Ambient Hydrophobic Paper Substrate” *J. Am Soc. Mass Spectrom.*, **2017**, 28(4), 647–654
3. Qiongqiong Wan, Suming Chen, and Abraham K. Badu-Tawiah “Mass Spectrometry for Picomole-Scale Online Electrooxidation Reaction Screening” **submitted, 2017**
4. Savithraa Jayaraj and Abraham K. Badu-Tawiah “N-Substituted Auxiliaries for Visible Light-Mediated Dehydrogenation of Tetrahydroisoquinolines: A Theory-Guided Rational Catalytic Design Supported by Real-time Electrospray-based Photoreaction Screening” **submitted, 2017**

# Probing Ion Solvation and Charge Transfer at Electrochemical Interfaces Using Nonlinear Soft X Ray Spectroscopy

L. Robert Baker

Department of Chemistry and Biochemistry  
The Ohio State University, Columbus, OH 43210  
[baker.2364@osu.edu](mailto:baker.2364@osu.edu)

## 1. Program Scope

Understanding charge transfer across interfaces is an important challenge with both scientific and technological relevance because these interfacial processes largely determine the performance of batteries, fuel cells, catalysts, opto-electronic devices, and photovoltaics. To significantly improve the efficiency of these energy conversion technologies will require a much better fundamental understanding of the molecular and electronic processes occurring at interfaces that drive energy conversion. Probing the femtosecond dynamics of charge transfer across interfaces with chemical state resolution is crucial for engineering materials with desirable optical and electronic properties for better energy conversion applications.

Towards this goal, we have constructed a tabletop extreme ultraviolet (XUV) spectrometer that operates in reflection at near grazing ( $8^\circ$ ) incidence angle. XUV spectroscopy is well suited for studying charge carrier dynamics because it is element specific, sensitive to oxidation state, spin-state, and coordination geometry of the metal center and because these experiments can be performed in the laboratory with femtosecond time resolution. Unlike transmission measurements, XUV reflectivity is not limited by sample thickness, which extends the use of XUV spectroscopy to functional surfaces without restriction to material thickness or substrate. Moreover, reflectivity offers the advantage of surface specificity having a recently measured probe depth of only a few nm, indicating that this technique can selectively follow charge transfer dynamics at the surface of a material. This gives us the ability to track the state of photoexcited charge carriers at a catalyst surface in real time with state-specific precision.

Much more is currently known about molecular photophysics and photochemical reaction dynamics compared to surface photochemistry due to the inability to probe surfaces selectively with sensitivity to oxidation state, spin state, carrier thermalization, lattice distortions, and charge trapping at defect states. Femtosecond soft x-ray reflectivity developed here is now enabling such studies with the goal of advancing the field of surface chemical physics. It is anticipated that in the near future, this technique will also enable the study of ion solvation and de-solvation dynamics at biased electrode-electrolyte interfaces.

## 2. Progress Report

### *Summary of Progress*

We have recently demonstrated that XUV reflection spectroscopy can probe element specific resonances from the early to late  $3d$  transition metal oxides with oxidation and spin state resolution.<sup>1</sup> We have also investigated the ultrafast carrier dynamics of two transition metal oxides with relevance for photocatalytic water oxidation:  $\text{Fe}_2\text{O}_3$  and  $\text{NiO}$ .<sup>1, 2</sup> In the case of  $\text{Fe}_2\text{O}_3$ , we observe that photoexcited electrons in  $\text{Fe}_2\text{O}_3$  trap at the surface within  $\sim 650$  fs and that this surface trapping is accompanied by fast expansion of the oxide lattice.<sup>2</sup> Further, we observe that surface electron trapping occurs on identical time scales for single crystalline and polycrystalline  $\text{Fe}_2\text{O}_3$ , indicating that surface defect states do not play a significant role in this process. Rather, the strong correlation between surface electron trapping and the corresponding lattice expansion suggests that small polaron formation in this material represents the primary driving force for electron localization to the surface.

We are currently applying this technique to study mixed metal Fe-Ni oxide, a widely used material for water oxidation. Despite numerous studies, the exact mechanism for the enhanced kinetics of

this mixed metal oxide catalyst is still not fully understood. We are currently investigating the dynamics of ultrafast charge separation across the heterojunction composed of NiO<sub>x</sub> thin films on a Fe<sub>2</sub>O<sub>3</sub> substrate. Early studies of this system show that immediately after excitation with 400 nm light, there is a transient response at the Fe M-edge, reflecting selective photoexcitation of Fe<sub>2</sub>O<sub>3</sub>. This is followed by hole transfer from the Fe<sub>2</sub>O<sub>3</sub> valence band to the NiO valence band with a time constant of ~8 ps. Ongoing spectral analysis promises to differentiate between O 2*p* and Ni 3*d* as the primary hole acceptor states in NiO. Lastly, we are investigating the ultrafast dynamics of Fe-doped NiO to simultaneously probe changes in the electronic structure and lattice environment of both Ni and Fe centers..

### *M<sub>2,3</sub>-Edge Reflection-Absorption of Transition Metal Oxides*

Because RA spectra probe both the real (*n*, i.e., reflection) and imaginary (*k*, i.e., attenuation) part of the refractive index, measured lineshapes are significantly different from corresponding transmission spectra. We have recently developed a general method to analyze RA spectra using ligand field multiplet theory coupled with electromagnetic theory.<sup>1</sup> We find that the imaginary part of the refractive index reports on the chemical state of the metal center, while the real part is additionally sensitive to the surface morphology of the material.

To demonstrate the ability to quantitatively account for surface morphology, Figure 1 compares the results of our general simulation procedure (black lines) with the experimental RA spectra (red lines) for three samples: single crystalline (SC) Fe<sub>2</sub>O<sub>3</sub>, polycrystalline (PC) Fe<sub>2</sub>O<sub>3</sub>, and PC CuFeO<sub>2</sub>. As shown in Figure 1, the RA spectra for SC Fe<sub>2</sub>O<sub>3</sub>, PC Fe<sub>2</sub>O<sub>3</sub>, and CuFeO<sub>2</sub> differ in spectral width and peak position. The CuFeO<sub>2</sub> also displays a pronounced irregularity in its baseline, which is the result of wavelength-dependent, non-resonant surface scattering from this rougher surface, and has been accounted for in our simulation. We have reported a general approach that is capable of quantitatively reproducing our measured results. Furthermore, to demonstrate the elemental and chemical state specificity of XUV RA spectroscopy, the spectra for PC samples of TiO<sub>2</sub>, Cr<sub>2</sub>O<sub>3</sub>, NiO were also collected. We show that the elemental specificity is retained in XUV RA spectroscopy. The energy of the M-edge transition increases from TiO<sub>2</sub> to NiO as expected.<sup>1</sup>

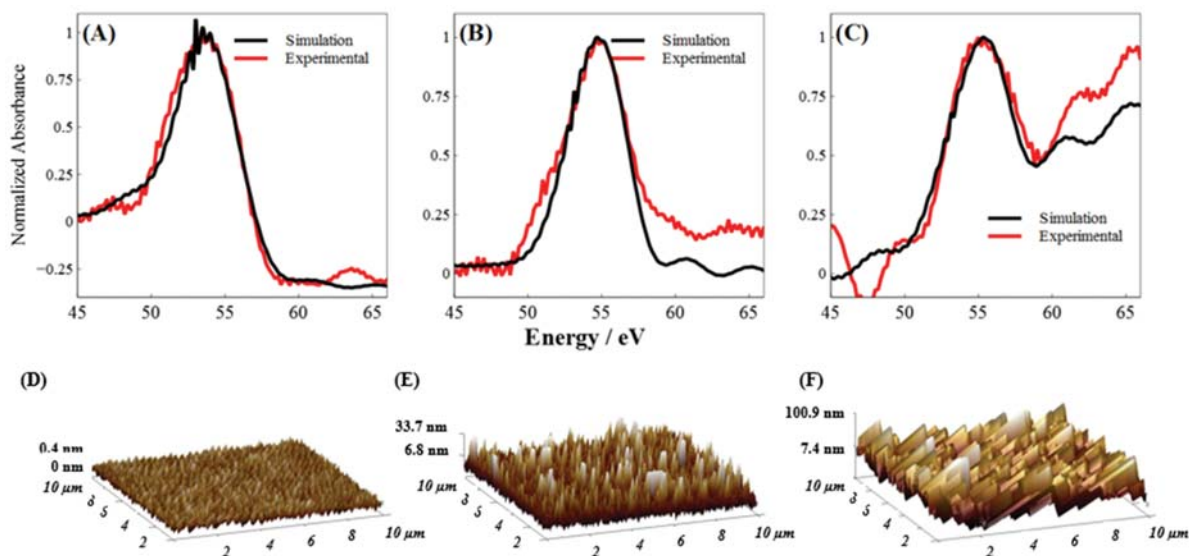


**Figure 1.** Simulated (black) and experimental (red) RA spectra for (A) SC Fe<sub>2</sub>O<sub>3</sub>, (B) PC Fe<sub>2</sub>O<sub>3</sub>, and (C) CuFeO<sub>2</sub>. All RA simulations differ only by adjusting a wavelength-independent offset in *n* to take into account the relative surface morphology. Below each spectrum is a representative AFM image of the surface roughness for each material ((D) SC Fe<sub>2</sub>O<sub>3</sub>,  $R_q < 0.2$  nm; (E) PC Fe<sub>2</sub>O<sub>3</sub>,  $R_q = 10$  nm; (F) CuFeO<sub>2</sub>,  $R_q \approx 27$  nm).

### Ultrafast Surface Electron Trapping and Polaron Formation in Hematite ( $\alpha\text{-Fe}_2\text{O}_3$ )

Hematite has been used as a potential photocatalyst due to its favorable optical bandgap ( $\sim 2$  eV), low cost, high earth abundance, and long-term stability. However, its major limitation as an efficient catalyst is the low mobility of charge carriers. It has been proposed that the formation of surface trapping via small polaron formation is responsible for low charge carrier mobility and hence poor catalytic efficiency. However, due to the lack of surface sensitive and chemical state specific spectroscopic techniques, it has been challenging to directly probe the surface trapping of polarons. XUV reflection spectroscopy is a well-suited technique to probe the surface trapping of polarons on the femtosecond time scale with chemical state resolution.

We have measured the transient XUV reflectivity of photoexcited hematite. Interpretation of the transient dynamics requires knowledge of  $n$  and  $k$  for both the ground and transient excited states involved in the photoexcitation. The simulation suggests that both the initial and final photoexcited states (Figure 2A and 2B) of hematite are ligand to metal charge transfer (LMCT) states where an electron from an O  $2p$  band has been transferred to the Fe  $3d$  band. Furthermore, by considering  $n$  and  $k$  of both the excited ( $\text{Fe}^{2+}$ ) and ground ( $\text{Fe}^{3+}$ ) state, the simulation indicates the delocalized nature of the initially photoexcited state, which subsequently evolves to a surface localized LMCT state within 660 fs. Correlation between experimental results and spectral simulations reveals that the lattice expansion during small polaron formation occurs on the same time scale as surface trapping and represents the probable driving force for sub-ps electron localization to hematite surface. Moreover, comparison of the charge carrier dynamics for single and polycrystalline hematite samples shows that the observed dynamics are negligibly influenced by grain boundaries and surface defects.

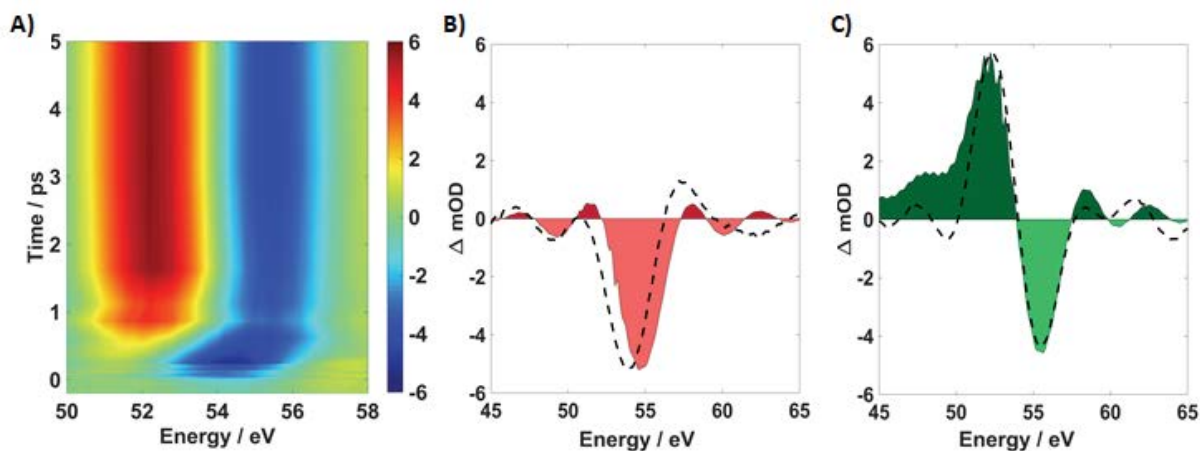


**Figure 2.** (A) Experimental contour plot showing the transient response at the Fe M-edge of photoexcited  $\text{Fe}_2\text{O}_3$  (B) Experimental (shaded red) and simulated (dashed line) initial photoexcited state of  $\text{Fe}_2\text{O}_3$  (C) Experimental (shaded green) and simulated (dashed line) final photoexcited state of  $\text{Fe}_2\text{O}_3$ .

### 3.Future directions

Charge carrier dynamics at a  $\text{NiO}_x/\text{Fe}_2\text{O}_3$  heterojunction with respect to pure NiO and  $\text{Fe}_2\text{O}_3$  are important to understand its catalytic activity for water oxidation. To investigate the electronic structure of a  $\text{NiO}_x/\text{Fe}_2\text{O}_3$  heterojunction, XUV RA spectra of  $\text{NiO}_x$  thin films of various thicknesses (2, 5, 7, and 10 nm) deposited on  $\text{Fe}_2\text{O}_3$  have been measured. Figure 3 compares the ground state XUV RA spectra of these  $\text{NiO}_x/\text{Fe}_2\text{O}_3$  heterojunctions with pure NiO (purple) and pure  $\text{Fe}_2\text{O}_3$  (red). These results clearly suggest that there are significant differences in the electronic structure of both Ni and Fe in the heterojunctions compared to pure NiO and  $\text{Fe}_2\text{O}_3$ . The RA spectrum of a heterojunction with a very thin layer of  $\text{NiO}_x$  (2 nm) is similar to pure  $\text{Fe}_2\text{O}_3$ , but displays a distorted Ni spectrum. However, with

increasing thickness of the NiO<sub>x</sub> layer, the Ni edge evolves towards the pure NiO spectrum.

To investigate the charge carrier dynamics across the type II heterojunction of NiO and  $\alpha$ -Fe<sub>2</sub>O<sub>3</sub>, photoexcited carrier dynamics of pure NiO and pure  $\alpha$ -Fe<sub>2</sub>O<sub>3</sub> have been performed separately, revealing transient LMCT excited states in both NiO and  $\alpha$ -Fe<sub>2</sub>O<sub>3</sub>.<sup>1, 2</sup> Photoexcitation of the heterojunction at 267 nm shows the signature of similar LMCT states in both Fe and Ni edges as observed in pure NiO and  $\alpha$ -Fe<sub>2</sub>O<sub>3</sub> (Figure 4B). However, photoexcitation of the heterojunction at 400 nm shows a delayed response at the Ni M-edge (Figure 4C) but a similar response in the Fe M-edge. Due to the wide band gap (~ 4 eV) of NiO compared to  $\alpha$ -Fe<sub>2</sub>O<sub>3</sub> (~ 2 eV), it is expected that the photoexcitation of the heterojunction at 400 nm light will selectively excite the charge carriers in  $\alpha$ -Fe<sub>2</sub>O<sub>3</sub> as shown in Figure 4A. Because the valence band offset of these two materials is well suited for hole transfer to produce spatially separated charge carriers, hole migration from Fe<sub>2</sub>O<sub>3</sub> to the valence band of NiO is responsible for a delayed response at the Ni edge when pumping at 400 nm. Figure 4D compares the instantaneous response at the Ni M-edge following excitation at 267 nm with the delayed response following excitation at 400 nm. From this data, the measured time constant for hole transfer across the heterojunction is ~8 ps. We are also in the process of performing transient reflectivity measurement on Fe-doped NiO to characterize the electronic structure and carrier dynamics of this material. These results will provide fundamental understanding of the photophysics leading to enhanced efficiency for water oxidation by these mixed Fe–Ni oxide systems.

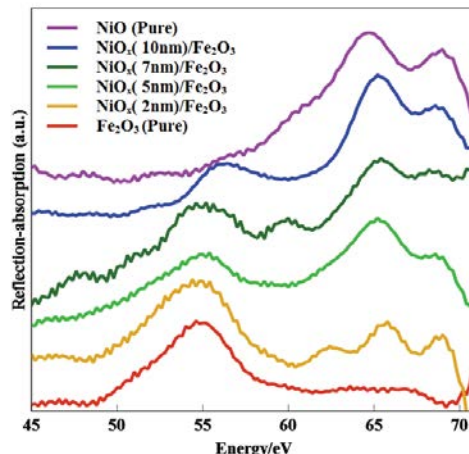


**Figure 3** Ground state RA spectra of several NiO<sub>x</sub>/Fe<sub>2</sub>O<sub>3</sub> heterojunctions compared with pure NiO (purple) and Fe<sub>2</sub>O<sub>3</sub> (red).

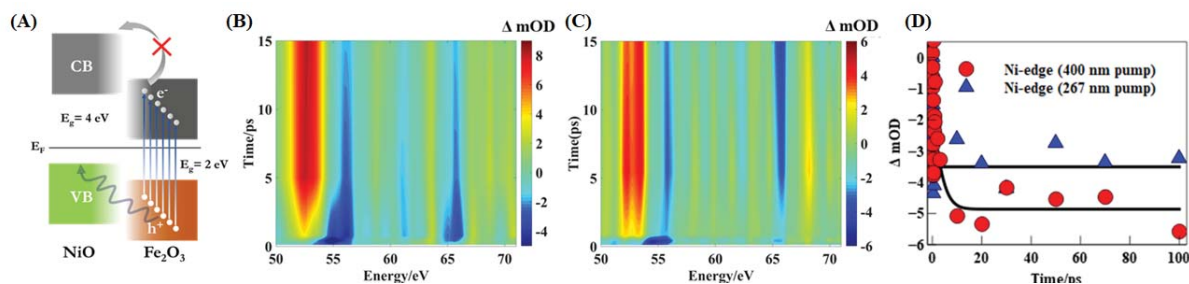


**Figure 4** (A) Band diagram of NiO/ Fe<sub>2</sub>O<sub>3</sub> heterojunction, showing the hole transfer across the interface. (B,C) Contour plots of the heterojunction photoexcited at 267 nm (B) and 400 nm (C), respectively. (D) Kinetic traces at the Ni edge pumped at 267 nm (blue markers) and 400 nm (red markers). Black solid lines show the fitted kinetics.

#### 4. Publications Acknowledging DOE Support

1. Cirri, A., Husek, J., Biswas, S. & Baker, L.R. Achieving Surface Sensitivity in Ultrafast XUV Spectroscopy: M<sub>2,3</sub>-Edge Reflection–Absorption of Transition Metal Oxides. *The Journal of Physical Chemistry C* **121**, 15861-15869 (2017).
2. Husek, J., Cirri, A., Biswas, S. & Baker, L.R. Surface Electron Dynamics in Hematite ( $\alpha$ -Fe<sub>2</sub>O<sub>3</sub>): Correlation Between Ultrafast Surface Electron Trapping and Small Polaron Formation, Under review.

## DEVELOPMENT OF APPROACHES TO MODEL EXCITED STATE CHARGE AND ENERGY TRANSFER IN SOLUTION

Aurora Clark, [auclark@wsu.edu](mailto:auclark@wsu.edu), Washington State University  
Christine Isborn, [cisborn@ucmerced.edu](mailto:cisborn@ucmerced.edu), University of California Merced  
Thomas Markland, [tmarkland@stanford.edu](mailto:tmarkland@stanford.edu), Stanford University

### Program Scope

The development of next generation energy conversion and catalytic systems requires a fundamental understanding of the interplay between photo-excitation and the resulting proton and electron transfer processes that occur in solution. To address these challenges requires accurate and efficient methods to compute ground and excited states, as well as the ability to treat the dynamics of electrons, protons, and electronic energy transfer in the presence of solvent fluctuations occurring over a range of time-scales. With this ability in hand, new analysis methods are being developed to elucidate the important roles of molecular motion, multiscale correlations, and statistical ensembles upon proton and energy transfer processes.

Our team is developing accurate and efficient theoretical models for solution phase reactions, and new analyses that explore multiscale correlations within time-dependent statistical ensembles. For reliable condensed phase simulations, an accurate model that includes both short- and long-range interactions is required. Short- and long-range interactions may be particularly strong in aqueous solution, where hydrogen-bonding and proton transfer may play a large role at short range and polarization may play a large role at long-range. For realistic condensed phase calculations that take into account solute-solvent interactions large-scale quantum mechanical (QM) calculations that include the condensed phase environment are necessary. These large-scale calculations can also help us determine what physics is necessary for more approximate models.

The Clark group is using graph theoretical methods to analyze proton transfer processes in aqueous solution, and creating new ways to elucidate correlated molecular motions and dynamics along generalized collective reaction coordinates. We are analyzing classical, ab-initio, and ring-polymer molecular dynamics trajectories so as to compare and contrast the influence of the interatomic interactions and quantum nuclear effects upon solution phase organization, molecular motion, and reaction pathways.

### Recent Progress

- 1) *Multi-body transition matrices to elucidate molecular motion.* Understanding molecular motions is essential toward understanding chemical reactions like proton transfer in solution. However, it is often difficult to learn what motions are essential to a process and if other, more nuanced multi-body concerted motions are relevant. The configurational state of a multi-body arrangement of molecules has been identified by its pattern of intermolecular interactions (e.g. HB network). Using enumeration methods, we obtain all possible patterns of interactions within a many-body system to define all possible configurational representations. Trajectories of molecular dynamics simulations are then used to populate the transitions between those states. Specifically, a three-state approach is taken where we keep track of all intermediary configurations as one pattern is changed to another. We have demonstrated that this concept captures significantly more patterns of molecular motion than one would normally intuit using chemical reasoning. This is demonstrated for the case of water rotation, where the full range of motions (small and large angle rotational jumps) are easily quantified, in addition to concerted motions where multiple interactions (HBs) are broken at the same time.
- 2) *Weighted intermolecular networks to understand correlations within proton transfer.* Ongoing work is focused upon the study of chemical information contained within

weighted networks of intermolecular interaction, based upon the probability of interactions from path integral molecular dynamics. Examples of ongoing work include: a) understanding correlations in ring polymer shape with successful proton transfer events, and 2) tracking proton conducting hydrogen bonded water wires as a function of solution phase conditions.

- 3) *Multi-layered microstates to sample free energy surfaces and the prediction of Shannon Entropy.* Configurations (microstates) of a system are represented as non-isomorphic graphs of their intermolecular interactions and topological metrics are added as parameters to emphasize the chemical importance of defects, network connectivity, compactness of a network, etc. Using the microstate distribution, transitions between microstates are being used to understand fluctuations associated with the energy surface, and the ensemble of microstates is used to calculate the Shannon Entropy. An optimization function is employed using machine learning to determine the set of topological parameters such that the change in Shannon Entropy can effectively track Chemical Entropy given a variety of perturbations (phase changes, mixing, etc.).

## Future Plans

### **Award Number DE-SC0014437: Development of Approaches to Model Excited State Charge and Energy Transfer in Solution**

**PI and co-PI(s):** Christine Isborn (Merced, PI), Aurora Clark (WSU, co-PI), Thomas Markland (Stanford, co-PI)

**Clark Group Postdoc(s):** Lance Edens (previous: now post-doc on DOE IDREAM EFRC), Andrew Launder (current)

**Clark Group Student:** Lelee Ounkham

## DOE Sponsored Publications

[1] Identifying Molecular Motions Using Many-body Transition Matrices of Intermolecular Networks. T. Zhou, L. Edens, J. Napoli, T. Markland, A. E. Clark *J. Chem. Phys.* (2017) *In Preparation.*

[2] Predicting Proton Transfer Events Using Weighted Intermolecular Networks. L. Ounkham, L. Edens, J. Napoli, T. Markland, A. E. Clark *J. Chem. Theory Comp.* (2017) *In Preparation.*

[3] Does Shannon Entropy Track Chemical Entropy? A. Launder, A. Ozkanlar, J. Kaminsky, A. E. Clark *J. Chem. Phys.* (2017) *In Preparation.*

# Rate Theory of Ion Pairing at Liquid Interfaces

## Recent Progress and Future Plans

Liem X. Dang  
Physical Sciences Division  
Pacific Northwest National Laboratory  
Richland, WA 93352  
[liem.dang@pnnl.gov](mailto:liem.dang@pnnl.gov)

### Background and Significance

The thermodynamics and kinetics of ion pairings at interfaces are fundamental processes encountered in a wide range of physical and chemical systems. Considerable progress has been made in understanding the equilibrium and dynamical properties of ion pairings at liquid interfaces. The main goal of our work, in addition to studying ion-ion potentials of mean force (PMF), is to provide detailed kinetic properties of ion pairings at the liquid–vapor interface of water using a variety of rate theory approaches. Moreover, we will determine how the inclusion of polarizable interactions influences the differences that arise at the interface versus the bulk liquid. Subsequently, our studies will be expanded to other interfaces, such as liquid–liquid interfaces. Knowledge of free energy profiles and rate theory evaluations is important for understanding a wide range of physical and chemical phenomena for ion solvation and pairing. These also provide a challenging test of the accuracy of the predictive information derived from force field models. Our work is distinguished from earlier contributions by the methodology and the extent in which we have exploited rate theory approaches, including classical transition-state theory (TST), the reactive flux (RF) formalism, and Grote-Hynes (GH) theory. In addition, we 1) explicitly include polarization effects in the potential models and compare them to results from nonpolarizable models; 2) evaluate solvent responses at the interface and in the bulk using a variety of classical rate theory approaches; and 3) compute and compare the dissociation lifetimes for the ion pair for different potential models and theories.

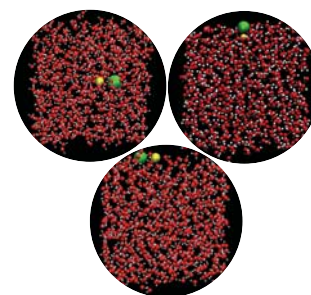


**Figure 1.** Schematic description of the NaCl/NaI–H<sub>2</sub>O system under study. The left panel is for the ion pair in the bulk region, and the right and center panel is for the ion pair at the GDS, with different orientations.

### Recent Progress

#### A. Kinetics of interfacial ion pairing with polarizable models

We begin this section by presenting results on the kinetic properties of the NaCl ion pair formation at the interface and in the bulk, and then continue with rate theory results determined using the RF and GH methods.

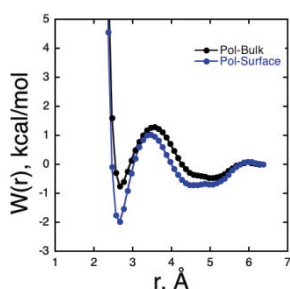


**Figure 2.** Computed PMFs for the NaCl ion pair in the bulk and at the interface: polarizable.

Figure 2 shows the computed PMF plots as a function of NaCl separation at the interface and in the bulk for the polarizable model. Although the shapes for both of the PMFs are quite similar, the details of the barriers are different, which may result in dissimilarities in the kinetics of ion pairing. From Figure 2, the PMF at the interface has a deeper minimum at the contact ion pair and a larger barrier height to dissociate compared to the corresponding bulk PMF results. This demonstrates that the interfacial ion pair is more strongly associated at the interface, which can be attributed to rearrangement of the interfacial water hydrogen networks to accommodate the ion pair at the interface. Moreover, it is well known that Cl<sup>−</sup> has a larger induced dipole at the interface, which should further strengthen NaCl pairing at the interface. Another interesting aspect of the PMF is that the solvent-separated ion pair

probability (its free energy is lower near 4.5 Å) is slightly enhanced at the interface with respect to the bulk. Overall, this shows that ions are more likely to not just be paired, but to be paired within their first two solvation shells near the interface. The free energy barriers for ion pair dissociation are found to be approximately 3.0 and 2.0 kcal/mol for the interfacial and bulk ion pairs, respectively. The computed rate constants from the PMFs using TST are 0.28 and 0.07 ps<sup>-1</sup>. These results show that the 1.0 kcal/mol higher barrier for dissociation at the interface has a major effect on dissociation rate. In Figure 3, we present the computed time-dependent  $\kappa(t)$  for both ion pair locations using the RF method. The transmission coefficients,  $\kappa_{RF}$ , are 0.14 and 0.25. We made two notable observations: 1) the plateaus of the transmission coefficient curves are very flat after 1.5 ps and 2) the transmission coefficients decrease from the interface to the bulk. Our results show that in addition to affecting the free energy of solvation, moving ion pairs from the bulk to the surface should significantly influence the kinetics of ion pairing.

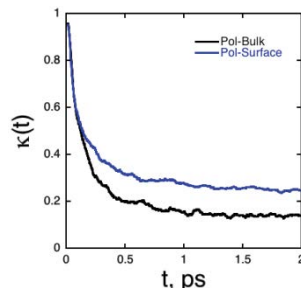


**Figure 3.** Computed  $\kappa(t)$  using the RF method for the NaCl ion pair in the bulk and at the Gibbs dividing surface.

## B. Kinetics of interfacial ion pairing with nonpolarizable model

To better understand the specific role that polarizability plays in dissociation kinetics, we made similar calculations using nonpolarizable models. For these calculations, we employed the Tip4P-Ew water model, and the ion parameters were derived to reproduce many experimental properties. In Figure 4, we present the computed PMF plots for the interfacial ion pair and the bulk ion pair for the nonpolarizable models.

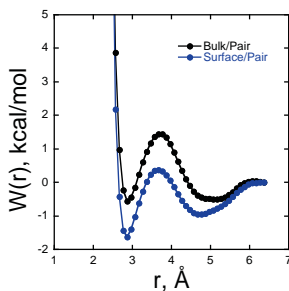
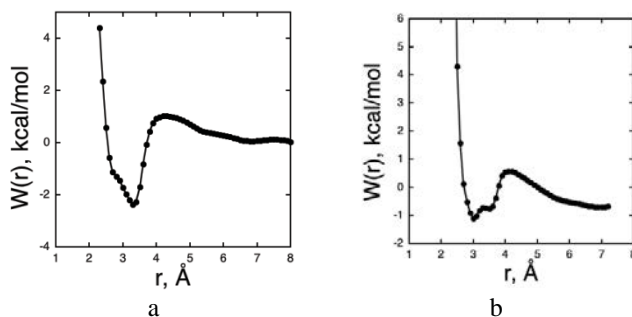


**Figure 4.** Computed PMFs for the NaCl ion pair in the bulk and at the interface: nonpolarizable.

Similar to results from the polarizable models, there is a deeper free energy minimum at the contact ion pair (around  $r = 3$  Å); however, the barrier heights for dissociation are very similar at the interface and the bulk (i.e., approximately 2.0 kcal/mol). This result is in contrast with the results obtained from the corresponding PMF described above that used polarizable models. Also, the free energy at the solvent-separated ion pair is significantly different at the interface than in the bulk, with the surface results being more than 0.5 kcal/mol more negative in free energy at a distance around 4.8 Å than the bulk value. This is greater than the difference observed in Figure 2 for the polarizable model. Overall, it seems that the interface stabilizes the contact ion pair for both models, while the nonpolarizable model provides slightly less, but still a significant degree of, stabilization of the solvent-separated ion pair due to the interface. Rate constants were calculated using the PMFs shown in Figure 4 and TST. These rate constants are a similar, albeit slightly lower, compared with the bulk rate constant value (0.28 ps<sup>-1</sup>) calculated for the polarizable model. This is consistent with our finding that polarizable models yielded faster dynamics. Of significant interest is the finding that the interface has slightly faster dissociation dynamics than the bulk for the nonpolarizable model, which is in sharp contrast with our finding for the polarizable model. For the polarizable model, the rate constant was four times higher in the bulk than at the interface, which is consistent with the much higher barrier for NaCl dissociation at the interface when compared to the barrier height in the bulk. The transmission coefficients were computed for the nonpolarizable model in the bulk and at the interface using both the RF method and GH theory. The computed values from both approaches are near 0.2, with the bulk and interfacial values nearly identical after 2 ps. Again, this is in contrast to the results from use of the polarizable model, which had a much higher transmission coefficient at the interface than in the bulk, indicating a different dissociation mechanism.

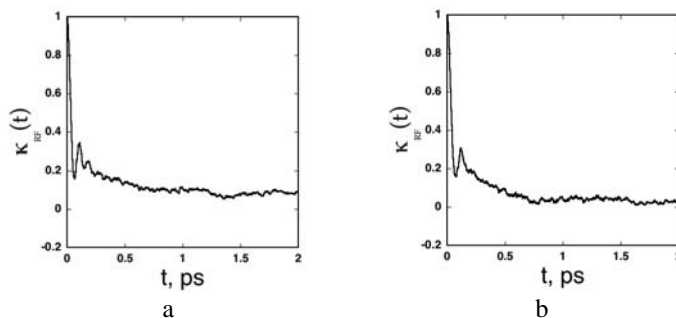
## C. Kinetics of ion pairing in liquid ethylene carbonate

We continue our research effort on lithium ion battery (LIB) systems by presenting results for the kinetics of Li<sup>+</sup>-[BF<sub>4</sub>]/[PF<sub>6</sub>] ion pairs in liquid ethyl carbonate (EC). In future work, we will extend our study of these liquid EC systems to the graphite-EC solid-liquid interface. We start with PMFs for the Li<sup>+</sup>-[BF<sub>4</sub>]/[PF<sub>6</sub>] pair, and then continue with the rate theory results determined using the RF and GH methods. We end this section with a comparison of results obtained using the different rate theory methods. In Figures 5a and 5b, we present PMF plots as a function of center-of-mass separation between the two ions in liquid EC.



**Figures 5a and 5b.** Computed PMFs for  $\text{Li}^+[\text{BF}_4]/\text{Li}^+[\text{PF}_6]$  in EC at 330K.

We notice that the PMF for the ion pair containing  $[\text{BF}_4]$  as the anion has a deeper contact ion pair minimum compared to the corresponding  $[\text{PF}_6]$ -based LIB. This demonstrates that the anion with a small (spherical) shape is more strongly associated with the  $\text{Li}^+$  in EC. The free energy barriers for the ion pair dissociation are found to be about  $-3.4$  and  $-1.7$  kcal/mol for  $\text{Li}^+[\text{BF}_4]$  and  $\text{Li}^+[\text{PF}_6]$ , respectively. Correspondingly, the computed rate constants from the PMFs using TST are determined to be  $5.4 \times 10^{-2}$  and  $4.6 \times 10^{-1}$ . These results clearly indicate that a free energy difference of 1.7 kcal/mol can have a noticeable effect on the rate constants. In addition, we also see that there is no well-defined solvent-separated ion pair as routinely observed for ion pairs in non-aqueous solutions. The reason for this is probably the absence of strong preferred interactions between ion-solvent and solvent-solvent systems. We computed time-dependent  $\kappa(t)$  for both ion pairs using the RF method as shown in Figures 6a and 6b.



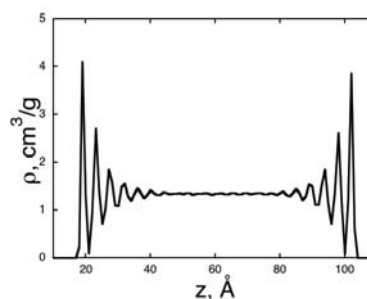
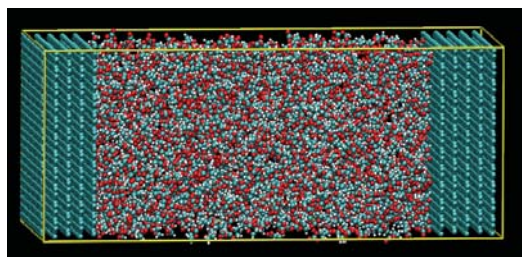
**Figures 6a and 6b.** Computed time-dependent transmission coefficients,  $\kappa(t)$ , for  $\text{Li}^+[\text{BF}_4]$ , (b) for  $\text{Li}^+[\text{PF}_6]$  in EC using the RF method.

The transmission coefficients, estimated as outlined above are  $8.4 \times 10^{-2}$  and  $2.5 \times 10^{-2}$ , respectively. The results are consistent with the computed PMFs, and we observed that the rate constants decrease from  $\text{Li}^+[\text{BF}_4]$  to  $\text{Li}^+[\text{PF}_6]$ . Our results show that anion type, in addition to affecting the free energy of solvation into EC, also should significantly influence the kinetics of ion pairing. The persistence of the ion pair can have important consequence on the dynamical properties of the ions and, thus, affect the ionic conductivity as observed in previous studies.

### Future Plans

Much effort has been put into LIB system development for electric vehicles, plug-in hybrid electrical vehicles, and other electrical system applications. During LIB operation, a solid electrolyte interphase (SEI) layer forms on the typical graphite anode surface. This SEI is the result of side reactions with the electrolyte solvent and salt. It is accepted that the SEI layer is essential to the performance of LIBs, and it has an impact on initial capacity loss, self-discharge characteristics, cycle life, rate capability, and safety. While the presence of the anode SEI layer is vital, its formation and growth is difficult to control because the chemical composition, morphology, and stability depend on several factors. Such as the type of graphite used, graphite morphology, electrolyte composition, electrochemical conditions, and cell temperature. Thus, SEI layer formation and electrochemical stability over long-term operation should be a primary topic of investigation in further development of LIB technology. Our goal is to develop/apply rate theory methods to study solvation of  $\text{Li}^+(\text{aq})$  and  $\text{Li}^+$ -ion pairings at the graphite-EC solid/liquid interface.

Following is a snapshot produced from a molecular dynamics study of the graphite-EC solid-liquid interface at 330K. Note that the EC molecules near the interface are less mobile, while molecules at the center have the density of the bulk liquid.



### References to publications of U.S. Department of Energy-sponsored research (2016 to the present)

1. **Liem X. Dang** and Gregory K. Schenter, Solvent Exchange in Liquid Methanol and Rate Theory. *Chemical Physics Letters*, 643, 142 (2016). Frontiers Article, Invited.
2. Computer Simulation of Methanol Exchange Dynamics around Cations and Anions. Santanu Roy and **Liem X. Dang**, *J. Phys. Chem. B*, 2016, 120, 1440-1445.
3. Quantifying Dimer and Trimer Formation by Tri-n-butyl Phosphates in n-Dodecane: Molecular Dynamics Simulations. Quynh N. Vo, **Liem X. Dang**, Mikael Nilsson, and Hung D. Nguyen, *J. Phys. Chem. B*, 2016, 120 6985–6994.
4. Rate Theory of Solvent Exchange and Kinetics of  $\text{Li}^+ - \text{BF}_4^- / \text{PF}_6^-$  Ion Pairs in Acetonitrile. **Liem X. Dang** and Tsun-Mei Chang, *J. Chem. Phys.* 145, 094502 (2016).
5. Unexpected Inhibition of  $\text{CO}_2$  Gas Hydrate Formation in Dilute TBAB Solutions and the Critical Role of Interfacial Water Structure. Ngoc N. Nguyen, Anh V. Nguyen, Khoi T. Nguyen, Llew Rintoul, **Liem X. Dang**, *Fuel* 185 (2016) 517–523.
6. The inhibition of methane hydrate formation by water alignment underneath surface adsorption of surfactants. Nguyen, Ngoc N., Nguyen, Anh V. and **Liem X. Dang** *FUEL* 197, 488-496 (2017).
7. Rate Theory of Ion Pairing at the Water Liquid-Vapor Interface. **Liem X. Dang**, Gregory K. Schenter, and Collin D. Wick, *J. Phys. Chem. C* 12, 10018-10026 (2017).
8. Rate Theory on Water Exchange in Aqueous Uranyl Ion. **Liem X. Dang**, Vo N. Quynh, Mikael Nilsson, Nguyen, Hung D. *Chemical Physics Letters*, 671, 58-62 (2017).
9. Interfacial Gas Enrichment at Hydrophobic Surfaces and the Origin of Promotion of Gas Hydrate Formation by Hydrophobic Solid Particles. Ngoc N. Nguyen, Anh V. Nguyen, Karen M. Steel, **Liem X. Dang** and Mirza Galib, *J. Phys. Chem. C* 121, 3830-3840 (2017).
10.  $\text{Li}^+$  Solvation and Kinetics of  $\text{Li}^+ - \text{BF}_4^- / \text{PF}_6^-$  Ion Pairs in Ethylene Carbonate. A Molecular Dynamics Study with Classical Rate Theories. Tun-Mei Chang and **Liem X. Dang**. *J. Chem. Phys* 147, 161709 (2017). (Invited)

## Nanoporous Materials and Ionic Liquids: Dynamics, Structure, and Interactions

Michael D. Fayer

Department of Chemistry, Stanford University, Stanford, CA 94305-5080

[fayer@stanford.edu](mailto:fayer@stanford.edu)

This program is investigating the dynamics, interactions, and structures of nanoporous materials, ionic liquids, and related systems. We are interested in the fundamental properties of these systems and in materials that are important in energy applications, e.g., fuel cell membranes and CO<sub>2</sub> capture. The methods that are being employed are ultrafast 2D IR spectroscopy using both a broad bandwidth system and a pulse shaping system that can perform experiments on highly scattering samples, IR polarization selective pump-probe experiments (PSPP), fast time resolved fluorescence and fluorescence depolarization experiments, and optical heterodyne detected optical Kerr effect (OHD-OKE) experiments.

Room temperature ionic liquids (RTILs), as the name implies, are ionic liquids that are liquid at and below room temperature. They are generally composed of complex cations and anions. Because the nature of the ions, crystallization does not occur at room temperature. RTILs are being considered for or used in a wide variety of applications. They generally have mesoscopic structure that consists of ionic regions and apolar organic regions. Because they are made up of nominally organic cations and anions, there are a vast number of combinations of the ions that yield a wide range of properties that are not found in non-ionic organic liquids. The influence of different types of solutes, different anions, cations, and alkyl chain lengths are being studied. One solute of particular interest is CO<sub>2</sub>. We have studied CO<sub>2</sub> in bulk RTILs, and we have now extended these studies to supported ionic liquid membranes (SILM), which are being developed for applications in CO<sub>2</sub> capture. The membranes are composed of polymers (PES – polyethersulfone) and are porous materials that are available with a variety of pore sizes. An important question is how does confinement in the nanopores of the membranes change the RTIL properties from those of the bulk liquid? We have performed 2D IR and PPSP experiments on CO<sub>2</sub> and SeCN<sup>-</sup> in EmimNTf<sub>2</sub> (1-ethyl-3-methylimidazolium bis(trifluoromethylsulfonyl)imide). The detailed studies of these two solutes in the bulk liquid and the SILMs showed that the RTIL structural dynamics slowed substantially in the membrane pores. The truly remarkable feature of the studies is that the pores are very large, on average ~350 nm. Generally liquids in nanoconfined systems display bulk properties once the diameter is >10 nm. We proposed that the polymer interface, because of the sulfone moieties, is attractive to cations, which changes the charge ordering that is normally found in the bulk ionic liquid. Because of long range Columbic interactions, the change in charge ordering at the interface persists for long distances, >100 nm, with the result that the structure and dynamics are different in the pores than in the bulk liquid. These results have important implications for use of SILMs in CO<sub>2</sub> capture.

Most RTILs are very hygroscopic. In applications it is frequently difficult to eliminate water from the RTIL. We have studied the influence of water as well as solutes, particularly Li<sup>+</sup>, on the dynamics of RTILs. We have studied these effects as a function of RTILs in which the cations have increasing alkyl chain lengths. Water and ions will locate in the ionic regions of RTILs. Using the ultrafast IR methods and vibrational probes that reside in the ionic regions, we studied the effects of water and Li<sup>+</sup> vs. chain length on RTIL dynamics associated with the ionic regions. We also compared measurements on a small anionic vibrational probe and a vibrational probe that was synthetically attached to the cation. The large cation probe experienced different dynamics than the small anion. To understand how water concentration and chain length influence dynamics and structure in the alkyl apolar regions of RTILs, we used a non-polar fluorescent probe that locates in the apolar regions, to perform fast fluorescence depolarization experiments. From the measurements we obtained friction coefficients as a function of water content and chain length. The friction coefficients are very sensitive to changes in the alkyl chain packing structure. We also studied bulk RTILs as a function of chain length and water content with OHD-OKE experiments. These are non-resonant experiments that provide information on the dynamics of the bulk liquids without the need to introduce a probe molecule. These experiments were very useful

for comparing dynamics that a probe molecule located in a particular region of the RTIL experiences to the total dynamics of the RTIL.

Proton transfer in the nanoscopic water channels of polyelectrolyte fuel cell membranes was studied using a photoacid, 8-hydroxypyrene-1,3,6-trisulfonic acid sodium salt (HPTS) put into the channels. The local environment of the probe was determined using 8-methoxypyrene-1,3,6-trisulfonic acid sodium salt (MPTS), which is not a photoacid. Three fully hydrated membranes, Nafion (DuPont) and two 3M membranes, were studied to determine the impact of different pendant chains and equivalent weights on proton transfer. Fluorescence anisotropy and excited state population decay data that characterized the local environment of the fluorescent probes and proton transfer dynamics were measured. The MPTS lifetime and anisotropy results show that most of the fluorescent probes have a bulk-like water environment with a relatively small fraction interacting with the channel wall. Measurements of the HPTS protonated and deprotonated fluorescent bands' population decays provided information on the proton transport dynamics. The decay of the protonated band from  $\sim 0.5$  ns to tens of ns is in part determined by dissociation, proton migration, and recombination with the HPTS, providing information on the ability of protons to move in the channels. The dissociation and recombination is manifested as a power law component in the protonated band fluorescence decay. The results show that equivalent weight differences between two 3M membranes resulted in a small difference in proton transfer. However, differences in pendant chain structure did significantly influence the proton transfer ability, with the 3M membranes displaying more facile transfer than Nafion.

Functionalized self-assembled monolayers (SAMs) are the focus of many ongoing investigations because they can be chemically tuned to control their structure and dynamics for a wide variety of applications, including electrochemistry, catalysis, and as models of biological interfaces. We developed the method and performed reflection two dimensional infrared vibrational echo spectroscopy (R-2D IR) and molecular dynamics simulations to determine the relationship between the structures of functionalized alkanethiol SAMs on gold surfaces and their underlying molecular motions on timescales of tens to hundreds of picoseconds. The simulations were performed in collaboration with my colleague Professor Thomas Markland. The alkyl chains were functionalized with a metal carbonyl head group, and a carbonyl stretching mode was used as the vibrational probe. These were the first 2D IR experiment to be performed in reflection; it was determined that the signal is sensitive to the angles of IR beams relative to the gold substrate and that there is a best angle. Two head group densities with the same overall chain densities were studied. We found that at the higher head group density, the monolayers have more disorder in the alkyl chain packing and faster dynamics. The dynamics of alkanethiol SAMs on gold are much slower than the dynamics of alkylsiloxane SAMs on silica. The simulations were in very good agreement with the data and allowed us to identify the nature of changes in structure and dynamics with the head group density. The simulations also enabled identification of important chain motions that contributed to the observed dynamics. For example trans-gauche isomerization on a chain caused surrounding chains to reconfigure.

We also performed a number of other 2D IR and PSPP studied. For the first time, we made direct measurement of the dynamics of waters of hydration in two minerals. These were literally 2D IR of rocks and required a new method to eliminate the deleterious effects of extreme scattered light from the powdered rocks. We performed studies of the dynamics of the small anion  $\text{SeCN}^-$  in bulk water and observed spectral diffusion, which was virtually identical to our previous studies of the dynamics of bulk water in which the OD stretch of dilute HOD in  $\text{H}_2\text{O}$  was studied. Detailed MD simulations with Professor Ward Thompson, University of Kansas, showed that the  $\text{SeCN}^-$  spectral diffusion was caused by the water hydrogen bond dynamics like the OD stretch in water. We examined the dynamics of water in reverse micelles in a thin layer near but not at the interface by studying  $\text{SeCN}^-$ . The reverse micelles were sufficiently large that they had a bulk water core in which the  $\text{SeCN}^-$  displayed bulk water dynamics. The dynamics of the anions on the interface were also observed. We were able to observe

dynamics that were neither bulk nor interfacial. We also did two important combined theoretical and experimental studies that are important for applying and interpreting 2D IR experiments.

The research will continue to address a range of problems. We are investigating different RTILs in the SILMs. We will study the effect of the alkyl chain length on dynamics in the membrane pores compared to the bulk liquids to gain understanding of the long distance influence of the interface on dynamics. In applications of SILMs for CO<sub>2</sub> capture, the RTIL will be saturated with water. Although at saturation, the concentration of water is not large, water has a large influence on viscosity and dynamics. We will investigate how water influences the bulk RTIL dynamics vs. in the pores. The dynamics of protic RTILs in the bulk and in SLIMs will be compared to the equivalent aprotic RTILs. We used photoacids to investigate proton transport in the nanochannels of three types of fuel cell membranes. We are now examining the behavior of water in the nanochannels using 2D IR and PSPP experiments to relate differences in proton transport to differences in H-bond dynamics. We are also extending our studies of proton transport to non-aqueous solvents. Our studies of SeCN<sup>-</sup> in bulk water and the associated simulations show that this anion can be used to probe water dynamics. We are using this probe, with its long vibrational lifetime, to study the dynamics of water in different size pores of nanoporous SiO<sub>2</sub>. The SiO<sub>2</sub> particles scatter a great deal of light. The experiments are made possible by our advances in using pulse shaping methods to reduce the effects of scattered light on the ultrafast IR experiments.

## Publications

### Room Temperature Ionic Liquids

1. “Coupling of Carbon Dioxide Stretch and Bend Vibrations Reveals Thermal Population Dynamics in an Ionic Liquid,” Chiara H. Giammanco, Patrick L. Kramer, Steven A. Yamada, Jun Nishida, Amr Tamimi, and Michael D. Fayer *J. Phys. Chem. B* 120, 549-556 (2016).
2. “Carbon Dioxide in an Ionic Liquid: Structural and Rotational Dynamics,” Chiara H. Giammanco, Patrick L. Kramer, Steven A. Yamada, Jun Nishida, Amr Tamimi, and Michael D. Fayer *J. Phys. Chem. B* 144, 104506 (2016).
3. “Ionic Liquid Dynamics Measured with 2D IR and IR Pump-probe Experiments on a Linear Anion and the Influence of Potassium Cations,” Amr Tamimi and Michael D. Fayer *J. Phys. Chem. B* 120, 5842-5854 (2016).
4. “Structural and rotational dynamics of carbon dioxide in 1-alkyl-3-methylimidazolium bis(trifluoromethylsulfonyl)imide ionic liquids: The effect of chain length,” Chiara H. Giammanco, Steven A. Yamada, Patrick L. Kramer, Amr Tamimi, and Michael D. Fayer *J. Phys. Chem. B* 120, 6698-6711 (2016).
5. “Ionic Liquid vs. Li<sup>+</sup> Aqueous Solutions - Water Dynamics near Bistriflimide Anions,” Chiara H. Giammanco, Patrick L. Kramer, and Michael D. Fayer *J. Phys. Chem. B* 120, 9997-10009 (2016).
6. “The Influence of Water on the Alkyl Region Structure in Variable Chain Length Imidazolium-Based Ionic Liquid/Water Mixtures,” Joseph E. Thomaz, Christian M. Lawler, and Michael D. Fayer *J. Phys. Chem. B* 120, 10350-10357 (2016).
7. “Water Dynamics in 1-Alkyl-3-Methylimidazolium Tetrafluoroborate Ionic Liquids,” Chiara H. Giammanco, Patrick L. Kramer, Daryl B. Wong, and Michael D. Fayer *J. Phys. Chem. B* 120, 11523-11538 (2016).

8. “Dynamics in a Room Temperature Ionic Liquid from the Cation Perspective: 2D IR Vibrational Echo Spectroscopy,” Steven A. Yamada, Heather E. Bailey, Amr Tamimi, Chunya Li, and Michael D. Fayer J. Am. Chem. Soc. 139, 2408-2420 (2017).

### **Nanoconfined Systems and Water Dynamics**

9. “Unraveling the dynamics and structure of self-assembled monolayers on gold using reflection 2D IR spectroscopy and molecular dynamics simulations,” Chang Yan, Rongfeng Yuan, William C. Pfalzgraff, Jun Nishida, Lu Wang, Thomas E. Markland, and Michael D. Fayer Proc. Nat. Ac. Sci. 113, 4929-4934 (2016).

10. “Water of Hydration Dynamics in the Minerals Gypsum and Bassanite: Ultrafast 2D IR Spectroscopy of Rocks,” Chang Yan, Jun Nishida, Rongfeng Yuan, and Michael D. Fayer J. Am. Chem. Soc. 138, 9694-9703 (2016).

11. “Dynamics of a Room Temperature Ionic Liquid in Supported Ionic Liquid Membranes vs. the Bulk Liquid: 2D IR and Polarized IR Pump-Probe Experiments,” Jae Yoon Shin, Steven A. Yamada, and Michael D. Fayer J. Am. Chem. Soc. 139, 311-323 (2017).

12. “Dynamics in a Water Interfacial Boundary Layer Investigated with IR Polarization Selective Pump-probe Experiments,” Rongfeng Yuan, Chang Yan, Jun Nishida, Michael D. Fayer J. Phys. Chem. B 121, 4530-4537 (2017)

13. “Proton Transfer in Perfluorosulfonic Acid Fuel Cell Membranes with Differing Pendant Chains and Equivalent Weights,” Joseph E. Thomaz, Christian M. Lawler, and Michael D. Fayer J. Phys. Chem. B 121, 4544-4553 (2017).

14. “Carbon Dioxide in a Supported Ionic Liquid Membrane: Structural and Rotational Dynamics Measured with 2D IR and Pump-Probe Experiments,” Jae Yoon Shin, Steven A. Yamada, and Michael D. Fayer J. Am. Chem. Soc. 139, 11222-11232 (2017).

15. “Molecular Anion Hydrogen Bonding Dynamics in Aqueous Solution,” Rongfeng Yuan, Chang Yan, Amr Tamimi, and Michael D. Fayer J. Phys. Chem. B 119, 13407-13415 (2015).

16. “Water-Anion Hydrogen Bonding Dynamics: Ultrafast IR Experiments and Simulations,” Steven A. Yamada, Ward H. Thompson, and Michael D. Fayer J. Chem. Phys. 146, 234501 (2017).

### **Method Development**

17. “Separation of Experimental 2D IR Frequency-Frequency Correlation Functions into Structural and Reorientation-induced Contributions,” Patrick L. Kramer, Jun Nishida, and Michael D. Fayer J. Chem. Phys. 143, 124505 (2015).

18. “The Quasi-Rotating Frame: accurate line shape determination with increased efficiency in non-collinear 2D optical spectroscopy,” Patrick L. Kramer, Chiara H. Giammanco, Amr Tamimi, David J. Hoffman, Kathleen P. Sokolowsky, and Michael D. Fayer J. Opt. Soc. Am. B 33, 1143-1156 (2016).

DOE-BES CPIMS  
Condensed Phase and Interfacial Molecular Science  
PI Miriam A. Freedman  
The Pennsylvania State University  
Department of Chemistry  
104 Chemistry Building  
University Park, PA 16802  
maf43@psu.edu

## Program Scope

***Size Dependence of Liquid-Liquid Phase Separation in Aerosol Particles:*** The central goal of this proposal is to construct experimental phase diagrams for submicron organic aerosol particles composed of organic compounds, salts, and water. In particular, some organic aerosol particles undergo liquid-liquid phase separation due to the limited solubility of the organic component in the salt solution. My research group has determined for several model systems that this phase transition is inhibited for particles  $< 40$  nm [1, 2]. This inhibition stems from a finite size effect where small particles cannot overcome the activation barrier needed to form a new phase [2, 3]. We have shown that the absence of this phase transition has an effect on the ability of these particles to form cloud droplets. For aerosol-resolved atmospheric models, we need to determine the relative humidity at which this phase transition takes place for sizes of particles where the phase transition is not inhibited. Determining this transition relative humidity for different systems and compositions, as well as the location of the critical point where the binodal and spinodal curves meet, will allow us to construct experimental phase diagrams. In addition, we plan to extend this work from organic aerosol systems to polymer mixtures to determine the extent to which our results can be extended into a field of interest to materials chemists.

[1] D. P. Veghte, M. B. Altaf, M. A. Freedman, *J. Am. Chem. Soc.* 135, 16046 (2013).

[2] M. B. Altaf, M. A. Freedman, *J. Phys. Chem. Lett.* 8, 3613 (2017).

[3] M. B. Altaf, A. Zuend, M. A. Freedman, *Chem. Commun.* 52, 9220 (2016).

## Recent Progress

Our recent work has focused on determining the origins for the size dependent morphology as well as demonstrating its application to atmospheric processes, as briefly discussed in the previous section.

In our first studies under this DOE grant, we have explored several fundamental aspects of the liquid-liquid phase separation process:

1) We have explored the role of low pH on liquid-liquid phase separation in supermicron particles. We have previously shown that in systems consisting of 3-methylglutaric acid, ammonium sulfate, sodium hydroxide, and water (pH 3 – 6), deprotonation of the organic acid shifts the relative humidity at which phase separation takes place (separation relative humidity, SRH) to lower values. This result stems from the increased solubility of the deprotonated organic acid in the salt solution [4]. Most organic aerosol particles, however, are predicted to have pH values ranging from 0.5 – 3. We have therefore explored multiple systems consisting of one organic compound, ammonium sulfate, sulfuric acid, and water (pH

0.3 - 5). As the particles become more acidic, SRH decreases because the ammonium sulfate is transformed to letovicite (intermediate pH) and ammonium bisulfate (low pH). These salts are not as efficient toward salting out the organic component as ammonium sulfate, which results in the lower values of SRH.

2) We have built a system to flash-freeze submicron aqueous aerosol particles. Our previous results for submicron particles were performed on particles that were dried in the gas phase to < 2 % relative humidity and analyzed by cryo-transmission electron microscopy (cryo-TEM) and complementary spectroscopies. This method allows us to track morphology, but not to determine SRH, which is necessary for construction of phase diagrams. The flash-freeze system will allow us to track morphology using cryo-TEM as a function of the relative humidity. We will therefore be able to determine SRH for submicron particles.

3) We have begun to explore particles composed of the polymers poly(ethylene glycol) and dextran. Our preliminary results show a size dependent morphology of this system, and we are beginning to explore the available parameter space.

[4] D. J. Losey, R. G. Parker, M. A. Freedman, *J. Phys. Chem. Lett.*, 7, 3865 (2016).

### **Future Plans**

In the first year of this DOE grant, our goals are:

1) To finish our study of the SRH of low pH aerosol particles.

2) To validate our flash-freeze system for the study of the morphology of submicron aerosol particles. After validation, we will apply this technique to model systems that are well-studied in my research laboratory to determine SRH for these systems, and particularly, how the submicron SRH differs from predictions for supermicron (bulk) systems. In addition, we will apply this technique to systems that are closer proxies for atmospheric aerosol such as those containing secondary organic material.

3) To continue to explore the phase separation behavior of aerosol particles consisting of poly(ethylene glycol) and dextran. We plan to map out the available parameter space for this system.

### **Publications**

None (Grant start date: 09/01/2017)

## Chemical Kinetics and Dynamics at Interfaces

### *Fundamentals of Solvation under Extreme Conditions*

**John L. Fulton**

Physical Sciences Division  
Pacific Northwest National Laboratory  
902 Battelle Blvd., Mail Stop K2-57  
Richland, WA 99354  
[john.fulton@pnl.gov](mailto:john.fulton@pnl.gov)

Collaborators: G. K. Schenter, C. J. Mundy, N. Govind, M. Galib.

### **Program Scope**

The primary objective of this project is to describe, on a molecular level, the solvent/solute structure and dynamics in fluids such as water under extremely non-ideal conditions. The scope of studies includes solute–solvent interactions, clustering, ion-pair formation, and hydrogen bonding occurring under extremes of temperature, concentration and pH. The effort entails the use of spectroscopic techniques such as x-ray absorption fine structure (XAFS) spectroscopy, high-energy x-ray scattering, coupled with theoretical methods such as molecular dynamics (MD-XAFS), and electronic structure calculations in order to test and refine structural models of these systems. In total, these methods allow for a comprehensive assessment of solvation and the chemical state of an ion or solute under any condition. The research is answering major scientific questions in areas related to energy, environmental and biological processes including specific areas of relevance to DOE such as mixed hazardous waste processing, power plant chemistry, and geologic carbon dioxide sequestration. This program provides the structural information that is the scientific basis for the chemical thermodynamic data and models in these systems under non-ideal conditions.

### **Recent Progress**

*The structure of carbonate and bicarbonate pairing with  $\text{Ca}^{2+}$ .* The interaction of anions with cations in aqueous solutions underlies broad areas in separations, catalysis, geochemistry and biochemistry. There is a decades-old problem regarding the question of ion pairing of carbonate,  $\text{CO}_3^-$ , with  $\text{Ca}^{2+}$ . At the core of this debate is the question about whether the calcium carbonate nucleation process at the phase boundary follows classical models involving only ion pair species or proceeds via a more specialized pathway involving “pre-nucleation” clusters or nano-clusters.

Many different experimental techniques (titration, x-ray scattering, centrifugation, TEM, etc.) have been used to probe the  $\text{Ca}^{2+}$  structure in the region near the phase transition. The challenge of these methods for the  $\text{CaCO}_3$  system is the very low concentration at the phase transition ( $\sim 10^{-4}$  M  $\text{Ca}^{2+}$ ). In addition, these methods primarily probe only changes in the macroscopic properties making it difficult to relate these changes to the local molecular structure about  $\text{Ca}^{2+}$  at these low concentrations. There is a unique advantage of Ca XANES since it is an element-specific method that directly probes the local molecular structure about the  $\text{Ca}^{2+}$  and readily lends itself to in situ measurements. Further, the advent of a new generation of undulator beamlines has enabled, for the first time, measurements with high sensitivity at these very low concentrations. For aqueous  $\text{Ca}^{2+}$ , the XANES spectra are exquisitely sensitive to the local

structure of both water and anions in the regions of the first *and* second solvent shells about the Ca absorber. From a series of Ca XANES measurements taken near the phase boundary, we have been able to show conclusively that this system follows classical nucleation theory.

Figure 1 compares the experimental Ca XANES spectra with the calculated spectra generated using the processing steps of 1) generating the DFT-based potential of mean force (PMF) between  $\text{CO}_3^-$ , with  $\text{Ca}^{2+}$ , 2) calculating the relative distribution of ion pair species, and 3) then creating the species-average TDDFT XANES spectrum. It was not known if  $\text{Ca}^{2+}$  forms either monodentate or bidentate contact ion pairs (CIP) or solvent-shared ion pairs (SSIP) with  $\text{CO}_3^-$ . Thus the DFT-based PMFs were used to calculate this ion-pair equilibrium with free  $\text{Ca}^{2+}$  (as shown in Figure 1 for pH 9.75). As a test of the validity of this XANES modeling strategy we applied this method to a set of three solid-phase crystalline standards, and found that the calculated and experimental spectra were in good agreement.

As expected, the perturbation of the aqueous  $\text{Ca}^{2+}$  structure due to the presence of the anion in the first or second solvation shells alters the spectra. Most notably, the monodentate carbonate configuration leads to significant deviations in the edge region that are likely due to its larger

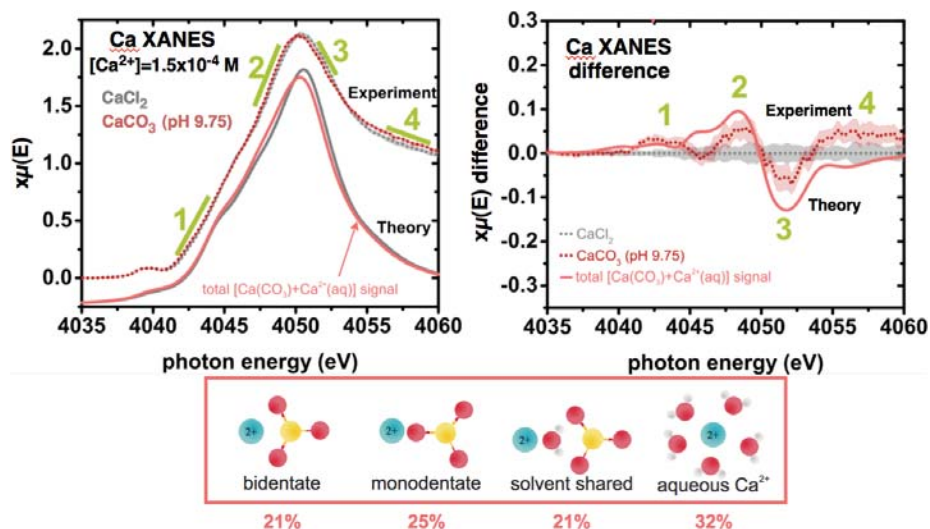


Figure 1. Experimental and theoretical (TDDFT-MD) XANES spectra for aqueous  $10^{-4} \text{ M Ca}^+$  (left) at pH 9.75. The difference spectra (right) represents the deviation due to the ion pair association with respect to that from the fully hydrated  $\text{Ca}^{2+}$ . The percentage distribution (lower) of three different ion pair species derived from the DFT potential of mean force. This distribution was used to calculate the theory XANES spectra.

impact on the water orientations in the first and second shells. The predicted difference spectrum (Fig. 1, right) shows exceptional agreement with both the position of the experimental spectral features and their amplitudes. The near-quantitative agreement between the calculated and experimental spectra strongly supports the conclusion that the solution structure is dominated by this ion-pair distribution near the liquid-liquid phase boundary. The overall picture from a combination of experimental XANES data, the classical solution thermodynamics and TDDFT theory shows that the existence of ion pair species is consistent with a classical model of nucleation for this system.

**DFT water hydrates  $\text{Na}^+$  differently.** We have previously shown that DFT-based simulations predict the structure of pure water with a fidelity that meets or exceeds the very best empirical models.<sup>5</sup> These DFT-based simulations also accurately predict the water structural response to significant changes in pressure (density) and temperature.<sup>5</sup> There is however a difficulty using

the same DFT models for predicting the hydrated structure of monovalent cations. The Na-water structure from the DFT simulation is too disordered and at a substantially longer Na-O distance than the experimental value<sup>6</sup> while the classical potential reasonably captures this structure derived from x-ray scattering experiments. One hypothesis is that the Na<sup>+</sup>/water dispersion treatment has been incorrectly parameterized within the DFT-Grimme treatment. We find further problems regarding structure in that both DFT- and classical-potentials do not quantitatively reproduce the experimental XANES spectrum (Figure 2a).

A quantitative evaluation of the Na<sup>+</sup> XANES spectrum through the comparison of contributions from various structural classes (order parameters) provides new insights into the first and second water shell structure. By identifying various structural contributions to the XANES spectral features it is possible to find specific configurations that are more favorable. For instance we have evaluated the contributions of a) the coordination number in the first shell, b) the degree of octahedral symmetry, c) the number of first-shell hydrogen bonds, d) the water tilt angle, e) and the interstitial water between first and second shell (INT6). The parameter that most significantly affects the XANES spectrum, and thereby moves closer to the experiment, is this interstitial water parameter.

The interstitial waters are known to play a large role in the understanding of pure water structure, especially when the bulk symmetric structure is perturbed by solute or by applying pressure.<sup>5</sup> If water is seen as a predominately tetrahedral 4-coordinated network, the presence of interstitial

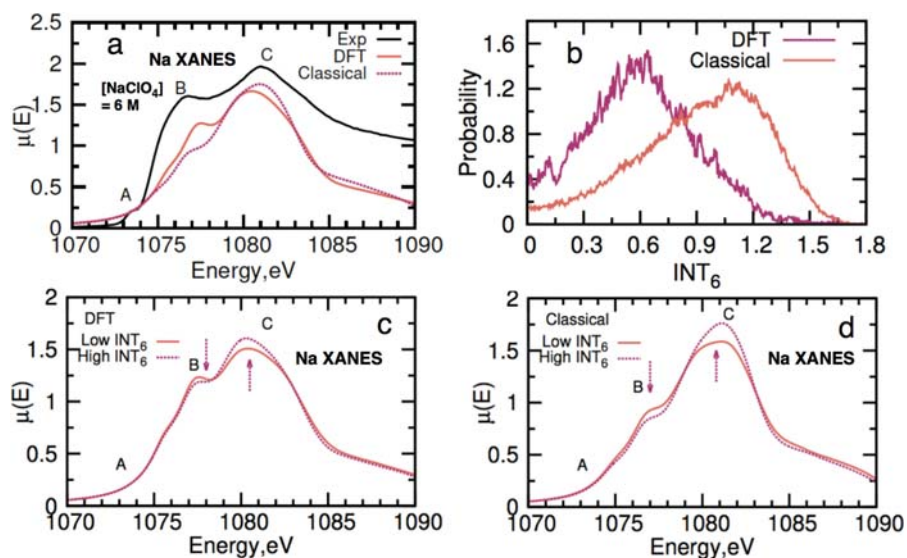


Figure 2. (a) Experimental XANES spectrum for Na<sup>+</sup> compared to TDDFT calculations for classical- and DFT-models that were generated from an ensemble average of 40 MD simulation snapshots, (b) the interstitial order parameter (INT6) for the 6<sup>th</sup> water hydrating Na<sup>+</sup>, (c,d) XANES spectra due to changes in the INT6 order parameter for DFT and classical models

waters can be used as a probe for the presence of defects in bulk water or, for instance, defects in the hydration structure about Na<sup>+</sup>. Figure 2b shows the probability distribution function for the 6<sup>th</sup>-water interstitial order parameters (INT6) for both the classical and DFT trajectories. An INT6 value of 0 indicates more interstitial water whereas a higher positive value indicates an empty region between the first and second solvation shell. As shown in Figure 2b, the DFT model has much more interstitial character while the classical model has mostly separated first

and second solvation shells. For both models, more interstitial water moves their XANES spectra closer to the experimental spectrum.

For classical waters, the ion-water interaction is quite strong producing a clear separation between the first and second shells. In contrast, DFT waters are less attracted to the ion separation producing more interstitial water. Since DFT potential has the luxury of having explicit electronic structure representation, we would expect that DFT describing of the interstitial water be more realistic. These results suggest that the true structure may lie between the two models while the results are helping to better define the deficiencies of DFT in this particular case.

### **Future Plans**

The objective is to gain a fundamental understanding of the molecular structure that provides the basis for understanding ion chemistry and dynamics. We propose exploring ion-water structure for systems in which the local structure has not yet been measured or the structure is not yet fully understood. Our goal is to identify the underlying structural factors that govern the macroscopic properties of ions that have so far eluded a comprehensive theoretical treatment. The proposed work also involves a comprehensive study of ion pairing in concentrated solutions and at high temperatures. The objective is to describe how the ion-pair structure is governed by a range of different types of solvent interactions.

### **References to publications of DOE sponsored research (2015 - present)**

1. Gregory K. Schenter, John L. Fulton, "Molecular Dynamics Simulations and XAFS (MD-XAFS)", In "XAFS Techniques for Catalysts, Nanomaterials, and Surfaces", Yasuhiro Iwasawa, Kiyotaka Asakura, and Mizuki Tada, editors, Springer, New York, Invited Book Chapter, 2017.
2. John C. Linehan, Mahalingam Balasubramanian, John L. Fulton, "Homogeneous catalysis: from metal atoms to small clusters", In "XAFS Techniques for Catalysts, Nanomaterials, and Surfaces", Yasuhiro Iwasawa, Kiyotaka Asakura, and Mizuki Tada, editors, Springer, New York, Invited Book Chapter, 2017.
3. "Electronic and Chemical State of Aluminum from the Single- (K) and Double-Electron Excitation ( $KL_{II\&III}$ ,  $KL_I$ ) X-ray Absorption Near-Edge Spectra of alpha-Alumina, Sodium Aluminate, Aqueous  $Al^{3+}\cdot(H_2O)_6$ , and Aqueous  $Al(OH)_4^-$ ", John L. Fulton, Niranjana Govind, Thomas Huthwelker, Eric J. Bylaska, Aleksei Vjunov, Sonia Pin, Tricia D. Smurthwaite, **J. Phys. Chem. B**, 119, 8380-8388, 2015.
4. "High-resolution Measurement of Contact Ion-pair Structures in Aqueous RbCl Solutions from the Simultaneous Corefinement of their Rb and Cl K-edge XAFS and XRD Spectra", Van-Thai Pham, John L. Fulton, **J. Solution Chem.**, 45, 1061-70, 2016.
5. "The structure of liquid water up to 360 MPa from x-ray diffraction measurements using a high Q-range and from molecular simulation", L. B. Skinner, M. Galib, J. L. Fulton, C. J. Mundy, J. B. Parise, V. -T. Pham, G. K. Schenter, C. J. Benmore, **J. Chem. Phys.**, 144, 134504, 2016.
6. "Revisiting the hydration structure of aqueous  $Na^+$ ", M. Galib, M. D. Baer, L. B. Skinner, C. J. Mundy, T. Huthwelker, G. K. Schenter, C. J. Benmore, N. Govind, J. L. Fulton, **J. Chem. Phys.** 146, 084504, 2017

# Probing Chromophore Energetics and Couplings for Singlet Fission in Solar Cell Applications

DE-FG02-13ER16393

Etienne Garand

Department of Chemistry, University of Wisconsin-Madison, Madison, WI 53706

[egarand@chem.wisc.edu](mailto:egarand@chem.wisc.edu)

## *Program scope*

Our studies aim to provide a molecular-level understanding of processes that can improve efficiencies of alternative sources of energy such as those found in dye-sensitized solar cells. In particular, the mechanisms and molecular requirements for efficient exciton multiplication through singlet fission will be explored using high-resolution anion photoelectron (PE) spectroscopy. To achieve this, we built an instrument capable of probing these chromophore systems, allowing us to study: (1) the evolution of the electronic structure as a function of cluster size to understand singlet fission in crystals; (2) the relationship between the nature of linkers and the electronic structure in covalently-bonded chromophore dimers; and (3) the differences, including exciton delocalization and the effects of solvent interactions, between the crystalline species and the isolated covalently-bonded dimers.

We will probe the electronic states of organic chromophores using PE spectroscopy of mass-selected anion precursors. Starting from the radical anion with a doublet ground state, all the low-lying singlet and triplet states of the neutral molecule that involve removal of a single electron can be accessed via one-photon photodetachment. Therefore, with the exception of the doubly excited state, all the electronic states relevant to singlet fission are accessible on equal footing in our experiments. To extract precise information about the electronic state energies and couplings, it is important to obtain well-resolved PE spectra. This can be achieved by using the slow electron velocity-map imaging (SEVI) technique, which combines velocity-map imaging (VMI) detection with tunable lasers to yield PE spectrum with sub-meV resolution. Comparisons of the different chromophore systems can reveal the electronic interactions responsible for the observed differences in their singlet fission efficiency. The results can also benchmark theoretical methods, a necessary step in applying rational design to integrate singlet fission into solar cells.

We will also explore the influences of solvent molecules by using a dual-ion-trap instrument that allows for temperature-controlled formation of solvated clusters in the first trap. Solvation can significantly perturb the geometry and electronic structures of a complex, altering, for example, the photophysics of a chromophore or proton-coupled-electron-transfer processes. These changes as a function of cluster size will be studied via vibrational predissociation as well as PE spectroscopy.

## Recent Progress

The experimental results discussed in this progress report are acquired using our home-built cryogenic ion SEVI apparatus, the details and performance capabilities of this instrument is published in a recently paper.[3]

Our SEVI instrument has a highly modular source region, capable of interfacing with an electrospray ionization (ESI) source, a heated oven expansion discharge source, and an Even-Lavie pulsed valve with hot filament ionizer. This built-in flexibility makes it easier for us to explore different means of producing the reactive and short-lived radical anion precursors. The anions, once formed, are cooled inside a quadrupole ion trap. This cooling allows for a better spectral resolution by narrowing the rotational profiles of the PE features. The cooled ions are gently extracted into a linear time-of-flight (TOF) mass spectrometer coupled to our newly designed multi-plate VMI. This VMI has a dual-lens design, with a series of forty evenly spaced electrodes extending the entire VMI region to provide a well-defined electric field environment. Photoelectrons, velocity focused by the VMI optics, are mapped onto a detector assembly providing both the conventional PE spectra via angular integration as well as anisotropy information on the individual vibronic transitions. Overall, our instrument is capable of maintaining a good VMI focus across a relatively large energy range, simplifying the data acquisition process.

We acquired the SEVI spectra of anthracene in two separate energy ranges, corresponding to the transition from the  ${}^2B_{3u}$  ground state of the radical anion to the  $S_0$  ( ${}^1A_g$ ) state and  $T_1$  ( ${}^3B_{1u}$ ) state of the neutral molecule and shown in Figure 1. Anthracene has a relatively low electron affinity (EA), observed at 0.532 eV, in agreement with previous experiments. Transition to the lowest triplet state provides the experimentally measured  $S_0$ - $T_1$  splitting of 1.870 eV.

The 0-0 transition is the strongest feature in the  $S_0$  state SEVI spectrum, but there are considerable vibrational activities observed, indicating some geometry changes upon removing the unpaired electron from the  $\pi$ -system. While most of the PE features can be assigned based on the FC simulation, there are a few features that are present in the experimental spectrum, but absent in the FC simulation. Most notable of these are the features near eBE = 5100  $\text{cm}^{-1}$ . The  $a_g$   $\nu_{10}$  vibration would appear at eBE = 5045  $\text{cm}^{-1}$ , accounting for one of the features. Its absence in the FC simulation points to possible errors in the calculated anion geometry. There is no  $a_g$

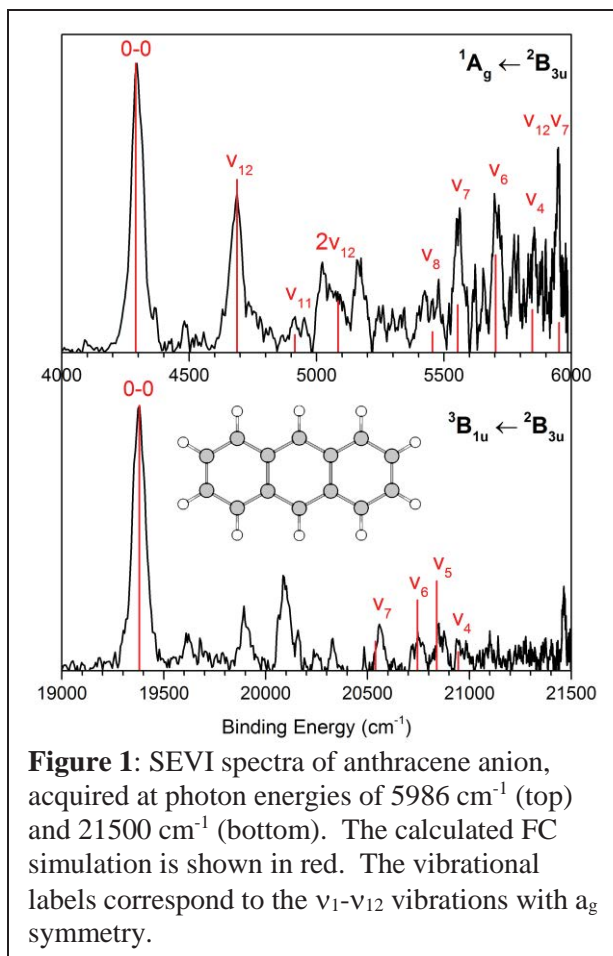


**Figure 1:** SEVI spectra of anthracene anion, acquired at photon energies of 5986  $\text{cm}^{-1}$  (top) and 21500  $\text{cm}^{-1}$  (bottom). The calculated FC simulation is shown in red. The vibrational labels correspond to the  $\nu_1$ - $\nu_{12}$  vibrations with  $a_g$  symmetry.

vibration, or combination bands, that can account for the feature at  $eBE = 5170 \text{ cm}^{-1}$ . This feature is most likely a vibration with  $b_{1u}$  symmetry, borrowing intensity from the optically bright  $S_1 \ ^1B_{1u}$  state, which lies  $\sim 3.4 \text{ eV}$  above  $S_0$ .

Similar to the  $S_0$  state, the SEVI spectrum of  $T_1$  state also shows the 0-0 transition as the most intense feature. However, the experimental spectrum here exhibits more deviation from the corresponding FC simulation. The feature at  $eBE = 20090 \text{ cm}^{-1}$  can possibly be accounted for by the  $a_g \nu_{10}$  vibration, which again has no calculated FC intensity. Alternatively, vibronic coupling on the  $T_1 \ (^3B_{1u})$  state, where the  $b_{1u}$  vibrations would have an  $a_g$  symmetry in the fully vibronically coupled picture, may account for the  $eBE = 20090 \text{ cm}^{-1}$  feature. In this case, the FC simulation would have minimal usefulness. There are additional complications in the triplet manifold. TD-DFT results indicate the  $T_2 \ (^3B_{2u})$  state is  $\sim 1 \text{ eV}$  above the  $T_1$  state and maybe provide intensities for  $b_{2u}$  symmetry modes, accounting for, for example,  $eBE = 19900 \text{ cm}^{-1}$  feature.

These experimental evidences for vibronic coupling are important for understanding the SF process. Already, the comparably simple anthracene monomer highlight the need to properly benchmark theoretical results, and establish a baseline for understanding the experimental spectra. The results for the similar fluoranthene molecule, shown in Figure 2, further demonstrate this need. This nominally  $C_{2v}$  molecule can be considered as a benzene bonded to a naphthalene, and serves as a simple example of covalently linked chromophore dimer, providing a contrast to the fully aromatic anthracene. It has a higher EA of  $0.756 \text{ eV}$ , with a larger singlet-triplet splitting of  $2.321 \text{ eV}$ . It is not yet clear whether the more extensive disagreement between calculation and experiment for the  $S_0$  state is due to inaccuracy in the anion calculation or vibronic coupling. There is a  $S_2 \ (^1A_1)$  state with a strong oscillator strength at  $\sim 4 \text{ eV}$  above  $S_0$  that may account for some of the discrepancies. Furthermore, the optimized geometry for the  $T_1$  state has a  $C_s$  symmetry, with the  $T_2$  state calculated to be only  $\sim 0.25 \text{ eV}$  above  $T_1$ , possibly causing an artificial symmetry breaking. Analysis here likely requires extrapolation of understandings from the anthracene molecule.

Together with the SEVI experiments, we also implemented a dual ion trap instrument that allows us to controllably form weakly bound clusters inside a liquid nitrogen cooled reaction

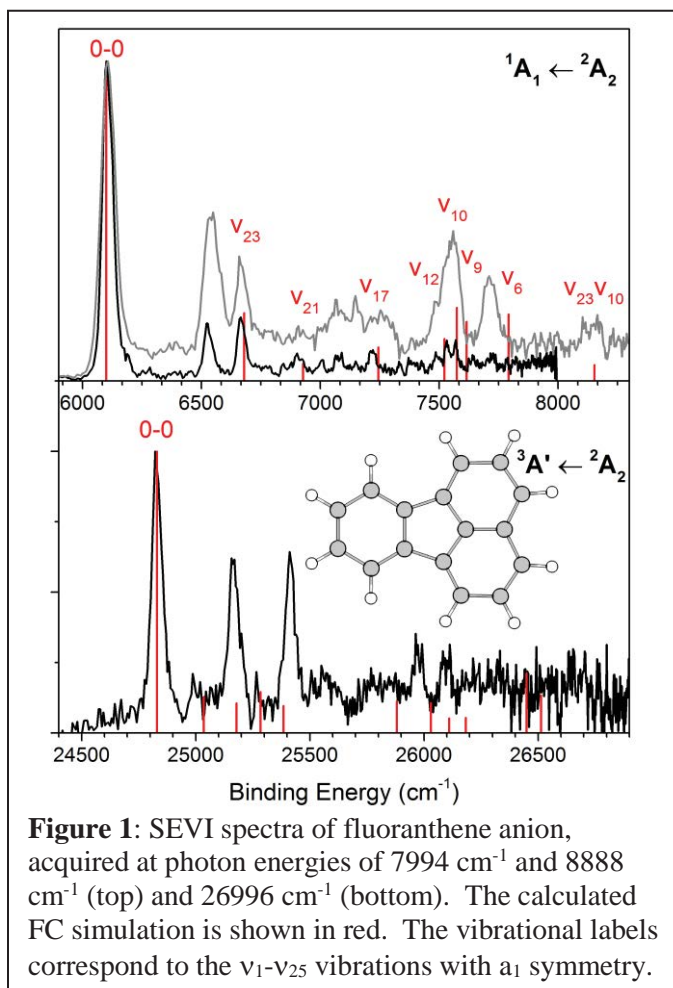


**Figure 1:** SEVI spectra of fluoranthene anion, acquired at photon energies of  $7994 \text{ cm}^{-1}$  and  $8888 \text{ cm}^{-1}$  (top) and  $26996 \text{ cm}^{-1}$  (bottom). The calculated FC simulation is shown in red. The vibrational labels correspond to the  $\nu_1$ - $\nu_{25}$  vibrations with  $a_1$  symmetry.

trap.[1, 2] Further temperature control of these clusters are possible inside the liquid helium quadrupole tagging trap. This two-stage trapping and cooling gives us the flexibility to generate different types of weakly bound clusters, while still maintaining the ability to cool the clusters for vibrational predissociation studies. This opens the path to study geometry and electronic structures of chromophore clusters as well as microsolvated chromophores.

We are currently using the capability of the dual-trap instrument to explore the dynamics of H/D exchange. When D<sub>2</sub>O is introduced at 300 K inside the reaction trap, we see extensive H/D exchange of the (Gly)<sub>4</sub>H<sup>+</sup> N-H and O-H protons. At 80 K, the results indicate there is insufficient energy to allow for H/D exchange during the ~10 ms residence time of the ion inside the trap, and we observe mainly the formation of (Gly)<sub>4</sub>H<sup>+</sup>(D<sub>2</sub>O)<sub>n</sub> clusters. A series of data spanning the 80-300 K temperature range allow us to directly probe the kinetics of the isotope exchange, providing experimental measures of the barriers. These studies will allow us to make use of selective isotope labeling to disentangle vibrational features in large solvated clusters.

With increasing cluster sizes, it is likely that multiple conformations are present even at 10 K. We have recently implement a novel two-laser isomer burning scheme to obtain isomer specific spectral signatures.[4] Our setup has one laser focused directly inside the 10 K tagging trap, while the other functions as a typical predissociation laser. This allows for both an isomer-burning scheme as well as an ion-dip scheme, providing flexibility for tackling different systems of interest. We applied our IR-IR ion-dip double resonance approach to disentangle the vibrational spectrum of Na<sup>+</sup>(glucose), revealing the presence of three  $\alpha$ -conformers and five  $\beta$ -conformers.

### ***Future Plans***

The SEVI data presented in this progress report are currently being prepared for publication. We will expand our studies to non-covalently bonded clusters, utilizing our dual-trap instrument, as well as covalently bonded dimers, to probe and compare the extend of electron delocalization and electronic state couplings in these chromophore systems. We will also continue the isotope exchange studies to determine the reaction barrier and elucidate the mechanism. Using the D<sub>2</sub>O clusters and conformer-specific double resonance spectroscopy, we will explore the structural changes induced by solvation in simple peptide systems. These results can serve to guide our studies on the solvated chromophores.

### ***Publications***

- 1) B.M. Marsh, J.M. Voss and E. Garand, *A dual cryogenic ion trap spectrometer for the formation and characterization of solvated ionic clusters*, **J. Chem. Phys.**, 143, 204201 (2015)
- 2) J. M. Voss, B. M. Marsh, J. Zhou and E. Garand, *Interaction between ionic liquid cation and water: Infrared predissociation study of [bmim]<sup>+</sup>·(H<sub>2</sub>O)<sub>n</sub> clusters*, **Phys. Chem. Chem. Phys.**, 18, 18905-18913 (2016)
- 3) S. J. Kregel, G. K. Thurston, J. Zhou and E. Garand, *A multi-plates velocity-map imaging design for high-resolution photoelectron spectroscopy*, **J. Chem. Phys.**, 147, 094201 (2017)
- 4) J. M. Voss, S. J. Kregel, K. C. Fischer, and E. Garand, *IR-IR conformation specific spectroscopy of Na<sup>+</sup>(glucose) adducts*, **J. Am. Soc. Mass. Spectrom.**, (Accepted)

## **Methods for addressing strongly heterogeneous and far-from-equilibrium systems**

Phillip L. Geissler (plgeissler@lbl.gov),  
Teresa Head-Gordon (thg@berkeley.edu), Kranthi Mandadapu (kkmandadapu@lbl.gov), and  
Kevin Wilson (krwilson@lbl.gov)

*Lawrence Berkeley National Laboratory, Chemical Sciences Division  
1 Cyclotron Road, Berkeley, CA 94720*

### **Program Scope**

A significant gap exists between basic studies of molecular chemical physics and the operation of real devices and natural systems. This effort comprises efforts to establish the chemical methods and insight that will enable understanding of systems that are profoundly complex in composition, heterogeneity, preparation, and organization.

Theoretical and computational aspects of this effort are advanced by Geissler, Head-Gordon, and Mandadapu. Their work aims to provide general techniques for addressing microscopic organization under conditions that profoundly challenge conventional approaches of simulation and analysis. Such behavior typically also presents formidable challenges for experimental measurement. Complementary method development in the laboratory is thus an important partner to these efforts.

Like theory, experimental advances are needed to develop novel ways for observing reactions in liquids and at their surfaces. In particular, liquids present a substantial challenge for detecting short lived reaction intermediates produced in thermal reactions. Furthermore, in many realistic systems, reactants reside both at the interface as well as the fully coordinated environment of the bulk solution. As laboratory work in other subtasks trends towards systems with slowly relaxing mesoscale disorder, we anticipate growth of the experimental component of this subtask aimed at developing new sample environments and approaches aimed at more robust connections to theory.

### **Recent Progress**

Mandadapu studies the nature of the glass transition in atomistic models of glass formers using cooling protocols at constant rates from a temperature above the onset of glassy dynamics to  $T = 0$  (Hudson et. al.). These non-equilibrium cooling protocols drive the supercooled liquids into a far-from-equilibrium frozen glassy state. Motivated by the East model, a kinetically constrained lattice model with inherent glassy behaviors, several predictions are made about the behavior of the supercooled liquid as it passes through the glass transition. These predictions are then compared with the results of our atomistic simulations. Consistent with the lattice model predictions, it is shown that the relaxation time of the material undergoes a crossover from super-Arrhenius to Arrhenius behavior at a cooling-rate-dependent glass transition temperature. Additionally, the limiting value of the energy barriers from the Arrhenius behaviors at low temperatures in the glassy state shows remarkable quantitative agreement with the lattice model predictions. The atomistic results also show that the rate of short-time particle displacements deviates from the equilibrium linear scaling around the glass transition temperature, asymptotically approaching a different linear scaling. Surprisingly, these short-time displacements, the dynamic indicators of the underlying excitations responsible for structural relaxation, show no spatial

correlations beyond a few particle diameters, both above and below the glass transition. This final result is contrary to our expectations, based on previous results for East model glasses formed by cooling, that inter-excitation correlations should emerge as the liquid vitrifies.

Head-Gordon performs theoretical studies on strongly heterogeneous and far-from-equilibrium systems. The mobility of radiocesium in geomeia is largely mediated by cation exchange in non-swelling clay minerals that naturally contain interlayer  $K^+$ , but which have high affinity for  $Cs^+$ . Although exchange of interlayer  $K^+$  for  $Cs^+$  is thermodynamically non-selective, recent experiments show that direct, anhydrous  $Cs^+$ - $K^+$  exchange is kinetically viable and leads to the formation of phase-separated interlayers through a mechanism that is unknown. We identified a “chemical-mechanical coupling” positive feedback mechanism in which exchange of the larger  $Cs^+$  for the smaller  $K^+$  significantly lowered the migration barrier of neighboring  $K^+$ , allowing exchange to propagate rapidly once initiated at the clay edge. We used these atomistic outcomes to inform a model for an activation energy barrier that depends on the fraction of Cs neighbors in the local environment of either ion, and the number of isomorphic substitutions of the site that the ion occupies. Using kinetic Monte Carlo simulations, we abstracted the model to a binary system of particles of dissimilar size confined between semiflexible planar surfaces, where the activation energy barrier to diffusion decreases with the local fraction of the larger particles. The system autonomously reaches a cyclical non-equilibrium state characterized by the formation and dissolution of metastable micelle-like clusters with the small particles in the core and the large ones in the surrounding corona. The power spectrum of the fluctuations in the aggregation number exhibits  $1/f$  noise reminiscent of self-organized critical systems. We propose that the dynamical metastability of the micellar structures arises from an inversion of the energy landscape, in which the relaxation dynamics of one of the species induces a metastable phase for the other species.

Geissler is advancing computational techniques that systematically explore the space of dynamical trajectories. Accessing dynamical behavior on time scales much longer than those of basic microscopic motions (say, ps to ns) is a ubiquitous challenge in molecular simulation. A variety of methods have been developed for one-step transformations in relatively simple environments, e.g., elementary chemical reactions in solution. These focus on the existence of a well-defined barrier whose crossing determines long-time dynamics. For much more complex situations that are not dominated by a single barrier, these computational approaches generally fail. From glassy systems to self-assembling nanostructures to systems driven out of equilibrium, examining typical trajectories is a challenge, and examining atypical yet especially informative trajectories is deeply problematic. We are building a new generation of path sampling techniques for this purpose.

Transition path sampling (TPS) is a survey of trajectories biased by a well-defined probability distribution of dynamical paths. Its important strength lies in not requiring advance knowledge of mechanism. The intrinsic strengths of importance sampling, applied to the space of trajectories, guarantees exact generation of path ensembles that obey constraints of interest (e.g., starting in a “reactant” state and ending in a “product” state). Successful applications of this methodology have ranged from autoionization in liquid water to protein folding and phase change. But addressing problems with extremely rugged landscapes, with transit time scales much longer than those of chaos, and without stable attractors in phase space currently lies beyond TPS capabilities. A next generation of path sampling tools is under development in this subtask, with example applications to phenomena of experimental interest such as self-assembly in aerosol droplets.

We have devised a basic scheme for circumventing the problems of chaotic divergence and intermediate kinetic trapping that plague existing TPS protocols. It draws on several recent advances in simulation methodology, adapted to the sampling of trajectory ensembles. First, our Monte Carlo trial moves modify time evolution in limited segments, requiring path displacements with both initial and final conditions constrained. This task is achieved with the use of Brownian bridges, i.e., exact sampling of Langevin dynamics with fixed endpoints under constant force, corrected by a non-unit acceptance probability. Second, traversing a landscape of metastable states is facilitated with an enhanced sampling approach akin to nonequilibrium driving methods based on Crooks's fluctuation theorem. Here, we alter a physical parameter like temperature over the course of many path sampling moves to achieve a kind of annealing. This driving incurs an effective dissipation, whose value determines the probability with which such an excursion can be accepted. A key feature of this approach is that perturbations can be applied on a limited scale, e.g., driving only a modest part of the system over a modest interval of time. As a result, the scale of dissipation can be managed, allowing reasonable acceptance rates.

Geissler has also adapted path sampling techniques to examine how molecular systems can be driven out of equilibrium with low dissipation. Manipulating chemical kinetics in complex environments, which often feature slow relaxation, essentially requires nonequilibrium driving. Doing so without excessive energy waste is a desirable but highly nontrivial goal. We have formulated a statistical ensemble of driving protocols, biased according to their average dissipation, as a way to explore efficient driving routes and also to quantify their diversity. Analogies with conventional equilibrium ensembles, together with symmetries imposed by the fluctuation theorem, allow a very effective numerical survey of protocols, which we demonstrated in an application that inverts the magnetization of an Ising model. From this survey we identify which features of time-dependent driving are essential for thermodynamic efficiency and which are unimportant.

### **Future Plans**

Mandadapu plans to develop novel tools and techniques to analyze the nature of the short time displacements in the glassy state in different atomistic models of glass formers, given the observation of the lack of non-trivial correlation length in the glassy state. These tools and techniques used to study the supercooled and glassy states of bulk systems will be applied to understand the phase-behaviors of grain interfaces in solids. The group also plans to incorporate the physics of the glass transition into coarse-grained lattice based models to study the competitions between vitrification and crystal coarsening. These studies are motivated by systems such as water and other solids that may exist in different physical states such as liquid, supercooled liquid, crystalline and glassy states.

Head-Gordon plans to generalize the findings reported above to other binary system where the diffusivity or mobility of the species, particles, or agents, depends on their local concentration, and where one of the species diffuses faster than the other, given the same local environment. For example, our model could be used to describe non-equilibrium spatial clustering of active matter systems, such as bacterial species that exhibit concentration-dependent mobilities, or the phase behavior of binary granular monolayers. We would like to work with other experimental CPIMS colleagues on exploring systems where dynamical inversion of the energy landscape (DIEL) might be operative.

Geissler plans to refine and demonstrate novel path sampling methods, en route to applications involving complex molecular transformations. As a testing ground, we will study established model systems, e.g., structural rearrangements within small clusters of Lennard-Jones particles. Despite their apparent simplicity, these systems already pose severe sampling challenges akin to those we aim to overcome in contexts of self-assembly and nonequilibrium response.

Wilson work with other LBNL experimentalists (Saykally and Ahmed) to explore a number of rapid mixing approaches that may allow the direct detection of short lived reaction intermediates in liquid phase chemical reactions. Direct detection of reaction intermediates is an important step in unraveling complex mechanisms in condensed and interfacial systems. Colliding microdroplet reactors currently under development show some promise of achieving very fast inertial mixing times in the microsecond range, which would allow short lived reactive intermediates (such as radicals) to be observed directly either by spectroscopy or mass spectrometry. Additionally, we will also investigate and quantify the mixing dynamics in colliding "sheet" jets to evaluate whether chemical reactions can be initiated and whether quantitative kinetics can be reliably extracted from the complex mixing dynamics. The use of colliding droplet reactors or liquid "sheets" could allow new studies of condensed phase liquid chemistry using X-ray methods at the Advanced Light Source. Liquid jet sheets have dynamically evolving surfaces, affording the potential to examine the real time evolution of surface chemistry. Additionally droplets could allow new studies of self-assembly chemistry initiated by surfactant photochemistry at the droplet interface.

#### **Publications Acknowledging DOE support:**

T.R. Gingrich and P.L. Geissler, "Preserving correlation between trajectories for efficient path sampling," *J. Chem. Phys.* (2015) **142**, 234104, doi: 10.1063/1.4922343

T. R. Gingrich, G.M. Rotskoff, G.E. Crooks, and P.L. Geissler. "Near-optimal protocols in complex nonequilibrium transformations", *Proc. Natl. Acad. Sci. USA* **113**, 10263 (2016), doi:10.1073/pnas.1606273113.

A. Bhowmick, S. Sharma, T. Head-Gordon, "The role of side chain entropy and mutual information for improving the de novo design of Kemp Eliminases KE07 and KE70," *Phys. Chem. Chem. Phys.* In press (2016).

L. E. Felberg, A. Doshi, G. L. Hura, J. Sly, V. A. Plunova, R. Miller, J. E. Rice, W. C. Swope, T. Head-Gordon, "Controlling the structural transition of polymers with pH using chemical composition and star polymer architecture," *Mol. Phys.* In press. (2016).

L. R. Pestana, K. Kolluri, T. Head-Gordon, and L. Nielsen Lammers (2017). Direct exchange mechanism for interlayer ions in non-swelling clays. *Environ. Sci. & Tech.* **51** (1), 393–400

L. R. Pestana, N. Minnetian, L. Nielsen Lammers, T. Head-Gordon, (2017). Dynamical inversion of the energy landscape promotes non-equilibrium self-assembly of binary mixtures. *Submitted*.

## Chemical Kinetics and Dynamics at Interfaces

*Laser-induced dynamics, reactions and spectroscopy at surfaces*

**Wayne P. Hess (PI) Alan G. Joly and Patrick Z. El-Khoury**

Physical Sciences Division  
Pacific Northwest National Laboratory  
P.O. Box 999, Mail Stop K8-88,  
Richland, WA 99352, USA  
[wayne.hess@pnnl.gov](mailto:wayne.hess@pnnl.gov)

Additional collaborators include: Y. Gong, M.T.E. Halliday, D. Hu, A.L. Shluger, P.V. Sushko, V.A. Apkarian, C.J. Cramer, M. Zamkov, A. Tarnovsky, N.D. Browning, R. F. Haglund Jr., P. Abellan, Q.M. Ramasse, I.V. Novikova, A. Bhattarai, G.E. Johnson, J. Laskin, J.E. Evans, E. Aprà, and N. Govind

### Program Scope

The interaction between light, metals, insulators and molecules is fundamentally important in photochemistry, microelectronics, sensor technology, and materials processing. The chemistry and physics of electronically excited solids and surfaces is relevant to the fields of photocatalysis, radiation physics, and solar energy conversion. Irradiation of solid surfaces by UV, or higher energy photons, produces energetic transient species such as core holes and free electrons that subsequently relax to form electron-hole pairs, excitons and plasmons. Specifically, the interaction between light and metal nanostructures can lead to intense field enhancement and strong optical absorption through excitation of surface plasmon polaritons. Such plasmon excitation can be used for a variety of purposes such as ultrasensitive chemical detection, solar energy generation, or to drive chemical reactions. Large electric field enhancements can be localized at particular sites by careful design of nanoscale plasmonic structures. Similar to near field optics, field localization below the diffraction limit can be obtained. Through this field enhancement and localization, surface and tip enhanced Raman spectroscopy (SERS and TERS), capable of single molecule sensitivity, becomes possible. Greater understanding of spectroscopic observables is gained using a combined experiment/theory approach. We therefore use *ab initio* calculations to model results from our SERS and TERS studies. The dynamics of plasmonic excitations is complex and we use finite difference time domain calculations to model field enhancements and optical properties of complex structures including substrate couplings or interactions with dielectric materials.

### *Approach:*

We are developing a combined photoemission electron microscopy (PEEM) and femtosecond laser approach to probe plasmonic nanostructures such as solid metal particles or lithographically produced nanostructures such as gratings, trenches, or nanohole arrays. Finite difference time domain (FDTD) calculations are used to interpret field enhancements measured by the electron and optical techniques. The effects of extreme electric field enhancement on Raman spectra is investigated using plasmonic nanostructures constructed from a metal nanoparticles or metal covered atomic force microscopy (AFM) tips on thin film metal/silica substrates. The Raman scattering from molecules positioned between these structures show greatly enhanced scattering and often highly perturbed spectra depending on nanogap dimensions or whether a conductive junction is created between tip and substrate.

In photodesorption studies, photon energies are chosen to excite specific surface structural features that lead to particular desorption reactions. The photon energy selective approach takes advantage of energetic differences between surface and bulk exciton states and probes the surface exciton directly. We measure velocities and state distributions of desorbed atoms or molecules from ionic crystals using resonance enhanced multiphoton ionization and time-of-flight mass spectrometry. We have demonstrated surface-selective excitation and reaction on alkali halides and generalized our exciton model to oxide materials and shown that desorbed atom product states can be selected by careful choice of laser wavelength, pulse duration, and delay between laser pulses.

### **Recent Progress**

Plasmonic applications require the ability to launch, focus, and guide surface plasmon polaritons (SPPs) to specific remote locations. The relative intensities of SPPs simultaneously launched from opposing edges of a symmetric trench structure, etched into a silver thin film, may be controllably varied by tuning the linear polarization of the driving field. This is demonstrated through transient multiphoton PEEM measurements performed using phase-locked femtosecond pulse pairs. Our measurements are rationalized using FDTD simulations, which reveal that the coupling efficiency into SPP modes is inversely proportional to the magnitude of the localized surface plasmon (LSP) fields excited at the trench edges. Additional experiments on single step edges also show asymmetric SPP launching with respect to polarization, analogous to the trench results. Our combined experimental and computational results allude to the interplay between localized and propagating surface plasmon modes in the trench; strong coupling to the localized modes at the edges correlates to weak coupling to the SPP modes. Simultaneous excitation of the electric fields localized at both edges of the trench results in complex interactions between the right- and left-side SPP modes with Fabry-Perot and cylindrical modes. This results in a trench width-dependent SPP intensity ratio using otherwise identical driving fields. A systematic exploration of polarization directed SPP launching from a series of trench structures reveals an optimal SPP contrast ratio of 4.2 using a 500 nm-wide trench.

A square trench structure can be considered an individual element of the toolbox needed for SPP control. The trench structure reveals phenomena that is generally neglected in literature specifically, interplay between LSPs and SPPs. Polarization dependent SPP coupling is a general feature of step edges. For trenches whose edges are separated by a few microns or less, coupling between opposite edges can lead to an increase in SPP launching asymmetry. Similarly, linear polarization may be used to direct SPPs launched from a protruded silver spherical cap structures. Experiment and theory reveal that SPP coupling efficiency, of spherical caps structures, is comparable to conventional etched-in plasmonic coupling structures. Additionally, plasmon propagation direction and coupling using spherical cap structures can be controlled by laser polarization. These results lead directly to application of spherical cap couplers as gate devices. To explain these results we propose simple geometric model in which the plasmon direction selectivity is proportional to the projection of the linear laser polarization on the surface normal. Overall, our results indicate that protruded cap structures hold great promise as additional elements in the tool-kit for surface plasmon applications.

We recorded time-resolved PEEM (tr-PEEM) images of propagating surface plasmons launched from lithographically patterned holes and rectangular trenches milled on a flat gold surface. Our tr-PEEM scheme involves a pair of identical, spatially separated, and interferometrically-locked femtosecond laser pulses. Using a combination of tr-PEEM and FDTD simulations, we imaged plasmon propagation properties and including focusing and dispersion. Power dependent PEEM images provide experimental evidence for a sequential coherent nonlinear photoemission process, in which one laser source launches a propagating surface plasmons (SPPs) through a linear

interaction, and the second subsequently probes the SPP *via* two-photon photoemission. The recorded time-resolved movies of a SPP allow us to directly measure various properties of the surface-bound wave packet, including its carrier wavelength (783 nm) and group velocity. In addition, tr-PEEM images reveal that the launched SPP may be detected at least 250 microns away from the coupling trench structure. The experimentally measured SPP properties demonstrate that surface plasmons propagating on nominally flat gold surfaces may potentially be harnessed for use in mesoscale plasmonic devices.

Using a locked pair of identical femtosecond laser pulses, we imaged propagating surface plasmons, launched from a lithographically patterned rectangular trench, on a flat gold surface. The use of spatially and temporally offset pump and probe pulse pairs allowed the determination of the plasmon group velocity of  $0.95c$ . A series of PEEM images recorded using sequentially delayed probe pulses produces a nearly light speed SPP movie, at 220 attoseconds per frame, and a 50 nm spatial resolution. Using a combination of tr-PEEM and FDTD simulations, we determined that the upper limit for the  $1/e$  decay length of the plasmon field is 88 microns. The recorded time-resolved movies of a SPP allow us to directly measure various properties of the surface-bound wave packet, including its carrier wavelength (783 nm) and group velocity. The experimentally measured SPP properties demonstrate that surface plasmons propagating on nominally flat gold surfaces may potentially be harnessed for use in plasmonic devices.

### **Future Plans**

Future research plans involve fabrication of well-defined plasmonic nanostructures capable of broadcasting the optical response of a single molecule. We stress that nanometric precision in structure is needed to achieve the required local electric fields used for ultrasensitive detection and chemical imaging experiments. This will be achieved through (a) established methods, including modified colloidal syntheses and focused gallium ion beam lithography, and (b) using our state-of-the-art fabrication method of choice for this project, namely helium ion lithography (HIL). All structural motif in these plasmonic constructs consist of interacting nanometric sub-components (e.g. nanometric holes, triangles, rectangles) that cooperatively support optically-accessible LSP resonances. In a recent proof-of-principle application of HIL, we demonstrated that ultrafine plasmonic trenches can be reproducibly etched in metallic thin films. The use of a focused helium ion beam for fabrication will not only afford us plasmonic nanojunctions as fine as a few nm, but will also ensure that the plasmonic properties of the surrounding substrate are not contaminated, e.g., via Ga implantation using standard focused ion beam lithography or by organic contaminants using conventional colloidal sample preparation methods. We now have the tools needed to correlate field enhancement with SERS and TERS response and by adding a two-color photoemission scheme to our PEEM set up, the path opens to an entirely new set of measurements capable of correlating structure and dynamics of a variety of designer plasmonic constructs. These developments will eventually enable us to examine photochemical transformations at the ultimate detection limit of a single molecule in ultrasensitive nanoscale chemical imaging experiments or possibly characterize the atomistic nature of SERS hot spots.

In a similar vein, we will extend our prior work to understand the effect of tailored electromagnetic fields on individual molecules and molecular assemblies. Such comparison will provide insights on emergent behavior in the few molecule and single-molecule regime where the 3D structure (vector components) and absolute magnitude of the local electric field can be inferred from the SERS/TERS spectra/images of carefully selected target molecules. The first step involves engineering and characterizing plasmonic constructs which support LSPs and/or SPPs. The inclusion of HIL into our arsenal, now allows sub 10 nm structures to be fabricated enabling correlated femtosecond PEEM with transmission electron microscopy (TEM), tip-enhanced Raman spectroscopy and electron energy loss spectroscopy (EELS). We envision EELS

spectroscopy of vibrational and electronic states of molecules adsorbed on such plasmonic metal constructs.

### References to publications of DOE BES sponsored research (2015 to present)

1. P. Z. El-Khoury, Y. Gong, P. Abellan, B. W. Arey, A. G. Joly, D. Hu, J. E. Evans, N. D. Browning and W. P. Hess "Tip-Enhanced Raman Nanographs: Mapping Topography and Local Electric Fields" *Nano Lett.* **15**, 2385 (2015).
2. Y. Gong, A. G. Joly, D. Hu, P. Z. El-Khoury and W. P. Hess, "Ultrafast Imaging of Surface Plasmons Propagating on a Gold Surface" *Nano Lett.* **15**, 3472 (2015).
3. R. B. Davidson II, J. I. Ziegler, G. Vargas, S. M. Avanesyan, Y. Gong, W. Hess and R. F. Haglund Jr., "Efficient Forward Second-Harmonic Generation from Planar Archimedean Nanospirals" *Nanophotonics*, **4**, 108 (2015).
4. M. T. E. Halliday, W. P. Hess and A. L. Shluger, "Structure and properties of electronic and hole centers in CsBr from theoretical calculations" *J. Phys. Condens. Matter* **27**, 245501 (2015).
5. P. Z. El-Khoury, G. E. Johnson, I. V. Novikova, Y. Gong, A. G. Joly, J. E. Evans, M. Zamkov, J. Laskin and W. P. Hess "Enhanced Raman Scattering from Aromatic Dithiols Electrospayed into Plasmonic Nanojunctions" *Faraday Discuss.* **184**, 339-357 (2015).
6. M. T. E. Halliday, A. G. Joly, W. P. Hess and A. L. Shluger, "Photo-Induced Br Desorption From CsBr Thin Films Grown on Cu(100)" *J. Phys. Chem. C.* (2015) **119**, 24036
7. M. T. E. Halliday, W. P. Hess and A. L. Shluger, "A mechanism of Cu work function reduction in CsBr/Cu photocathodes" *Phys. Chem. Chem. Phys.* **18**, 7427-7434 (2016).
8. T. Ueltschi, S. Fischer, E. Aprà, A. Tarnovsky, N. Govind, P. Z. El-Khoury, W. P. Hess, "Time-Domain Simulations of Transient Species in Experimentally Relevant Environments" *J. Phys. Chem. A*, **120**, 556 (2016).
9. P. Z. El-Khoury, P. Abellan, R. L. Chantry, Y. Gong, A. G. Joly, I. V. Novikova, J. E. Evans, E. Aprà, D. Hu, Q. M. Ramasse and W. P. Hess, "On the information content in single molecule Raman nanoscopy" *Advances in Physics: X*, **1**, 35 (2016).
10. S. A. Fischer, T. W. Ueltschi, P. Z. El-Khoury, A. L. Mifflin W. P. Hess, H.-F. Wang, C. J. Cramer, and N. Govind, "Infrared and Raman Spectroscopy from Ab Initio Molecular Dynamics and Static Normal Mode Analysis: The C-H Region of DMSO as a Case Study" *J. Phys. Chem. B* **120**, 1429 (2016).
11. P. Z. El-Khoury, A. G. Joly and W. P. Hess, "Hyperspectral Dark Field Optical Microscopy of Single Silver Nanospheres," *J. Phys. Chem. C*, **120**, 7295 (2016).
12. P. Z. El-Khoury, P. Abellan, Y. Gong, F. S. Hage, J. Cottom, A. G. Joly R. Brydson, Q. M. Ramasse and W. P. Hess, "Visualizing Surface Plasmons with Photons, Photoelectrons, and Electrons", *Analyst* **141**, 3562-3572 (2016).
13. Y. Gong, A. G. Joly, P. Z. El-Khoury, and W. P. Hess, "Enhanced Propagating Surface Plasmon Signal Detection" *ACS Photonics* **3**, 2413 (2016)
14. Y. Gong, A. G. Joly, P. Z. El-Khoury, and W. P. Hess "Polarization Directed Surface Plasmon Polariton Launching" *J. Phys. Chem. Lett.* **8**, 49 (2017).
15. S. A. Fischer, E. Aprà, N. Govind, W. P. Hess, and P. Z. El-Khoury, "Nonequilibrium Chemical Effects in Single-Molecule SERS Revealed by Ab Initio Molecular Dynamics Simulations," *J. Phys. Chem. A* **121**, 1344 – 1350 (2017)
16. Y. Gong, A. G. Joly, P. Z. El-Khoury, and W. P. Hess, "Plasmon Coupling and Polarization Control Using Spherical Cap Structures" *J. Phys. Chem. Lett.* **8**, 2695 (2017).
17. I. Novikova, C. R. Smallwood, Y. Gong, D. Hu, L. Hendricks, J. E. Evans, A. Bhattarai, W. P. Hess, P. Z. El-Khoury, "Multimodal hyperspectral optical microscopy" *Chem. Phys.* (2017) DOI: 10.1016/j.chemphys.2017.08.011

**DEVELOPMENT OF APPROACHES TO MODEL EXCITED STATE CHARGE AND ENERGY TRANSFER IN SOLUTION: MODELING EXCITED STATES IN THE CONDENSED PHASE**

Christine Isborn<sup>1</sup> (PI), Aurora Clark (co-PI)<sup>2</sup>, Thomas Markland (co-PI)<sup>3</sup>

1. University of California Merced, Email: [cisborn@ucmerced.edu](mailto:cisborn@ucmerced.edu)
2. Washington State University, Email: [auclark@wsu.edu](mailto:auclark@wsu.edu)
3. Stanford University, Email: [tmarkland@stanford.edu](mailto:tmarkland@stanford.edu)

**PROGRAM SCOPE**

The development of next generation energy conversion and catalytic systems requires fundamental understanding of the interplay between photo-excitation and the resulting proton and electron transfer processes that occur in solution. To address these challenges requires accurate and efficient methods to compute ground and excited states, as well as the ability to treat the dynamics of energy transfer in the presence of solvent fluctuations. Our team is developing accurate and efficient theoretical models for solution phase reactions. These developments provide an improved understanding of photo-initiated excitations, electron transfer, and proton coupled electron transfer processes.

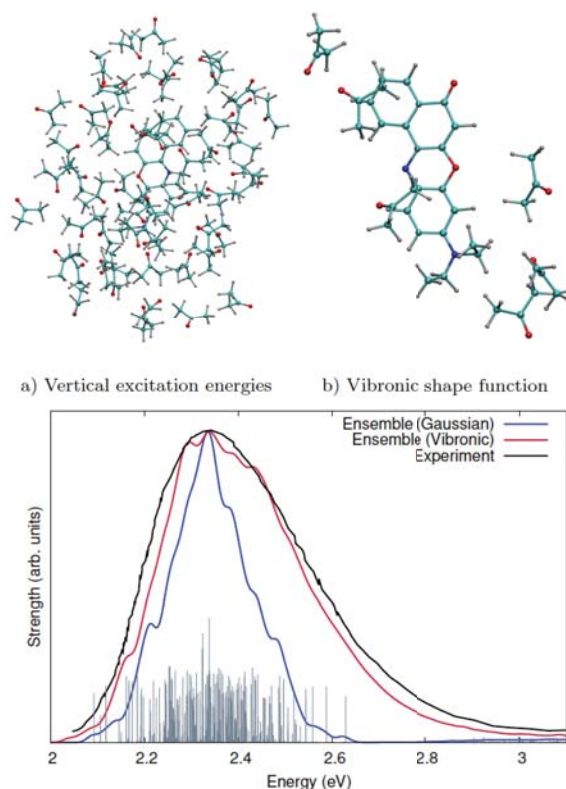
Our research team brings together expertise in electron and nuclear dynamics (classical and quantum), electronic structure, and analysis of solvation networks. We are developing and validating techniques for modeling condensed phase reactions. For reliable condensed phase simulations, an accurate model that includes both short- and long-range interactions is required. Short- and long-range interactions may be particularly strong in aqueous solution, where hydrogen-bonding and proton transfer may play a large role at short range and polarization may play a large role at long-range. For realistic condensed phase calculations that take into account solute-solvent interactions large-scale quantum mechanical (QM) calculations that include the condensed phase environment are necessary. These large-scale calculations can also help us determine what physics is necessary for more approximate models. The Isborn group is using excited state time-dependent density functional theory calculations that include the condensed phase to determine how to accurately model chromophores in solution. We are exploring various aspects of modeling condensed phase systems, including examination of basis set and density functional dependence [1], the limitations of the adiabatic approximation in time-dependent density functional theory [2], the role of nuclear quantum effects [3] and vibronic effects [7] on computed absorption spectra, the best choice of classical solvent model [4], and how much QM solvent to include in a calculation [4, 5, 6].

**RECENT PROGRESS**

To determine how much solvent should be treated with QM in a condensed phase calculation, we have examined convergence trends for solutes of different polarity [4, 5, 6]. Although short-range solute-solvent interactions such as charge-transfer, hydrogen bonding, and solute-solvent polarization can be taken into account with a QM treatment of the solvent, it is

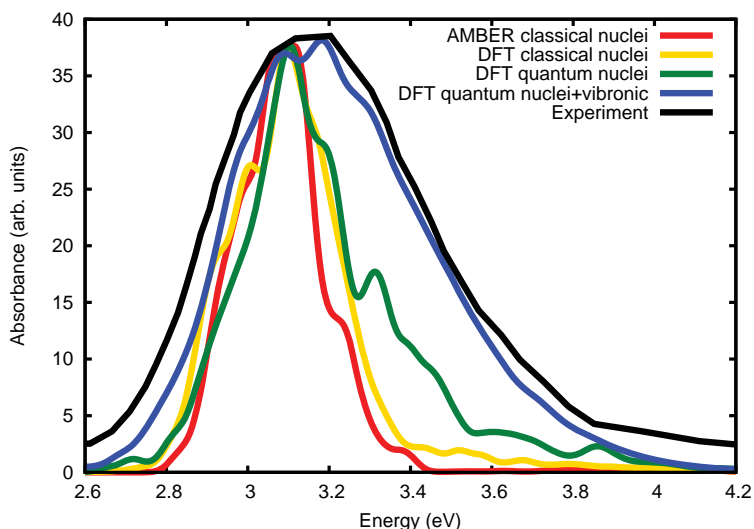
unclear how much QM solvent is necessary to accurately model interactions with different solutes. We investigated the effect of explicit QM solvent on absorption spectra computed for a series of solutes with decreasing polarity. By adjusting the boundary between QM and classical molecular mechanical solvent, convergence of the calculated absorption spectra with respect to the size of the QM region is achieved. We found that the rate of convergence does not correlate with solute polarity when excitation energies are calculated using time dependent density functional theory with a range-separated hybrid functional, but does correlate with solute polarity when using configuration interaction singles. We also found that larger basis sets converge the computed spectrum with fewer QM solvent molecules. To optimize the computational cost with respect to convergence, we tested a mixed basis set with more basis functions for atoms of the chromophore and the solvent molecules that are nearest to it and fewer basis functions for the atoms of the remaining solvent molecules in the QM region. Our results show that using a mixed basis sets is potentially an effective way to significantly lower the computational cost while reproducing the results computed with larger basis sets. We also have tested which classical solvation method best interfaces with large amounts of QM solvent, and have found that the convergence of excitation energies is similar for molecular mechanical point charges and a polarizable continuum model (PCM). We found that although the van der Waals (VDW) definition of the PCM cavity is adequate for molecular structures with small amounts of QM solvent, larger QM solvent layers had gaps in the VDW PCM cavity, leading to asymptotically incorrect excitation energies. Given that the VDW cavity leads to unphysical solute-solvent interactions, we advise the computational community to instead use a solvent excluded surface cavity for QM/PCM calculations that include QM solvent. We showed that the sign and magnitude of the error in the PCM excitation energies is correlated with the ground to excited state difference dipole moment.

One of the goals in our group is accurately modeling absorption spectra in solution. Reproducing experimental spectra serves as a good way to validate: the ground state sampling of solute-solvent configurations, the ground and excited state methodology, and the importance of what causes spectral broadening, including lifetime and vibronic effects. By gaining a better understanding of which effects are necessary to reproduce absorption spectra, we will know which effects are important for a correct model of condensed phase reactivity. We've explored the accuracy of both the ensemble and Franck-Condon approaches of modeling absorption spectra, and have found that neither approach accurately captures both the full inhomogeneous broadening due to the non-Gaussian solvent distributions along with the vibronic transitions. We have developed a combined approach to model the absorption spectrum of semi-flexible chromophores in solution that includes full sampling of solute-solvent degrees of freedom at the desired temperature using a large QM region for the calculation of vertical excitation energies, and then combines this ensemble



sampling with the zero temperature Franck-Condon vibronic shape function to simulate the vibronic contributions to the spectrum at a particular solvent configuration. [7] This combined approach models the full inhomogeneous broadening of the explicit solvent environment, and is also able to reproduce the high-energy tail of the spectrum due to vibronic transitions. For Nile Red in acetone, the ensemble + vibronic approach with no phenomenological broadening shows significant improvement in spectral shape compared to the ensemble approach with standard Gaussian broadening (see first Figure).

In our work with the Clark and Markland groups, we are analyzing which solvent effects are important to include for accurate simulation of aqueous absorption spectral shapes by comparing our computed spectra to experimental spectra for different chromophores. We are comparing absorption spectra computed from configurations obtained from classical force field molecular dynamics to ab initio density functional theory Born-Oppenheimer molecular dynamics that can simulate proton transfer, and also examining the importance of nuclear quantum effects via path integral molecular dynamics. Our initial studies show that including nuclear quantum effects and vibronic effects are important for reproducing experimental results (see second Figure).



## FUTURE PLANS

In addition to continuing our analysis of the role of nuclear quantum effects on electronic excitations, we plan to continue working with the Clark and Markland groups to analyze the hydrogen bonding dynamics in different potentials (classical vs quantum) and explore how hydrogen bonding and solvent environment affects the electronic excitations. With the Markland group, we will pursue a comparison between our recently developed ensemble plus Franck-Condon approach and an energy gap time-correlation function approach in which we consider terms beyond 2<sup>nd</sup> order in the cumulant expansion. We also have a new graduate student in the group working to examine the accuracy of real-time TDDFT for modeling charge-transfer effects.

### Award Number DE-SC0014437: Development of Approaches to Model Excited State Charge and Energy Transfer in Solution

**PI and co-PI(s):** Christine Isborn (University of California Merced, PI), Aurora Clark (Washington State University, co-PI), Thomas Markland (Stanford, co-PI)

**Isborn Group Postdoc(s):** Makenzie Provorse (now an Assistant Professor at University of Central Arkansas), Tim Zuehlsdorff

## Up to Ten Publications Acknowledging this Grant (started September 2015), Isborn Group

- [1] “Size-dependent error of the density functional theory ionization potential in vacuum and solution.” X. A. Sosa Vazquez and C. M. Isborn. *J. Chem. Phys.* 143, 244105 (2015)
- [2] “Electron Dynamics with Real-Time Time-Dependent Density Functional Theory.” M. R. Provorse and C. M. Isborn. “*Int. J. Quantum Chem.* 116, 739-749 (2016)
- [3] “Simulating Nuclear and Electronic Quantum Effects in Enzymes.” L. Wang, C. M. Isborn, and T. E. Markland. *Methods in Enzymology*, 577, 389-418 (2016)
- [4] “Convergence of Excitation Energies in Mixed Quantum and Classical Solvent: Comparison of Continuum and Point Charge Models.” M. R. Provorse, T. Peev, C. Xiong, C. M. Isborn. *J. Phys. Chem. B* 120, 12148-12159 (2016)
- [5] “Convergence of Computed Aqueous Absorption Spectra with Explicit Quantum Mechanical Solvent.” J. M. Milanese, M. R. Provorse, E. Alameda, C. M. Isborn. *J. Chem. Theory Comput.* 13, 2159-2171 (2016)
- [6] “Combining Explicit Quantum Solvent with a Polarizable Continuum Model.” M. R. Provorse and C. M. Isborn. *Submitted*.
- [7] “Combining the Ensemble and Franck-Condon Approaches for Spectral Shapes of Molecules in Solution.” T. J. Zuehlsdorff and C. M. Isborn. *Submitted*.

# DE-FG02-07ER15889: Probing catalytic activity in defect sites in transition metal oxides and sulfides using cluster models: A combined experimental and theoretical approach

Caroline Chick Jarrold and Krishnan Raghavachari

Indiana University, Department of Chemistry, 800 East Kirkwood Ave.

Bloomington, IN 47405

[cjarrold@indiana.edu](mailto:cjarrold@indiana.edu), [kraghava@indiana.edu](mailto:kraghava@indiana.edu)

## I. Program Scope

Our research program combines experimental and computational methods to study a range of cluster models for heterogeneous catalytic materials. The focus of our studies has been transition metal oxide and sulfide clusters in non-traditional oxidation states, and their chemical and physical interactions with water, though recent efforts have been broadened to include more complex applied systems. Over the past year, experimental capabilities for generated isotopically pure metal hyper-sulfide clusters have been expanded, because these cluster systems have recently emerged as stable solution-phase catalysts for the hydrogen evolution reaction (HER). In addition, we have further developed our studies on sacrificial reagents for full-cycle catalysis of  $H_2$  production from water decomposition to understand the very specific way in which the model sacrificial reagent interacts with the small clusters. The experiments and calculations are designed to probe fundamental, cluster-substrate molecular-scale interactions that are governed by charge state, peculiar oxidation states, and unique molecular structures.

The general strategy of our studies continues to be as follows: (1) Determine how the molecular and electronic structures of transition metal suboxide and subsulfide clusters evolve as a function of oxidation state by reconciling anion photoelectron spectra of the bare clusters with high-level DFT calculations. Anions are of particular interest because of the propensity of metal oxide and sulfides to accumulate electrons in applied systems. (2) Measure and analyze the kinetics of cluster reactivity with water, with and without the inclusion of sacrificial reagents. (3) Dissect possible reaction mechanisms computationally,

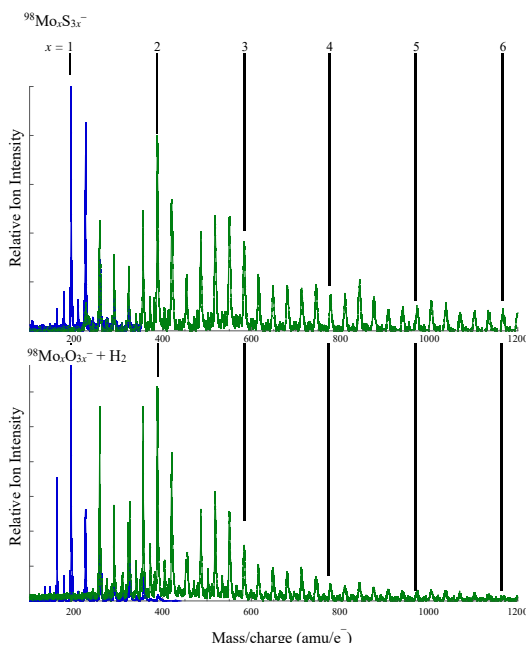


**Figure 1.** Top: Mass spectra of clusters generated from ablation of  $^{98}\text{MoS}_2$  powder, with  $\text{Mo}_x\text{S}_{3x}^-$  hypbersulfide clusters indicated. Bottom: cluster distribution following reactions with  $\text{H}_2$ . Blue and green traces are spectra obtained under low- and high-mass range settings on the mass spectrometer.

to determine whether catalytically relevant interactions are involved. (4) Verify these challenging computational studies by spectroscopic investigation [typically, anion photoelectron (PE) spectroscopy] of observed reactive intermediates. (5) Probe the effect of local electronic excitation on bare clusters and cluster complexes, to evaluate photocatalytic processes. The overarching goal of this project is to identify particular defect structures that balance structural stability with electronic activity, both of which are necessary for a site to be simultaneously robust and catalytically active, and to find trends and patterns in activity that can lead to improvement of existing applied catalytic systems, or the discovery of new systems.

## II. Recent Progress

**A. Chemistry of transition metal sulfide clusters:** While our combined computational and experimental approach to studying catalytically driven energy-relevant reactions have implemented clusters as models for defect sites in bulk heterogeneous catalyst materials, small molybdenum hypersulfide clusters with one to 3 Mo centers have been shown to be electrocatalysts for HER in solution.<sup>i</sup> The hypothesis is that the disulfide groups

<sup>i</sup>H.I. Karunadasa *et al.*, *Science* **335**, 698 (2012); Z. Huang, *et al.*, *Angew. Chem. Int. Ed.* **54**, 15181 (2015); J. Kibsgaard *et al.*, *Nat. Chem.* **6**, 248 (2014).

in the solution phase clusters mimic the MoS<sub>2</sub> bulk edge sites that have been implicated as the active sites, which is in contrast to the oxygen vacancies implicated as active site in bulk metal oxides. Experimentally, the move from the Group 6 transition metal oxides to the sulfides has been complicated by the rapid oxidation of the metal sulfides, the mass coincidence between sulfur and two oxygen atoms, and the broad distribution of isotopes naturally abundant in Mo and W. However, we have used high-temperature solid state reactions to generate <sup>98</sup>MoS<sub>2</sub> and <sup>184</sup>WS<sub>2</sub> using isotopically enriched oxidized metal powders, and have begun reactivity studies with H<sub>2</sub> and H<sub>2</sub>O. The top panel of Figure 1 shows the broad range of Mo<sub>x</sub>S<sub>y</sub><sup>-</sup> cluster sizes and stoichiometries made from ablation of targets prepared by pressing the freshly synthesized <sup>98</sup>MoS<sub>2</sub> powder, with the Mo<sub>x</sub>S<sub>3x</sub><sup>-</sup> hypersulfide cluster stoichiometries indicated. In addition, the relative intensities of the hypersulfides can be reduced by introducing H<sub>2</sub> into the carrier gas mixture, presumably via Mo<sub>x</sub>S<sub>y</sub><sup>-</sup> + H<sub>2</sub> → Mo<sub>x</sub>S<sub>y-1</sub><sup>-</sup> + H<sub>2</sub>S (*vide infra*) reaction, as is evident in the lower panel of Fig.1. The distribution of stoichiometries for the <sup>98</sup>Mo<sub>x</sub>S<sub>y</sub><sup>-</sup> clusters show an interesting distinction from the oxide congeners, which is that the distribution of sulfides for any given number of metal centers is much broader than the oxide distribution, and relatively flat in terms of relative intensities. For example, the Mo<sub>2</sub>S<sub>y</sub><sup>-</sup> series ranges from y = 1 through 8.

<sup>98</sup>Mo<sub>x</sub>S<sub>y</sub><sup>-</sup> + H<sub>2</sub>, H<sub>2</sub>O: Overall, the <sup>98</sup>Mo<sub>x</sub>S<sub>y</sub> clusters in the distribution of stoichiometries generated via ablation of the <sup>98</sup>MoS<sub>2</sub> powder are relatively unreactive toward water and hydrogen. However, an unexpected result of the <sup>98</sup>Mo<sub>x</sub>S<sub>y</sub><sup>-</sup> + H<sub>2</sub> reactivity studies is the high specificity of H<sub>2</sub> addition products observed. For example, small quantities of Mo<sub>2</sub>S<sub>3</sub>H<sub>2</sub><sup>-</sup> products are observed for the lowest values of y, but Mo<sub>2</sub>S<sub>4</sub><sup>-</sup> specifically shows high reactivity toward H<sub>2</sub> addition, as does Mo<sub>3</sub>S<sub>5</sub><sup>-</sup>. Clearly, there is some unique structural or electronic feature of these two systems that promotes H<sub>2</sub> addition that is not present in the other species. We are currently investigating this result computationally to understand this reactivity and to explore its implications.

Compared to the Mo<sub>x</sub>O<sub>y</sub><sup>-</sup> congeners, Mo<sub>x</sub>S<sub>y</sub><sup>-</sup> clusters are less reactive toward H<sub>2</sub>O in the gas phase, though direct oxidation (Mo<sub>x</sub>S<sub>y</sub><sup>-</sup> + H<sub>2</sub>O → Mo<sub>x</sub>S<sub>y</sub>O<sup>-</sup> + H<sub>2</sub>) is observed. There is no evidence of sequential oxidation, as was observed in the oxide studies. Comparing products formed in reactions with D<sub>2</sub>O and H<sub>2</sub>O suggests that molybdenum sulfide thiols may play an important role in HER from hypersulfide clusters in solution. In previous studies comparing Mo<sub>x</sub>O<sub>y</sub><sup>-</sup> with W<sub>x</sub>O<sub>y</sub><sup>-</sup> reactions with water, several striking differences in the reaction kinetics and product distributions were observed. W<sub>x</sub>S<sub>y</sub><sup>-</sup> + H<sub>2</sub>O reactivity studies are currently underway.

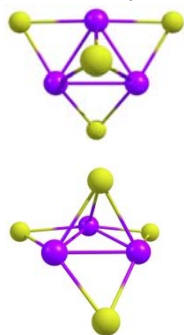


**Figure 3.** Top and side views of the optimized Mo<sub>3</sub>S<sub>4</sub><sup>-</sup> cluster structure.

**Computational studies on Mo<sub>3</sub>S<sub>4</sub><sup>-</sup> and W<sub>3</sub>S<sub>4</sub><sup>-</sup> reactions with H<sub>2</sub>O:** We carried out a careful computational investigation of the water reactivity of a cluster involving some key structural elements. Mo<sub>3</sub>S<sub>4</sub><sup>-</sup> and W<sub>3</sub>S<sub>4</sub><sup>-</sup> were chosen in this study for two reasons: they contain three undercoordinated sulfurs (see Fig. 3) reminiscent of some edge sites in the metal sulfides such as MoS<sub>2</sub> that have shown some correlation with reactivity in solution phase studies, and they contain a triply bridging sulfur that is another structural motif commonly associated with reactivity. The reaction pathways leading up to H<sub>2</sub> release were characterized carefully to understand the possible roles of different structural elements in this cluster. In particular, the triply bridging sulfur has a significant impact on the energetic barriers for the reaction as well as its site selectivity. The overall barriers for structures containing the triply-bridging motif were somewhat lower than for comparable structures without this motif. Additionally, this structural motif also increases the cluster's overall stability and appears to protect it from partial dissociation.

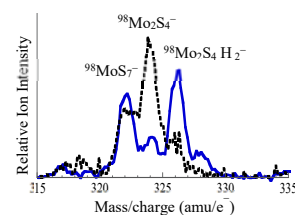


**Figure 2.** Mo<sub>2</sub>S<sub>4</sub><sup>-</sup>, a cluster with bulk stoichiometry, is one of a small number of clusters that are uniquely reactive toward H<sub>2</sub>. Dotted black trace is initial distribution, blue trace is post H<sub>2</sub> reaction.

## B. Complex reactions between $\text{Mo}_x\text{O}_y^-$ clusters and $\text{C}_2\text{H}_4/\text{H}_2\text{O}$ gas mixtures

In a series of studies investigating  $\text{H}_2\text{O}$  reactions with Group 6 transition metal suboxide clusters, we observed sequential direct oxidation with  $\text{H}_2$  production, which generally terminated with dihydroxide formation as the cluster oxidation state approached the bulk. Subsequently, a computational study on the feasibility of introducing a sacrificial reagent, **A** ( $\text{A} = \text{CO}, \text{C}_2\text{H}_2, \text{C}_2\text{H}_4, \text{C}_3\text{H}_6$ ) which would reduce newly oxidized clusters prior to the terminating step in a computational study on the system,



While the calculations predicted deeply bound complexes formed between “**A**” and the cluster, the internal energy gained in the oxidation step (Reaction I) experimentally is not instantaneously dissipated under experimental conditions. Ethylene was selected to be the sacrificial reagent for the experimental follow-up because it is less directly reactive toward the clusters compared to  $\text{CO}$  and  $\text{C}_2\text{H}_2$ , and has two unique bonds, rather than the five unique bonds in  $\text{C}_3\text{H}_6$ . The experiments involved comparing product distributions from  $\text{Mo}_x\text{O}_y^-$  clusters reacting individually with  $\text{C}_2\text{H}_4$  and  $\text{H}_2\text{O}$  with those from reactions with a  $\text{C}_2\text{H}_4 + \text{H}_2\text{O}$  mixture, and results were interpreted with supporting computational thermochemistry. The results revealed that the molecular interactions at play were more involved than previously considered.

**Chemifragmentation:** Results of experiments on reactions between  $\text{Mo}_x\text{O}_y^-$  and  $\text{C}_2\text{H}_4$ , compared with reactions involving  $\text{C}_2\text{H}_4/\text{H}_2\text{O}$  gas mixtures suggested that several competing and unanticipated reactions take place. First, there are several pieces of evidence pointing to chemifragmentation of larger clusters undergoing reactions with  $\text{C}_2\text{H}_4$  to form small  $\text{MoO}_y\text{C}_n\text{H}_m^-$  complexes. With a combination of anion photoelectron spectroscopy, reconciled with spectral simulations generated from DFT computed structures and energies, we have determined that these complexes feature  $\eta^2$  acetylene ligands (see Fig. 4) rather than vinylidene ligands, suggesting that such  $\eta^2$ -interactions between ethylene and larger  $\text{Mo}_x\text{O}_y^-$  are important, which opens a new direction in how we approach the reaction free energy pathway computationally. Additionally, evidence of photodissociation of  $\eta^2$ -acetylene complexes suggests that net  $2 \text{C}_2\text{H}_4 \rightarrow \text{C}_2\text{H}_2 + \text{C}_2\text{H}_6$  disproportionation may be occurring. Thermochemical calculations support mechanisms that invoke participation of two ethylene molecules on thermodynamically favorable pathways leading to experimentally observed products.

**Cooperative reactions:** Unique species observed in reactions exclusively with the  $\text{C}_2\text{H}_4 + \text{H}_2\text{O}$  mixture,  $\text{Mo}_2\text{O}_5\text{C}_2\text{H}_2^-$  and  $\text{MoO}_3\text{C}_2\text{H}_4^-$ , suggest that the internal energy gained in new  $\text{Mo}-\text{O}$  bond formation from oxidation by  $\text{H}_2\text{O}$  opens additional reaction channels with  $\text{C}_2\text{H}_4$ . Further,  $\text{C}_2\text{H}_3\text{O}^-$  is observed uniquely in reactions with the  $\text{C}_2\text{H}_4 + \text{H}_2\text{O}$  mixture, giving indirect evidence of  $\text{CH}_3\text{CHO}$  formation via the cluster mediated  $\text{H}_2\text{O} + \text{C}_2\text{H}_4 \rightarrow \text{H}_2 + \text{CH}_3\text{CHO}$  reaction;  $\text{C}_2\text{H}_3\text{O}^-$  can form via dissociative electron attachment to  $\text{CH}_3\text{CHO}$ .

## C. Understanding the mechanism and selectivity of complex catalytic systems

The oxygen reduction reaction (ORR) is a crucial step in devices such as fuel cells to directly convert fuels to electricity at modest temperature. While systems such as N-doped graphitic structures are being explored

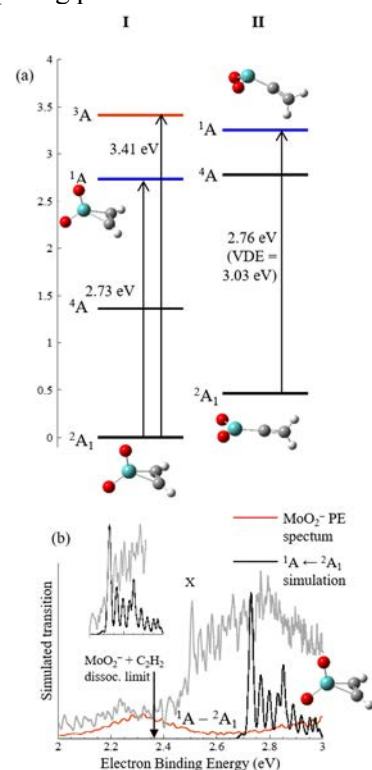


**Figure 4.** (a) Summary of computed  $\text{MoO}_2\text{C}_2\text{H}_2^-$  structures and spin states. (b) the PE spectrum of  $\text{MoO}_2\text{C}_2\text{H}_2^-$  formed in chemifragmentation reactions between larger  $\text{Mo}_x\text{O}_y^-$  clusters and  $\text{C}_2\text{H}_4$ , with calculated simulation based on structure I.

to replace expensive Pt-based electrocatalysts, little is known about the catalytic mechanisms, including the parameters that determine the selectivity of the reaction. In particular, experimental studies suggest a four-electron pathway (leading to H<sub>2</sub>O) under alkaline conditions (high pH) while a two-electron pathway (leading to H<sub>2</sub>O<sub>2</sub>) is preferred at lower pH. We have now developed a model based on interfacial solvation around the active sites to understand this pH-dependent selectivity. The model has been carefully calibrated by comparing quantum chemical calculations of a well-defined graphene nanostructure with experimental results, and is able to provide a clear understanding of the pH-dependent ORR selectivity catalyzed by nearly all of the previously reported graphitic materials.

### III. Future Plans

As illustrated in the previous section, the enduring strength of the research program is the synergistic interplay between theory and experiment. While we bring the sacrificial reagent study to a conclusion with the final free energy pathway calculations, taking into account the detailed molecular interactions and competing reactions determined experimentally. Further expansion of our new experiments and calculations on metal sulfides will include comparing the reactivity of <sup>186</sup>W<sub>x</sub>S<sub>y</sub><sup>-</sup> toward both water and H<sub>2</sub> with surprising new results on Mo<sub>x</sub>S<sub>y</sub><sup>-</sup> reactivity, along with a detailed theoretical study on the electronic and molecular structures of the various sulfide cluster anions, in order to learn which characteristics result in hydride complex formation. The differences in reducibility and M–S bond energies of the clusters are likely to result in an interesting electronic and structural environment that will strongly influence interactions with water. Finally, we will implement our new ion carpet-based reactor that will allow us to filter out a narrow range of clusters between the cluster source and the reactor. With this new stage in the source/reactor setup, we can more strongly correlate initial cluster distributions with cluster fragment and oxidized sacrificial reagent formation.

### IV. References to publications of DOE sponsored research that have appeared in 2015–present or that have been accepted for publication

1. "Reactions of Molybdenum Oxide Cluster Anions with C<sub>2</sub>H<sub>4</sub> and H<sub>2</sub>O for a Full Catalytic Cycle of H<sub>2</sub> Production," Manisha Ray, Richard N. Schaugaard, Josey E. Topolski, Jared O. Kafader, Krishnan Raghavachari, and Caroline Chick Jarrold, under second review, *Topics in Catalysis*, June, 2017.
2. "Bond Activation and Hydrogen Evolution from Water through Reactions with M<sub>3</sub>S<sub>4</sub> (M = Mo, W) and W<sub>3</sub>S<sub>3</sub> anionic clusters", Corrine A. Kumar, Arjun Saha, and Krishnan Raghavachari, *J. Phys. Chem. A* **121**, 1760-1767 (2017). <http://dx.doi.org/10.1021/acs.jpca.6b11879>
3. "A Model for the pH-Dependent Selectivity of the Oxygen Reduction Reaction Electrocatalyzed by N-Doped Graphitic Carbon", Benjamin W. Noffke, Qiqi Li, Krishnan Raghavachari, and Liang-shi Li", *J. Am. Chem. Soc.* **138**, 13923–13929, (2016). <http://dx.doi.org/10.1021/jacs.6b06778>
4. "Hydrogen evolution from water using Mo-oxide clusters in the gas phase: DFT modeling of a complete catalytic cycle using a Mo<sub>2</sub>O<sub>4</sub><sup>-</sup>/Mo<sub>2</sub>O<sub>5</sub><sup>-</sup> cluster couple," Manisha Ray, Arjun Saha, and Krishnan Raghavachari, *Phys. Chem. Chem. Phys.* **18**, 25687-25692 (2016). <http://dx.doi.org/10.1039/c6cp04259g>
5. "Effect of alkyl group on M<sub>x</sub>O<sub>y</sub><sup>-</sup> + ROH (M = Mo, W; R = Me, Et) reaction rates," Manisha Ray, Sarah E. Waller, and Caroline Chick Jarrold, *J. Phys. Chem. A* **120**, 1508-1519 (2016). <http://dx.doi.org/10.1021/acs.jpca.6b00102>
6. "Role of weakly-bound complexes in temperature-dependence and relative rates of M<sub>x</sub>O<sub>y</sub><sup>-</sup> + H<sub>2</sub>O (M = Mo, W) reactions," Jared O. Kafader, Manisha Ray, Krishnan Raghavachari, and Caroline Chick Jarrold, *J. Chem. Phys.* **144**, 074307(1-9) (2016). <http://dx.doi.org/10.1063/1.4941829>
7. "H<sub>2</sub>S reactivity on oxygen-deficient heterotrimetallic cores: Cluster fluxionality simulates dynamic aspects of surface chemical reactions," Debashis Adhikari and Krishnan Raghavachari, *J. Phys. Chem. A* **120**, 447-472 (2016). <http://dx.doi.org/10.1021/acs.jpca.5b10899>
8. "Direct Reduction of Alkyl Halides at Silver in Dimethylformamide: Effects of Position and Identity of the Halogen", Lauren M. Strawsine, Arkajyoti Sengupta, Krishnan Raghavachari, and Dennis G. Peters, *ChemElectroChem.* **2**, 726–736 (2015). <http://dx.doi.org/10.1002/celec.201402410>

# Unmasking the Mechanics of Proton Defect Accommodation and Transport in Water through Rational Control of Water Cluster Scaffolds

RE: DE-FG02-00ER15066 and DE-FG02-06ER15800

Program Managers: Dr. Mark Pederson and Dr. Gregory Fiechtner

K. D. Jordan (jordan@pitt.edu), Dept. of Chemistry, University of Pittsburgh, Pittsburgh, PA 15260

M. A. Johnson (mark.johnson@yale.edu), Dept. of Chemistry, Yale University, New Haven, CT 06520

## Program Scope:

Our program exploits size-selected clusters as a medium with which to unravel molecular level pictures of key transient species and solvent speciation motifs that underlie condensed phase and interfacial chemistry. To this end, we are increasingly focused on understanding the molecular nature of the hydrated proton “defect” - the situation arising when a proton is either injected into or removed from a water network - and the microscopic interactions that control the macroscopic behavior of ionic liquids (ILs). We have made significant progress in both of these focus areas over the past year, as we outline below in sections I and II. Because aqueous processes are central to most of practical interfacial chemistry, we continue to address the origin of behaviors unique to this regime regarding the role of fast dynamics in the vibrationally excited states. This requires the development of new theoretical tools based on the spectroscopic properties of vibrationally adiabatic potential energy surfaces, an endeavor that we initiated over a decade ago. Recent results indicate that the effects are much more general than was initially apparent, and consequently we have refined the approach as discussed in section III.

## I. Unraveling the quantum signature of excess proton motion in water networks

The highest profile aspect of our work in this area was discussed in the CPIMS 2016 abstract, in which we joined forces with Knut Asmis’s group in Leipzig to identify and

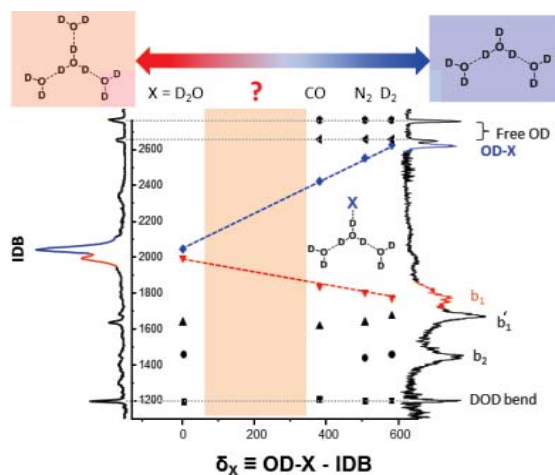


**Fig. 1.** The interpolation of band patterns from  $D^+(D_2O)_3$  (3D) to  $D^+(D_2O)_4$  (4D) using the OD-X band displacement relative to the location of the bound OD stretch fundamentals in 4D as an empirical index of intermediate distortion. The red “?” below the color bar emphasizes the need to add another tag species to quantify the band pattern in this range of the transformation from 3D to 4D.

characterize the spectral correlations across the IR spectrum that, together, encode the transfer of a proton from one water molecule to another. The results of this joint experiment/theory effort were reported in *Science* (ref. [4]), and followed an enabling study published in *PCCP* (ref. [6]), in which we identified the role of isomers and temperature in the spectrum of the protonated water pentamer. Both studies leveraged the strong dependence of anharmonic coupling on the hydrogen mass, with the perdeuterated systems displaying much simpler spectra than those of the all H isotopologues. This indicates that the spectral features result from large excursions along the potential energy surface for hydron motion. To explore this effect more quantitatively, we engaged a collaboration with the Bowman and McCoy groups to understand the isotope dependence of the protonated water trimer. This required addressing the vibrational quantum mechanics on an extended potential energy surface (with the 3-body contribution anchored to  $\sim 52,000$  ab initio points) with explicit coupling between 18 vibrational modes. On the experimental side, we introduced a new scheme for acquiring the vibrational spectra based on IR-IR double resonance of the bare ions, thus eliminating complications arising from the widely used “messenger tagging” approach. The important aspect of the study, published in 2017 in *J. Phy. Chem.-Letters*, (ref. [9]) is that recovering even qualitative aspects of the experimental spectra of both isotopologues *required* refinement of the three-body portion of the potential energy surface (PES).

With the more accurate PES in hand, we are now addressing the assignments of many “extra” features in the spectra of all the small protonated water clusters. This effort involves a variation of the approach we used to map out the spectral trajectories associated with proton transfer in which we purposefully followed the perturbations caused by a series of increasingly strongly interacting “tag” molecules. This yields an experimental way to follow the incremental evolution of the various bands when a network is systematically “tuned” from one water cluster size to the next, as illustrated by the trajectories associated with morphing  $D^+(D_2O)_3$  into  $D^+(D_2O)_4$  (Fig. 1). The surprising result here is that the strongest bands near  $1700\text{ cm}^{-1}$ , long thought to be derived from the OD stretches bound to the two flanking water molecules in the protonated trimer, do NOT evolve toward the analogous feature in the Eigen form of the tetramer! We will next resolve these assignments for all the strong bands in the  $n = 3$  to 7 clusters through a combination of theoretical approaches ranging from vibrational self-consistent field methods (VSCF) to vibrational configuration interaction calculations (VCI) to multi-reference vibrational second-order perturbation theory (VPT2).

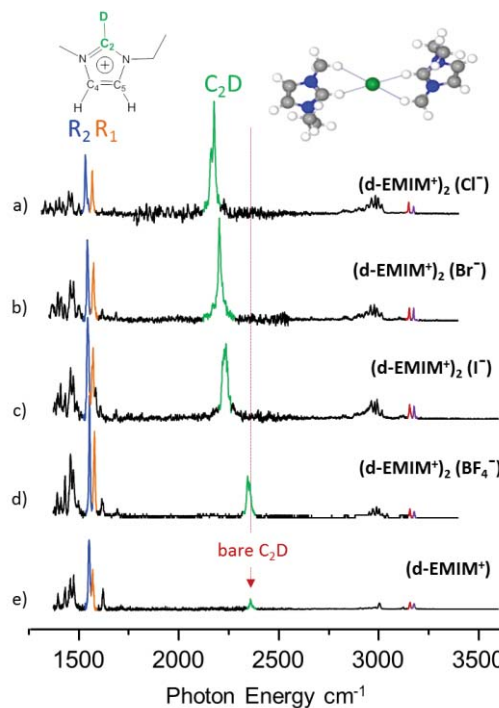


**Fig. 2.**  $N_2$ -tagged vibrational spectra of the cationic ternary clusters,  $(d\text{-EMIM}^+)_2X^-$ , where d-EMIM indicates selective deuteration at the  $C_{(2)}$  position. The green band near  $2300\text{ cm}^{-1}$  arises from the antisymmetric stretch of the  $C_{(2)}$ -D groups bound to the anions.

## II. Quantifying the role of H-bonding in EMIM-based ionic liquids

Our early work using vibrational spectroscopy to understand the intermolecular interactions in EMIM-based ionic liquids highlighted the importance of isolating the key acidic CH proton on the imidazole ring with selective deuteration. Together with measurement of the intrinsic frequency of this oscillator in the bare d-EMIM ion, we demonstrated that the  $C_{(2)}$ -D band was essentially unshifted in the ternary  $(EMIM^+)_2BF_4^-$  system, thus establishing a minimal role for traditional hydrogen bonding to the anion. We have extended this study to include the complexes with the smaller halide ions, and the resulting spectra shown in Fig. 2 reveal clear signatures of hydrogen bonding through the red-shift and intensity enhancement of the key  $C_{(2)}$ -D bands. Symmetry-adapted perturbation theory (SAPT) was employed to characterize the interactions in  $EMIM^+(BF_4^-)_{n=1,2}$  and  $EMIM^+(Cl^-)_{n=1,2}$  clusters. These calculations help delineate the relative importance of polarization and charge transfer. In both sets of clusters polarization is found to be much more important than charge transfer, although charge transfer does play a more important role in the  $Cl^-$  complexes.

## III. Adiabatic ID Potentials for Treating Anharmonic Effects in Ion-Water Clusters

The OH stretch vibrational spectra of clusters such as  $CH_3NO_2^-(H_2O)$ ,  $CH_3CO_2^-(H_2O)$ , and  $NO_3^-(H_2O)$ , display progressions with a spacing of  $\sim 80\text{ cm}^{-1}$ . These progressions arise from strong anharmonic coupling between the OH stretch and water rock vibrations. A simple way of understanding the origin of this structure is to make an adiabatic-type separation of the OH stretch and rock vibrations which leads to separate one-dimensional potentials for the water rock vibration with zero and one quanta of OH stretch. The progression can then be obtained by calculation of the Franck-Condon overlaps between the zero-point level in the rock potential for  $n = 0$  stretch and the various levels of the rock potential for  $n = 1$  OH stretch. The adiabatic potentials for  $NO_3^-(H_2O)$  calculated at the CCSD(T)-F12 level are shown in Fig. 3. Calculation of the vibrational spectra using these potentials and values of the reduced mass appropriate for the potential energy minima results in spacings of  $120\text{-}131\text{ cm}^{-1}$  between consecutive members of the progression, much larger than the observed  $73\text{-}82\text{ cm}^{-1}$  spacings for  $NO_3^-(H_2O)$ . Agreement with experiment is considerably improved by allowing the reduced mass to depend on geometry. With this modification, the calculated spacings are reduced to  $90\text{-}109\text{ cm}^{-1}$ . Part of the remaining discrepancy between the calculated and observed spectra is due to the use of harmonic frequencies in constructing the adiabatic potentials. However, it is clear that simple one-dimensional adiabatic models are most useful for providing qualitative insight rather than quantitative prediction of the observed vibrational spectra. On the experimental side, in the past year we have carried out an isotopic study of the archetypal formate monohydrate, and verified the predicted collapse in the extent of the vibrational progression found in  $HCO_2^-(H_2O)$  in the spectrum of the  $HCO_2^-(D_2O)$  ion.

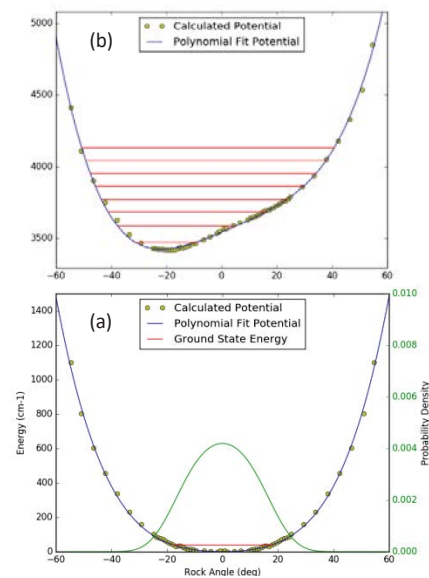


**Fig. 3.** Adiabatic potentials for water rock of  $NO_3^-(H_2O)$ . For (a)  $n = 0$  and (b)  $n = 1$  OH stretch adiabatic potentials. The wave function for the ground state rock level in  $n = 1$

#### IV. Focus for the next year

Beyond the ongoing projects discussed above, we will directly address the nature of the intra- and inter-molecular couplings underlying the complex spectra of hydrated protons using our new IR-IR double resonance approach to determine the features due to a *single* H atom embedded in an otherwise perdeuterated cluster. Of particular interest here is the direct determination of the coupling between the intramolecular bending vibrations of nearby water molecules with the H-bonded OH stretching fundamentals. We will also expand our investigations of the H-bonding interactions in ionic liquids to challenge the recently advanced hypothesis that H-bonds among the hydrocarbon tails in cationic components can yield an attractive interaction that can partially overcome the Coulomb repulsion to yield a new design parameter in the tailoring of ILs for specific applications.

#### V. Papers in the past two years under this grant:

1. **“Comparison of the Local Binding Motifs in the Imidazolium-based Ionic Liquids [EMIM][BF<sub>4</sub>] and [EMMIM][BF<sub>4</sub>] through Cryogenic Ion Vibrational Predissociation Spectroscopy: Unraveling the Roles of Anharmonicity and Intermolecular Interactions”**, J. A. Fournier, C. T. Wolke, C. J. Johnson, A. B. McCoy, and M. A. Johnson, *J. Chem. Phys.*, **17**, 8518–8529 (2015).
2. **“Understanding the Ionic Liquid [NC<sub>4111</sub>][Tf<sub>2</sub>N] from Individual Building Blocks: An IR Spectroscopic Study”**, K. Hanke, M. Kaufmann, G. Schwaab, M. Havenith, C. T. Wolke, O. Gorlova, M. A. Johnson, B. Kar, W. Sander, and E. Sanchez-Garcia, *Phys. Chem. Chem. Phys.*, **17**, 8518 (2015).
3. **“Water Network-Mediated Electron-Induced Proton Transfer in Anionic [C<sub>5</sub>H<sub>5</sub>N<sup>•</sup>(H<sub>2</sub>O)<sub>n</sub>] Clusters: Size-Dependent Formation of the Pyridinium Radical for n > 3”**, A. F. DeBlase, C. T. Wolke, G. H. Weddle, K. A. Archer, K. D. Jordan, J. T. Kelly, G. S. Tschumper, N. I. Hammer, and M. A. Johnson, *J. Chem. Phys.*, **143**, 144305 (2015).
4. **“Spectroscopic Snapshots of the Proton Transfer Mechanism in Water”**, C. T. Wolke, J. A. Fournier, L. C. Dzugas, M. R. Fagiani, T. T. Odbadrakh, H. Knorke, K. D. Jordan, A. B. McCoy, K. R. Asmis, and M. A. Johnson, *Science*, **354**, 1131–1135 (2016).
5. **“Characterization of the Primary Hydration Shell of the Hydroxide Ion with H<sub>2</sub> Tagging Vibrational Spectroscopy of the OH<sup>-</sup>(H<sub>2</sub>O)<sub>n=2,3</sub> and OD<sup>-</sup>(D<sub>2</sub>O)<sub>n=2,3</sub> Clusters”**, O. Gorlova, J. W. DePalma, C. T. Wolke, A. Brathwaite, T. T. Odbadrakh, K. D. Jordan, A. B. McCoy, and M. A. Johnson, *J. Chem. Phys.*, **145**, 134304 (2016).
6. **“Gas Phase Vibrational Spectroscopy of the Protonated Water Pentamer: the Role of Isomers and Nuclear Quantum Effects”**, M. R. Fagiani, H. Knorke, T. Esser, N. Heine, C. T. Wolke, S. Gewinner, W. Schöllkopf, M.-P. Gaigeot, R. Spezia, M.A. Johnson, and K.R. Asmis, *Phys. Chem. Chem. Phys.*, **18**, 26743 (2016).
7. **“Proton-coupled Electron Transfer in [Pyridine•(H<sub>2</sub>O)<sub>n</sub>]<sup>-</sup>, n = 3, 4, Clusters”**, K. A. Archer, and K. D. Jordan, *Chem. Phys. Lett.*, **661**, 196–199 (2016).
8. **“Theoretical Studies of Charged and Neutral Water Clusters”**, K. Sen and K. D. Jordan, *Specialist Periodic Reports on Computational Chemistry*, **13**, 105–131 (2016).
9. **“Disentangling the Complex Vibrational Spectrum of the Protonated Water Trimer, H<sup>+</sup>(H<sub>2</sub>O)<sub>3</sub> with Two-color IR-IR Photodissociation of the Bare Ion and Anharmonic VSCF/VCI Theory”**, C. H. Duong, O. Gorlova, N. Yang, P. J. Kelleher, M. A. Johnson, A. B. McCoy, Q. Yu, and J. M. Bowman, *J. Phys. Chem. Lett.*, **8**, 3782–3789 (2017).

## Nucleation Chemical Physics

Shawn M. Kathmann  
Physical Sciences Division  
Pacific Northwest National Laboratory  
902 Battelle Blvd.  
Mail Stop K1-83  
Richland, WA 99352  
[shawn.kathmann@pnl.gov](mailto:shawn.kathmann@pnl.gov)

### Program Scope

The objective of this work is to develop an understanding of the chemical physics governing nucleation. The thermodynamics and kinetics of the embryos of the nucleating phase are important because they have a strong dependence on size, shape and composition and differ significantly from bulk or isolated molecules. The technological need in these areas is to control chemical transformations to produce specific atomic or molecular nanoparticles with specific properties. Computing reaction barriers and understanding condensed phase mechanisms is much more complicated than those in the gas phase because the reactants are surrounded by solvent molecules and the configurations, energy flow, quantum and classical electric fields and potentials, and ground and excited state electronic structure of the entire statistical assembly must be considered.

### Recent Progress and Future Directions

#### Quantum Description of Liquid Water's Mean Inner Potential

Water's interfacial electric potential, arising from the quantum mechanical distribution of nuclei and electrons, alter the path and hence the phase of an electron wave passing through it. Consequently,

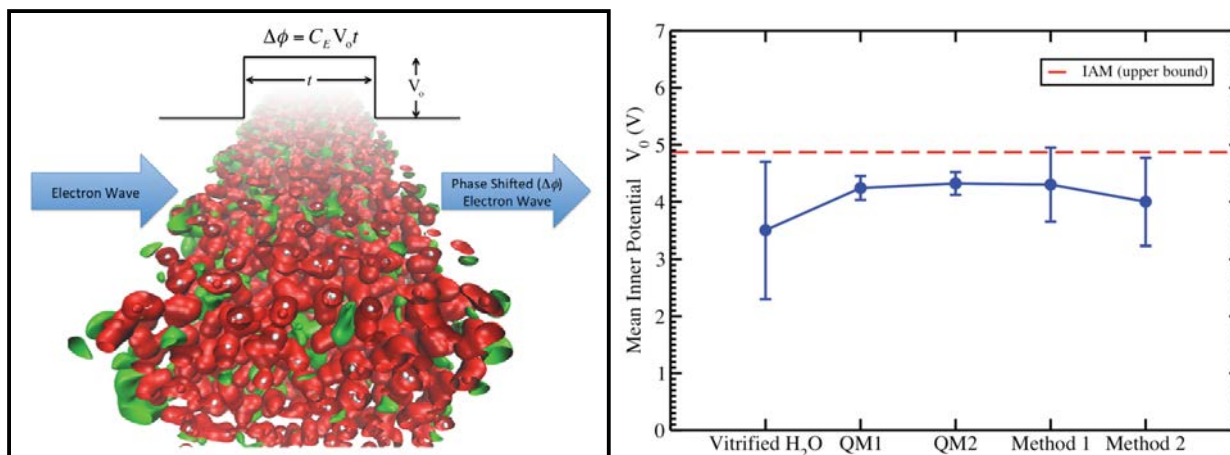


**Figure 1.** (Left) Illustration of how the MIP ( $V_0$ ) is related to the electron wave phase shift ( $\Delta\phi$ ) as a consequence of passing through voltages of liquid water of thickness  $t$  ( $C_E$  is an experimental constant). Red isosurfaces denotes positive voltage regions (greater than 0V) and green denotes negative voltage regions (less than -2.7V). (Right) Comparison of previous measurement on *vitrified* water, best current measurement on *liquid* water (Method 1), and the best theoretical results from resampling (QM1) and direct (QM2) quantum mechanical calculations. The Independent Atom Model (IAM) uses a superposition of Dirac-Fock atomic Hartree potentials.

experimental measurements of electron wave phase changes provide direct quantitative metrics of the electrical properties of liquid water – see Figure 1. Here we compare the first quantitative electron holographic (EH) measurement of the Mean Inner Potential (MIP) for liquid water. The MIP of liquid

water has been recently measured, using off-axis liquid phase electron holography, to be  $V_o = +4.30 \pm 0.65$  V and is used to assess dominant factors for quantum mechanical simulations of liquid water. Our quantum mechanical calculations are in excellent agreement with these latest EH experiments. The ( $\sim 0.6$ V) difference between the IAM model and the quantum results (or EH experimental results) represents the difference due to electronic charge redistribution and OH bond formation compared to a superposition of Dirac-Fock atomic densities calculated in vacuum.

Additionally, recent measurements and quantum simulations of the vibrational sum frequency generation spectroscopy of water's interface and dipolar surface potential ( $\phi_D = +0.47$ V), computed using maximally localized Wannier functions, can be related to liquid phase electron holography measurements. The sign of the Wannier surface dipole potential is consistent with the surface dipole potential estimated from electrochemical measurements ( $\chi = +0.14$ V). But, even though there is consistency between these values they were obtained from very different physical considerations and one should remain cautious until better experiments and electrochemical theory are devised to provide a more fundamental quantum-based description of the electrochemical observables. Stable and reproducible off-axis liquid phase electron holography is successfully demonstrated and provides essential benchmarks toward a better understanding of liquid water's surface vibrational spectroscopy, electron density, electric potentials and fields inside and at the interface of liquids.

### Voltage Fluctuations in Small NaCl Clusters

The observations of luminescence during crystallization as well as electric field induced crystallization suggest that the process of crystallization may not be purely classical but also involves an essential electronic structure component. Strong electric field and/or voltage fluctuations may play an important role in this process by providing the necessary driving force for the observed electronic structure changes. The importance of electric field fluctuations driving electron transfer has been a topic of intense research since the seminal work of Marcus. The main objective of this work is to provide basic understanding of the fluctuations in charge, electric potentials, and electric fields, both classically and quantum mechanically, for concentrated aqueous NaCl electrolytes.

The stability of each ion in a finite cluster depends upon the Madelung voltages of the individual ions, each sensitive to its own environment – see Figure 2. As the salt clusters approach their ultimate crystal cubic symmetry, they pass through various non-cubic distorted or amorphous configurations, including the presence of trapped water molecules. Thus, the Madelung voltages for each ion within a salt cluster can be used as an order

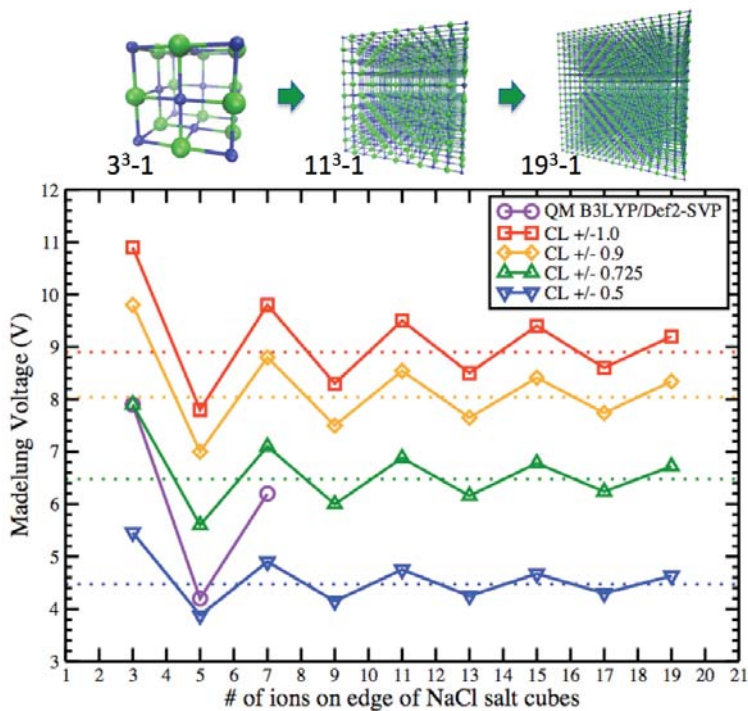


**Figure 2.** Classical (CL) and Quantum Mechanical (QM) Madelung voltage variations experienced by a central Cl<sup>-</sup> ion in NaCl clusters as a function of cluster size and ion charge. The QM voltages *cannot* be obtained by uniform scaling of the CL charges ( $|q| = 1.0, 0.9, 0.725, \text{ and } 0.5e$ ).

parameter (in addition to other order parameters e.g., the distance between ions, the angle between ion triplets, and electric fields at the ion sites) characterizing their progress along various nucleation pathways. Figure 2 shows the progression of voltages experienced by a central Cl<sup>-</sup> ion due to all other charges within the cubic clusters. However, these classical voltages do not include quantum effects due to the delocalized nature of electron densities. The variations in voltages, shown in Fig.2, for both classical and quantum descriptions show large changes with the size of the salt cluster. This is significant because the voltages govern the interaction energy between the ions making up the salt clusters and hence their thermodynamic stability. Importantly, there is a large discrepancy between the classical ( $\pm 1.0e$ ) and quantum voltages – a situation compounded by the fact that the QM results cannot be obtained by uniform charge scaling. Our previous classical molecular dynamics studies of concentrated aqueous NaCl electrolytes showed that the distribution of voltages for all the ions in the solution, including those ions trapped within salt clusters, spanned a broad range that included the bulk Madelung voltages ( $\pm 8.9V$  for ion charges of  $\pm 1.0e$ ). However, in that study we did not separate the voltage distributions between solvated ions and those ions involved in salt clusters. Our calculations and analyses provide the first steps toward understanding the magnitude and fluctuations of charge, classical point charge sources of electric potentials and fields in aqueous electrolytes and what role these fields may play in driving charge redistribution/transfer during crystallization as well as inducing crystal formation itself.

### *Coupling Cluster Formation, Vibrational Spectroscopy, Voltages and Electric Fields*

The influence of internal and externally applied voltages and electric fields on the vibrational response of clustering molecules and ions has a long history and is relevant to many chemical processes in condensed phases and their interfaces. The central concept is the use of a particular vibrational mode as a kind of antenna or probe capable of sensing the *effective* electrostatic fluctuations due to its surrounding environment. Early work in this area employed continuum descriptions of electrostatics while more recent work utilized electric fields arising from classical point charges. These voltages and fields must be considered as *effectively* arising from the surrounding atoms as this construction formally neglects the self-voltages and/or self-electric fields arising from the ions or atoms within the molecule for which the field is being probed as well as the response of the surrounding environment to this probe's charge distribution. Specifically, the voltages and electric fields on the ion/atomic sites are calculated as those arising from

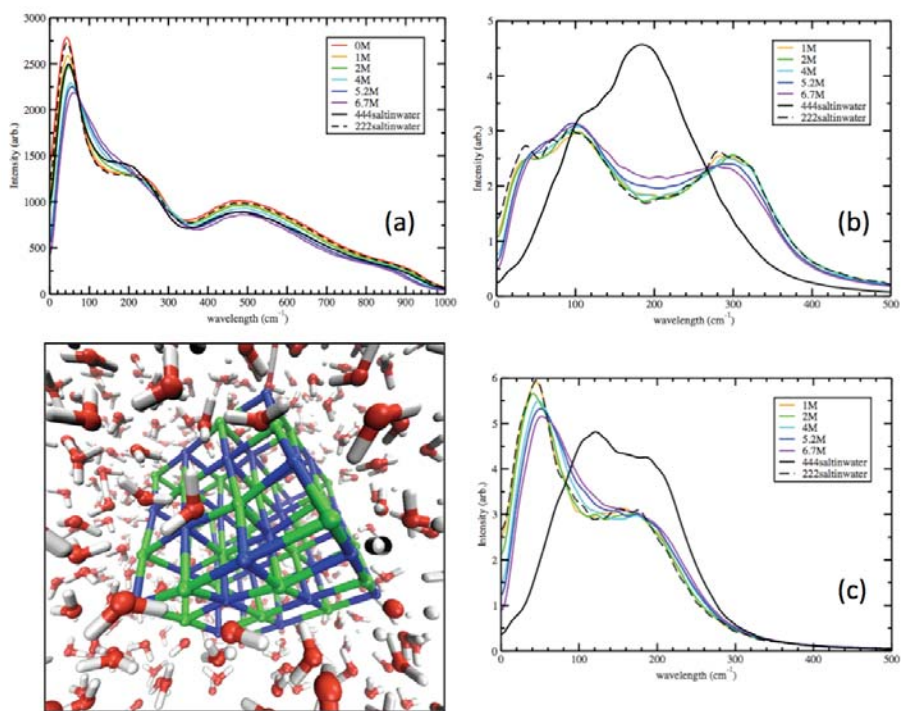


**Figure 3.** (a) Total vibrational power spectra for water and various concentrated NaCl electrolyte solutions including spectra for an unstable (dissociated)  $2^3$  NaCl crystal and stable (intact)  $4^3$  NaCl crystal (bottom left). (b) Sodium (Na) and (c) Chloride (Cl) spectra showing the vibrational signature corresponding to crystal formation.

the quantum mechanical charge densities of all the other atoms in the system, excluding only those ions/atoms at which the voltage or field is being evaluated. The resulting electric fields at these sites, either classical or quantum mechanical, are extremely large (ca.  $\sim 2 \text{ V/\AA}$ ). So large that, in fact, they could easily break the OH bond within water as it only takes  $0.6 \text{ V/\AA}$ . Thus, there is an inconsistency between the fields evaluated at atomic sites when the water molecule being probed is not included in the quantum mechanical calculation and the field evaluated including the probe water molecule. Resolving these inconsistencies is the focus of our ongoing research.

An order parameter, or cluster definition, provides a low-dimensional means of understanding the mechanism of crystallization while differentiating between various amorphous or crystalline pre-critical clusters leading to different nucleation pathways. Furthermore, we anticipate that these order parameters are very sensitive indicators of the structure of salt clusters underlying crystallization. To better understand the role of either voltages or fields as useful order parameters, we will correlate their distributions to the vibrational signatures. Figure 3(a) shows the total vibrational power spectra for pure water, various concentrated NaCl electrolytes, and dissociated  $2^3$  and stable  $4^3$  NaCl crystals. Figures 3 (b) and (c) show the individual Na and Cl vibrational power spectra displaying the vibrational signatures corresponding to crystal formation. Below  $1000\text{cm}^{-1}$ , these crystallization signatures are obscured by the water oxygen contributions to the spectra. Ongoing studies are exploring water's higher frequency OH vibrational spectral signatures present in ab initio molecular dynamics.

Direct PNNL collaborators on this project include G.K. Schenter, C.J. Mundy, S.S. Xantheas, M. Valiev, X. Wang, J. Fulton, L. Dang, and M. Baer and Postdoctoral Fellow Will Isley III. Outside collaborations with Kristian Molhave at the Technical University of Denmark on the connections between electron holography and voltages inside and at the interface of liquid water and Mark Johnson at Yale on connections between electric fields and vibrational spectroscopy have been beneficial.

*Acknowledgement:* This research was performed in part using the DOE NERSC facility. Battelle operates PNNL for DOE.

### **Publications of DOE Sponsored Research (2015-present)**

S.J. Cox, **S.M. Kathmann**, B. Slater, and A. Michaelides, "Molecular simulations of heterogeneous ice nucleation. I. Controlling ice nucleation through surface hydrophilicity", *Journal of Chemical Physics*, **142**, 184704 (2015).

S.J. Cox, **S.M. Kathmann**, B. Slater, and A. Michaelides, "Molecular Simulations of Heterogeneous Ice Nucleation. II. Peeling back the Layers", *Journal of Chemical Physics*, **142**, 184705 (2015).

**Feature Cover Article** - J.A. Fournier, C.T. Wolke, M.A. Johnson, T.T. Odbadrakh, K.D. Jordan, **S.M. Kathmann** and S.S. Xantheas, "Snapshots of Proton Accommodation at a Microscopic Water Surface: Understanding the Vibrational Spectral Signatures of the Charge Defect in Cryogenically Cooled  $\text{H}^+(\text{H}_2\text{O})_{n=2-28}$  Clusters", *Journal of Physical Chemistry A*, **119**, 9425 (2015).

J.L. Stinson, **S.M. Kathmann**, and I.J. Ford, "A classical reactive potential for molecular clusters of sulphuric acid and water", *Molecular Physics*, DOI:10.1080/00268976.2015.1090027 (2015).

C.T. Wolke, J.A. Fournier, E. Miliordos, **S.M. Kathmann**, S.S. Xantheas, and M.A. Johnson, "Isotopomer-selective spectra of a single intact  $\text{H}_2\text{O}$  molecule in the  $\text{Cs}^+(\text{D}_2\text{O})_5\text{H}_2\text{O}$  isotopologue: Going beyond pattern recognition to harvest the structural information encoded in vibrational spectra", *Journal of Chemical Physics*, **144**, 074305 (2016).

## **Chemical Kinetics and Dynamics at Interfaces**

*Structure and Reactivity of Ices, Oxides, and Amorphous Materials*

**Bruce D. Kay (PI), R. Scott Smith, and Zdenek Dohnálek**

Physical Sciences Division  
Pacific Northwest National Laboratory  
P.O. Box 999, Mail Stop K8-88  
Richland, Washington 99352  
bruce.kay@pnnl.gov

Collaborators include: GA Kimmel, NG Petrik, Yuntao Xu, and C. Yuan

### **Program Scope**

The objective of this program is to examine physiochemical phenomena occurring at the surface and within the bulk of ices, oxides, and amorphous materials. The microscopic details of physisorption, chemisorption, and reactivity of these materials are important to unravel the kinetics and dynamic mechanisms involved in heterogeneous (i.e., gas/liquid) processes. This fundamental research is relevant to solvation and liquid solutions, glasses and deeply supercooled liquids, heterogeneous catalysis, environmental chemistry, and astrochemistry. Our research provides a quantitative understanding of elementary kinetic processes in these complex systems. For example, the reactivity and solvation of polar molecules on ice surfaces play an important role in complicated reaction processes that occur in the environment. These same molecular processes are germane to understanding dissolution, precipitation, and crystallization kinetics in multiphase, multicomponent, complex systems. Amorphous solid water (ASW) is of special importance for many reasons, including the open question over its applicability as a model for liquid water, and fundamental interest in the properties of glassy materials. In addition to the properties of ASW itself, understanding the intermolecular interactions between ASW and an adsorbate is important in such diverse areas as solvation in aqueous solutions, cryobiology, and desorption phenomena in cometary and interstellar ices. Metal oxides are often used as catalysts or as supports for catalysts, making the interaction of adsorbates with their surfaces of much interest. Additionally, oxide interfaces are important in the subsurface environment; specifically, molecular-level interactions at mineral surfaces are responsible for the transport and reactivity of subsurface contaminants. Thus, detailed molecular-level studies are germane to DOE programs in environmental restoration, waste processing, and contaminant fate/transport.

Our approach is to use molecular beams to synthesize “chemically tailored” nanoscale films as model systems to study ices, amorphous materials, supercooled liquids, and metal oxides. In addition to their utility as a synthetic tool, molecular beams are ideally suited for investigating the heterogeneous chemical properties of these novel films. Modulated molecular beam techniques enable us to determine the adsorption, diffusion, sequestration, reaction, and desorption kinetics in real-time. In support of the experimental studies, kinetic modeling and simulation techniques are used to analyze and interpret the experimental data.

Recently, in collaboration with Greg Kimmel, we have developed a pulsed laser heating method that will allow us to investigate deeply supercooled liquids by producing transiently heated films, which become liquids that last for approximately 10 ns per laser pulse. Subsequent rapid cooling due to the dissipation of the heat pulse into the metal substrate effectively quenches the liquid dynamics until the next laser heating pulse arrives. The rapid heating and cooling allows the system to reach previously unattainable supercooled liquid temperatures and return to the amorphous state before significant crystallization can occur.

## Recent Progress and Future Directions

*Distinguishing between bulk and interface-enhanced crystallization in nanoscale films of amorphous solid water* Amorphous solid water (ASW) is a metastable glassy phase form of water that can be created in the laboratory by vapor deposition onto a cold substrate. The properties of ASW are of interest for a variety of reasons including its use as a model for liquid and supercooled liquid water, its use as a model for studying the properties of amorphous solids, and because it is believed to be the predominant form of water in astrophysical and planetary environments.

One motivation for the study of ASW is to extract the nucleation and growth parameters for the formation of crystalline ice from deeply supercooled liquid water. The idea is that when ASW is heated above its glass transition, it will transform into a supercooled liquid prior to crystallization. The crystallization kinetics will provide information about the properties of supercooled liquid water in very low temperature regions of the phase diagram. In recent work (8), we investigated the crystallization kinetics of nanoscale ASW films using temperature programmed desorption (TPD) and reflection absorption infrared spectroscopy (RAIRS). Desorption measurements are used to probe surface crystallization and RAIRS measurements are used to probe bulk crystallization. The desorption results show that surface crystallization is independent of the film thickness (from 100 to 1000 ML). Conversely, the RAIRS measurements show that the bulk crystallization time increases linearly with increasing film thickness. These results suggested that nucleation and crystallization begin at the ASW/vacuum interface and then a crystallization growth front propagates linearly into the bulk. This mechanism was tested by selective placement of an isotopic layer (5% D<sub>2</sub>O in H<sub>2</sub>O) at various positions in an ASW (H<sub>2</sub>O) film. In this case, the closer the isotopic layer was to the vacuum interface, the earlier the isotopic layer crystallized. These experiments provided direct evidence to confirm that ASW crystallization in vacuum proceeds by a “top-down” crystallization mechanism.

The preference for nucleation at the vacuum interface is possibly due to the higher mobility that surface molecules have compared to those in the bulk. In subsequent work (10), we tested this hypothesis by investigating the crystallization kinetics of ASW films in two configurations. In one case the ASW films were deposited on top of and capped with a decane layer (the “sandwich” configuration). In the other case, the ASW films were deposited on top of a decane layer and not capped (the “no cap” configuration). The idea being that the presence of the decane overlayer will impede the mobility of surface water molecules. The results show that the crystallization kinetics in the “sandwich” configuration, were independent of the isotopic layer placement whereas in the “no cap” configuration, the closer the isotopic layer was to the vacuum interface, the earlier the isotopic layer crystallized (consistent with the work in 8). Further, the crystallization half-times for ASW films in the “sandwich” configuration were about eight times slower than in the “no cap” configuration. These results confirm that the presence of the decane overlayer changes the crystallization mechanism and suppresses the surface nucleation rate. This means that prior work using only surface sensitive techniques, such as desorption and adsorbate physisorption, likely do not provide information relevant to bulk nucleation. Thus, the nucleation rates extracted from these experiments are most likely over estimates. Future work will involve the further study of ASW crystallization in “sandwich” films to determine if information relevant to bulk nucleation of supercooled can be extracted. The use of “sandwich” layers eliminates the contributions of nucleation at the vacuum interface to the observed crystallization kinetics. The extraction of the nucleation and growth parameters from the

crystallization kinetics will require additional experiments and more detailed kinetic modeling that explicitly treat the interfacial and bulk nucleation and growth kinetics.

***Desorption Kinetics of Benzene and Cyclohexane from a Graphene Surface*** The interactions of adsorbates with graphene is of interest in a variety of fields including catalysis, material science, and electronics. In addition, theoreticians have studied adsorbate-graphene interactions as models to improve the calculation of weakly bound and van der Waals systems. Understanding the interactions and desorption kinetics from carbon-based substrates is also important for astrophysicists to create models for the composition of various astrophysical bodies (e.g., comets, interplanetary ices, interplanetary dust, and planetary surfaces). The interaction of benzene with graphene has been used as a model system for calculating  $\pi$ - $\pi$  interactions that are believed to be important in biological systems (e.g., protein and DNA structure).

The desorption kinetics for benzene and cyclohexane from a graphene covered Pt(111) surface were investigated using temperature-programmed desorption (TPD) (9). The benzene desorption spectra have well-resolved monolayer and multilayer desorption peaks. The benzene monolayer and submonolayer TPD spectra for coverages greater than  $\sim 0.1$  ML have nearly the same desorption peak temperature and have line shapes which are consistent with first-order desorption kinetics. For benzene coverages greater than 1 ML, the TPD spectra align on a common leading edge which is consistent with zero-order desorption. An “inversion” procedure in which the prefactor is varied to find the value that best reproduces the entire set of experimental desorption spectra was used to analyze the benzene data. The inversion analysis of the benzene TPD spectra yielded a desorption activation energy of  $54 \pm 3$  kJ/mol with a prefactor of  $10^{17 \pm 1} \text{ s}^{-1}$ . The TPD spectra for cyclohexane also have well-resolved monolayer and multilayer desorption features. The desorption leading edges for the monolayer and the multilayer TPD spectra are aligned indicating zero-order desorption kinetics in both cases. An Arrhenius analysis of the monolayer cyclohexane TPD spectra yielded a desorption activation energy of  $53.5 \pm 2$  kJ/mol with a prefactor of  $10^{16 \pm 1} \text{ ML s}^{-1}$ .

It is interesting that the desorption kinetics for benzene on graphene covered Pt are first-order while for cyclohexane the desorption kinetics are zero-order. Zero-order desorption kinetics for submonolayer coverages can occur if the adsorbate behaves as a two-dimensional gas with isolated adsorbates rapidly diffusing on the surface in equilibrium with adsorbate islands. The observation of first-order desorption for benzene may mean that the island formation is not favored due to the lack of attractive adsorbate interactions. For example, benzene has an order of magnitude larger quadrupole moment compared to cyclohexane ( $-28.9 \text{ Cm}^2 \times 10^{-40}$  versus  $3.0 \text{ Cm}^2 \times 10^{-40}$ ). The positively charged outer region of the molecule (the hydrogens) may result in repulsive interactions between coplanar molecules that limit or prohibit the formation of islands. This would account for the observed first-order desorption kinetics. On the other hand, cyclohexane has an order of magnitude smaller quadrupole and the configurational flexibility that may allow for stronger attractive interactions and the formation of two-dimensional islands. This would explain the observation of zero-order desorption kinetics in this case. Future work will further explore how these lateral interactions affect the desorption kinetics of other adsorbates on graphene.

***Growth rate of crystalline ice and the diffusivity of supercooled water from 126 to 262 K*** Understanding the properties of deeply supercooled water is key to unraveling many of water’s anomalous properties. However, developing this understanding has proven difficult due to rapid and uncontrolled crystallization. To circumvent the rapid crystallization of supercooled liquid

water that occurs between 180 and 262 K, we employed a nanosecond pulsed-laser-heating technique. Our approach is to transiently heat compositionally tailored nanoscale films to the temperature of interest for a brief time (nanoseconds) and then it rapidly cools back to the pre-laser pulse temperature effectively “freezing” the kinetics. Processes that occur at these elevated temperatures are followed via a post-mortem analysis using surface spectroscopic techniques. In recent work (7) in collaboration with Greg Kimmel, we used this method to determine the crystalline-ice growth rate,  $G(T)$ , for temperatures between 180 and 262 K in ultrahigh-vacuum conditions. The self-diffusion of supercooled liquid water,  $D(T)$ , is obtained from  $G(T)$  using the Wilson–Frenkel model of crystal growth. Over the temperature range from 126 to 262 K  $G(T)$  and  $D(T)$  smoothly vary by  $\sim 11$  orders of magnitude with no evidence of a singularity. The fact that  $G(T)$  and  $D(T)$  are smoothly varying rules out the hypothesis that liquid water’s properties have a singularity at or near 228 K at ambient pressures. This approach affords many future opportunities to explore deeply supercooled liquids in regions of the phase diagram that were previously inaccessible due to rapid crystallization.

### References to Publications of DOE sponsored Research (2015 - present)

- (1) Smith, R. S.; May, R. A.; Kay, B. D. Probing Toluene and Ethylbenzene Stable Glass Formation Using Inert Gas Permeation. *J. Phys. Chem. Lett.* **2015**, *6*, 3639-3644.
- (2) Thürmer, K.; Yuan, C.; Kimmel, G. A.; Kay, B. D.; Smith, R. S. Weak Interactions between Water and Clathrate-Forming Gases at Low Pressures. **2015**, *641*, 216-223.
- (3) Chen, L.; Smith, R. S.; Kay, B. D.; Dohnalek, Z. Adsorption of Small Hydrocarbons on Rutile TiO<sub>2</sub>(110). *Surf. Sci.* **2016**, *650*, 83-92.
- (4) Smith, R. S.; May, R. A.; Kay, B. D. Desorption Kinetics of Ar, Kr, Xe, N<sub>2</sub>, O<sub>2</sub>, CO, Methane, Ethane, and Propane from Graphene and Amorphous Solid Water Surfaces. *J. Phys. Chem. B* **2016**, *120*, 1979-1987.
- (5) Xu, Y. T.; Dibble, C. J.; Petrik, N. G.; Smith, R. S.; Joly, A. G.; Tonkyn, R. G.; Kay, B. D.; Kimmel, G. A. A Nanosecond Pulsed Laser Heating System for Studying Liquid and Supercooled Liquid Films in Ultrahigh Vacuum. *J. Chem. Phys.* **2016**, *144*, 164201.
- (6) Xu, Y. T.; Dibble, C. J.; Petrik, N. G.; Smith, R. S.; Kay, B. D.; Kimmel, G. A. Complete Wetting of Pt(111) by Nanoscale Liquid Water Films. *J. Phys. Chem. Lett.* **2016**, *7*, 541-547.
- (7) Xu, Y. T.; Petrik, N. G.; Smith, S.; Kay, B. D.; Kimmel, G. A. Growth Rate of Crystalline Ice and the Diffusivity of Supercooled Water from 126 to 262 K. *Proc. Natl. Acad. Sci. U. S. A.* **2016**, *113*, 14921-14925.
- (8) Yuan, C. Q.; Smith, R. S.; Kay, B. D. Surface and Bulk Crystallization of Amorphous Solid Water Films: Confirmation of "Top-Down" Crystallization. *Surf. Sci.* **2016**, *652*, 350-354.
- (9) Smith, R. S.; Kay, B. D. Desorption Kinetics of Benzene and Cyclohexane from a Graphene Surface. DOI: 10.1021/acs.jpcc.7b05102. **2017**.
- (10) Yuan, C. Q.; Smith, R. S.; Kay, B. D. Communication: Distinguishing between Bulk and Interface-Enhanced Crystallization in Nanoscale Films of Amorphous Solid Water. *J. Chem. Phys.* **2017**, *146*, 031102.

## Probing Ultrafast Electron (De)localization Dynamics in Mixed Valence Complexes Using Femtosecond X-ray Spectroscopy

**Lead PI:** Munira Khalil, University of Washington, Seattle, WA

**PI:** Niranjana Govind, EMSL, Pacific Northwest National Laboratory, Richland, WA

**PI:** Shaul Mukamel, University of California, Irvine, CA

**PI:** Robert Schoenlein, SLAC, Menlo Park, CA

### Project Goals

The overall goal of this project is to understand valence electron and vibrational motion following metal-to-metal charge transfer (MMCT) excitation in the following mixed valence complexes dissolved in aqueous solution:  $[(\text{NH}_3)_5\text{Ru}^{\text{III}}\text{NCFe}^{\text{II}}(\text{CN})_5]^-$  (**1**, FeRu),  $\text{trans}-[(\text{NC})_5\text{Fe}^{\text{II}}\text{CNPt}^{\text{IV}}(\text{NH}_3)_4\text{NCFe}^{\text{II}}(\text{CN})_5]^{4-}$  (**2**, FePtFe) and  $\text{trans}-[(\text{NC})_5\text{Fe}^{\text{III}}\text{CNRu}^{\text{II}}(\text{L})_4\text{NCFe}^{\text{III}}(\text{CN})_5]^{4+}$  (**3**, FeRuFe, L=pyridine). The project objectives are (i) to observe the time-dependent re-arrangement of *d* electrons across two transition metal sites and the bridging ligand following photoinduced MMCT excitation on a sub-50 fs timescale using femtosecond X-ray pulses generated at LCLS (ii) to simulate femtosecond X-ray absorption and emission spectra of solvated, photo-excited, transition metal mixed valence complexes using a realistic treatment of multi-electron correlations/transitions, spin-orbit coupling and final state lifetime effects and to propose and study the feasibility of nonlinear X-ray experiments on solvated transition metal mixed valence systems using future X-FEL light sources and (iii) to determine the role of coupled electronic and vibrational motions during ultrafast photoinduced charge transfer.

### Recent Progress

- ***Signatures of Vibronic Coupling in Two-Dimensional Vibrational-Electronic (2D VE) Spectroscopy.***

We have recently developed a Fourier transform (FT) 2D vibrational-electronic (2D VE) spectroscopy employing a sequence of mid-IR and optical pulses to interrogate coupled vibrational and electronic motions in the condensed phase. We simulated 2D VE spectra using a model Hamiltonian consisting of one anharmonic vibration and two electronic states. Equilibrium displacement of the vibrational coordinate and vibrational frequency shifts upon excitation to the first electronic excited state were included in our Hamiltonian through linear and quadratic vibronic coupling terms and we explicitly considered the nuclear dependence of the electronic transition dipole moment and demonstrated that these spectroscopies are sensitive to non-Condon effects. Our simulations showed that one of the following conditions must be met to observe signal: (1) non-zero linear and/or quadratic vibronic coupling in the electronic excited state, (2) vibrational-coordinate dependence of the electronic transition dipole moment, or (3) electronic-state-dependent vibrational dephasing dynamics.

- ***Equilibrium X-ray Absorption and X-ray Emission Spectroscopy of Transition Metal Mixed Valence Complexes in Solution.***

In order to understand the electronic configuration in the ground state of the transition metal complexes, we have obtained equilibrium X-ray absorption (XA) and X-ray emission (XE) spectra in water for the mixed valence complex complexes, FeRu, FeRuFe, FePtFe, and model complexes Fe(II)CN<sub>6</sub> and Fe(III)CN<sub>6</sub> at the Fe L-edge and the Fe K-edge. The spectra reveal that the oxidation state of the iron atoms in the FeRu and FePtFe complexes is Fe(II) and that of FeRuFe is Fe(III) in the ground electronic state. The successful collection of equilibrium spectra has allowed us to validate parameters in the simulation/computational codes for correctly modelling the electronic structure of the solvated mixed valence complexes. Our studies reveal the importance of carefully accounting for solute-solvent interactions for core-level spectroscopies. These spectra were obtained at APS 11 ID during August 2015 and at ALS BL 10.3.2 during January 2015 and January 2016. We are currently working on two manuscripts describing our equilibrium results.

- ***Femtosecond X-ray Absorption and X-ray Emission Spectroscopy of Transition Metal Mixed Valence Complexes in Solution.***

We were awarded beam time at LCLS under proposal LJ67 for five shifts in October 2015 and four shifts in December 2016. During 2015, experiments were performed at the X-ray pump probe (XPP) instrument at LCLS using 800 nm laser light to photo excite the sample preceding

X-ray measurements. Femtosecond XA and XE spectroscopies were used at the Fe K-edge to directly monitor transient oxidation states and orbital occupancy during charge transfer in a series of solvated mixed-valence complexes. A transition from Fe<sup>II</sup> to Fe<sup>III</sup> (as in FeRu) would result in a blue peak shift of ~0.2 eV and broadening of the K $\alpha_1$  peak consistent with the experimental transient XE result for FeRu. Transient XE spectra for FeRuFe exhibit the opposite, a red peak shift with spectral narrowing consistent with an Fe<sup>III</sup> to Fe<sup>II</sup> transition. Fits of the kinetic traces reveal that the initial MMCT from Fe<sup>II</sup>Ru<sup>III</sup> to Fe<sup>III</sup>Ru<sup>II</sup> and Fe<sup>III</sup>Ru<sup>II</sup>Fe<sup>III</sup> to Fe<sup>II</sup>Ru<sup>III</sup>Fe<sup>III</sup> occurs within the response of the instrument (50 fs) and the BET occurs within 100 fs for each compound. In the difference XA signal for FeRu, we see the growth of a transient feature upon MMCT which indicates that a hole is created in the t<sub>2g</sub> orbital. The other XANES peaks undergo shifts to the blue upon photoexcitation and a change in the linewidth indicating the adjustments of the metal d orbitals following the initial MMCT. Simulations of the transient XANES features reveal the extent of electron delocalization during the MMCT process. In a related effort, the Schoenlein group (in collaboration with Prof. T.-K. Kim, U. Pusan) has focused on the CN- bridged mixed valence transition-metal complex Ru<sup>II</sup>-CN-Cr<sup>III</sup>-CN-Ru<sup>II</sup> complex as a prototypical model system. Compared to the typical CN-bridged model complex (Ru<sup>II</sup>-CN-Ru<sup>III</sup>), the use of the covalently linked Cr<sup>III</sup> electron acceptor leads to remarkably long-lived charge-separated intermediates, attributed to the existence of electronic states of different spin multiplicity that effectively inhibit BET. The first time-resolved X-ray spectroscopy studies of this complex have recently been conducted at Advanced Photon Source. Transient XAS and XES at the Cr K-edge monitors changes in the local coordination geometry, changes in the spin multiplicity and electronic structure revealed by growth/disappearance of pre-edge features. The experimental results are now being analyzed via *ab initio* calculations to understand electron delocalization dynamics.

- **Simulating Valence-to-Core X-ray Emission Spectroscopy.** Valence-to-Core X-ray Emission Spectroscopy (VtC-XES) is a sensitive tool to identify ligands and characterize ligand valence orbitals in transition metal complexes. In the past year we studied how linear-response time-dependent density functional theory (LR-TDDFT) can be extended to simulate K-edge VtC-XES reliably. LR-TDDFT allows one to go beyond the single-particle picture. Specifically, we developed a “black box” protocol in NWChem to simulate these spectra. A systematic study of the K-edge VtC-XES spectra of a series of low- and high-spin model Fe-, Mn- and Cr-complexes was performed and compared with experiment. Our results are in good agreement with experiment. The study also revealed that our method has advantages over the conventional single-particle DFT approach in describing VtC-XES features that have multi-configuration character. These results have been published in the Journal of Chemical Theory and Computation in November 2015. We are in the process of calculating of simulating the VtC-XES for the dimer (FeRu) and trimer (FeRuFe) complexes. We have recently applied this technique to solid-state transition metal compounds (Physical Review B, September 2017). Simulating VtC-XES for transient species is also possible with our approach.

- **Ab Initio Molecular Dynamics/Molecular Mechanics (AIMD/MM), XA, UV/Vis and IR Spectroscopies of Model Transition Metal and Mixed Valence Complexes in Water on the Ground and Electronic Excited States.** The goal of this study is to elucidate the structural and spectroscopic changes of the dimer complex in a solvent environment both in the ground and excited states. In order to study solvated model Fe(CN)<sub>6</sub><sup>4-</sup> and Fe(CN)<sub>6</sub><sup>3-</sup> complexes in water, we have performed extensive hybrid AIMD/MM based molecular dynamics simulations with NWChem. The FeRu dimer complex QM/MM model involved the solvation in a simulation box containing the dimer complex with 5000 water molecules to give a density close to 1 g/cm<sup>3</sup>. The FeRuFe and FePtFe complexes contained 7919 and 5842 water molecules respectively to give a density close to 1 g/cm<sup>3</sup>. The QM region in our approach comprises the transition metal complex, while the aqueous environment was treated using a MM representation. The QM region was treated with a hybrid exchange-correlation functional (PBE0). Following the AIMD/MM runs, we extracted snapshots of the complex with an explicit solvation environment of water molecules from the trajectory to perform the XANES, UV/Vis, IR, EXAFS spectra calculations. The Fe K-edge XANES and UV/Vis spectra were calculated with our restricted excitation window (REW) TDDFT approach. We have extended our TDDFT code to capture the quadrupole transitions in the Fe K-edge XANES. For FePtFe, our extensive ground state calculations reveal that the closed-shell singlet configuration is the lowest energy state compared with the

triplet configuration in agreement with experiment. This is in contrast to previously published theoretical work on this system that reported a lower triplet state. For the FeRu and FeRuFe complexes, we have developed a new theoretical approach to tackle the transient-XAS to probe the x-ray absorption response of the UV-Vis excited transition metal complex. Our calculations, so far, are in good agreement with experiment. We have also performed VtC-XES calculations on representative clusters of the FeRu and FeRuFe complexes. For these calculations, we treat the solvent environment explicitly, which results in systems of approx. 300-350 atoms. VtC-XES calculations using the ground and excited-state geometries for the FeRu and FeRuFe complexes have also been performed.

- **Simulations of Core-Resonant Circular Dichroism Signals.** Core-resonant circular dichroism (CD) signals are induced by molecular chirality and vanish for achiral molecules and racemic mixtures. The highly localized nature of core excitations makes them ideal probes of local chirality within molecules. Our simulations of the circular dichroism spectra of several molecular families illustrate how these signals vary with the electronic coupling to substitution groups, the distance between the X-ray chromophore and the chiral center, geometry, and chemical structure. Clear insight into the molecular structure is obtained through analysis of the X-ray CD spectra. These proof-of-principle results were published in *Chemical Science* in 2017. Spin-orbit coupling (SOC) of the 2p electrons splits the XANES spectra and the electron-hole exchange interaction blurs the physical picture of the independent particle, thus the experimental intensity branching ratio of the transitions from the  $2p_{3/2}$  and  $2p_{1/2}$  orbitals may stray far from the ideal value of 2:1. Similarly, SOC should also play an important role in L-edge XCD. We neglected spin-orbit effects in our paper. However, there is every reason to expect that SOC should not affect the most important findings, *i.e.*, for molecules with a chiral center the amplitude of the XCD signals strongly decreases with the distance between the X-ray chromophore and the chiral center if the corresponding excitations are very localized to the excited atom, and that for globally chiral molecules the XCD signals also strongly depend on the chromophore position. A two-component TDDFT approach is under development for future XCD simulations including SOC of large molecules. This development potentially opens up new directions for our project.

- **Developments and new protocols in NWChem.** The following enhancements have been implemented or ongoing in the NWChem code over the course of this project:

1. Extensions to the TDDFT code in NWChem to capture quadrupole transitions ( $1s \rightarrow 3d$ ) which are relevant for transition metal K-edge XANES.
2. TDDFT restart capabilities that will allow a user to systematically increase the number of excitations from previously saved calculations.
3. Parallelization enhancements for TDDFT calculations up to 3000 basis functions.
4. “Black Box” valence-to-core x-ray emission spectroscopy (VtC-XES) protocol.
5. New QM/MM protocols for simulations of the model, dimer and trimer complexes in different solvents.
6. New transient XAS protocol to tackle simulations of pump (optical)-probe (X-ray) spectroscopy.
7. Development of TDDFT approach for XCD spectra.
8. Development of a simplified spin-orbit TDDFT approach for L-edge X-ray spectra
9. Development of two-component TDDFT to tackle spin-orbit effects in L-edge X-ray spectra (ongoing).

The enhancements described above (2 and 3) are especially relevant for response calculations on the trimer systems where the transition metal complex (solute) plus the explicit water molecules (solvent) can result in system sizes of ~300 atoms or more.

### Future Plans

We plan to accomplish the following in the next year. (i) Complete the data analysis of the transient X-ray spectroscopic and scattering signals for FeRu and FeRuFe in water. (ii) Perform transient IR experiments on FeRu and FeRuFe to follow vibrational relaxation following MMCT excitation. (iii) We are in the process of preparing several manuscripts combining experimental and computational data on the IR, electronic and core-hole spectroscopies on solvated mixed valence complexes. (iv) We will be performing further benchmark studies on our new transient XAS approach. (v) We will focus on the development of theoretical approaches for the calculation of L-edge and transient L-edge and RIXS spectra.

## DOE Supported Publications

1. B. E. V. Kuiken, M. R. Ross, M. L. Strader, A. A. Cordones, H. Cho, J. H. Lee, R. W. Schoenlein, and M. Khalil, "Picosecond sulfur K-edge x-ray absorption spectroscopy with applications to excited state proton transfer", *Structural Dynamics* **4** (2017) 044021.
2. S. Eckert, J. Norell, P. S. Miedema, M. Beye, M. Fondell, W. Quevedo, B. Kennedy, M. Hantschmann, A. Pietzsch, B. E. Van Kuiken, M. Ross, M. P. Minitti, S. P. Moeller, W. F. Schlotter, M. Khalil, M. Odelius, and A. Fohlisch, "Ultrafast independent N-H and N-C bond deformation investigated with resonant inelastic x-ray scattering", *Angew Chem Int Ed Engl* **56** (2017) 6088-6092.
3. J. D. Gaynor, and M. Khalil, "Signatures of vibronic coupling in two-dimensional electronic-vibrational and vibrational-electronic spectroscopies", *The Journal of chemical physics* **147** (2017) 094202.
4. B. E. Van Kuiken, H. Cho, K. Hong, M. Khalil, R. W. Schoenlein, T. K. Kim, and N. Huse, "Time-resolved x-ray spectroscopy in the water window: Elucidating transient valence charge distributions in an aqueous Fe(II) complex", *The Journal of Physical Chemistry Letters* **7** (2016) 465-470.
5. K. M. Slenkamp, M. S. Lynch, J. F. Brookes, C. C. Bannan, S. L. Daifuku, and M. Khalil, "Investigating vibrational relaxation in cyanide-bridged transition metal mixed-valence complexes using two-dimensional infrared and infrared pump-probe spectroscopies", *Structural Dynamics* **3** (2016) 023609.
6. Y. Zhang, S. Mukamel, M. Khalil, and N. Govind, "Simulating valence-to-core x-ray emission spectroscopy of transition metal complexes with time-dependent density functional theory", *Journal of Chemical Theory and Computation* **11** (2015) 5804-5809.
7. T. L. Courtney, Z. W. Fox, K. M. Slenkamp, and M. Khalil, "Two-dimensional vibrational-electronic spectroscopy", *The Journal of Chemical Physics* **143** (2015) 154201.
8. T. L. Courtney, Z. W. Fox, L. Estergreen, and M. Khalil, "Measuring coherently coupled intramolecular vibrational and charge-transfer dynamics with two-dimensional vibrational-electronic spectroscopy", *The Journal of Physical Chemistry Letters* **6** (2015) 1286-1292.
9. Y. Zhang, J. R. Rouxel, J. Autschbach, N. Govind, and S. Mukamel, "X-ray circular dichroism signals: a unique probe of local molecular chirality", *Chemical Science*, **8** (2017) 5969-5978.
10. D. R. Mortensen, G. T. Seidler, J. J. Kas, N. Govind, C. P. Schwartz, S. Pemmaraju, and D. G. Prendergast, "Benchmark results and theoretical treatments for valence-to-core x-ray emission spectroscopy in transition metal compounds", *Physical Review B* **96** (2017) 125136-125145.

## **Chemical Kinetics and Dynamics at Interfaces**

*Non-Thermal Reactions at Surfaces and Interfaces*

**Greg A. Kimmel (PI) and Nikolay G. Petrik**

Physical Sciences Division  
Pacific Northwest National Laboratory  
P.O. Box 999, Mail Stop K8-88  
Richland, WA 99352  
[gregory.kimmel@pnl.gov](mailto:gregory.kimmel@pnl.gov)

Collaborators include: BD Kay, RS Smith, and Y Xu

### **Program Scope**

The objectives of this program are to investigate 1) thermal and non-thermal reactions at surfaces and interfaces, and 2) the structure of thin adsorbate films and how this influences the thermal and non-thermal chemistry. Energetic processes at surfaces and interfaces are important in fields such as photocatalysis, radiation chemistry, radiation biology, waste processing, and advanced materials synthesis. Low-energy excitations (e.g. excitons, electrons, and holes) frequently play a dominant role in these energetic processes. For example, in radiation-induced processes, the high energy primary particles produce numerous, chemically active, secondary electrons with energies that are typically less than ~100 eV. In photocatalysis, non-thermal reactions are often initiated by holes or (conduction band) electrons produced by the absorption of visible and/or UV photons in the substrate. In addition, the presence of surfaces or interfaces modifies the physics and chemistry compared to what occurs in the bulk.

We use quadrupole mass spectroscopy, infrared reflection-absorption spectroscopy (IRAS), and other ultra-high vacuum (UHV) surface science techniques to investigate thermal, electron-stimulated, and photon-stimulated reactions at surfaces and interfaces, in nanoscale materials, and in thin molecular solids. Since the structure of water near interface plays a crucial role in the thermal and non-thermal chemistry occurring there, a significant component of our work involves investigating the structure of aqueous interfaces. A key element of our approach is the use of well-characterized model systems to unravel the complex non-thermal chemistry occurring at surfaces and interfaces. This work addresses several important issues, including understanding how the various types of low-energy excitations initiate reactions at interfaces, the relationship between the water structure near an interface and the non-thermal reactions, energy transfer at surfaces and interfaces, and new reaction pathways at surfaces.

In collaboration with Bruce Kay, we have developed a pulsed laser heating method that allows us to investigate deeply supercooled liquids by producing transiently heated films, which become liquids that last for approximately 10 ns per laser pulse. Subsequent rapid cooling due to the dissipation of the heat pulse into the metal substrate effectively quenches the liquid dynamics until the next laser heating pulse arrives. The rapid heating and cooling allows the system to reach previously unattainable supercooled liquid temperatures and return to the amorphous state before significant crystallization can occur.

## Recent Progress

### *The Growth Rate of Crystalline Ice and the Diffusivity of Supercooled Water from 126 K to 262 K*

A detailed understanding of supercooled water is crucial to solving many of the remaining mysteries of liquid water. A number of properties (both thermodynamic and transport) exhibit unusual behavior at low temperatures suggesting that there is a temperature,  $T_x \sim 228$  K, at which these properties diverge. For example, the diffusivity in normal liquid water exhibits Arrhenius behavior. However, upon supercooling (i.e., below  $\sim 273$  K) the temperature behavior of the diffusivity becomes markedly non-Arrhenius and the diffusivity rapidly decreases. Such a super-Arrhenius behavior is the hallmark of a so-called “fragile liquid” (In contrast, “strong” liquids exhibit Arrhenius behavior). Supercooled, glass forming liquids have been examined theoretically, and a number of different models have been proposed to explain the anomalous behaviors observed experimentally. Experimental measurements at temperatures near  $T_x$  are vital for resolving these outstanding issues. However, rapid homogeneous nucleation of crystalline ice has prevented experiments on bulk water below  $\sim 235$  K. Using our pulsed laser heating technique [7], we have measured the growth rate of crystalline ice,  $G(T)$ , for  $180 \text{ K} < T < 262 \text{ K}$ , i.e. deep within water’s “no man’s land” in ultrahigh vacuum conditions.[8] Isothermal measurements of  $G(T)$  were also made for  $126 \text{ K} \leq T \leq 151 \text{ K}$ . The self-diffusion of supercooled liquid water,  $D(T)$ , was obtained from  $G(T)$  using the Wilson-Frenkel model of crystal growth. For  $T > 237 \text{ K}$  and  $P \sim 10^{-8} \text{ Pa}$ ,  $G(T)$  and  $D(T)$  have super-Arrhenius (“fragile”) temperature dependences, but both crossover to Arrhenius (“strong”) behavior with a large activation energy in “no man’s land.” The fact that  $G(T)$  and  $D(T)$  are smoothly varying rules out the hypothesis that liquid water’s properties have a singularity at or near 228 K at ambient pressures. However the results are consistent with a previous prediction for  $D(T)$  that assumed no thermodynamic transitions occur in “no man’s land.”

### *Adsorption and Photodesorption of CO from Charged Point-Defects on TiO<sub>2</sub>(110)*

CO adsorption on the rutile TiO<sub>2</sub>(110) surface has been extensively studied theoretically and experimentally. CO, which has a small dipole moment, adsorbs on the five-fold coordinated Ti sites (Ti<sub>5c</sub>) normal to the surface with the more negative carbon atom down. The interaction of CO with the bridging oxygen vacancy (V<sub>O</sub>) on the reduced surface has been a controversial topic for many years. Many DFT calculations indicate that the binding energy for CO in a vacancy is higher by 0.01 – 0.15 eV than on the Ti<sub>5c</sub> sites. On the other hand, the first scanning tunneling microscopy (STM) study at 80 K reported that CO molecules are mobile and spend relatively little time in the vacancies or in the Ti<sub>5c</sub> sites directly adjacent to them. Instead, most of the CO was found at Ti<sub>5c</sub> sites that are next-nearest to the vacancy. The study concluded that these sites are the primary locations for the CO adsorption on reduced TiO<sub>2</sub>(110). We recently studied the adsorption and photochemistry of CO on rutile TiO<sub>2</sub>(110) using scanning tunneling microscopy (STM), temperature-programmed desorption and angle-resolved photon-stimulated desorption (PSD) at low temperatures.[9] In contrast to previous studies, we found that the adsorption probability was the highest for the bridging oxygen vacancies (V<sub>O</sub>) and that, except for the Ti<sub>5c</sub> site next to the vacancies, the adsorption probabilities for the other sites were all comparable. The probability distribution for the various adsorption sites corresponds to very small differences

in CO adsorption energies ( $< 0.02$  eV). We also found that UV irradiation stimulates diffusion and desorption of CO at low temperature. The CO photodesorbs primarily from the vacancies with a bi-modal angular distribution, indicating some scattering from the surface which also leads to photo-stimulated diffusion. Hydroxylation of  $V_O$ 's does not significantly change the CO PSD yield or the angular distribution, which suggests that photodesorption can be initiated by recombination of photo-generated holes with excess electrons localized near the charged point defect (either  $V_O$  or bridging hydroxyl).

### ***Quenching of Electron Transfer Reactions Through Coadsorption: A Study of Oxygen Photodesorption from $TiO_2(110)$***

$TiO_2$  is a widely used photocatalyst. Its ability to oxidize organic contaminants makes it useful, for example, in air and water purification systems and as a thin-film coating for self-cleaning surfaces. As a result of titanium oxide's practical applications and its potential use in photocatalytic water splitting, it has been the subject of a tremendous amount of research. Despite this, fundamental questions regarding the roles of photo-generated electrons and holes, band bending, and defects in the photochemistry remain unresolved. Using temperature programmed desorption (TPD) and photon stimulated desorption (PSD), we investigated the influence of a variety of adsorbates on the photodesorption of  $O_2$  from rutile  $TiO_2(110)$ . [6] We showed that coadsorbates of varying binding energies on the  $TiO_2(110)$  surface exert a commensurate inhibiting influence on the hole-mediated photodesorption of adsorbed  $O_2$ . A variety of coadsorbates (Ar, Kr, Xe,  $N_2$ , CO,  $CO_2$ ,  $CH_4$ ,  $N_2O$ , acetone, methanol or water) were shown to quench  $O_2$  photoactivity, with the extent correlating with the coadsorbate's gas phase basicity, which in turn determines the strength of the coadsorbate- $Ti^{4+}$  bond. Coadsorbed rare gases inhibited the photodesorption of  $O_2$  by  $\sim 10$ -25%, whereas strongly bound species (water, methanol and acetone) nearly completely inhibited  $O_2$  PSD. We suggest that coadsorption of these molecules inhibit the arrival probability of holes to the surface. Band bending effects, which vary with the extent of charge transfer between the coadsorbate and the  $TiO_2(110)$  surface, are not expected to be significant in the cases of the rare gases and physisorbed species. These results indicate that neutral coadsorbates can exert a significant influence on charge transfer events by altering the interfacial dipole in the vicinity of the target molecule.

### **Future Directions:**

Important questions remain concerning the factors that determine the structure of thin water films on various substrates. We plan to continue investigating the structure of thin water films on non-metal surfaces, such as oxides, and on metals where the first layer of water does not wet the substrate. For the non-thermal reactions in water films, we will use IRAS to characterize the electron-stimulated reaction products and precursors. We will also continue our investigations into the photochemistry of small molecules on  $TiO_2(110)$ . The pulsed laser heating experiments will focus on exploring diffusion, crystallization, and isotope exchange kinetics of supercooled water in the temperature range 180-273K.

### **References to publications of DOE-sponsored research (FY 2015 – present)**

- [1] Nikolay G. Petrik, Michael A. Henderson, and Greg A. Kimmel, "Insights into Acetone Photochemistry on Rutile  $TiO_2(110)$ . 1. Off-Normal  $CH_3$  Ejection from Acetone Diolate," *J. Phys. Chem. C.*, **119**, 12262 (2015). (DOI: 10.1021/acs.jpcc.5b02477).

- [2] Nikolay G. Petrik, Michael A. Henderson, and Greg A. Kimmel, "Insights into Acetone Photochemistry on Rutile TiO<sub>2</sub>(110). 2. New Photodesorption Channel with CH<sub>3</sub> Ejection along the Surface Normal," *J. Phys. Chem. C.*, **119**, 12273 (2015). (DOI: 10.1021/acs.jpcc.5b02478).
- [3] Konrad Thürmer, Chunqing Yuan, Greg A. Kimmel, Bruce D. Kay, R. Scott Smith, "Weak interactions between water and clathrate-forming gases at low pressures," *Surf. Sci.* **641**, 216-223 (2015). (DOI: 10.1016/j.susc.2015.07.013).
- [4] Nikolay G. Petrik and Greg A. Kimmel, "Reaction Kinetics of Water Molecules with Oxygen Vacancies on Rutile TiO<sub>2</sub>(110)," *J. Phys. Chem.* **119**, 23059 (2015) (DOI: 10.1021/acs.jpcc.5b07526).
- [5] Yuntao Xu, Collin J. Dibble, Nikolay G. Petrik, R. Scott Smith, Bruce D. Kay, and Greg A. Kimmel, "Complete Wetting of Pt(111) by Nanoscale Liquid Water Films," *J. Phys. Chem. Lett.* **7**, 541 (2016). (DOI: 10.1021/acs.jpcclett.5b02748).
- [6] Nikolay G. Petrik, Greg A. Kimmel, Mingmin Shen, Michael A. Henderson, "Quenching of Electron Transfer Reactions Through Coadsorption: A Study of Oxygen Photodesorption from TiO<sub>2</sub>(110)," *Surf. Sci.* **562** (2016) 183 (DOI: 10.1016/j.susc.2015.12.038).
- [7] Yuntao Xu, Collin J. Dibble, Nikolay G. Petrik, R. Scott Smith, Alan G. Joly, Russel G. Tonkyn, Bruce D. Kay, and Greg A. Kimmel, "A Nanosecond Pulsed Laser Heating System for Studying Liquid and Supercooled Liquid Films in Ultrahigh Vacuum," *J. Chem. Phys.* **144** (2016) 164201 (DOI: 10.1063/1.4947304).
- [8] Yuntao Xu, Nikolay G. Petrik, R. Scott Smith, Bruce D. Kay and Greg A. Kimmel, "The growth rate of crystalline ice and the diffusivity of supercooled water from 126 K to 262," *Proc. Nat. Aca. Sci.* **52** (2016) 14921. (DOI: 10.1073/pnas.1611395114).
- [9] Rentao Mu, Arjun Dahal, Zhi-Tao Wang, Zdenek Dohnálek, Greg A. Kimmel, Nikolay G. Petrik, and Igor Lyubinetsky, "Adsorption and Photodesorption of CO from Charged Point-Defects on TiO<sub>2</sub>(110)," *J. Phys. Chem. Lett.* **8**, 4565 (2017) (DOI: 10.1021/acs.jpcclett.7b02052).

# 2D IR Microscopy—Technology for Visualizing Chemical Dynamics in Heterogeneous Environments

PI: Amber T. Krummel

Colorado State University, 200 W. Lake Street, Fort Collins, CO 80525

[amber.krummel@colostate.edu](mailto:amber.krummel@colostate.edu)

## 1. Program Scope

Chemistries crucial for energy technologies including battery technology, fuel cell technology, and enhanced oil recovery take place in heterogeneous environments. Understanding and predicting chemical dynamics, including solute-solvent interactions, adsorption processes, and transport processes, to name a few, requires the ability to probe these events directly and ultimately visualizing these processes via microscopy. The overarching goal of this project is to develop two-dimensional infrared (2D IR) imaging tools to directly probe chemical interactions in heterogeneous environments, with geochemical systems being our primary target in this project. A combination of experiments directed toward technology development, the exploration of fundamental chemical physics of large macrocycles and acidic oils, and culminating with the direct visualization of chemical interactions in model pore structures. This project builds from our expertise in fabricating IR compatible microfluidic structures, in developing a 100 kHz 2D IR spectrometer, and in probing the nanoaggregates of large macrocycles.

The large number of observables offered by 2D IR spectroscopy allows us to disentangle and quantify complex chemical interactions in ways that were not previously feasible. These observables include the direct measurement of the frequency-frequency correlation function, which is a direct measure of the homogeneous and inhomogeneous contributions to the vibrational lifetime; and the peak positions (both diagonal peaks and cross peaks) and intensities, which are a direct measure of molecular structure. Each of these observables can be spatially resolved. We will interface a microscope with a high-speed 2D IR spectrometer, thus we will be able to perform 2D IR imaging at acquisition rates suitable for probing length scales beyond the micrometer length scale, resulting in connections being made between molecular length scale interactions to mesoscale phenomena.

## 2. Recent Progress & Current Efforts

The start date of this project was July 15, 2016. In the past 15 months our efforts have been two-fold: 1. Interface a 2D IR spectrometer with microfluidic device technology, and 2. Integrate a microscope head with our high-repetition rate 2D IR spectrometer.

Microfluidic devices afford precision control over sample handling and mixing, as well as a path to reduce the amounts of materials required in a kinetics experiment. At this time, we can produce IR compatible microfluidic devices in hard materials such as CaF<sub>2</sub> and in polymeric materials including PDMS (poly(dimethyl siloxane)) and COC (cyclic olefin copolymers). Producing IR compatible devices in polymeric materials allows inexpensive, bench-top fabrication processes to be employed. As such, a broad range of investigators can use this microfluidic device technology. Producing high-throughput 2D IR spectroscopy measurements allows us to observe the vibrational response of mixed solvent environments across a microfluidic device without having to create numerous samples, successfully minimizing chemical usage and experiment time. Furthermore, we improved the quality of our 2D IR spectroscopy measurements in the past year to produce 2D IR spectra on-chip that are scatter-free, Figure 1.<sup>1</sup> In order to improve the quality of the 2D IR spectra acquired, we

implemented a rotating frame in the pulse shaper and utilized irises to spatially filter scatter that was not fully removed by the rotating frame.

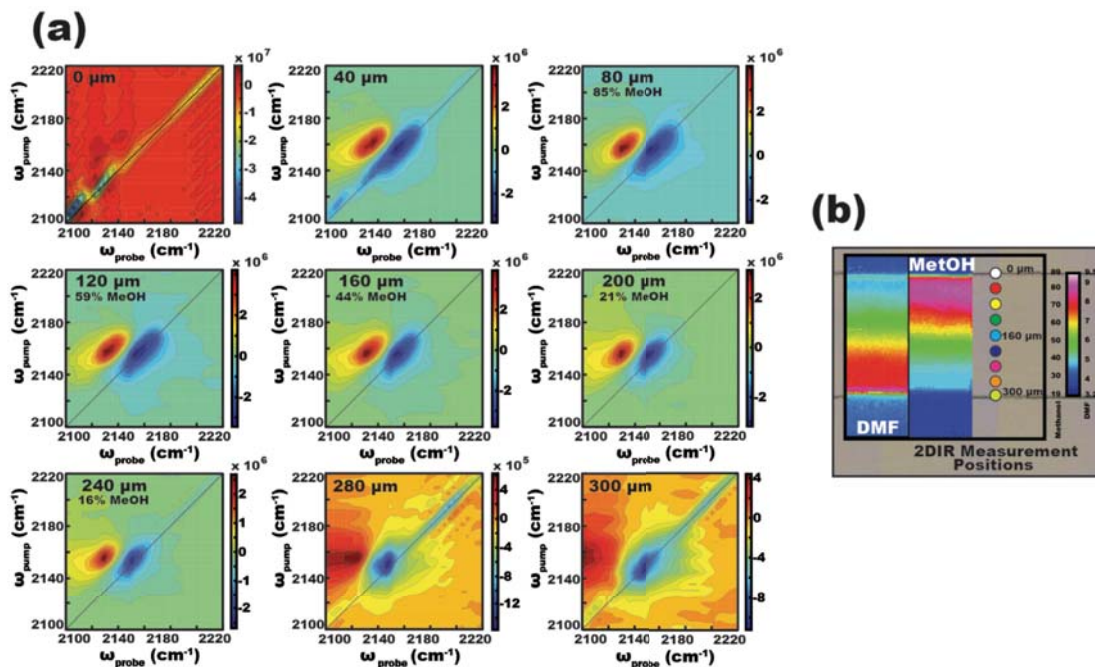


**Figure 1.** (a) 2D IR spectra collected across the microfluidic channel moving from 100% methanol to 100% dimethyl formamide by volume and (b) the IR chemical map images integrated from 3136 to 3189  $\text{cm}^{-1}$  for the solvent methanol and from 1720 to 1728  $\text{cm}^{-1}$  for the solvent DMF. The dots indicate the locations of 2D IR measurements across the channel.

In a parallel effort we have designed and built a microscope head to interface with our high repetition rate 2D IR spectrometer. Recently, 2D IR microscopy in a point scanning geometry<sup>2</sup> and a wide-field geometry were demonstrated;<sup>3</sup> in each experiment a polystyrene bead containing metal carbonyl molecules were imaged. In each case, the images were acquired over a period of hours due to the intrinsic spectral acquisition rate associated with a 1 kHz laser system. Taking advantage of our 100 kHz mid-IR laser system that drives our high-repetition rate 2D IR spectrometer, we have been able to improve acquisition rates of 2D IR microscopy images. Currently we shape mid-IR pulses and detect the mid-IR signal fields at a 100 kHz repetition rate—the current speed limit of shaping and detection technology. In order to maintain these acquisition speeds we have designed a microscope head to utilize the point scanning geometry. The general layout of our 2D IR microscope is given in Figure 2.

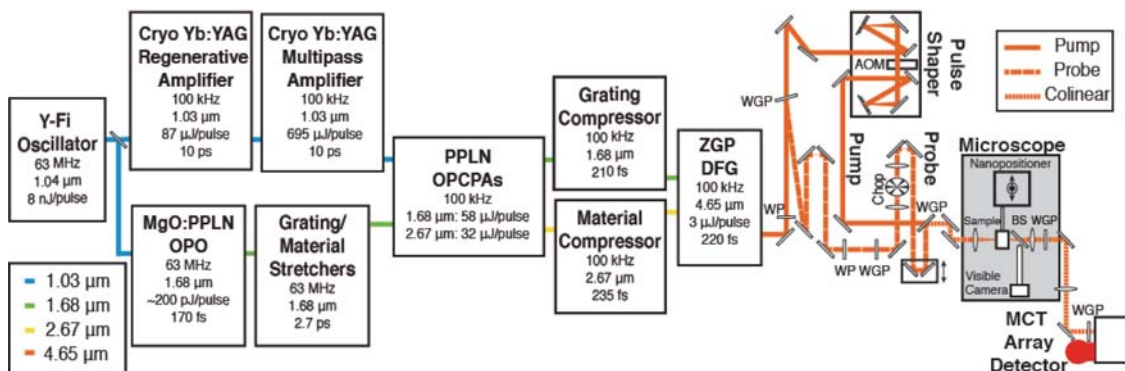


**Figure 2.** The general layout of 100 kHz mid-IR laser system and 2D IR microscope.

In order to perform 2D IR microscopy, a collinear beam geometry is utilized and spectra are collected in a cross polarization (XXYY) geometry. To implement this approach, the probe pulse polarization is rotated by  $90^\circ$  with a  $\lambda/2$  plate, creating an S-polarized probe. In order to be able to collect data in both a 4- and 8-frame phase cycling set up, we also included a chopper in the probe line. The probe pulse is then overlapped with the P-polarized pump in a wire-grid polarizer, which transmits the two pump pulses and reflects the probe pulse. The three pulses are focused into the sample by a Ge/Si Achromatic lens and then re-collimated using a Si lens and sent to the detector. The two polarizers before the detector are used to block the pump pulses and transmit the probe and signal. The sample positioning for the microscope utilizes a combination of nanopositioners and micropositioners to raster scan the sample. Nanopositioners are used in X-Y-Z in order to navigate  $200\ \mu\text{m}$  in each dimension with high precision and speed. The three-axis nanopositioners are integrated on a X-Y micropositioner with  $25\ \text{mm}$  of travel in each dimension. This combination of stages affords the potential of performing linear IR and 2D IR microscopy across multiple length scales. The initial objectives that have been employed are long working distance objectives with 2x and 5x magnifications; these objectives were chosen based on the anticipated beam diameters at the image plane. In addition, a CMOS camera has been incorporated into the system in order to capture bright field images along with chemical maps generated from linear IR and 2D IR spectral acquisitions.

We have been able to collect a 2D IR chemical map of a polystyrene bead that had been soaked in methyl thiocyanate in chloroform and then dried and placed between two  $\text{CaF}_2$  plates. We were able to successfully collect the image in a 4-frame phase cycling scheme, Figure 3. We have designed our 2D IR microscope to collect up to 10,000 points of 2D IR spectra in 40 minutes under fully automated conditions. Current efforts are focused on using our 2D IR microscope to investigate chemical systems that are relevant to energy technologies.

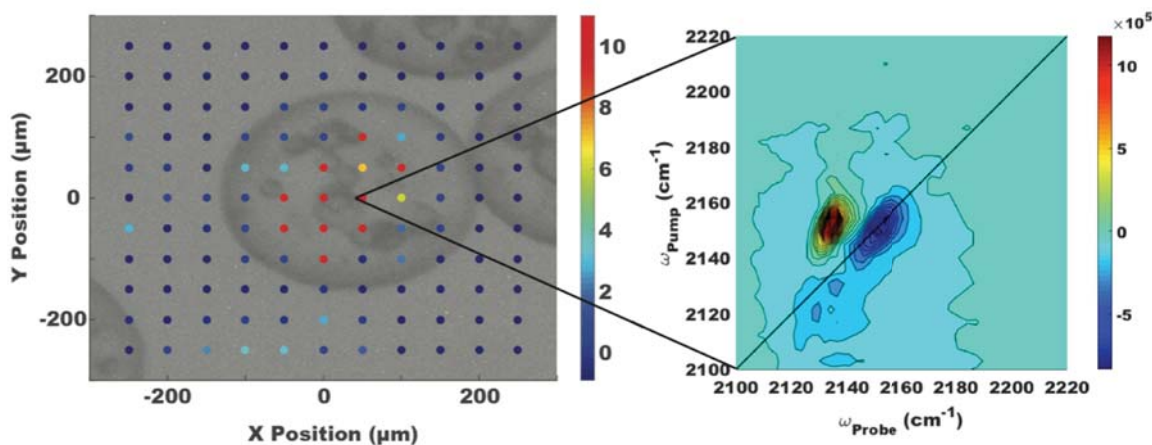


**Figure 3.** 2D IR microscopy image of a polystyrene bead with methyl thiocyanate in chloroform. The color bar represents the integrated intensity of the peak in the 2D IR spectrum associated with the  $\nu=1$  to  $\nu=2$  transition.

### 3. Future Plans

The second year of this project is focused on calibrating our 2D IR microscope and using it to collect 2D IR microscopy images of chemical systems that are relevant to energy technologies. As part of these efforts we will also improve the tunability of the 100 kHz midIR OPCPA that drives these 2D IR spectroscopy and microscopy experiments. Our

approach to add more tunability to this system will be to generate continuum in a YAG crystal and use the continuum to seed our existing ZGP OPA. It is expected that this approach will yield tunable midIR light that spans the 3.0  $\mu\text{m}$  to 8.0  $\mu\text{m}$  wavelength region. Thus, opening the ability to use this 2D IR spectrometer and microscope to probe macrocyclic molecules and acids directly.

#### 4. Publications

Given the July 15, 2016 start date of this project, no publications have been produced under this award, but one manuscript is in preparation at this time.

#### References:

<sup>1</sup>Tracy, K. M.; Barich, M. V.; Carver, C. L.; Luther, B. M.; Krummel, A. T. *The Journal of Physical Chemistry Letters* **2016**, 7 (23), 4865–4870.

<sup>2</sup>Baiz, C. R.; Schach, D.; Tokmakoff, A. *Opt. Express*, OE 2014, 22 (15), 18724–18735.

<sup>3</sup>Ostrander, J. S.; Serrano, A. L.; Ghosh, A.; Zanni, M. T. *ACS Photonics* 2016.

# Probing charge density and surface chemistry of nanostructured electrodes using single-particle spectro-electrochemistry

Christy F. Landes and Stephan Link

Department of Chemistry, Department of Electrical and Computer Engineering  
Rice University, Houston, TX 77005 USA  
*cflandes@rice.edu, slink@rice.edu*

13<sup>th</sup> Condensed Phase and Interfacial Molecular Science Research PI Meeting  
US Department of Energy, Basic Energy Sciences  
October 16-18, 2017

## 1. Program Scope

*The goal of this project is to correlate the activity of plasmonic electrocatalysts with nanoparticle morphology, surface chemistry, and 'hot' carrier physics using single particle spectroelectrochemical microscopy. One of the keys to developing compact, robust, and affordable power sources is the identification of novel catalytic supports and reactions. Nanoparticles are of increasing interest because they provide a larger surface to volume ratio compared to flat surfaces. Additionally, new selectivities and activities are achievable with nanoparticle based electrocatalysts compared to single crystalline metal electrodes. For example, 'noble metal' Au nanoparticles with diameters of 5-100 nm, initially considered inert and not suited for catalysis, show a significant catalytic activity for many reactions including methanol oxidation, oxygen reduction, and hydrogen peroxide reduction. However, it still remains controversial how nanoscale properties determine the catalytic activity because most previous studies measured innately heterogeneous distributions of nanoparticles. It is therefore not known if the average catalytic activity arises from an almost equal contribution of all nanoparticles or if only a few, 'superactive' nanoparticles dominate the signal. To resolve this and other issues and to be able to optimize electrocatalysts, it is thus necessary to characterize the catalytic activity at the single nanoparticle level. The central hypothesis is that the catalytic activity of plasmonic electrocatalysts can be tuned via controlling the population and dynamics of excited charge carriers, and strongly depends on size, shape, crystal facet, and surface chemistry. State of the art single particle and single molecule spectroscopic techniques are employed to probe electrocatalytic activities. Further, the redox events associated with molecular affinity or electric field hot spots, which are typically localized to dimensions much smaller than the diffraction limit of light, are investigated. Specifically, the following two aims are pursued:*

(1) Determine the catalytic activities of single nanoelectrocatalysts and correlate them with their structural morphologies. (2) Investigate the effects of plasmon enhancement on the electrocatalytic activities of single metal nanoparticles and demonstrate feasibility of superresolution mapping of catalytic activity.

## 2. Recent Progress

In the last year, we addressed the project's central hypothesis, that the catalytic activity of plasmonic electrocatalysts can be tuned via controlling the population and dynamics of excited charge carriers, and that the activity strongly depends on size, shape, crystal facet and surface chemistry. One existing controversy in charge dependent plasmonics is how the plasmon resonance, linewidth, and intensity tune with shape and relative surface area. Our work pursued a detailed experimental and theoretical treatment of this issue. We studied the shape dependent spectral response of the gold nanoparticle surface plasmon resonance at various electron densities to provide mechanistic insight into the role of capacitive charging, a topic of some debate. We demonstrated a morphology dependent spectral response for gold nanoparticles due to capacitive charging using single particle spectroscopy in an inert electrochemical environment. A decrease in plasmon energy and increase in spectral width for gold nanospheres and nanorods was observed as the electron density was tuned through a potential window of -0.3 to 0.1 V (Figure 1). The combined observations could not be explained by existing theories. A new quantum theory for charging based on the random phase approximation was developed along with our Rice collaborators. Additionally, the redox reaction of gold oxide formation was probed using single particle plasmon voltammetry to reproduce the reduction peak from the bulk cyclic voltammetry. These results deepen our understanding of the relationship between optical and electronic properties in plasmonic nanoparticles and provide insight towards their potential applications in directed electrocatalysis. This work was published in the *Journal of Physical Chemistry Letters* (Ref. 1).

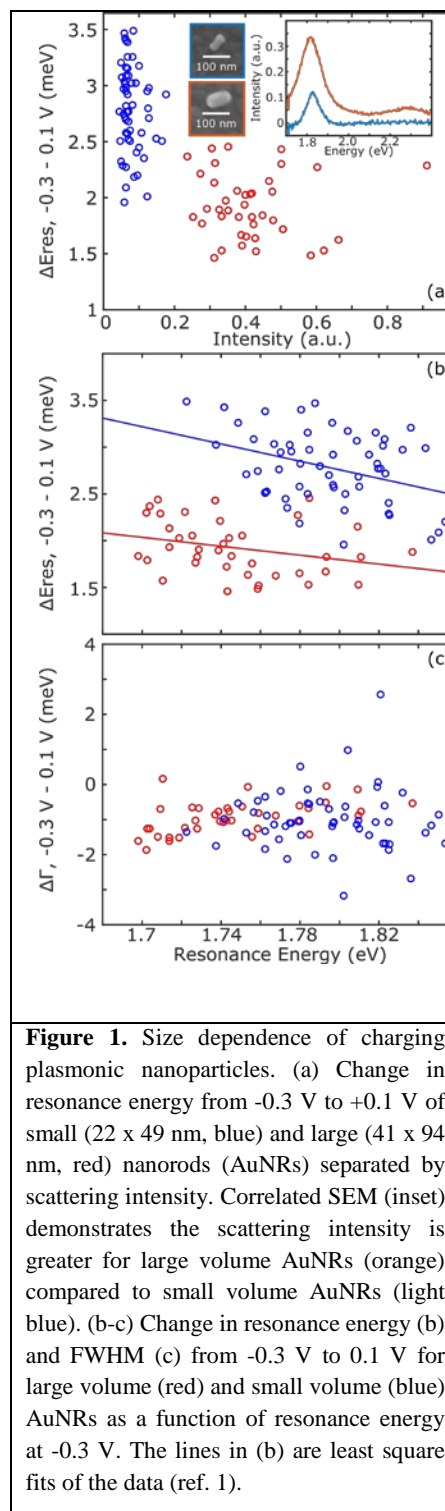
We additionally have exciting unpublished results on spectroelectrochemically directed dissolution. The ability to select the surface facet on which adsorptive catalysis occurs can strongly influence selectivity and yields. The goal is achieve a mechanistic understanding of selective dissolution. The ability to select the surface facet on which reactant adsorption occurs is one important goal towards improving selectivity and yields, as well as reducing catalyst fouling. We also directed our attention towards the unsolved problem that spectroelectrocatalysis often introduces irreversible changes to the nanocatalysts and/or their surroundings. The challenge lies in monitoring heterogeneous nonequilibrium dynamics via the slow, serial methods that are intrinsic to almost all spectral acquisition methods with suitable spatial and/or spectral resolution. We have overcome this challenge with a new metrology, *snapshot hyperspectral imaging (SHI)* that facilitates *in situ* readout of the 0th and 1st order diffractions of the dark-field

scattering from many individual plasmonic nanoparticles to simultaneously extract their respective spectra. Evanescent wave excitation with a supercontinuum laser enabled signal to noise ratios greater than 100 with a time resolution of only 1 ms. Throughput of  $\sim 100$  simultaneous spectra was achieved with a highly ordered nanoparticle array, yielding a spectral resolution of 0.21 nm/pixel (Figure 2). Additionally, an alternative dark-field excitation geometry utilized a combination of a supercontinuum laser and a reflecting objective for polarization controlled snapshot hyperspectral imaging. With SHI it will be possible to understand the influence of particle heterogeneity on the kinetics of irreversible plasmon mediated processes, and in general advance a variety of research fields in nanoscience and nanotechnology.

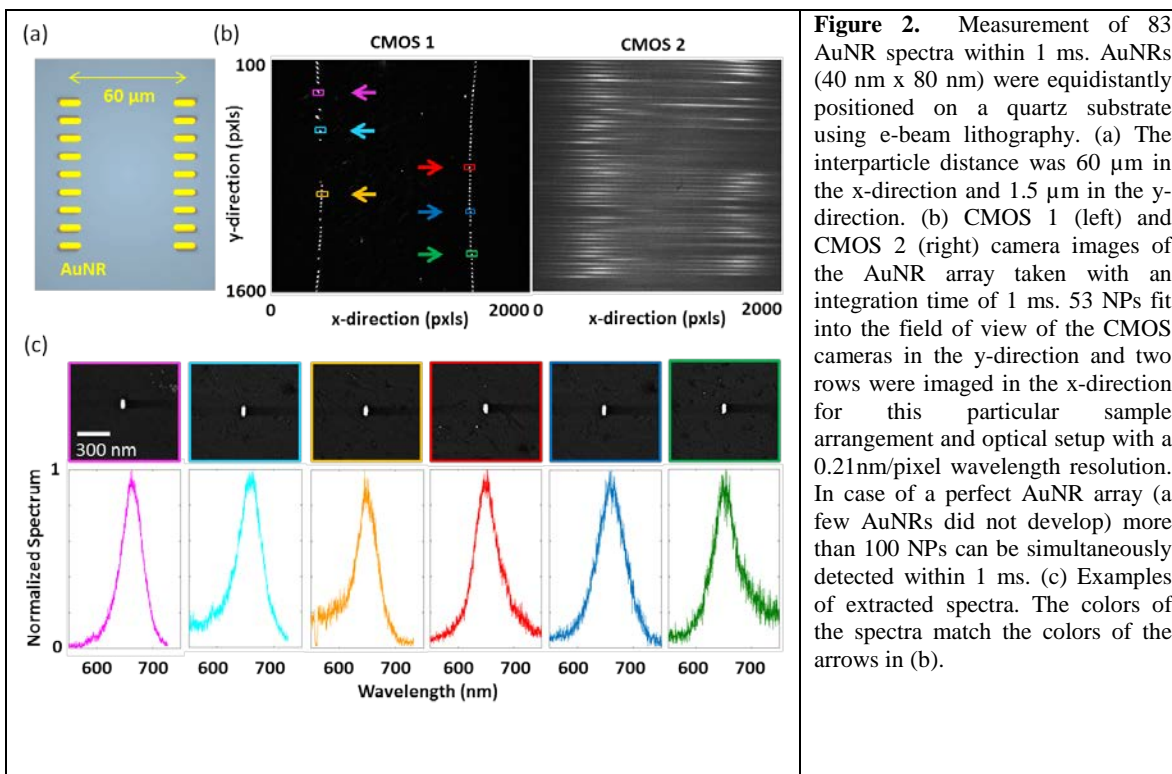
The benefit of this project lies in that if the interparticle and intraparticle heterogeneity using single nanoparticle spectroscopies can be resolved, it is possible to elucidate information about how excited charge carriers participate in electrocatalysis by correlating the catalytic activities with nanoparticle morphology, surface chemistry, and carrier physics. The outcomes gained from this work will lead to the rational design of optimized plasmonic electrocatalysts for various redox reactions, a crucial step in realizing portable, reusable power sources. Furthermore, several new, sophisticated single particle spectroscopy techniques are developed and students are trained on a wide range of physical characterization tools and electromagnetic modeling which can prepare the students to be leading experts in the energy sector.

### 3. Future Plans

The main focus of future studies is to understand the role of hot carriers on the electrocatalytic properties of plasmonic nanoparticles (aim 2). While we have so far used



the plasmon resonance as an optical probe to follow charging and surface adsorption, plasmon excitation, especially if carried out with selective laser wavelengths with varying powers, can create hot carriers that shift the Fermi level and enable selective redox reactions that are otherwise only possible at much higher electrochemical potentials. Electrogenerated chemiluminescence from redox reactions on single gold nanoparticles will be monitored with and without illumination with a plasmon resonant laser. The use of electrogenerated chemiluminescence has the advantage that no probe light is needed to follow the corresponding redox reaction: Products in an excited state are created at an applied electrochemical potential and emit.



#### 4. References

- 1) B. S. Hoener, H. Zhang, T. S. Heiderscheid, S. R. Kirchner, A. S. De Silva Indrasekara, R. Baiyasi, Y. Cai, P. Nordlander, S. Link, C. F. Landes, W.-S. Chang *Spectral Response of Plasmonic Gold Nanoparticles to Capacitive Charging: Morphology Effects*. *J. Phys. Chem. Lett.* 8, 2681–2688 (2017).
- 2) S. R. Kirchner, K. Smith, W. Wang, Y.-Y. Cai, C. Kinnear, H. Zhang, W.-S. Chang, P. Mulvaney, C. F. Landes, S. Link *Snapshot Hyperspectral Imaging (SHI) for Revealing Irreversible and Heterogeneous Plasmonic Processes*. Submitted.

**DEVELOPMENT OF APPROACHES TO MODEL EXCITED STATE CHARGE AND ENERGY TRANSFER IN SOLUTION: QUANTUM DYNAMICS APPROACHES FOR MODELLING CHARGE AND ENERGY TRANSFER IN SOLUTION**

Christine Isborn<sup>1</sup> (PI), Aurora Clark (co-PI)<sup>2</sup>, Thomas Markland (co-PI)<sup>3</sup>

1. University of California Merced, Email: cisborn@ucmerced.edu

2. Washington State University, Email: auclark@wsu.edu

3. Stanford University, Email: tmarkland@stanford.edu

Andres Montoya-Castillo, William C. Pfalzgraff, Aaron Kelly, Thomas E. Markland  
Department of Chemistry, Stanford University, Stanford, California, USA

### **Program Scope**

The development of next generation energy conversion and catalytic systems requires fundamental understanding of the interplay between photo-excitation and the resulting proton and electron transfer processes that occur in solution. To address these challenges requires accurate and efficient methods to compute ground and excited states, as well as the ability to treat the dynamics of energy transfer in the presence of solvent fluctuations. Our team is developing accurate and efficient theoretical models for solution phase reactions. These developments provide an improved understanding of photo-initiated excitations, electron transfer, and proton coupled electron transfer processes.

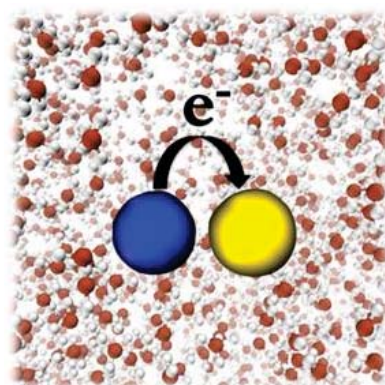
Our research team brings together expertise in electron and nuclear dynamics (classical and quantum), electronic structure, and analysis of solvation networks. We are developing and validating techniques for modeling condensed phase reactions. For reliable condensed phase simulations, an accurate model that includes both short- and long-range interactions is required. Short- and long-range interactions may be particularly strong in aqueous solution, where hydrogen-bonding and proton transfer may play a large role at short range and polarization may play a large role at long-range. For realistic condensed phase calculations that take into account solute-solvent interactions large-scale quantum mechanical (QM) calculations that include the condensed phase environment are necessary. These large-scale calculations can also help us determine what physics is necessary for more approximate models. The Isborn group is using excited state time-dependent density functional theory calculations that include the condensed phase to determine how to accurately model chromophores in solution. We are exploring various aspects of modeling condensed phase systems, including examination of basis set and density functional dependence [1], the limitations of the adiabatic approximation in time-dependent density functional theory [2], the role of nuclear quantum effects [3] and vibronic effects [7] on computed absorption spectra, the best choice of classical solvent model [4], and how much QM solvent to include in a calculation [4, 5, 6].

### **Recent Progress**

The development of next generation energy conversion and catalytic systems requires fundamental understanding of the interplay between photo-excitation and the resulting proton and electron transfer processes that occur in solution. To address these challenges requires accurate and efficient methods to compute ground and excited states, as well as the ability to treat the dynamics of energy transfer in the presence of solvent fluctuations. Our team is developing accurate and efficient theoretical models for solution phase reactions. These developments provide an improved understanding of photo-initiated

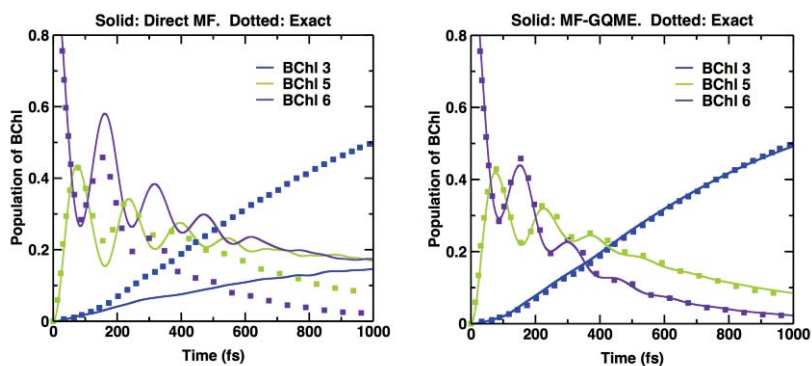
excitations, electron transfer, and proton coupled electron transfer processes.

The exact treatment of real time nonadiabatic quantum dynamics in condensed phase chemical systems remains a significant challenge that spurs the ongoing development of approximate methods that are accurate, efficient, and can treat large systems with a wide range of different forms of interactions. Quantum-classical (semiclassical) trajectory based methods provide some of the most appealing solutions to this problem that offer a hierarchy of approaches with different balances between accuracy and computational cost. However, since moving up this hierarchy typically requires orders of magnitude more computational effort, only the lowest tiers are likely to be practical, both now and in the foreseeable future, for nonadiabatic problems containing large quantum subsystems. In this talk, I will discuss our recent research showing how quantum-classical approaches can be made both more accurate and efficient by combining them with the formally exact quantum master equation framework. This combination of quantum-classical theory and master equation techniques makes it possible to obtain the accuracy of much more computationally expensive approaches at a cost an order of magnitude lower than even the most efficient trajectory-based approaches, providing the ability to treat the quantum dynamics of atomistic condensed phase systems for long times. In our recent research, we have applied the MF-GQME method to study the non-equilibrium quantum dynamics of an atomistic model of electron transfer incorporating two molecules that can exchange charge in a fully atomistic environment (liquid water) [7]. This demonstrates that proceeding via the GQME to generate quantum dynamics offers efficiency and accuracy benefits beyond the assumptions of harmonic environments and linear subsystem-environment coupling [7]. The successful treatment of electron transfer builds towards the further objective of accurately treating proton coupled electron transfer (PCET) in solution and at electrode interfaces.



We have also shown analytically the cases where a GQME approach is likely to be able to give a more accurate solution than direct application of the approximate method [2]. When approximate methods, such as those arising from the quantum-classical and semiclassical hierarchies, are used to calculate the memory kernel, significant improvements in accuracy have been observed when compared to their direct application. However, such improvements sensitively depend on how one calculates the projection-free partial kernels that are used to construct the memory kernel. These observations naturally raise questions as to why this is and when proceeding via the projection operator formalism will be advantageous. In our recent work we have demonstrated the conditions which must be satisfied to obtain gains in accuracy when proceeding via the GQME formalism.

However, one can also use manipulations that are satisfied by exact quantum mechanics (but which may not be satisfied by an approximate method), to cast the expression for the memory kernel into a different form. We show that this alternate form of the memory kernel is *guaranteed* to give an identical result to that obtained from the direct dynamics. By considering the connections between these forms of the kernel, we derive the conditions that approximate methods must satisfy if they are to offer different results when used in conjunction with the GQME formalism. This research thus uncovers the origins of why the



GQME approach is able to improve the accuracy of some approaches and hence informs the application of these approaches.

A concern that has been raised about the ability to use the GQME formalism to accelerate and improve the accuracy of quantum classical methods is that, for a system with  $N_s$  subsystem states, the size of the memory kernel that must be generated formally grows as  $N_s^4$ . One might imagine that this unfavorable scaling would present a barrier to applying the same approach to problems with larger numbers of subsystem states. Recently, we have therefore shown how quantum-classical methods can be used to evaluate the memory kernel in the GQME can be scaled to problems with many subsystem states. The figure below shows our results obtained for the Fenna Mathews Olsen complex (FMO) with 7 subsystem states. Although for this problem there are 2,401 memory kernel elements, one can show that one can generate them with Ehrenfest trajectories with only 28 different initial conditions. As we saw for systems with smaller numbers of subsystem states, proceeding via the memory kernel formalism recovers the exact result almost perfectly, even though a direct application of mean-field theory is qualitatively incorrect. In addition, we are currently investigating how one can use importance sampling to preferentially sample initial conditions that are needed to capture the particular initial excitation of the system which one is interested in. Our initial tests using an importance sampling algorithm for the memory kernel elements already indicate that, in FMO, one can obtain more than an order of magnitude acceleration by using such an approach, making MF-GQME less computationally expensive than even direct mean-field theory, even for this many-level system. With these advanced sampling algorithms implemented, we intend to demonstrate the ability to scale MF-GQME to large subsystems by applying it to electronic energy transfer in the LHC-II light harvesting complex, which has a 14 state quantum subsystem and thus presents a significant challenge to many nonadiabatic quantum dynamics methods.

These extensions now allow us to simulate the GQME dynamics using memory kernels generated from a wide variety of quantum-classical approaches for large quantum subsystems coupled to fully atomistic environments.

## Future Plans

In the next stage of this research we are using our insights into when GQME methods can offer accuracy advantages to provide similar improvements for nonequilibrium systems as well as treating problems incorporating vibrational modes that are strongly coupled to the electronic subsystem. We are also developing improved mappings of the fermionic degrees of freedom which are compatible with the GQME framework. These developments are essential for PCET in solution and at interfaces.

## Award Number DE-SC0014437: Development of Approaches to Model Excited State Charge and Energy Transfer in Solution

**PI and co-PI(s):** Christine Isborn (Merced, PI), Aurora Clark (WSU, co-PI), Thomas Markland (Stanford, co-PI)

**Markland Group Postdoc(s):** Andres Montoya-Castillo (current), Ondrej Marsalek (previous: now Assistant Professor, Charles University, Czech Republic), Aaron Kelly (previous: now Assistant Professor, Dalhousie University, Canada)

## Up to Ten Publications Acknowledging this Grant (since September 2015), Markland Group

[1.] Electrostatic control of regioselectivity in Au(I)-catalyzed hydroarylation. *V. M. Lau, W. C.*

- Pfalzgraff, T. E. Markland and M. W. Kanan J. Am. Chem. Soc., 139 (11), 4035-4041 (2017)*
- [2.] Generalized Quantum Master Equations In and Out of Equilibrium: When Can One Win? *A. Kelly, A. Montoya-Castillo, L. Wang and T. E. Markland, J. Chem. Phys. 144, 184105 (2016)*
- [3.] Simulating Nuclear and Electronic Quantum Effects in Enzymes. *L. Wang, C. M. Isborn, and T. E. Markland, Methods in Enzymology, 577, 389-418 (2016)*
- [4.] Unraveling the dynamics and structure of functionalized self-assembled monolayers on gold using 2D IR spectroscopy and MD simulations. *Yan, R. Yuan, W. C. Pfalzgraff, J. Nishida, L. Wang, T. E. Markland, M. D. Fayer, Proc. Natl. Acad. Sci., 113 (18), 4929-4934 (2016)*
- [5.] Nuclear Quantum Effects in Water and Aqueous Systems: Experiment, Theory, and Current Challenges. *M. Ceriotti, W. Fang, P. G. Kusalik, R. H. McKenzie, M. A. Morales, A. Michaelides and T. E. Markland, Chem. Rev., 116 (13), 7529-7550 (2016)*
- [6.] Ab initio molecular dynamics with nuclear quantum effects at classical cost: ring polymer contraction for density functional theory. *O. Marsalek and T. E. Markland, J. Chem. Phys. 144, 054112 (2016)*
- [7.] Nonadiabatic dynamics in atomistic environments: harnessing quantum-classical theory with generalized quantum master equations. *W. C. Pfalzgraff, A. Kelly and T. E. Markland, J. Phys. Chem. Lett., 6, 4743-4748 (2015)*

## *Intrinsic to collective properties of ions in solution*

Christopher J. Mundy  
Physical Sciences Division  
Pacific Northwest National Laboratory  
902 Battelle Blvd, Mail Stop K1-83  
Richland, WA 99352  
[chris.mundy@pnnl.gov](mailto:chris.mundy@pnnl.gov)

### Program Scope

The long-term objective of this research is to develop a fundamental understanding of processes, such as transport mechanisms and chemical transformations, at interfaces of hydrogen-bonded liquids. Liquid surfaces and interfaces play a central role in many chemical, physical, and biological processes. Many important processes occur at the interface between water and a hydrophobic liquid. Separation techniques are possible because of the hydrophobic/hydrophilic properties of liquid/liquid interfaces. Reactions that proceed at interfaces are also highly dependent on the interactions between the interfacial solvent and solute molecules. The interfacial structure and properties of molecules at interfaces are generally very different from those in the bulk liquid. Therefore, an understanding of the chemical and physical properties of these systems is dependent on an understanding of both the bulk and interfacial solvation structure. The adsorption and speciation of ions at aqueous liquid interfaces are fundamental processes encountered in a wide range of physical systems. In particular, the manner in which solvent molecules solvate ions at the interface is relevant to problems in a variety of areas. Another major focus lies in the development of reduced models of interaction based on the potential of mean force (PMF) and solvation free energies to provide accurate descriptions of both single ion and ion-ion interactions. These reduced models can be used with appropriate simulation techniques for sampling statistical mechanical ensembles to obtain the desired collective properties such as nucleation.

### Progress Report

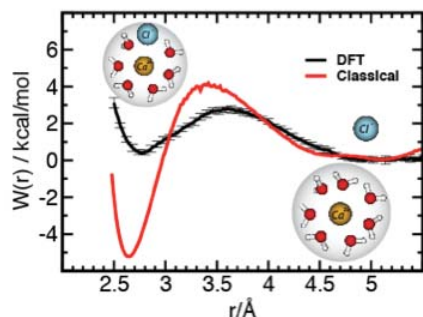


**Figure 1:** PMF for ion pairing of  $\text{CaCl}_2$  using different levels of molecular interaction. The DFT is consistent with a picture little ion pairing in agreement with experiment.[1] The classical force field would suggest that  $\text{CaCl}_2$  forms strong ion pairs.

*A microscopic picture of collective properties of ions in solution* [6-8]: In current and previous funding periods we have studied both the structure and solvation free energetics of single ions in solution. We have demonstrated that the accuracy of the ion-water and water-water interaction afforded by DFT are good enough to reproduce the local aqueous structure of anions as determined by extended x-ray fine structure spectroscopy (EXAFS). Nevertheless, questions pertaining to the collective nature of concentrated electrolyte solutions still remain. Moreover, producing well converged ensembles of trajectories of electrolyte solutions at finite concentrations using DFT based interaction potentials remains a challenge. Questions pertaining to the extent of

an accurate representation of the short-ranged structure is necessary to predict the long-range collective response of a concentrated electrolyte solution remains. We have shown that DFT based interaction potentials reproduce the local aqueous solvation structure as determined by EXAFS of both isolated  $\text{Ca}^{2+}$  and  $\text{Cl}^-$  ions.[6] Having established this notionally “intrinsic” measure of accuracy with DFT interaction potentials, we can compute the PMF between two ions in water. **Figure 1** depicts the potential of mean force (PMF) as computed from DFT interaction potentials and classical empirical potential. Also shown in **Figure 1** is the same PMF computed with a classical empirical potential that is known to give good agreement with EXAFS. The PMFs are remarkably different. [6] It is well known in the literature that  $\text{CaCl}_2$  does not ion-pair until concentrations above 6M.[6] Although data provided in **Figure 1** provides qualitative evidence of how an accurate description of local structure impacts collective properties such as activity and osmotic coefficients, a more rigorous connection is needed.

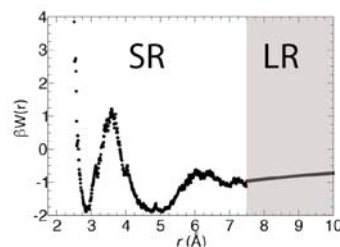


**Figure 2** demonstrates schematically how our research is making connections between “intrinsic” properties at infinite dilutions and collective properties at finite concentration. [7] To this end we provided a model for ion pairing of NaCl using

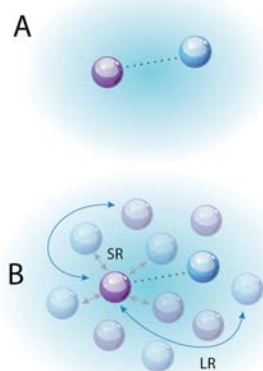


**Figure 2:** A schematic of a PMF of ion-pairing in the dilute limit (A) that was computed in **Figure 1**. (B) how the dilute limit PMF informs collective behavior. This will require the delicate interplay between the slowly varying long-range (LR) interaction and the complex short-range (SR) interaction.

the short-range (SR) interaction as determined by DFT and the long-range (LR) interaction being determined by simple Coulomb form as shown in **Figure 3**. Using this simple two-body potential for the ion-ion interaction as the input in an integral equation with the hypernetted-chain closure, we

can efficiently access the osmotic coefficients at finite concentration. [7] The result, as shown in **Figure 3** shows that the coarse grained two-body interaction potential indeed yields reasonable osmotic coefficients up to concentrations of 1 M. Using the ideas of the intrinsic PMF from accurate representations of interaction based in quantum mechanics to inform our understanding of collective properties such as clustering in solution up to moderate concentrations will be the focus of future studies. Specifically, it will be the differences in the SR component between quantum versus classical empirical interaction potentials that will drive much of the interesting phenomena. [8]

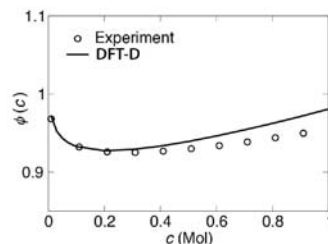


**Figure 3:** (top) the potential of mean force for an isolated  $\text{Na}^+-\text{Cl}^-$ . The SR is determined by DFT. The LR is a simple electrostatic term. (bottom) The computed and experimentally determined osmotic coefficients for NaCl as a function of concentration.

**Solvation Free Energies:** [1,5] Ionic solvation free energies are one of the most fundamental and important properties in physical chemistry and yet there is still debate and uncertainty about what they are. In particular, the contribution from the surface potential of the air-water interface is poorly understood. Our research is aimed at providing clear

and rigorous definition of single ion solvation free energies (see **Figure 4**). Starting with model systems we calculate solvation free energies for positive and negative charged hard spheres using interaction potentials based in quantum density functional theory (DFT). For charged hard

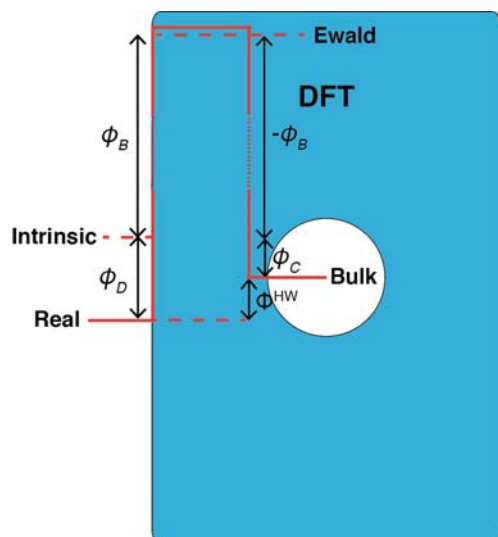


**Figure 4:** Four different definitions of the electrostatic contributions to the solvation free energies: **Real**, **Intrinsic**, **Ewald** (inherently unphysical because they contain the Bethe potential  $-\phi_B$ ), and **Bulk**. The conversion between each of the definitions is denoted schematically by the addition/subtraction of well-defined potentials, namely the Bethe potential  $-\phi_B$ , the dipole potential due to the presence of an interface  $\phi_D$ , the cavity potential  $\phi_C$ . Note, for the case of quantum based potentials such as DFT,  $\phi_B$  is large and positive. See Remsing *et al.* *J. Phys. Chem. Lett.* **5**, 2767 (2014) for details.

spheres we show that DFT water responds linearly to the charge in the center of the cavity but exhibits a very large charge hydration asymmetry that is much larger than experimental estimates for real ions. [1] This indicates that real ions, particularly anions, are significantly more complex than the simple charged hard spheres they are often considered to be. We have used these methods developed on model systems to compute single ion free energies of both aqueous  $\text{Li}^+$  and  $\text{F}^-$ . As stated previously, our research suggests that the  $\text{Li}^+$  behaves similar to a charged hard-sphere whereas  $\text{F}^-$  takes on much more complex behavior that relies on an accurate description of the short-range quantum mechanical interaction. [5]

**Acknowledgements.** This work was performed with Mirza Galib (PNNL), Santanu Roy (PNNL), Tim Duignan (PNNL), John D. Weeks (U. Maryland), Rick Remsing (Temple), Ilja Siepmann (U. Minn.), Greg Schenter (PNNL), Marcel D. Baer (PNNL), Shawn M. Kathmann (PNNL), Greg Kimmel (PNNL), and John Fulton (PNNL). We also

acknowledge computer resources from NERSC. Battelle operates Pacific Northwest National Laboratory for the US Department of Energy. The Molecular Theory and Modeling FWP 16249 is co-managed by CTC and CPIMS programs of DOE Office of Basic Energy Sciences Division of Chemical Sciences, Geosciences, and Biosciences.

#### Publications with BES support (2016-present):

1. T. Duignan, MD Baer, GK Schenter, and **CJM**, “Electrostatic solvation free energies of charged hard spheres using molecular dynamics with density functional theory interactions” arXiv:1702.05203v2 [To appear in *The Journal of Chemical Physics*]
2. [**Cover Article**] A. Prakash, J. Pfaendtner, J. Chun, and **CJM**, “Quantifying the Molecular-Scale Aqueous Response to the Mica Surface” *J. Phys. Chem. C* **121**, 18496–18504 (2017)
3. S. Roy, MD Baer, **CJM**, G.K. Schenter, “Marcus Theory of Ion Pairing” *J. Chem. Theory Comput.* **13** 3470–3477 (2017)

4. [Editors Choice] M. Galib, T. Duignan, Y. Misteli, MD Baer, GK Schenter, J. Hutter, and **CJM**, “Mass Density Fluctuations in quantum and classical descriptions of liquid water” *The Journal of Chemical Physics* **146**, 244501 (2017)
5. T. Duignan, MD Baer, GK Schenter, and **CJM**, “Real single ion solvation free energies with quantum mechanical simulation” *Chem. Sci.* **8**, 6131-6140 (2017)
6. M Galib, MD Baer, LB Skinner, **CJM**, T Huthwelker, GK Schenter, CJ Benmore, N Govind, JL Fulton, “Revisiting the hydration structure of aqueous Na<sup>+</sup>” *The Journal of Chemical Physics* **146**, 084504
7. Marcel D. Baer and **CJM**, “Local aqueous solvation structure around Ca<sup>2+</sup> during Ca<sup>2+</sup>--Cl<sup>-</sup> pair formation” *Journal of Physical Chemistry B* **120**, 1885, (2016)
8. Duignan, T.; Baer, M.D.; **CJM**, “Ions Interacting in Solution: Moving from Intrinsic to Collective Properties” *Current Opinion in Colloid & Interface Science* **23**, 58 (2016)
9. Daily M.; Baer, Marcel, **CJM**, “Divalent Ion Parameterization Strongly Affects Conformation and Interactions of an Anionic Biomimetic Polymer” *The Journal of Physical Chemistry B* **120**, 2198 (2016)
10. L. B. Skinner, L.B.; Galib, M.; Fulton, J.L. **CJM**; Parise, J. B.; Pham, V.-T.; Schenter, G.K. and Benmore, C.J., “The structure of liquid water up to 360 MPa from x-ray diffraction measurements using a high Q-range and from molecular simulation, *The Journal of Chemical Physics* **144**, 134504 (2016)
11. Roy, S; Baer, M.D.; **CJM**; Schenter, G.K., “Reaction Rate Theory in Coordination Number Space: An Application to Ion Solvation” *The Journal of Physical Chemistry C* **120**, 7597 (2016)
12. Lei, H.; Baker, N.A.; Wu, L.; Schenter, G.K.; **CJM**, and Tartakovsky, A, “Smoothed Dissipative Particle Dynamics model for mesoscopic multiphase flows in the presence of thermal fluctuations,” *Physical Review E* **94**, 023304 (2016)

# Studies of surface adsorbate electronic structure and femtochemistry at the fundamental length and time scales

Hrvoje Petek (*petek@pitt.edu*)

Department of Physics and Astronomy and Chemistry University of Pittsburgh

We study the dynamical properties of solid surfaces on the femtosecond temporal and nanometer spatial scales by time-resolved photoemission and scanning tunneling microscopy methods. The chemical and physical properties at molecule-solid interfaces are fundamentally important to solar energy conversion processes. Here we report on the first experimental time-domain measurement of a coherent multi-electron response triggered by interfacial photoinduced charge-transfer excitation. Our results relate to other electron correlation phenomena such as autoionization of atoms, final state effects in photoemission, core hole spectroscopy, multi-exciton generation in semiconductors, etc.

In the past year we have applied multidimensional coherent multiphoton photoemission (MDCMP) spectroscopy to study the coherent electron dynamics at metal surfaces. We observe a coherent multi-electron response provoked by photoinduced charge transfer excitation from the Shockley surface (SS) of Cu(111) to chemisorbed Rb or Cs. We interpret the dynamics as a “final state effect”, which is often invoked in frequency domain photoemission spectroscopy to explain non-band structure features in photoemission spectra. Excitation of a photoelectron suddenly turns on the charge of its hole, which prompts secondary excitations of the Fermi sea that screen the Coulomb potential of the nascent charge; because energy must be conserved, the photoelectrons can carry away information on these secondary excitations causing photoelectron spectra to deviate from single-particle band structures. The corresponding time domain dynamics of such multi-electron processes have not yet been reported.

The multi-electron dynamics are triggered on Cs(Rb)/Cu(111) surfaces by the charge transfer excitation from the SS of Cu(111) to the unoccupied  $\sigma$  resonance of chemisorbed alkali atoms at small ( $\sim 0.01$  monolayer) coverages. The  $\sigma$  resonances correlate with the  $6s(5s)$  valence states of the free Cs(Rb) atoms. At  $\sim 1$  eV above the  $\sigma$  resonance there is a  $\pi$  resonance, whose primary character derives from the degenerate  $np_x$  and  $np_y$  orbitals. The valence  $ns$  electron in front of a metal experiences attraction of its own image charge and repulsion from the *negative* image charge of the alkali ion core. The net interaction is repulsive with  $+1/4z$  dependence on the distance from the image plane; consequently, charge transfer excitation of the  $\sigma$  resonance suddenly turns on a Coulomb potential with a strength of  $\sim 2$  eV.

A representative multiphoton photoemission (mPP)  $E(k)$  spectrum of Cs/Cu(111) surface excited with  $\hbar\omega_i = 1.92$  eV light is shown in Fig. 1. Also

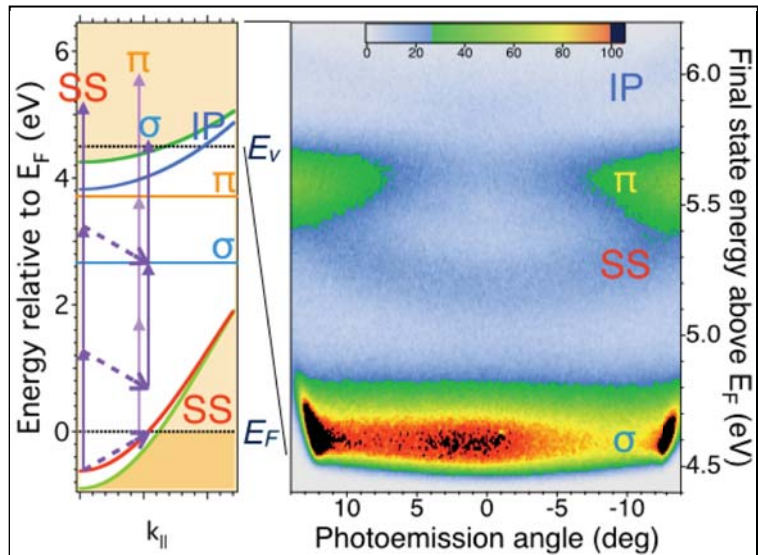


**Fig. 1.** 3PP-spectrum of Rb/Cu(111) surface with  $\hbar\omega_i = 1.92$  eV excitation and the surface projected band structure showing mPP excitation pathways. The two-photon state from SS is detuned by 0.6 eV from the SS- $\sigma$  resonant transition. The  $\sigma$  resonance, nevertheless, is excited by a multi-electron process, which excites electrons by an interband process in SS (upward dashed arrow) to simultaneously conserve energy and momentum in the two-photon transition (downward dashed arrows).

shown is an energy-band diagram indicating the possible excitation pathways for multiphoton photoemission (mPP) involving the SS as the initial state, and the  $\sigma$  and  $\pi$  resonances as the intermediate states. Photoemission from SS is excited by a non-resonant 3PP process; its spectrum is similar to that of the clean Cu(111) surface. The  $\pi$  resonance is excited by a two-photon resonant transition from SS for  $k_{\parallel}$  near its crossing with  $E_F$ , as shown in Fig. 1. Because the  $\pi$  resonance is localized on alkali atoms,  $k$ -conservation in the optical transition is relaxed; a resonance at one  $k$ -point enables excitation at all  $k$ . According to the diagram in Fig. 1b, the two-photon absorption from SS at  $k_{\parallel} = 0$  excites an electron to a virtual state  $\sim 0.6$  eV above the  $\sigma$  resonance, so there is no excitation process to the  $\sigma$  resonance via dipole transitions that conserves energy. There is a dichotomy, therefore, in that the  $\sigma$  resonance, for which there is *no resonant excitation pathway*, dominates the mPP spectra in Fig. 1b.

MDCMP measurements of mPP from Cs and Rb/Cu(111) surfaces using 2.10-1.85 eV light reveal the multi-electron character of the nonresonant mPP process via the  $\sigma$  resonance. Figure 2a shows a cross section for  $k_{\parallel} = 0$  through an MDCMP movie obtained by recording  $E(k)$  spectra for Rb/Cu(111), such as in Fig. 1b, for pump-probe delay intervals of  $\sim 50$  as between identical  $\sim 15$  fs pulses at with  $\hbar\omega_i = 1.92$  eV. Essentially the same results are obtained for Cs/Cu(111). Figure 2b further shows cross sections through the data in Fig. 2a at the final state energies of the  $\sigma$  and  $\pi$  resonances. These interferometric two-pulse correlation (I2PC) measurements show the interferences between the pump and probe-induced polarization fields that contribute to 3PP processes at particular  $E$  and  $k$  via the alkali atom resonance intermediate states. Focusing just on the coherent fringes within the duration of the third-order autocorrelation (AC;  $\pm 30$  fs), it is immediately evident that the coherent response at the  $\sigma$  resonance is anomalous: whereas the interference fringes near zero delay at the  $\pi$  resonance follow the laser AC, for the  $\sigma$  resonance there is evident beating with a period of  $\sim 6.5$  fs *within* the AC. This polarization frequency modulation seemingly violates the energy-time uncertainty, because it requires the laser pulse to create coherent frequency components *outside* of its frequency bandwidth on a time scale of a single optical cycle of the excitation light. The polarization beating is not observed for  $\hbar\omega_i > 1.95$  eV, but appears with less regular pattern for  $\hbar\omega_i < 1.92$  eV. Clearly, the polarization beating and energy non-conservation in the excitation are related.

The paradox of the sample undergoing coherent evolution at frequencies that are far outside of the bandwidth of the driving field and do not correspond to the single particle band structure can be illuminated by performing a Fourier transform (FT) of the signal in Fig. 2a with respect to time, which is shown in Fig. 3a. This analysis gives the dominant frequency components of the coherent polarization, which are plotted along the vertical FT axis, and the final state energies that they correlate with. According

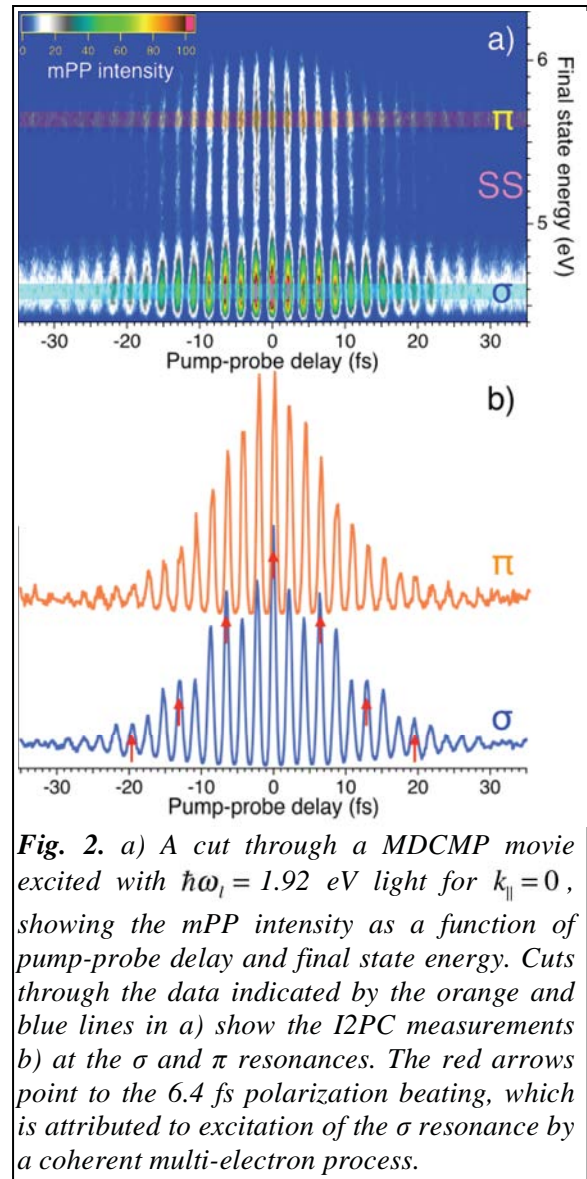


**Fig. 2.** a) A cut through a MDCMP movie excited with  $\hbar\omega_i = 1.92$  eV light for  $k_{\parallel} = 0$ , showing the mPP intensity as a function of pump-probe delay and final state energy. Cuts through the data indicated by the orange and blue lines in a) show the I2PC measurements b) at the  $\sigma$  and  $\pi$  resonances. The red arrows point to the 6.4 fs polarization beating, which is attributed to excitation of the  $\sigma$  resonance by a coherent multi-electron process.

to Fig. 3a, the coherent response is dominated by harmonics of the driving field, which is expected for a coherent mPP process. What is surprising, based on years of experience with similar measurements, for example, for the bare Cu(111) or alkali covered Cu(111) and Ru(0001) surfaces, is that the 2D spectra in Fig. 3a and their cross sections at the  $\sigma$  and  $\pi$  resonances (Fig. 3b), show *additional* frequency responses at frequencies corresponding to approximately  $\frac{1}{3}\omega_l$ ,  $\frac{2}{3}\omega_l$ , and  $\frac{5}{3}\omega_l$  exclusively for the 3PP process via the  $\sigma$  resonance. These additional polarization components have broad line shapes with cutoffs for  $\sim 0.6$  eV detuning from the main peaks at the  $0\omega_l$ ,  $1\omega_l$ , and  $2\omega_l$  frequencies.

One can immediately deduce that the  $\frac{1}{3}\omega_l$  component is related to the detuning  $\Delta$  of the virtual state reached by two-photon dipole excitation ( $W_{\mu E}$ ) of an electron from SS by the driving frequency  $\omega_l$  and the  $\sigma$  resonance ( $2\omega_l - \omega_\sigma = \Delta$ ; the downward dashed arrows in Fig. 3c). For the nonresonant excitation from SS to terminate at the  $\sigma$  resonance, energy conservation requires other excitations of the system, *e.g.*, photons or electrons, to take up the detuning energy. The coupling to photons via an electronic hyper-Raman process is unlikely to have  $\sim 10\%$  efficiency with respect to  $2\omega_l$  polarization and would not depend strongly on  $\omega_l$ . We conclude, therefore that the two photon state decays into a multi-electron final state through Coulomb interaction ( $W_C$ ). This process conserves energy and momentum by excitation of an electron to the  $\sigma$  resonance and concomitant excitation of one or more *e-h* pairs in the 2D electron gas (2DEG) formed by the SS at the Cu(111) surface (upward dashed arrow in Fig. 1 and 3a). We note that charge transfer from alkali atoms to SS causes its band minimum to decrease from 0.4 eV for the clean surface to 0.6 eV below  $E_F$ . Thus, the 0.6 eV detuning energy of the virtual state from the  $\sigma$  resonance is sufficient to excite any electron within the 2DEG.

Based on the above analysis, we interpret the fractional frequency components in the 2D spectra as follows. Alkali atoms exist as ionized impurities imbedded in the 2DEG. The 2DEG screens the ionic charges. Exciting an electron from SS to a virtual state, which derives transition strength from the alkali  $\sigma$  resonance, instantaneously excites a new charge distribution that evolves to that of the *neutral* alkali atom, and thereby turns on the repulsive Coulomb interaction of strength  $W_C \sim 2$  eV with the preexisting image charge of the alkali ion core. The redistribution of charge provokes many-body excitations within the 2DEG that screen the new charge distribution. The localization of the  $\sigma$  resonance on the impurity atoms relaxes the momentum conservation enabling intraband transitions to occur within SS. We find that the maximum multi-electron response occurs at  $\hbar\omega_l = 1.92$  eV; most likely this is

because 1)  $\Delta$  is sufficiently large to excite any *e-h* pair within the entire 2DEG; and 2) intraband transitions terminating at the Fermi level are probably enhanced by a many-body excitonic effect called the Fermi edge singularity (FES). Because  $\hbar\omega_l \sim W_C$  the joint action of the driving optical field and the Coulomb interaction can couple the single-particle and multi-

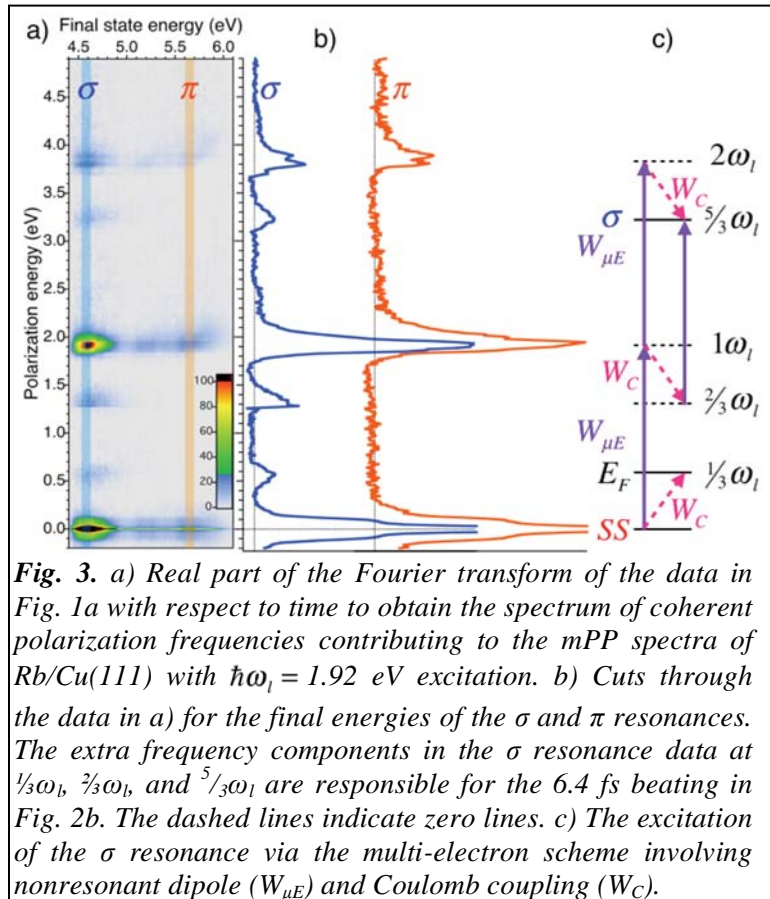


**Fig. 3.** a) Real part of the Fourier transform of the data in Fig. 1a with respect to time to obtain the spectrum of coherent polarization frequencies contributing to the mPP spectra of Rb/Cu(111) with  $\hbar\omega_l = 1.92$  eV excitation. b) Cuts through the data in a) for the final energies of the  $\sigma$  and  $\pi$  resonances. The extra frequency components in the  $\sigma$  resonance data at  $\frac{1}{3}\omega_l$ ,  $\frac{2}{3}\omega_l$ , and  $\frac{5}{3}\omega_l$  are responsible for the 6.4 fs beating in Fig. 2b. The dashed lines indicate zero lines. c) The excitation of the  $\sigma$  resonance via the multi-electron scheme involving nonresonant dipole ( $W_{\mu E}$ ) and Coulomb coupling ( $W_C$ ).

electron states on the single optical cycle time scale. We believe that the multi-electron response involves a novel manifestation of FES in the case of impurity alkali atoms on Cu(111) surface. Here, the impurity ions take on the role of massive holes in core hole spectroscopy, and the free electrons occupying the SS respond to a sudden change in the charge state of alkali atoms.

Based on the above analysis, we construct the following physical picture for multi-electron excitation in mPP of Rb and Cs/Cu(111) surfaces. Electric-dipole transitions drive single-electron two-photon excitation from SS to alkali atom localized virtual state with predominantly  $\sigma$  resonance character. The  $\sigma$  resonance is a coherent superposition with multi-electron states, which are dark for dipole transitions, but are coupled to the  $\sigma$  resonance through Coulomb interaction with a strength of  $\sim 2$  eV. The two-photon state thus decays into superposition states involving the  $\sigma$  resonance and intraband excitations in the Fermi sea, which satisfy the energy and momentum constraints for photons to be absorbed. The strength of the Coulomb interaction causes the virtual state to decay within single cycles of the excitation light into the multi-electron state, *i.e.*, faster than the virtual state lifetime, which is inversely related to  $\Delta$  by the energy-time uncertainty. Thus, within each cycle of the excitation light, electrons having absorbed two-quanta of  $\hbar\omega_i$  decay into a multi-electron state consisting of the  $\sigma$  resonance and screening excitations within the Fermi sea. The Coulomb coupling between the bright and dark state on single-cycle time scale preserves coherence that is recorded in the 2D spectra.

We believe that the observed coherent multi-electron dynamics could be observed in other systems, for example in Coulomb interaction mediated multi-exciton generation.

In other experiments we are working on the modification of electronic structure of graphite by alkali atom chemisorption. Doping of graphitic materials with alkali atoms has led to discovery of several superconducting materials, but the electronic interactions are poorly understood. In mPP experiments we identified the electronic states introduced by alkali atom chemisorption and found strong evidence for the 3D interlayer state of graphite, which is of fundamental importance for 2D layered materials. We are also studying the 2D topological insulator properties of metal organic networks on noble metal surfaces.

#### DOE supported publications 2013-2016.<sup>1-10</sup>

- 1 Feng, M. *et al.* Energy stabilization of the s-symmetry superatom molecular orbital by endohedral doping of C<sub>82</sub> fullerene with a lanthanum atom. *Phys. Rev. B* **88**, (2013).
- 2 Winkelmann, A. *et al.* in *Solar Energy Conversion: Dynamics of Interfacial Electron and Excitation Transfer* (ed Piotr Piotrowiak) Ch. 8, 225-260 (The Royal Society of Chemistry, 2013).
- 3 Cui, X. *et al.* Transient Excitons at Metal Surfaces. *Nat Phys* **10**, 505-509 (2014).
- 4 Feng, M., Sun, H., Zhao, J. & Petek, H. Self-Catalyzed Carbon Dioxide Adsorption by Metal–Organic Chains on Gold Surfaces. *ACS Nano* **8**, 8644-8652 (2014).
- 5 Petek, H. Single-Molecule Femtochemistry: Molecular Imaging at the Space-Time Limit. *ACS Nano* **8**, 5-13 (2014).
- 6 Zhao, J., Feng, M., Dougherty, D. B., Sun, H. & Petek, H. Molecular Electronic Level Alignment at Weakly Coupled Organic Film/Metal Interfaces. *ACS Nano* **8**, 10988-10997 (2014).
- 7 Silkin, V. M., Lazić, P., Došlić, N., Petek, H. & Gumhalter, B. Ultrafast electronic response of Ag(111) and Cu(111) surfaces: From early excitonic transients to saturated image potential. *Phys. Rev. B* **92**, 155405 (2015).
- 8 Feng, M. *et al.* Cooperative Chemisorption-Induced Physisorption of CO<sub>2</sub> Molecules by Metal–Organic Chains. *ACS Nano* **9**, 12124-12136 (2015).
- 9 Feng, M. & Petek, H. (ed A. Popov) (Springer, in press).
- 10 Zhang, S. *et al.* Time-resolved photoemission study of the electronic structure and dynamics of chemisorbed alkali atoms on Ru(0001). *Phys. Rev. B* **93**, 045401 (2016).

# Probing Condensed-Phase Structure and Dynamics in Hierarchical Zeolites and Nanosheets for Catalytic Upgradation of Biomass

Neeraj Rai

330 Swalm Chemical, Mississippi State University, Mississippi State, MS, 39762

Email: neerajrai@che.msstate.edu

## Program Scope

Understanding complex reactions at the molecular level in systems characterized by multiscale collective coupling across time and space is a significant scientific challenge. This project is guided by the hypothesis that interactions of oligomers, solvents and active sites can be tailored by a suitable choice of solvent and also of pore architecture of solid-acid catalysts to promote chemical transformations during catalytic conversion of biomass. The architecture is determined by the choice of hierarchical zeolites, which provide large channels for macromolecule diffusion and small pores for catalysis. A multiscale computational approach will be used to elucidate physical and chemical interaction across multiple spatial and temporal scales. Furthermore, advanced first principles Monte Carlo algorithms will be developed to efficiently sample configurational space. We will use advanced first principles Monte Carlo and molecular dynamics simulations, and electronic structure calculations to answer fundamental scientific questions pertinent to acid catalyzed hydrolysis and hydrogenolysis of cellulose and lignin, respectively, in ordered mesoporous zeolitic structures. One outcome will be a better understanding of the fundamental interactions of reactant and solid acid catalysts in the presence of solvents, enabling rational design of catalytic systems that can upgrade biomass in a selective and energy efficient manner. Another outcome will be the development of sampling tools essential to detangle interactions in complex, reactive phenomena.

## Recent Progress

Diffusion of Glucose Molecules in Nanopores of Beta Zeolite in the Condensed Phase: Our initial focus has been to understand diffusion of cellulose and lignin monomers in the nanopores of zeolites with selected topologies. We have conducted molecular dynamics simulations in *isothermal isobaric ensemble* to elucidate diffusion mechanism and solvation environment in nanopores of Beta zeolite. A model of zeolite supercell with approximate dimensions of  $6 \times 6 \times 6$  nm was constructed and then placed in a cubic box with cell length of 13 nm. Glucose and solvent molecules were subsequently added to the system. These simulations have provided information on probability density map of solvent and glucose molecules (see Figure 1), effect of confinement on dynamics of solvent and monomers, and potential of mean force for diffusion of glucose into the pores, and collision frequencies with the zeolite framework. We find that dynamics of solvent and glucose inside the pores slows down by an order of magnitude compared to glucose solution outside the zeolite framework. Although water molecules are able to diffuse into the smaller pores, glucose molecules reside primarily in the large pores (pore diameter  $\approx 0.7$ nm). We have also investigated the effect of temperature on

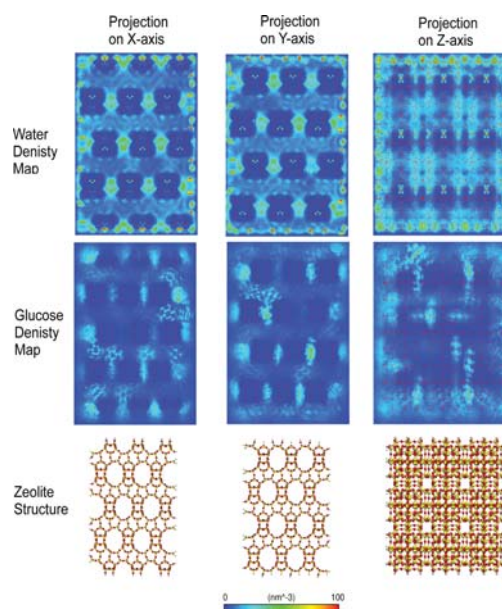


Figure 1. Two dimensional (2D) density map of water and glucose molecules projected along x, y and z-axis. Diffusion of water and glucose molecules across nano pores and sinusoidal channels were observed 2D density map projected in x and y axis. Higher density of molecules were found to be at nano pores of zeolite interior structure than sinusoidal channels.

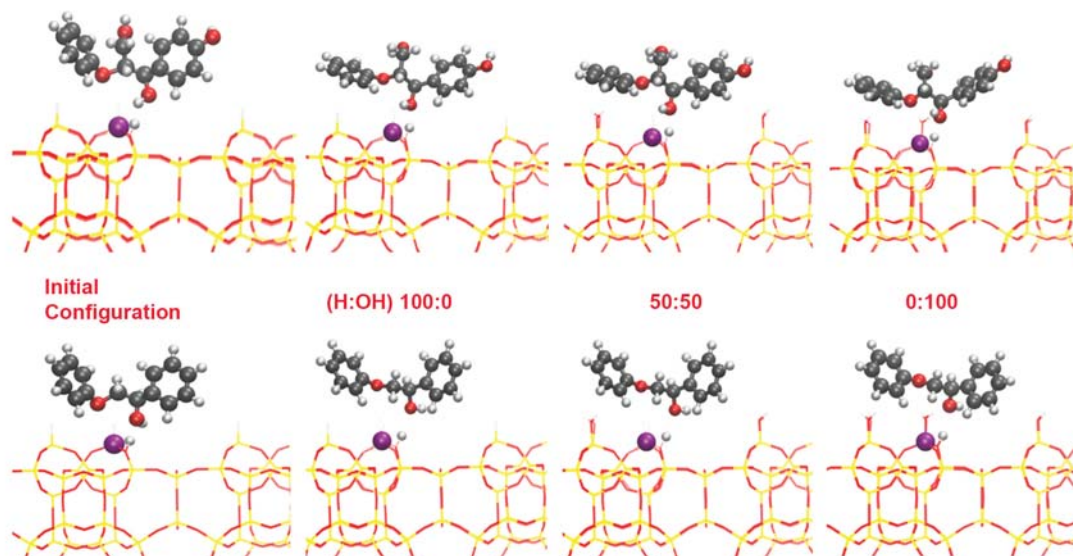


Figure 2. The effect of surface termination ( $-H$  vs  $-OH$ ) on the binding modes of model compounds with  $\beta$ -O-4 linkage (1-(4-hydroxyphenyl) 2-phenoxy-1,3-propanediol (HH, top) and 2-phenoxy-1-phenylethanol (PE, bottom)) on MWW nanosheet.

the monomer/solvent dynamics.

#### Effect of Nanosheet Surface Termination on Binding Modes of Model Compounds with Ether Linkage:

We have initiated electronic structure calculations to understand the binding modes of model compounds with  $\beta$ -O-4 linkages (1-(4-hydroxyphenyl) 2-phenoxy-1,3-propanediol (HH) and 2-phenoxy-1-phenylethanol (PE)) on MWW 2D zeolite nanosheets. Brønsted acid site was introduced by replacing one of the silicon atoms with aluminum atom and the charge was compensated by introducing proton on the bridging oxygen (see Figure 2). We have used PW91 and optB88-vdW density functionals for these calculations. The effect of different surface termination ( $-H$  vs  $-OH$ ) on binding mode is shown in Figure 2. The change in the binding mode (ring orientation) is more pronounced for HH. Although the binding energies for PW91 functional are 10-15 kcal/mol smaller than the optB88-vdW functional, the qualitative trends are similar, i.e. as we increase the density of  $-OH$  group on the surface of MWW 2D nanosheet, the binding energy increases. We have also carried out *ab initio* molecular dynamics simulations in the presence of solvents. Our initial work indicates that in the condensed phase C–O bond cleavage proceeds after protonation of the hydroxyl group on alkyl linker that connects aromatic rings.

#### **Future Plans**

##### Implement Fragment Based Configurational-Bias Monte Carlo Algorithm in CP2K:

The presence of aromatic rings in lignin polymer presents a significant challenge for first principles Monte Carlo algorithms. The implementation of highly efficient and parallelized configurational bias (CB) algorithms in first principles code such as CP2K can address one of the key sampling challenges when modeling chemical transformations at finite temperatures and pressures. The configurational bias (CB) growth in stepwise manner for complex molecules causes a serious problem for electronic structure codes as energy of broken fragments is so high that such CB moves will never get accepted. A solution to this problem is to utilize pre-sampling potential based on the underlying DFT functional and use it during the CB growth while the final acceptance criteria is based on the DFT energetics. Furthermore, we will use fragment based approach introduced by Macedonia and Maginn to sample intra-fragment configurations. As the cost of energy calculation with pre-sampling potential is expected to be at least three orders of magnitude smaller than single DFT SCF calculation, we can generate large number of trial configurations. The energy of each

of trial configurations will be parallelized using OpenMP paradigm.

*Probe Solvent Effect on Structure and Dynamics of Oligomers:*

A better understanding of oligomer structure in the condensed phase is necessary to design hierarchical systems for catalytic transformation of lignocellulosic biomass. We will build model oligomers of lignin and cellulose in a systematic manner by increasing number of monomers. For lignin, we will mimic lignin composition (distribution of monolignols and linkages) from different sources. Solvents with a range of polarity will be considered. The goal of condensed phase simulations will be to establish scaling laws for structural metrics such as radius of gyration and explore interaction of solvents with oligomer, structural evolution, and dynamics of conformational change as a function of solvent composition, temperature, and pressure. To understand oligomer structure, different structural metrics (such as solvent accessible surface area, principle components of moment of inertia, asphericity, and fractal dimensions) will be used to describe the structural features. Diffusion constants of oligomers and solvents will be estimated with mean squared displacement approach.

*Investigate Interaction of Solvent with Active Sites in Meso- and Micro-pores:*

Isomorphic substitution of Si with the selected elements will be considered to create Lewis/Brønsted acid sites (L/BAS). These elements will provide a range of acidic character to investigate depolymerization reactions. The density of H/OH terminated Si bonds on the surface will be additional parameters that will be explored. Large scale atomistic simulations will provide well equilibrated structures of solvents in micro- and meso-pores. From these simulations, system size will be reduced to perform accurate QM/MM MD simulations to understand interaction of solvent with the catalytic sites. For sampling solvent reorganization on the surface, MD approach will suffice as solvents have faster relaxation/reorganization time. QM region will be decided based on the radial distribution function from the atomistic calculations to include at least two solvation shells and second nearest Si atoms in the zeolite framework. We will identify key geometric features such as solvent orientation and binding modes (monodentate/bidentate). Furthermore, hydrogen bond dynamics will be determined by means of auto-correlation function of hydrogen bond population operator. This will allow us to study hydrogen bond life time, and determine whether the dynamics of h-bonds near the active site differs from molecules beyond second solvation shell. The effect of co-solvent on the H-bond dynamics will also be elucidated. We expect the h-bond dynamics will be different in micro- and meso-pores. This will be quantified in terms of long and short timescale behavior of H-bond dynamics.

*Probe Brønsted and Lewis Acidity of Hierarchical Zeolites:*

One of the biggest challenge in the modeling liquid phase reactions with DFT is the treatment of solvation effects. Currently, either solvents are completely ignored or treated with implicit solvent models when employing cluster models to represent zeolite active sites. This can be a problem especially when considering reactions that occur in the liquid medium (biomass conversion). We will probe acidity of B/LAS by calculating binding energies, deprotonation energies, and vibrational frequencies of selected probe molecules: ammonia, pyridine, and CO. We will first determine these properties without considering solvents to establish baseline for the acidity. This will also allow us to benchmark acidity with respect to other well studied model systems of 3D zeolite.

**List of Publications**

Due to a recent start date (09/01/2017), this project has not resulted in any publications.

# MOLECULAR STRUCTURE, BONDING AND ASSEMBLY AT NANOEMULSION AND LIPOSOME SURFACES

PI: Geraldine Richmond, University of Oregon

Email: richmond@uoregon.edu

## ***Program Scope and Definition***

Nanoemulsions and microemulsions are environments where oil and water can be solubilized in one another to provide a unique platform for many different biological and industrial applications. Nanoemulsions, unlike microemulsions, have seen little work done to characterize molecular interactions at their surfaces. Reverse nanoemulsions are water droplets suspended in oil and are gaining increasing interest for emulsified fuel technologies, reactors for nanoparticle synthesis, carriers for slow drug release, and models for confined water environments. With time, nanoemulsions will destabilize and eventually separate into their separate phases with the process initialized by either coalescence or Ostwald ripening mechanisms. Molecular species, such as surfactants adsorbed to the droplet interface play a significant role in nanoemulsion stability by increasing the steric hindrance or electrostatic repulsions between droplets and lowering the interfacial tension between the oil and water phases. Although there have been many studies of nanoemulsion stability in bulk solutions and nanoemulsions at air/water interfaces there is a lack of understanding on a molecular level of how molecules assemble and bond at the oil/water junction at the surface of nanoemulsions.



The objective of these studies is just that: *to advance our understanding of the molecular structure, orientation and bonding of surfactants at the surface of nanoemulsions and liposomes, and the bonding characteristics of interfacial water that is either confined or surrounding the surfactant coated soft particle surfaces.* Our approach involves measuring the surface vibrational spectroscopy of the surfactant coated particle surfaces in-situ using vibrational sum frequency scattering spectroscopy (VSFSS), with related complementary studies of

these surfactant systems examined at the more well-defined planar oil/water interface by vibrational sum frequency spectroscopy (VSFS). Classical molecular dynamics (MD) calculations coupled with density functional theory (DFT) methods are employed to assist in spectral assignments and understanding solvation effects. Other experimental techniques such as dynamic light scattering (DLS), zeta potential and interfacial tensiometry are being used.

## ***Recent Progress***

Over the past year we have been furthering our investigations of sodium di-2-ethylhexylsulfocinate (AOT) at the nanoemulsion and planar oil/water interface and particle sizes of ~200 nm. AOT was selected for these studies of nanoemulsion surfaces for several reasons. In addition to its many applications, as with microemulsions, AOT also has the ability to form both regular and reverse nanoemulsions without a cosurfactant.<sup>1</sup> Its efficacy at forming reverse emulsions is attributed to its wedge-like shape and enhanced aqueous solubility.

The success of our studies described below are significantly aided by our prior work at neat oil-water interfaces as examined by VSFS and computational studies on planar interfaces.<sup>2-5</sup>

What has been learned from these studies is that weak bonding interactions between interfacial water and various hydrophobic oils is a general trait for these oil-water systems which results in significant molecular ordering and structuring of both solvent phases near the interfacial region. The interfacial electric field at the oil-water interface has been shown to facilitate the adsorption of simple electrolyte ions at the interface, surfactant adsorption,<sup>6,7</sup> the ordered assembly of polyelectrolytes<sup>8</sup> and two-dimensional peptoid nanosheets.<sup>9</sup>

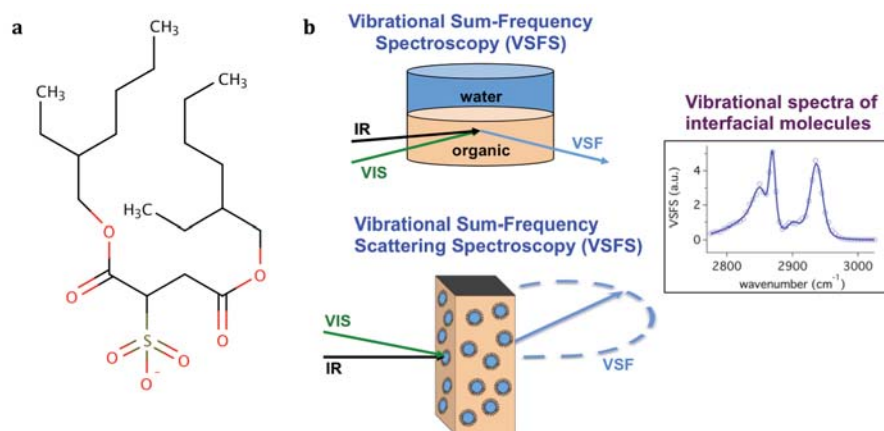


**Figure 1.** (a) The chemical structure of AOT. (b) A diagram of the planar and particle VSF experimental geometries, both involving an overlap of the incoming visible and IR beams at the planar interface (top) in a TIR geometry, or the center of a cuvette composed of a CaF<sub>2</sub> front window with a quartz back window and an optical path length of 200  $\mu$  m.

One of the unique aspects of our nanoemulsion studies is our ability to compare the interfacial molecular structure, bonding and orientation of AOT and interfacial water at the nanoemulsion surface with its behavior at the planar oil-water interface by VSFS and VSFSS respectively (Figure 1). More details of the experimental parameters can be found elsewhere.<sup>10</sup>

## Orientation and Solvation of the AOT Headgroup

Understanding the molecular structure and solvation of the ionic headgroup of a surfactant such as AOT is important because of its presence directly at the junction. In this investigation we have measured the vibrational spectroscopy of the sulfonate headgroup and surrounding water molecules of AOT at the planar and reverse nanoemulsion surface for M:AOT where M=Na, K and Mg. The strong sulfonate symmetric stretch signal found for all systems indicates that the dipole moment of the sulfonate group of AOT has a high degree of orientation perpendicular to the interface with frequencies of 1048 ( $\pm$  3) and 1045 ( $\pm$  3) cm<sup>-1</sup> for the planar

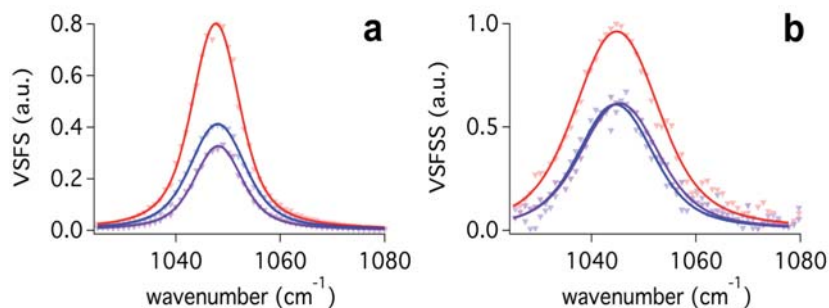


**Figure 2:** VSF SSP spectra of the S-O symmetric stretch of Na:AOT (blue), K:AOT (purple), and Mg:AOT (red) at the (a) planar isooctane/ D<sub>2</sub>O interface and (b) the CCl<sub>4</sub>/D<sub>2</sub>O reverse nanoemulsion interface. The spectral broadening is due to the difference in laser systems used.

and reverse nanoemulsion interfaces respectively. The absence of any peak broadening or spectral shifts found between the monoatomic and diatomic cations indicates that the hydration of the AOT headgroups is similar between counterion samples and interfacial geometries.<sup>11</sup>

For both the planar and the reverse nanoparticle surfaces Mg:AOT has a higher intensity than Na:AOT and K:AOT. One of the main factors contributing to this response is the higher surface concentration of Mg:AOT relative to the other

ion complexes due to the tighter bonding of magnesium ion to the headgroup and subsequent reduction neighboring AOT repulsion as described below.

### Alkyl Chain Ordering

As noted in the CPIMS 2016 abstract, the CH modes of the methylene and methyl groups on AOT are readily visible at the reverse and regular nanoemulsions and also the planar interface indicative of significant chain ordering. The spectra look remarkably similar for all three with subtle differences found with the spectra are fit and the ratio of the methyl to methylene intensities are compared. One complicating factor is that unlike many alkyl chain VSF studies that use this ratio as an indicator of chain ordering, AOT is double branched and with several small side chains. However, even taking this into account it is found that the ratio for the planar studies indicate a higher degree of overall chain ordering relative to the nanodroplets. The reverse and regular nanoemulsion give a very similar ratio indicative of quite similar hydrophobic structuring at the two spherical surfaces. Interestingly, when the nanodroplets are allowed to coalesce over time from sizes of 200-600 nm, the CH spectra are invariant.

### Interfacial Water Orientation and Bonding

Further understanding of interfacial water molecules in the presence of AOT and different counterions can be gleaned from studies of the O-H stretch modes of water in the 3 micron region. Overall the studies show a high degree of water orientation as would be expected from the charged interface in the presence of AOT. No significant difference between the planar and spherical geometries is found for the bound OH stretch modes. The surface concentration varies for different AOT counterions studied and follows the trend of Mg:AOT > K:AOT ~ Na:AOT, mirroring the size of the solvation spheres and counterion proximity (Figure 3). The interfacial water orientation follows the opposite trend with the highest degree of water orientation found for the less hydrated Na<sup>+</sup> ion and a significantly reduced water alignment found when the highly hydrated Mg<sup>2+</sup> ion complexes at the surface with AOT. Previous <sup>1</sup>H NMR studies show that the Mg<sup>2+</sup> counterion is more tightly coordinated to the sulphonate head group followed by K<sup>+</sup> and Na<sup>+</sup>.<sup>11</sup> We attribute this difference in water orientation to the higher degree

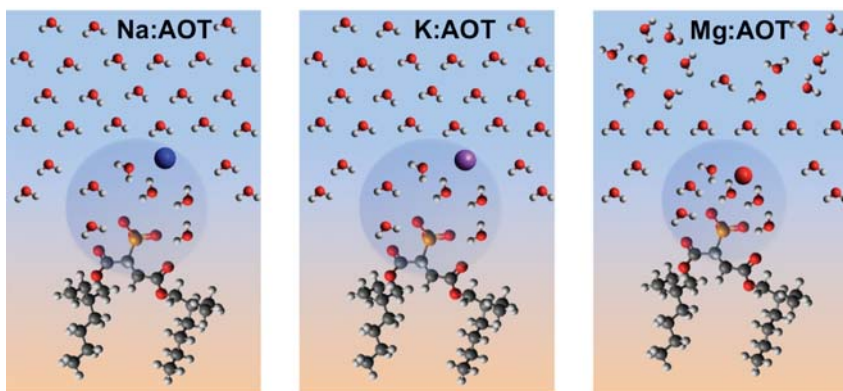


Figure 3. Illustration of Na:AOT, K:AOT and Mg:AOT and Na:AOT at the reverse nanoemulsion and planar oil/water surface.

of charge screening of the sulfonate headgroup that results in a reduction of the field that orients interfacial water molecules and reduces the VSF response. Even with this difference in water orientation, no significant difference is observed in the frequency or bandwidth of the sulfonate as the counterion is changed, indicative of similar levels of headgroup hydration. The overall picture obtained from AOT at the surface of a reverse nanoemulsion and also the planar interface is that the dipole moments of the hydrated sulfonate headgroup and neighboring water molecules in the interfacial region are highly oriented perpendicular to the surface (Figure 3).

### ***Future Studies***

**AOT:** We are continuing to pursue further AOT studies where we are seeking to also measure the CO mode on the AOT to obtain fuller analysis of its structure at the nanoemulsion interface. This is a particularly challenging spectral region for these studies for various experimental reasons. Another area of focus over the next year is to study the nanodroplets that appear to stabilize for degassed solutions and without a surfactant. There is much uncertainty in the field as what is responsible for this stabilization with surface adsorbed hydroxide ions assumed to be the factor. Our additional set of experiments involve studies CTAB at the oil-in-water nanoemulsions. Like with AOT, we want to be able to compare CTAB at the regular and reverse nanoemulsion interfaces. The advantage with CTAB is we can draw firmer conclusions as to surfactant conformational disorder at each interface by using the  $d^+/r^+$  ratio and computational work. Over the past year we have had considerable success in characterizing through planar studies the CH spectrum of CTAB through deuteration studies that allow us to distinguish peaks of the CH modes in the charged headgroup region from those of the alkyl tails. This will be of significant value to our studies of the nanoparticle surfaces. The use of  $C_n$ TAB in surfactant in PS studies cannot be overstated. It remains one of the most universally used surfactants.

- (1) Binks, b. P. M., J.; Abillon, O.; Langevin, D. Measurement of film rigidity and interfacial tensions in several ionic surfactant-oil-water microemulsion systems. *Langmuir* **1989**, *5* (2), 415.
- (2) Hore, D. K. W., D. S.; Richmond, G. L. Water at hydrophobic surfaces: When weaker is better. *Journal of the American Chemical Society* **2008**, *130*, 1800.
- (3) Moore, F. G.; Richmond, G. L. Integration or segregation: How do molecules behave at oil/water interfaces? *Acc. Chem. Res.* **2008**, *41* (6), 739.
- (4) McFearin, C. L.; Richmond, G. L. The unique molecular behavior of water at the chloroform-water interface. *Appl Spectrosc* **2010**, *64* (9), 986.
- (5) Scatena, L. F.; Brown, M. G.; Richmond, G. L. In *Science*, 2001; Vol. 292.
- (6) Conboy, J. C.; Messmer, M. C.; Richmond, G. L. Dependence of alkyl chain conformation of simple ionic surfactants on head group functionality as studied by vibrational sum-frequency spectroscopy. *J. Phys. Chem. B* **1997**, *101* (34), 6724.
- (7) Robertson, E. J.; Beaman, D. K.; Richmond, G. L. Designated Drivers: The Differing Roles of divalent metal ions in surfactant adsorption at the oil-water interface. *Langmuir* **2013**, *29* (50), 15511.
- (8) Beaman, D. K. R., E. J.; Richmond, G.L. Ordered polyelectrolyte assembly at the oil-water interface. *Proceedings of the National Academy of Sciences* **2012**, *109*, 3226.
- (9) Robertson, E. J. O., G.K.; Qian, M.; Pizano, R.; Prouix, C.; Zuckerman, R.N.; Richmond, G.L. Assembly and molecular order of two-dimensional peptoid nanosheets at the Oil-Water Interface. *Proceedings of the National Academy of Sciences* **2014**, *111*, 13284.
- (10) Hensel, J. K.; Carpenter, A. P.; Ciszewski, R. K.; Schabes, B. K.; Kittredge, C. T.; Moore, F. G.; Richmond, G. L. Molecular characterization of water and surfactant AOT at nanoemulsion surfaces. *P.N.A.S.* **2017**, *Early edition*.
- (11) Moran, P. D. B., G. A.; Cooney, R. P.; Bartlett, J. R.; Woolfrey, J. L. Vibrational spectra of metal salts of bis(2-ethylhexyl)sulfosuccinate (AOT). *Journal of Materials Chemistry* **1995**, *5*, 295.

### **Publications:**

“Molecular Characterization of Water and Surfactant AOT at Nanoemulsion Surfaces”, J.K. Hensel, A.P. Carpenter, R.K. Ciszewski, B.K. Schabes, C.T. Kittredge, F.G. Moore and G.L. Richmond, PNAS, July 31, 2017 Early Edition (doi: 10.1073/pnas.1700099114.)

**Enhancing Rare Events Sampling in Molecular Simulations of Complex Systems**  
**Sapna Sarupria, Assistant Professor in Chemical and Biomolecular Engineering,**  
**Clemson University, Clemson SC Phone: 864-656-3258 Email: [ssarupr@g.clemson.edu](mailto:ssarupr@g.clemson.edu)**

Birth of a new distinct phase is a phenomenon encountered in a myriad of processes, and has wide ranging consequences in material processing, biological self-assembly, separations and several other processes. Several phase transitions are nucleation driven. The nucleation events occur over nanosecond timescales and involve hundreds to thousands of molecules. These length and timescales are difficult to access in experiments, thereby making experimental studies of nucleation challenging. On the other hand, molecular simulations sample the nanosecond and nanometer scales making them ideal to study nucleation. However, nucleation is a rare event, meaning that the waiting time to observe one nucleation event is significant. This makes simulation studies of rare events challenging.

To address this challenge, new techniques such as transition path sampling (TPS), transition interface sampling (TIS) and forward flux sampling (FFS) have been developed recently that enable sampling of rare events in molecular simulations using reasonable computer resources. We focus on FFS. While the method is straightforward, its application to systems with complex free energy landscapes has revealed several weaknesses which make it computationally prohibitive to extend the use of techniques such as FFS to realistic systems (i.e. with complex and rugged energy landscapes) and to perform studies at realistic conditions (e.g. nucleation at low supersaturation where the rates are smaller). Our work addresses these challenges.

**Proposed Work:** The proposed work focuses on using a multi-pronged approach to address such challenges to develop the next generation FFS-based rare event sampling methods for molecular simulations. We specifically will be developing Multidimensional FFS (nDFFS), which is an FFS-based methodology that allows us to propagate transitions using multiple order parameters. In addition, We will apply machine learning algorithms to develop approaches that screen through the thousands of configurations and trajectories generated in the FFS calculations to distinguish between the reactive and the non-reactive trajectories.

**Previous Results:** In our previous work, we have developed a software program called Scalable Forward Flux Sampling (ScaFFS) to perform large scale forward flux sampling (FFS) calculations efficiently and effectively in high performance computing (HPC) infrastructure. In FFS, transitions from state A to state B are sampled through several intermediate transitions by dividing the phase space between A and B into interfaces. Several simulations are initiated at a given interface and configurations from those which reach the next interface are harvested. Then several simulations are initiated from the harvested configurations at the “new” interface to obtain configurations for the next interface. This process is continued until the final state is reached. While the process is straightforward, the application of the method to realistic systems can result in large number of simulation jobs and huge amount of data. To handle these large jobs and amounts of data effectively, we have developed ScaFFS.

ScaFFS represents a collaboration of state-of-the-art techniques in molecular simulations with those from Big Data to enable rare event simulations at massive scales. ScaFFS is designed to be adaptive, data-intensive, high-performance, elastic, and resilient. ScaFFS uses Hadoop in a novel

manner to handle the millions of simulations performed and files generated in FFS calculations. Through this approach we have been able to address all the challenges listed above. In addition, we do this in such a manner that the user only deals with the details of their FFS simulation. This is analogous to the MD software programs, where you only feed the details of the simulation system and parameters without worrying about how the parallelization would occur or what format the files can be written as. We use a similar approach here. We have now developed a new version of ScaFFS that is more user-friendly and also has updated back end for easier modifications. This will help us change the code as needed for nDFFS. We refer to this version of ScaFFS as SAFFIRE.

Advantages of SAFFIRE (also summarized in Fig. 1):

- Able to decide interfaces on-the-fly based on user specified criteria.
- There is no need for modification to the source codes for simulation i.e. if MD is being performed then no source code modification of GROMACS/LAMMPS or any other software is required.
- The status of each job is tracked and if needed, failed jobs are automatically re-run.
- Each file is tracked and intermediate data is not stored. However, if needed, the user can specify to retrieve it.
- The jobs are distributed over the nodes efficiently.
- SAFFIRE is capable of restarting the FFS simulation in case the calculations run over wall-time such that no data is lost.
- The biggest advantage from a user perspective is that the user needs to only modify one file that specifies all details about the FFS parameters and details of file storage etc.
- SAFFIRE has been tested extensively in both the institutional shared HPC environment at Clemson University as well as the publicly available HPC resources at XSEDE.

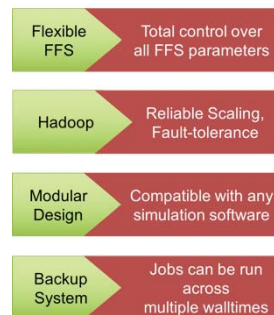


Figure 1:User friendly features of SAFFIRE

**Specific goals of proposed research:**

- Integration of nDFFS into SAFFIRE: We will develop and integrate nDFFS method into SAFFIRE thereby enabling us to run large scale simulations required to validate SAFFIRE on realistic systems.
- We will apply machine learning algorithms to develop approaches that screen through the thousands of configurations and trajectories generated in the FFS calculations to distinguish between the reactive and the non-reactive trajectories
- Validation of nDFFS method based on simulations of crystallization of Lennard Jones liquid: This system has been studied widely and the appropriate reaction coordinates for this transition have been determined based on other techniques.
- Application to ice and gas hydrate nucleation: Specifically, we will study the nucleation of ice near silver iodide surfaces and of gas hydrates. These provide “realistic” systems for testing the nDFFS method. Finding the appropriate reaction coordinate will improve the efficiency of FFS significantly and will become an important aspect as the systems and processes get more complex.

**Recent Progress:**

- We have developed a new version of ScaFFS that is more user-friendly and also has updated back end for easier modifications. We refer to this version of ScaFFS as SAFFIRE. We have tested this version and are developing a documentation for the same.
- We have developed a framework to perform 2DFFS on simple systems. We have identified six such simple test models that advance in complexity. We have performed langevin dynamics simulations to study the unbiased transition behavior and are now performing 1DFFS on these systems to evaluate the differences in sampling. Our previous results had indicated it is possible to have “bias in the sampling” of the transition paths when using 1DFFS. We were able to reduce this bias when we use 2DFFS, however, the methodology had other limitations. We are currently studying this phenomena in further detail on the newly developed test cases. Secondly, we are testing our hypothesis that local information about the trajectories can be used to navigate the direction of progress towards transition.
- We have completed large scale 1DFFS simulations for family of Lennard-Jones like potential at different temperature and pressure conditions. We also performed committor analysis on the configurations belonging to the transition paths and have identified some promising reaction coordinates. Our results conform with the previously reported studies of Lennard Jones liquid-to-solid nucleation studies. Based on this we will test our 2DFFS methods and evaluate if we our methods can identify the better reaction coordinates on-the-fly.
- We have performed largescale 1DFFS of ice nucleation on silver iodide surfaces. We are currently investigating various order parameters that best correlate to committor probability (and therefore, are closest to the reaction coordinate). Interestingly, we have not yet identified any one or two best order parameters. We further suspect that our system sizes for these simulations was small and therefore, we believe we will need to repeat our simulations for larger system sizes.
- We have also performed large scale 1DFFS simulations of hydrate nucleation and used committor probability to find the best reaction coordinates to describe this transition. This will form a dataset that we will use to evaluate the effectiveness of our nDFFS approaches in identifying reaction coordinates for complex systems.

**Conclusions:** The successful completion of our work will enable simulations to study the kinetics of complex processes -- an aspect that has greatly lagged behind so far. While our work is motivated by phase transitions and assembly processes in aqueous systems, rare events are relevant to a broad span of fields including telecommunications, finance, insurance, physics, chemistry, and biology. The techniques and software program developed here can easily be adapted to these systems. Therefore, our methodology and the simultaneous development of the software infrastructure to implement these methods will provide the broad scientific community with powerful tools to study previous inaccessible processes through molecular simulations.

**Grant Number and Title:**

DE-SC0015448 Enhancing Rare Events Sampling in Molecular Simulations of Complex Systems

**Students:** Ryan DeFever (PhD student)

Steven Hall (Undergraduate student)

## Equilibrium Structure and Dynamics of Aqueous Solutions and Interfaces

Richard Saykally (saykally@berkeley.edu), Musahid Ahmed (mahmed@lbl.gov), Phillip L. Geissler (plgeissler@lbl.gov), Kranthi Mandadapu (naani.m@gmail.com), and Teresa Head-Gordon (thg@berkeley.edu)

*Lawrence Berkeley National Laboratory, Chemical Sciences Division,  
1 Cyclotron Road, Berkeley, CA 94720*

**Program Scope:** It is widely recognized that the solvation properties of ions and molecules are central for governing transformations in many energy technologies. Key processes include electrochemical transport, ion pair formation and crystallization, corrosion, as well as chemical reactions in solutions and at interfaces. The ultimate goal of this work is to develop predictive models of electrolyte behavior in bulk solution, at interfaces and in confined environments.

**Progress Report:** Understanding solvation phenomena in microscopic physical detail has formed a central goal of our work, both for its relevance for atmospheric and electrochemistry and also for the basic gaps in chemical theory that it reveals. According to a popular mechanistic hypothesis, the charge asymmetry of ions' affinity for the air-water interface originates in the pre-existing anisotropy of the interfacial environment. Water molecules at the liquid's surface are orientationally biased, with a distinct population of hydroxyl groups pointing into vapor and lacking a hydrogen bond acceptor. The resulting average surface dipole density generates a drop in electrostatic potential across the interface, the so-called surface potential. Geissler and coworkers have recently performed a thorough set of calculations assessing whether anions' stronger preference for the surface can accurately be attributed to their motion across this potential gradient. A key component of this analysis was establishing finite size effects in computer simulations of periodically replicated liquid slabs. Such effects were known to be substantial in the case of bulk liquid simulations and had been rationalized quantitatively. We have generalized that result from a dielectric continuum perspective, obtaining a correction for periodic slab geometries that is quite different in form from the bulk case, and we demonstrated its accuracy in aqueous simulations.

In ongoing work, Saykally and coworkers examine ion adsorption to the model interface formed by water and graphene, comparing the results for this prototypical material interface to those from an earlier study with the Geissler group of the air/water interface. Deep UV second harmonic generation measurements of the SCN<sup>-</sup> ion, a prototypical chaotrope, determined a free energy of adsorption within error of that for air/water. However, unlike for the air/water interface, wherein repartitioning of the solvent energy drives interfacial ion adsorption, computer simulations reveal that direct ion/graphene interactions dominate the observed favorable enthalpy change. Moreover, the graphene sheets dampen capillary waves such that rotational anisotropy of the solute, if present, is the dominant entropy contribution, in contrast to the air/water interface.

As a route to further clarifying the mechanism that selectively drives ions to and away from the air/water interface, we have developed a new experiment (Deep UV Sum Frequency Generation) for measuring the complete charge transfer to solvent (CTTS) spectrum of interfacial anions, and have applied it to the prototypical case of the iodide anion. The spectrum shows significant differences from the bulk CTTS spectrum, and provides a new variable for constructing general theoretical models to explain interfacial ion behavior, which are underway in the Geissler group. Our studies of ion adsorption to solid-liquid interfaces were extended to polymer systems in a first

study of aqueous ion adsorption to the water-polystyrene interface, using SHG scattering spectroscopy of a polystyrene bead solution.

Flexible nanoscale confinement of solvent is critical to understanding the role that bending fluctuations play on geochemical and catalytic environments as well as in biological processes where soft interfaces are ubiquitous. Using molecular dynamics simulations, Head-Gordon and coworkers compare the phase behavior of water confined between flexible and rigid graphene sheets as a function of the in-plane density,  $\rho_{2D}$ . Both cases show commensurate mono-, bi-, and tri-layered states, however the water phase in those states and the transitions between them are qualitatively different for the rigid and flexible cases. The rigid systems exhibit discontinuous transitions between an (n)-layer and an (n+1)-layer state at particular values of  $\rho_{2D}$ , whereas under flexible confinement the graphene sheets bend to accommodate a coexistence of an (n)-layer and an (n+1)-layer state at the same density. Flexible walls introduce a very different sequence of ice phases and phase coexistence with vapor and/or liquid phases than that observed with rigid walls. A particularly striking example is seen at intermediate densities where the rigid walls invoke an aligned-stacking of hexagonal ice with a large number of defects at a solid-gas interface, whereas the flexible walls never nucleate a solid phase but instead exhibit coexistence between monolayer and bilayer liquid states.

Water encapsulated in silica microporous shells with controlled inner dimensions are used to experimentally probe water confinement. Ahmed and coworkers have measured the water uptake in these shells by IR spectroscopy and X-ray photoelectron spectroscopy. Changes in the OH asymmetric to symmetric stretch ratios provided a spectroscopic signature for water interactions with silica inside these shells. Electrospray ionization mass spectrometry coupled with microdroplet based X-ray spectroscopy was used to probe the chemical reactivity (chlorination and oxidation) of cobalt nanocrystals in the liquid phase. A novel mechanistic route was identified that leads to the formation of highly valent cobalt complexes with decreasing particle size. Site specific proton transfer in aqueous arginine nanoparticles and phase changes in super-cooled water nanoparticles were recorded with Velocity Map Imaging X-ray photoelectron spectroscopy. The dynamics of laser-induced formation and self-assembly of Ag nanoparticle gratings on mesostructured and amorphous titania substrate were probed by synchrotron X-ray absorption spectroscopy and imaging mass spectrometry

It has been previously established that dynamical heterogeneity plays a prominent role in understanding the dynamics of supercooled liquids on their way to forming glasses. In this context, the concept of dynamical phase transitions between the active and inactive phases played an important role in understanding glass formation. Particularly, it has been shown in models of glass formers, using path sampling techniques, that the system exhibits an active-inactive first order phase transition in the trajectory space. Mandadapu and coworkers are examining solvation and pre-transition effects in space-time in trajectories of a kinetically constrained model of glass formers (Katira et. al.). These effects are manifestations of the dynamical first-order phase transition between active and inactive trajectories, and are analogous to those observed for thermodynamic first-order phase transitions such as the hydrophobic effect in liquid water.

**Future Plans:** Theoretical work to date has highlighted our incomplete understanding of charge asymmetry even in the bulk liquid phase. The simpler homogeneous environment already features substantial solubility differences between cations and anions of the same size, differences that dielectric theory cannot explain. Geissler and coworkers have found in simulations that quadrupole contributions can account for this discrepancy, and have identified the geometric relationship

between water's dipole and quadrupole as an important source of charge asymmetry. These observations suggest an elaboration of dipole field theory that resolves a microscopic quadrupole field as well. Incorporating constraints between these fields poses a substantial theoretical challenge. As first steps, mean field treatments we will examine as well as models informed empirically from atomistic simulations.

The concepts of hydrophobic solvation like effects in trajectory space and the associated dynamical interfacial tension will be examined by Mandadapu and coworkers to quantitatively understand the melting of ultra-stable glasses. This will be explored by studying the spatial propagation of activity fronts when melted from an inactive phase, i.e., glassy phase. The current work on solvation in trajectory space establishes that immobile regions in supercooled liquids show correlations in space-time to effectively minimize the dynamical interfacial free energy.

The DUV-SHG experimental approach, described above, will be used by Saykally and coworkers to measure CTTS spectra of other surface-enhanced ions, emphasizing the study of counterion effects on the spectra. The goal is to develop a complete model of ion adsorption to liquid interface with the Geissler's group. Studies of ion adsorption will be extended beyond graphene-water interfaces to interfaces with both hydrophilic and hydrophobic polymers, and ultimately, to water-metal systems, seeking to extract entropy and enthalpy effects.

Head-Gordon and coworkers will study flexible interfaces, which are widely present in fundamental and technological processes, because it is of critical importance to understand nanoconfinement effects in the phase behavior of water under realistic conditions, beyond the idealized confinement conditions of infinitely rigid walls. This will be an important component for seeding future experimental directions for chemical reactivity under confinement.

### **Publications Acknowledging DOE support:**

T. R. Gingrich, G.M. Rotskoff, G.E. Crooks, and P.L. Geissler. "*Near-optimal protocols in complex nonequilibrium transformations*", Proc. Natl. Acad. Sci. 113, 10263 (2016).

A. Bhowmick, S. Sharma, T. Head-Gordon (2016). The role of side chain entropy and mutual information for improving the de novo design of Kemp Eliminases KE07 and KE70. *Phys. Chem. Chem. Phys.* In press

J. Yao, D. Lao, X. Sui, Y. Zhou, S. K. Nune, X. Ma, T. P. Troy, M. Ahmed, Z. Zhu, D. J. Heldebrant, X-Y Yu, *Two Coexisting Liquid Phases in Switchable Ionic Liquids*. PCCP 2017,19, 22627, DOI: 10.1039/C7CP03754F

B. Xu, M.I. Jacobs, O. Kostko, M. Ahmed, "*Guanidinium group is protonated in a strongly basic arginine solution*," Chem. Phys. Chem. 18, 1503 (2017), DOI 10.1002/cphc.201700197

N. Schwierz, R. K. Lam. Z. Gamlieli, J. J. Tills, A. Leung, P. L. Geissler, and R. J. Saykally, "Hydrogen and electric power generation from liquid microjets: Design principles for optimizing conversion efficiency", J. Phys. Chem. C doi: 10.1021/acs.jpcc.6b03788 (2016).

S. Vaikuntanathan, G. M. Rotskoff, A. Hudson, P. L. Geissler, "Necessity of capillary modes in a minimal model of nanoscale hydrophobic solvation", Proc. Natl. Acad. Sci. U.S.A. 113, E2224 (2016).

Lam, R. K., Smith, J. W., Saykally, R. J. "Communication: Hydrogen bonding interactions in water-alcohol mixtures from X-ray absorption spectroscopy" *J. Chem. Phys.*, **144**, 191103 (2016).

McCaffrey, D. L., Nguyen, S. C., Cox, S. J., Weller, H., Alivisatos, A. P., Geissler, P. L., Saykally, R.J. "*Mechanism of ion adsorption to aqueous interfaces: Graphene/water vs. air/water*\_" *PNAS*, Early Edition, (2017).

Lam, R. K., Shih, O., Smith, J. W., Sheardy, A. T., Rizzuto, A. M., Prendergast, D., Saykally, R. J. "*Erratum: "Electrokinetic detection for x-ray spectra of weakly interacting liquids: n-decane and n-nonane"*" [*J. Chem. Phys.* 140, 234202 (2014)]" *J. Chem. Phys.*, **146**, 249902 (2017).

Rizzuto, A. M., Irgen-Gioro, S., Eftekhari-Bafrooei, A., Saykally, R. J. "*Broadband Deep UV Spectra of Interfacial Aqueous Iodide*" *J. Phys. Chem. Lett.*, **7**, 3882-3885 (2016).

Smith, J. W., Lam, R. K., Shih, O., Rizzuto, A. M., Prendergast, D., Saykally, R. J. "*Properties of aqueous nitrate and nitrite from x-ray absorption spectroscopy*" *J. Chem. Phys.*, **2015**, 143, 084503.

O. Kostko, B. Bandyopadhyay, T.P. Troy and M. Ahmed. "*Proton transfer in acetaldehyde–water clusters mediated by a single water molecule*," *PCCP* (In press)

B. Bandyopadhyay, T. Stein, Y. Fang, O. Kostko, A. White, M. Head-Gordon, and M. Ahmed, "*Probing Ionic Complexes of Ethylene and Acetylene with Vacuum Ultraviolet Radiation*," *J. Phys. Chem A.* (2016) **120**, 5053, DOI: 10.1021/acs.jpca.6b00107

O. Kostko, B. Bandyopadhyay, and M. Ahmed, "*Vacuum Ultraviolet Photoionization of complex chemical systems*," *Ann. Rev. Phys. Chem.* (2016) Vol. 67, 19, DOI: 10.1146/annurev-physchem-040215-112553

B. Bandyopadhyay, O. Kostko, Y. Fang, and M. Ahmed, "*Probing Methanol Cluster Growth by Vacuum Ultraviolet Ionization*," *J. Phys. Chem. A.* (2015) **119**, 4083.

O. Kostko, B. Xu, M.I. Jacobs, M. Ahmed, "*Soft X-ray spectroscopy of nanoparticles by velocity map imaging*," *J. Chem. Phys.* (2017), 147, 013931, DOI: 10.1063/1.4982822

S. Alayoglu, D. Rosenberg, M. Ahmed, "*Hydrothermal Synthesis and Characterization under Dynamic Conditions of Cobalt Oxide Nanoparticles Supported over Magnesium Oxide Nanoplates*," *Dalton Trans.*, (2016) **45**, 9932, DOI: 10.1039/C6DT00204H

## Molecular Theory and Modeling

Gregory K. Schenter

Pacific Northwest National Laboratory

902 Battelle Blvd. Mail Stop K1-83

Richland WA 99352

greg.schenter@pnl.gov

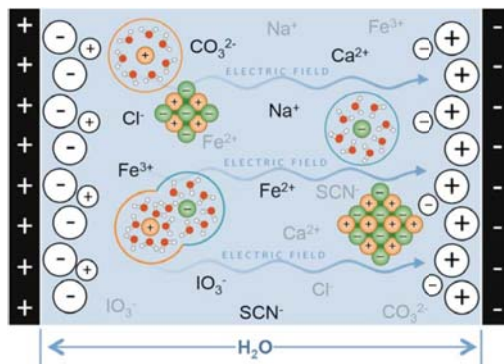
### Abstract

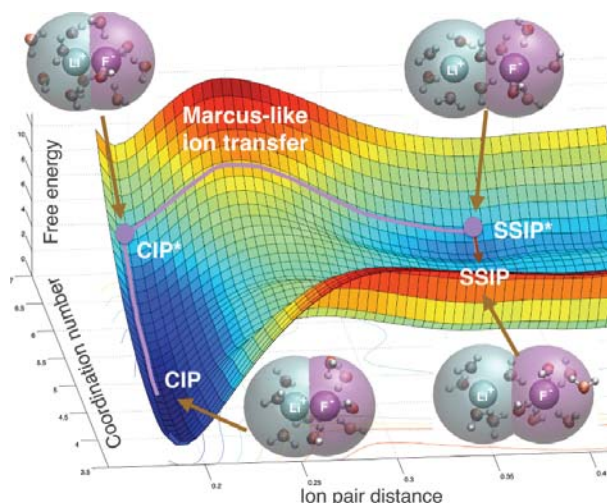
The Molecular Theory and Modeling group at Pacific Northwest National Laboratory consists of Gregory K. Schenter, Liem X. Dang, Shawn M. Kathmann, Chris J. Mundy, Sotiris S. Xantheas, and Marat Valiev. Please find contributions from individual PIs in the abstract book.

The overarching goals of the Molecular Theory & Modeling Program are: 1) development of a fundamental comprehension of the driving forces, processes and phenomena, such as solvation, nucleation, assembly, transport, and reaction, in complex condensed-phase, heterogeneous and interfacial molecular environments, and 2) development of theoretical and computational methods required to accelerate scientific advances in condensed-phase and interfacial molecular science.

In current work, we focus on the water exchange process about ions, comparing the dependence on the descriptions of molecular interaction. [5,6,8,9,10] In studying these exchange processes, it is necessary to find the proper balance between the ion-water and water-water interaction. [2,3,4,11] We are starting to extend some of these ideas to the process of nucleation in the condensed phase. Another significant component of our current and future work is to explore appropriate reaction coordinates and collective motions that control the phenomena. We are exploring system/bath decompositions and reduced descriptions of dynamics in terms of generalized Langevin equations. What is new is the focus of phenomena at interfaces and in inhomogeneous systems.

In our studies, we search for the appropriate amount of explicit treatment of electronic structure that allows for efficient sampling of a statistical mechanical ensemble of a system of interest. We have established that a Density Functional Theory (DFT) description of molecular interaction provides a quantitative representation of the short-range interaction and structure when compared to Extended X-ray Absorption Fine Structure (EXAFS) measurements. To do this we continue to develop our MD-EXAFS approach. [1] This direct comparison to experimental measurement gives us the confidence that the short range molecular phenomena are effectively and accurately described by DFT electronic structure coupled to statistical mechanical sampling. Much of our future efforts will concentrate on characterizing fluctuations, taking advantage of effective potentials of mean force and linear response kernels from density, charge and electromagnetic fluctuations. [7]





In Ref. [10] we explored the dynamics of  $\text{Li}^+ - \text{F}^-$  ion pairing in aqueous solvent, focusing on the transition from a contact ion-pair to a solvent separated ion pair. We constructed a generalized Langevin equation framework to compare DFT and empirical potential descriptions of molecular interaction. A key result of this study was the identification of high frequency coupling associated with “geometrically-frustrated charge pairing” that occurs in the empirical potential but not in the DFT description of molecular interaction. In Ref. [9] we explored the use of the coordination number as a reaction coordinate to describe water exchange rates about solvated ions. We developed a consistent transition state theory (TST) in this coordinate. This

allows us to more effectively characterize the important collective motions that lead to the rare event processes. Currently we are considering the two-dimension potential of mean force consisting of both distance based reaction coordinates (distance between ions) and coordination number. [See Figure] We are exploring how this energy landscape changes with the nature of the ions and the controlling factors that determine the transition thermodynamics and rates between the contact ion pair (CIP) and the solvent separated ion pair (SSIP). In doing so, we discovered a natural separation of motions. First involves restructuring of the solvent environment, characterized by the coordination number reaction coordinate. Next, the final stage of motion corresponds to ion separation. This separation of motions has allowed us to construct a “Marcus Theory of Ion-Pairing” [6], involving parabolic free energies and inverted regions of behavior.

### Molecular Theory and Modeling FWP 16249

**Postdoc(s):** Tim Duignan, Mirza Galib, and Santanu Roy

**Acknowledgements:** In addition to the postdocs in the group, the work described here was influenced by all members of the Molecular Theory and Modeling group. A majority of the work was performed with Chris Mundy and John Fulton of CPIMS.

The Molecular Theory and Modeling FWP 16249 is co-managed by CTC and CPIMS programs of DOE Office of Basic Energy Sciences Division of Chemical Sciences, Geosciences, and Biosciences.

### Publications Acknowledging this Grant

Publications of GK Schenter. For other Molecular Theory and Modeling efforts, see contributions Liem X. Dang, Shawn M. Kathmann, Chris J. Mundy, Sotiris S. Xantheas, and Marat Valiev in this abstract book.

1. Schenter GK, and JL Fulton. 2017. "Molecular Dynamics Simulations and XAFS (MD-XAFS)." Chapter 18 in *XAFS Techniques for Catalysts, Nanomaterials, and Surfaces*, ed. Y Iwasawa, K Asakura and M Tada, pp. 251-270. Springer International Publishing, Cham, Switzerland. doi:10.1007/978-3-319-43866-5\_18
2. Galib M, MD Baer, LB Skinner, CJ Mundy, T Huthwelker, GK Schenter, CJ Benmore, N Govind, and JL Fulton. 2017. "Revisiting the hydration structure of aqueous  $\text{Na}^+$ ." *Journal of Chemical Physics* 146(8):084504. doi:10.1063/1.4975608

3. Duignan TTS, MD Baer, GK Schenter, and CJ Mundy. 2017. "Electrostatic solvation free energies of charged hard spheres using molecular dynamics with density functional theory interactions." *Journal of Chemical Physics* 147, 161716. doi:10.1063/1.4994912
4. Duignan TTS, MD Baer, GK Schenter, and CJ Mundy. 2017. "Real single ion solvation free energies with quantum mechanical simulation." *Chem. Sci.*, 8, 6131-6140. doi:10.1039/c7sc02138k
5. Dang LX, GK Schenter, and CD Wick. 2017. "Rate Theory of Ion Pairing at the Water Liquid-Vapor Interface." *Journal of Physical Chemistry C* 121(18):10018-10026. doi:10.1021/acs.jpcc.7b02223
6. Roy S, MD Baer, CJ Mundy, and GK Schenter. 2017. "Marcus Theory of Ion-Pairing." *J. Chem. Theory Comput.*, 13 (8), pp 3470–3477. doi:10.1021/acs.jctc.7b00332
7. Galib M, TTS Duignan, YB Misteli, MD Baer, GK Schenter, J Hutter, and CJ Mundy. 2017. "Mass Density Fluctuations in Quantum and Classical descriptions of Liquid Water." *Journal of Chemical Physics* 146, 244501. doi:10.1063/1.4986284
8. Dang LX, and GK Schenter. 2016. "Solvent Exchange in Liquid Methanol and Rate Theory." *Chemical Physics Letters* 643:142-148. doi:10.1016/j.cplett.2015.10.045
9. Roy S, MD Baer, CJ Mundy, and GK Schenter. 2016. "Reaction Rate Theory in Coordination Number Space: An Application to Ion Solvation." *Journal of Physical Chemistry C* 120(14):7597-7605. doi:10.1021/acs.jpcc.6b00443
10. Pluharova E, MD Baer, GK Schenter, P Jungwirth, and CJ Mundy. 2016. "Dependence of the rate of LiF ion pairing on the description of molecular interaction." *Journal of Physical Chemistry B* 120(8):1749-1758. doi:10.1021/acs.jpcc.5b09344
11. Skinner LB, M Galib, JL Fulton, CJ Mundy, JB Parise, VT Pham, GK Schenter, and CJ Benmore. 2016. "The structure of liquid water up to 360 MPa from x-ray diffraction measurements using a high Q-range and from molecular simulation." *Journal of Chemical Physics* 144(13):134504. doi:10.1063/1.4944935

**Program Title:** Understanding Chemical Bond Dynamics in Liquids Using Mixed Quantum/Classical Molecular Dynamics Simulation

**Principal Investigator Info:** Professor Benjamin J. Schwartz  
Department of Chemistry and Biochemistry  
University of California, Los Angeles  
Los Angeles, CA 90095-1569 USA  
Voice: 310-206-4113; Fax: 310-206-4038  
E-mail: [schwartz@chem.ucla.edu](mailto:schwartz@chem.ucla.edu)

**Program Scope:** One of the central themes of modern physical chemistry is elucidating the elementary steps associated with chemical reactions. In the gas phase, our understanding is becoming largely complete. In principle, knowledge of the potential energy surfaces and the initial reactant trajectories is sufficient to predict the details of the reaction mechanism. In condensed phases, however, changes in reactant charge distribution or size during a reaction are strongly coupled to motions of the solvent molecules: solvent dynamics can stabilize (or destabilize) the energy of the transition state, controlling not only the effective barrier for a reaction but also how long that barrier persists. In addition, ‘caging’ by the solvent can promote recombination of recently-broken chemical bonds. All of these solvent effects, which play a crucial role in determining the rate or possibly even the products of chemical reactions, take place on picosecond or sub-picosecond time scales.

This program presents a description of both short- and longer-ranged studies designed to attack the frontiers of chemical reaction dynamics in the condensed phase. The results of these projects will elucidate the molecular basis for solvation, non-adiabatic relaxation, and multi-electron quantum mechanical effects in solution-phase chemical reactivity, with emphasis on the critical realms of equilibrium chemical bond dynamics and bond breaking/bond formation. The proposed research will utilize non-adiabatic mixed quantum/classical (MQC) MD simulations and will make direct ties to ultrafast spectroscopic experiments. The particular objectives that will be tackled include the following:

- Elucidating solvent effects on both ground- and excited-state chemical bonds, including the effects of exchange and correlation treated using configuration-interaction-with-singles-and-doubles (CISD) in MQC MD simulations. This includes understanding how Pauli repulsive forces from solvents compress bonding electrons ( $e^-$ s) to raise molecular vibrational frequencies, how even non-polar solvents can induce significant dipoles in non-polar molecular bonds, how polar liquids force  $e^-$  localization toward one side of a chemical bond, and how solvents generally control photodissociation dynamics, including caging, recombination and charge transfer between the fragments.
- Going beyond the frozen core approximation by developing pseudopotentials in MQC MD simulations that respond to changes in molecular coordinates. Improving polarization potentials. Understanding the implications of both of these on chemical bond dynamics.
- Making detailed ties between MQC MD calculations and ultrafast spectroscopy experiments.

Our plan is to study solution-phase bond dynamics initially by revisiting the equilibrium and photodissociation dynamics of simple diatomics. Our theoretical description of chemical bonds in solution will combine three recent advances made by the PI’s group. First, we will take advantage of our newly-developed coordinate-dependent pseudopotentials<sup>1</sup> to describe the

bonding  $e^-$ s in alkali metal dimers and alkali metal hydrides. These molecules can be well described by pseudopotentials because their chemical bonds are composed of  $s$ -type atomic  $e^-$ s that reside outside closed-shell cores; thus, our calculations need to treat only the two bonding electrons quantum mechanically. With only two quantum  $e^-$ s, we can then use our real-space, CISD non-adiabatic MQC MD algorithm<sup>2</sup> to find, for each solvent configuration, the *exact* electronic structure of the two QM bonding  $e^-$ s in the presence of the solvent (for a  $2-e^-$  system, CISD is equivalent to full CI). Moreover, CISD calculations will allow us to study dynamics on both the ground and electronic excited states, including dynamics near curve crossings where solvent motions can induce non-adiabatic transitions between electronic surfaces. In essence, we will be performing electronic dynamics by computing the full many-body condensed-phase PES on the fly. Finally, we will make use of our newly-developed quantum umbrella sampling algorithm<sup>3</sup> to construct PMFs along both the nuclear bond and various solvent coordinates, allowing us to investigate the nature of solvent-induced charge separation and curve-crossing.

Our specific objectives include addressing each of the following questions:

- 1) For photoexcited alkali metal dimers and hydrides, what is the branching ratio for dissociation versus geminate recombination in solution? How do the branching ratio and the nature of the solvent motions that induce the curve-crossing to new electronic states depend on the mass and/or polarity of the solvent? How does this vary with and without the FCA?
- 2) Is a PMF description, in which the solvent degrees of freedom are integrated out, accurate for solution-phase reactions or even for equilibrium bond dynamics? If not, can a PES-type picture be salvaged by explicitly including just a few important solvent degrees of freedom? What is the correct way to think about effects such as Pauli repulsion compressing bonding electrons and changing the electronic structure of a molecule? What about changes in bond length and vibrational frequency associated with charge transfer character induced by the solvent?
- 3) Where do the bonding electrons go during photodissociation? Can solvation by a polar solvent (e.g.,  $H_2O$ ) lead to dissociation into an ion pair (cation + anion) rather than a neutral (bi-radical) channel? If so, what is the branching ratio, and how does it compare to that in non-polar (e.g., Ar) or weakly-polar (e.g., THF) solvents? Are there non-adiabatic transitions between the two channels, such as occur in the photodissociation of NaI? Can partial charge transfer or ‘harpooning’ occur? If so, what solvent motions drive such electronic dynamics, and how does all this affect the nuclear bond (e.g. dissociation, recombination and any subsequent vibrational relaxation)?
- 4) How is correlation between the two bonding electrons lost when the bond breaks? The two electrons are highly correlated and thus indistinguishable at equilibrium, but as dissociation proceeds, the electrons (at least in the biradical channel) localize on separate atoms in different solvent environments and thus become distinguishable. How does the solvent induce this loss of correlation, and how long does it take?

**Recent Progress:** Although the grant has only been active for a few weeks, we have already obtained preliminary results simulating the ground-state of the  $Na_2$  molecule in liquid tetrahydrofuran (THF). The  $Na_2$  molecule is not bound at the Hartree-Fock level of theory, but our pseudopotential-plus-CISD treatment of the bonding electrons does an excellent job of describing the electronic structure of this molecule compared to higher-level calculations. It is well known that ethers have a predilection for chelating alkali metal cations, and THF is well

known to chelate  $\text{Na}^+$ . In fact, in previous work, we simulated<sup>4</sup> (and measured using ultrafast spectroscopy)<sup>5</sup> the solvation of neutral Na atoms in liquid THF, and found that the solvent pushes the valence electron of the atom off-center, exposing part of the  $\text{Na}^+$  core and making it available for chelation. In essence, by paying the energetic price to partially ionize the atom, the solvent is able to create up to 4 stable  $\text{Na}^+\text{-O}$  dative bonds, as well as a fairly large atomic dipole that can be solvated by the weakly polar solvent. It turns out that these same driving forces strongly alter the properties of the  $\text{Na}_2$  molecule in liquid THF; in fact, as described below, *we find that the solvent plays a direct role in the molecular identity of the solute.*

In previous work, we explored the properties of simulated  $\text{Na}_2$  dissolved in liquid Ar.<sup>6</sup> We found that placement in the condensed phase causes the vibrational frequency of the molecule to blue-shift for several reasons. First, caging by the surrounding solvent molecules creates an effectively steeper potential that increases the vibrational frequency, a purely classical effect. But, we also found that most of the vibronic blue-shift is the result of compression of the dimer bonding electrons by collisions with the surrounding solvent molecules. These collisions, on average, increase the bonding electron density between the atoms relative to that of the molecule in the gas phase. This provides a second, quantum mechanical effect whose effect on the vibronic blue shift is more than double the size of the classical effect. Moreover, even though the average dipole of the solvated dimer molecule is zero, the instantaneous dipole can be quite large, since collisions with the Ar atoms push the bonding electrons off-center. This means that immersion in the solvent induces a time-dependent dipole, and thus gives rise to IR absorption, even though the molecule is a homonuclear diatomic in a nonpolar solvent.<sup>6</sup>

When the  $\text{Na}_2$  molecule is placed in liquid THF, in contrast, we see several remarkable things. First, the average vibrational frequency of the molecule is strongly red-shifted, the exact opposite of what we saw in liquid Ar. We also see that the molecule has a much larger average dipole moment and thus an even more intense IR spectrum than what is predicted in liquid Ar. The reason for this is chelation: like with bare Na atoms in THF, the ether solvent strongly chelates both ends of the  $\text{Na}_2$  molecule, pushing the electron density off of the bond axis. In fact, on average, we see three THF molecules chelating one side of the molecule and four THF's chelating the other side (which we label the (3,4) configuration), although configurations with three THFs on each side ((3,3)) and two one side and four on the other ((2,4)) are also quite common. The dative bonds formed between the THF oxygen atoms and the Na cation cores are moderately strong, about the same strength as an H-bond in liquid water. As a result, the chelated solvation structures are quite stable, and the datively-bonded solvent molecules exchange relatively slowly, on a time scale of ten or a few tens of ps. When we calculate the PMF for chelation of the dimer along a coordination number order parameter, we find that each chelated state occupies a local free energy minimum, with barriers of 5 to 6  $k_B T$  separating the different chelation states.

As a result, each chelation state -- (2,4), (3,3) and (3,4) -- represents a distinct molecule, and the different chelation states are in effective equilibrium with other with interconversion rates that are well described by simple transition state theory. Moreover, the molecule associated with each chelation state has a different vibrational frequency and a different average dipole. In order to chelate each end of the molecule, the interaction with the datively-bonded solvents increases the bond length and lowers the internuclear bonding electron density. This, combination with the fact that the datively-bonded solvents vibrate along with the Na atoms, explains the lowering of the vibrational frequency. The (3,3) chelation state/molecule, by symmetry, has no average dipole, but the asymmetric (2,4) and (3,4) molecules effectively have

permanent dipoles, giving rise to strong IR transitions. The overall dipole moment is modulated at both the intermolecular frequency, which is lowered relative to that in the gas phase, and at the frequency of the Na–O dative bonds, which is significantly higher than that in the gas phase.

Overall, the mere presence of the solvent turns what had been a single Na<sub>2</sub> molecule into what is at least three different molecular species in equilibrium. Each of the three chelated species has a different IR spectrum, dipole and barrier to interconversion, and all three behave quite differently from the isolated gas-phase species. Thus, we have found that the solvent not only modulates chemical properties, but also plays a direct role in chemical identity.

**Future Plans:** For the immediate future, we plan on continuing our exploration of how local specific solvent interactions can alter molecular identity. The fact that the dative bond interactions responsible for changing identity here are comparable to the strengths of H-bonds means that the idea of the solvent playing an explicit role in molecular identity is likely general to any chemical system with local specific interactions of about this strength. This includes H-bonds in water and alcohol solvents, and the intramolecular forces responsible for secondary structure in proteins and peptides. We also plan to address how the solvent alters molecular identity for intrinsically asymmetric molecules such as Na-K or Na-H (the latter of which does not offer the possibility of chelation of the proton by the ether solvent). We also plan to extend the simulations to more polar solvents such as water (even though alkali metal dimers and hydrides react violently with water, we can still use classical water as a prototypical highly polar solvent in simulations since classical water cannot react to form H<sub>2</sub> gas or other products).

Over the longer term, we plan to directly address all the questions discussed under the project scope by simulating the excited-state dynamics of all of the above molecules. By promoting these dimers to their lowest dissociative excited-state surface, we can see how the condensed environment, and the local specific interactions present in THF in particular, alter the photodissociation dynamics relative to that in the gas phase. Our group already has a track record for simulating non-adiabatic dynamics using either in-house developed algorithms<sup>7</sup> or more standard surface-hopping algorithms found in the literature. The hope is also to develop experiments along these lines (sodium dimer molecules already have been studied in rare gas matrices, and should be stable in glass-forming solvents like 2-methyl-THF), either collaboratively or within the PI's group.

**Publications:** As the project was funded on Sept. 1, 2017, there are as of yet no publications supported by this award.

### References:

- <sup>1</sup> A. Kahros and B. J. Schwartz, "Going Beyond the Frozen Core Approximation: Development of Coordinate-Dependent Pseudopotentials and Application to Na<sub>2</sub><sup>+</sup>," *J. Chem. Phys.* **138**, 054110, 1-9 (2013).
- <sup>2</sup> W. J. Glover, R. E. Larsen and B. J. Schwartz, "First-Principles Multielectron Mixed Quantum/Classical Simulations in the Condensed Phase. I. An Efficient Fourier-Grid Method for Solving the Many-Electron Problem," *J. Chem. Phys.* **132**, 144101 (2010).
- <sup>3</sup> W. J. Glover, J. R. Casey and B. J. Schwartz, "Free Energies of Quantum Particles: The Coupled-Perturbed Quantum Umbrella Sampling Method," *J. Chem. Theor. Comput.* **10**, 4661-71 (2014).
- <sup>4</sup> W. J. Glover, R. E. Larsen and B. J. Schwartz, "Simulating the Formation of Sodium:Electron Tight-Contact Pairs: Watching the Solvation of Atoms in Liquids One Molecule at a Time," *J. Phys. Chem. A* **115**, 5887 (2011).
- <sup>5</sup> A. E. Bragg, W. J. Glover and B. J. Schwartz, "Watching the Solvation of Atoms in Liquids One Molecule at a Time," *Phys. Rev. Lett.* **104**, 233005 (2010).
- <sup>6</sup> W. J. Glover, R. E. Larsen and B. J. Schwartz, "How Does a Solvent Affect Chemical Bonds? Mixed Quantum-Classical Simulations with a Full CI Treatment of the Bonding Electrons," *J. Phys. Chem. Lett.* **1**, 165 (2009).
- <sup>7</sup> M. J. Bedard-Hearn, R. E. Larsen and B. J. Schwartz, "Mean-Field Dynamics with Stochastic Decoherence (MF-SD): A New Algorithm for Nonadiabatic Mixed Quantum/Classical Molecular Dynamics Simulations with Nuclear-Induced Decoherence," *J. Chem. Phys.* **123**, 234106 (2005).

# An Atomic-scale Approach for Understanding and Controlling Chemical Reactivity and Selectivity on Metal Alloys

E. Charles H. Sykes (charles.sykes@tufts.edu)

Department of Chemistry, Tufts University, 62 Talbot Ave, Medford, MA 02155

## Program Scope:

Catalytic hydrogenations are critical steps in many industries including agricultural, chemicals, foods and pharmaceuticals. In the petroleum refining industry, for instance, catalytic hydrogenations are performed to produce light, hydrogen rich products like gasoline. Hydrogen activation, uptake, and reaction are also important phenomena in fuel cells, hydrogen storage devices, materials processing, and sensing. Typical heterogeneous hydrogenation catalysts involve nanoparticles composed of expensive noble metals or alloys based on metals like Pt, Pd, and Rh. Our goal is to alloy these reactive metals, at the single atom limit, with more inert and often much cheaper hosts and to understand how the local atomic geometry affects reactivity.

The CPIMS program has supported Sykes lab work in developing a new class of model alloy catalysts that we have termed *single atom alloys* (SAAs) and understanding their ability to activate H<sub>2</sub> and enable spillover of hydrogen to the support where ultra-selective reactions can occur. *Spurred by our fundamental studies, many groups around the world have now shown that our SAA concept is valid in real catalysts working under ambient conditions.* For example, selective hydrogenation of acetylene and acrolein, as well as Uhlmann coupling have been demonstrated. *Our goal is to now push this work beyond hydrogenation chemistry and study the ability of SAAs to perform C-H activation chemistry and dehydrogenation reactions, as well as probing the ability of larger metal alloy ensembles to enable selective oxidations.* Mostly recently we have demonstrated that SAAs are robust to poisoning by CO, a common problem in Pt based catalysis.

## Recent Progress: Tackling CO Poisoning with Single Atom Alloys

Platinum is widely used for fuel cell anodes and hydrocarbon processing due to its superior catalytic performance. Pt metals are highly active for H<sub>2</sub> dissociation, but are very susceptible to CO poisoning. Due to its strong binding to Pt, even trace amounts of CO impurity, which is always present in H<sub>2</sub> gas produced from fuel reforming, can diminish H<sub>2</sub> activation and reactivity. This strong CO adsorption also hinders the fast conversion of CO to CO<sub>2</sub> at low temperatures (< 200°C), and becomes a technical challenge for efficient emission control and water-gas shift (WGS) for hydrogen upgrading. Recently, atomically dispersed Pt<sub>1</sub> (or Pd<sub>1</sub>)-O<sub>x</sub>- stabilized on a variety of supports, such as silica, titania, KLTL-Zeolite, MCM-41, alumina and iron oxide, were found to be highly active in WGS and CO oxidation reactions and Pd<sub>1</sub>/g-C<sub>3</sub>N<sub>4</sub> was reported to be active and stable in the selective hydrogenation of 1-hexyne to 1-hexene. The single platinum atom sites have a cationic nature that results in weak CO adsorption, and thus are the only sites capable of low temperature CO conversion. Although single-atom catalytic sites in Pt<sub>1</sub> (or Pd<sub>1</sub>)-O<sub>x</sub>-oxides possess the desired property of weaker CO adsorption, they may not be stable enough under hydrogenation conditions.

As the natural expansion of our SAA concept, we tackled the CO poisoning issue of platinum catalysts with Pt-based SAAs in which the Pt atoms are embedded in a host metal surface, like Cu. The situation for isolated Pt atoms may be different than traditional bimetallic alloys, where ensemble effects have

been shown to increase the CO binding strength at extended catalytic metal sites. From a fundamental perspective, metal alloys that alter the adsorption geometry of CO can exhibit weaker CO binding and enhanced CO tolerance.

By using model Pt-Cu SAAs, we determined the binding strength of CO to isolated Pt atoms in the surface of Cu(111) (Figure 1A). Weakly bound CO desorbs from Cu(111) below 200 K and after deposition of 0.01 ML Pt, a symmetrical CO desorption peak was observed in TPD traces at 350 K. At an increased coverage of 0.3 ML Pt, CO desorbed at 360 K with a high temperature tail. The high temperature tail developed into an additional peak at 480 K (0.6 ML Pt). At 5 ML, a desorption feature was observed at 410 K and the surface is assumed to be terminated as Pt(111).

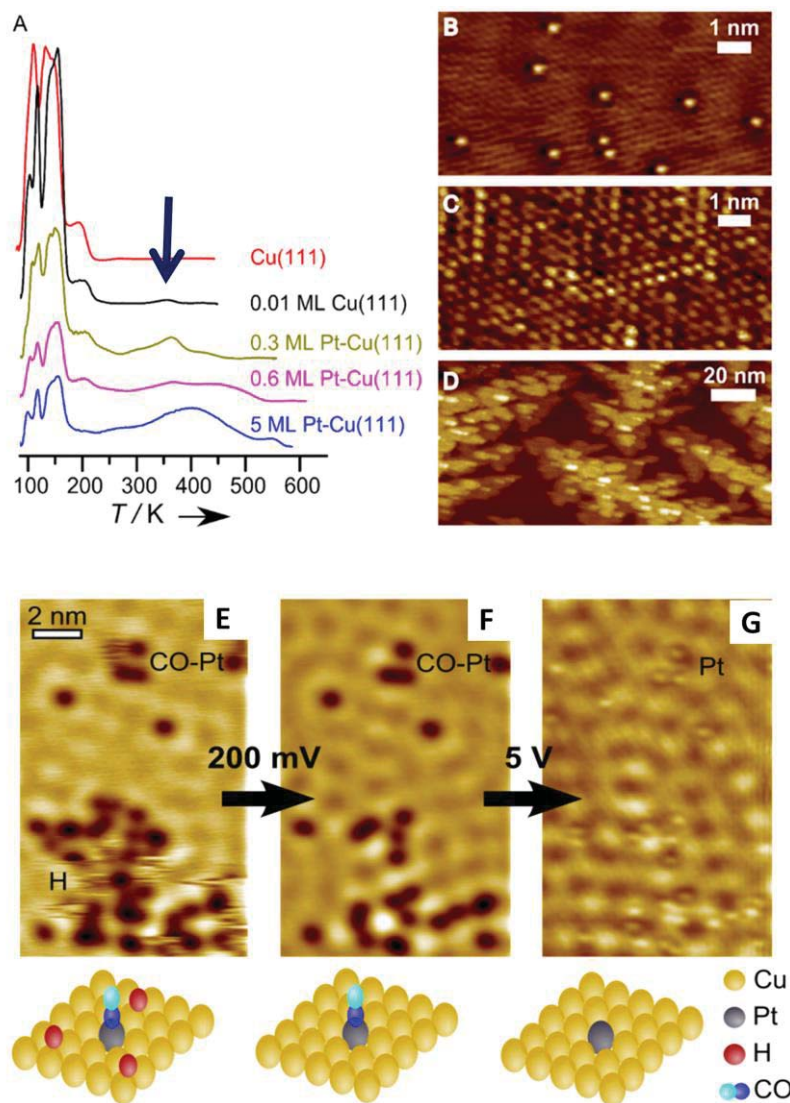


**Figure 1.** Measuring CO binding strength and atomic scale adsorption sites on PtCu alloys. Upper Panels: Binding strength of CO to Pt-Cu SAAs vs. pure Pt. (A) CO desorption and STM images of (B) 0.01 ML, (C) 0.3 ML and (D) 1 ML Pt-Cu(111) alloys prepared at 380 K. Lower Panels: STM images showing the co-adsorption of H and CO on a Pt-Cu(111) SAA surface and STM tip-induced adsorbate removal to reveal the binding sites beneath. (E) H and CO adsorbed on Pt-Cu(111) SAA. (F) Image of same area following scanning at elevated bias (200 mV) to remove adsorbed H from the image area. (G) After 5 V pulses to remove adsorbed CO, individual Pt atoms are seen underneath each removed CO molecule.

In agreement with the Pt surface structure observed by STM, the CO desorption traces reveal the development of 3 distinct Pt-Cu alloyed structures with increasing Pt coverage (Figure 1B-D). With atomic resolution, the Pt atoms image ~20 pm higher than the surrounding Cu lattice and appear as brighter protrusions. At low Pt coverages, CO desorbs from isolated Pt atoms (peak at 350 K highlighted by arrow) and at intermediate coverages, CO desorbs from extended ensembles of Pt atoms (peak at 480 K). At 5 ML Pt, the surface layer is composed primarily of continuous ordered Pt ensembles and CO desorbs at 410 K. At low CO coverages, CO desorption from Pt(111) is reported at 450 K and with increasing CO coverage desorption is observed at 400 K due to the repulsion between co-adsorbed CO molecules. In Pt-Cu alloys, CO adsorbs weakest on the Pt-Cu SAA and strongest on the extended Pt clusters. These results indicated that Pt atoms at the SAA limit exhibit the weakest binding to CO which DFT confirmed and indicated is due to an electronic effect and the inability of SAAs to bridge-bond CO to two adjacent Pt sites.

To probe the interaction of CO and H with the Pt catalytic sites at the atomic-scale, H and CO were co-adsorbed onto 0.01 ML Pt-Cu(111) (Figure 1E-G). We used the STM tip to interrogate the nature of the H and CO adsorption sites. Initially, we observed clusters of mobile depressions on the Cu terraces previously identified as H adatoms due to the low diffusion barrier of H on Cu (Figure 1E). Increasing the bias applied to the STM tip moved these H atoms to outside the imaging area (Figure 1F). Select immobile depressions remained on the surface that could only be removed by individual pulses locally delivered by the STM tip (5 V) (Figure 1G), hence, the dark immobile depressions are assigned as CO molecules as previously reported. After removal of the CO molecules, stationary surface protrusions were observed where each of the CO molecules was previously located. We identify the ~ 20 pm high protrusions as Pt atoms in the Cu surface, thus, providing further evidence of the selective adsorption of CO on the Pt sites.

Given that CO desorbs from Pt-Cu SAAs at 350 K vs. ~450 K on Pt nanoparticles these results indicate that SAAs are considerably more CO-tolerance than traditional Pt catalysts. The Flytzani-Stephanopoulos group at Tufts has now confirmed these results in real catalysts under hydrogenation conditions (3). Furthermore, we postulate that this SAA approach in other metal combinations can be used for the design of novel CO-tolerant catalysts for other industrially important reactions such as hydrocarbon and alcohol oxidation reactions, and for the present generation, low-temperature hydrogen fuel cells where the platinum electro-catalysts is prone to CO-poisoning.

### **Future Plans:**

Our surface science approach offers the opportunity to study the atomic-scale composition and structure of active sites and relate this information to their ability to activate, spillover and react industrially relevant small molecules. We will use these guiding principles to examine catalytic metal alloys from a new perspective and discover new processes. Future work is aimed at:

- 1) Interrogating the ability of single atom alloys (SAAs) to activate C-H bonds of importance to dehydrogenation and coupling reactions
- 2) Extending our SAA approach to understanding hydrogenations on Pd/Ag and Pt/Ag
- 3) Elucidating the optimal atomic geometry of Ag/Cu and Cu/Ag bimetallic surfaces for oxygen activation, spillover and reaction

These model systems will allow us a fundamental understanding of many important elementary steps in surface catalyzed chemistry. The atomic-scale structure of the active sites in metal alloy catalysts is hard, if not impossible, to characterize by conventional methods. Our surface science approach that includes scanning probes offers methods to characterize the structure, stoichiometry, and reactivity, and provides an atomic-scale view of local structure and adsorbate binding/diffusion. However, when working on well-defined model systems it is imperative to work with the same elements, structures and ensembles that are present in the real catalysts under working conditions. Implementation of the SAA approach to the design of real catalysts requires consideration of the effect of higher reaction temperature and pressure, which may cause the minority active element to segregate into the bulk of the more inert host and hence cause a loss in activity. Understanding and controlling surface segregation under reaction conditions will also be crucial for the efficient use of the costly elements of the alloy by keeping them in active sites on or near the surface. Promisingly, there are now many experimental and theoretical examples of metal alloys under realistic conditions in which the more active element is stabilized at the surface by adsorbates. All our proposed systems have been chosen with these considerations in mind. Active elements will be alloyed into more inert Cu, Ag, and Au surfaces. The (111) facet is chosen, as it is often the most commonly exposed facet on metal nanoparticles. While minority structures like step edges or defects often dominate the reactivity of metal surfaces, the chemistry of our alloyed systems is expected to be driven at the added metal atom sites and this will be checked with control experiments of the reactivity before and after alloying.

#### DOE-Sponsored Research Publications in the Last Two Years:

- 1) "Controlling Selectivity in the Ullmann Reaction on Cu(111)" E. A. Lewis, M. D. Marcinkowski, C. J. Murphy, M. L. Liriano, A. J. Therrien, A. Pronschinske, and E. C. H. Sykes *Chemical Communications* 2017, 53 7816-7819
- 2) "Selective Formic Acid Dehydrogenation on Pt-Cu Single Atom Alloys" M. D. Marcinkowski, J. Liu, C. J. Murphy, M. L. Liriano, N. A. Wasio, F. R. Lucci, M. Flytzani-Stephanopolous, and E. C. H. Sykes *ACS Catalysis* 2017, 7, 413-420(The surface science part of this project (Sykes) was solely funded by CPIMS – collaborator MFS was funded by DOE DE-FG02-05ER15730 for the catalysis side of the project)
- 3) "Tackling CO Poisoning with Single Atom Alloy Catalysts" J. Liu, F. R. Lucci, M. Yang, S. Lee, M. D. Marcinkowski, A. J. Therrien, C. T. Williams, E. C. H. Sykes, and M. Flytzani-Stephanopoulos *Journal of the American Chemical Society* 2016, 138, 6396-6399 [Cover Story] (The surface science part of this project (Sykes) was solely funded by CPIMS – collaborator MFS was funded by DOE DE-FG02-05ER15730 for the catalysis side of the project)
- 4) "Controlling Hydrogen Activation, Spillover, and Desorption with Pd-Au Single Atom Alloys" F. R. Lucci, M. T. Darby, M. F. G. Mattera, C. J. Ivimey, A. J. Therrien, A. Michaelides, M. Stamatakis, and E. C. H. Sykes *The Journal of Physical Chemistry Letters* 2016, 7, 480-485
- 5) "Squeezing and Stretching Pd Thin Films: A High-Resolution STM Study of Pd/Au(111) and Pd/Cu(111) Bimetallics" M. E. Blecher, E. A. Lewis, A. Pronschinske, C. J. Murphy, M. F. G. Mattera, M. L. Liriano, and E. C. H. Sykes *Surface Science* 2016, 646, 1-4
- 6) "A Microscopic View of the Active Sites for Selective Dehydrogenation of Formic Acid on Cu(111)" M. D. Marcinkowski, C. J. Murphy, M. L. Liriano, N. Wasio, F. R. Lucci, and E. C. H. Sykes *ACS Catalysis* 2015, 5, 7371-7378
- 7) "Collective Effects in Physisorbed Molecular Hydrogen on Ni/Au(111)" A. J. Therrien, A. Pronschinske, C. J. Murphy, E. A. Lewis, M. L. Liriano, M. D. Marcinkowski, and E. C. H. Sykes *Physical Review B* 2015, 92, 161407

# Imaging Interfacial Electric Fields on Ultrafast Timescales

William A. Tisdale

Department of Chemical Engineering  
Massachusetts Institute of Technology, Cambridge, MA 02139  
tisdale@mit.edu

## Program Scope

The goal of the project is to develop the experimental capability to dynamically probe interfacial electric fields on ultrafast timescales. The proposed technique could be applied to a variety of heterointerfaces, with particular emphasis on interfaces involving colloidal quantum dots. Research activities involve validation of the technical approach, construction of the microscope, and synthesis and characterization of materials to be studied using the instrument.

## Recent Progress I: *Phase-Modulated Optical Parametric Amplification Imaging*

Second harmonic generation (SHG) is a second order nonlinear optical process in which two photons at a fundamental frequency  $\omega$  combine to form a single photon at frequency  $2\omega$ . Like any even-ordered nonlinear optical process, SHG is dipole-forbidden in the bulk of centrosymmetric media such as many crystal structures, amorphous solids, liquids, and gases; observed SHG signals in these media originate from materials' interfaces.

In Year 2 of the project, we published a successful amplification of weak spontaneous SHG signals by optical stimulation in an idealized proof-of-principle demonstration (Goodman & Tisdale, *Phys. Rev. Lett.* **2015**).<sup>1</sup> Though the initial demonstration showed an improvement in SHG signal generation by a factor of  $10^4$  compared to the spontaneous signal, the signal suffered from large fluctuations due to optical phase instability. As we showed in the initial paper, the stimulated SHG signal is highly sensitive to the relative optical phase between the incident fundamental and second harmonic fields. While this sensitivity caused undesired signal fluctuations in the original intensity modulation scheme, we soon realized that we could use the phase sensitivity to our advantage by modulating the optical phase of the stimulating field rather than modulating its intensity. This approach has the added benefit of removing artifacts associated with intensity modulation of the second harmonic field, such as third-order phenomena and two-photon fluorescence.

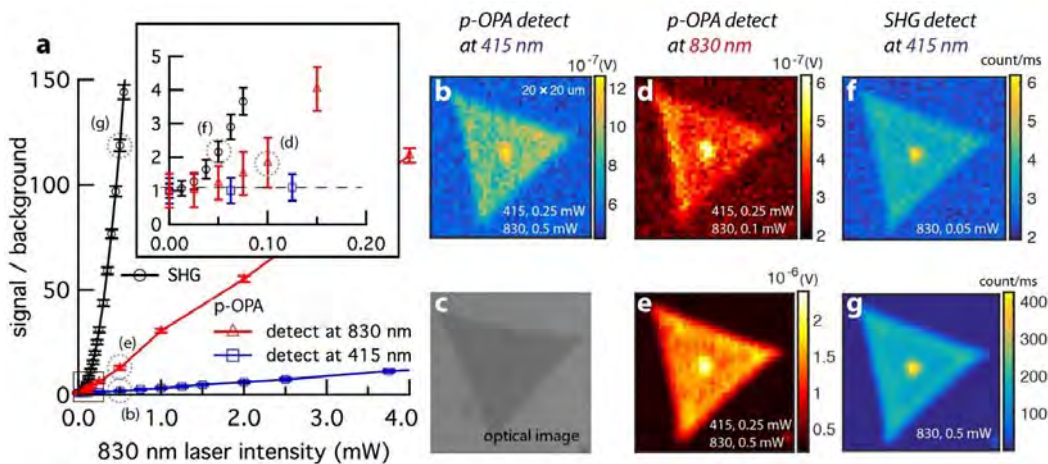
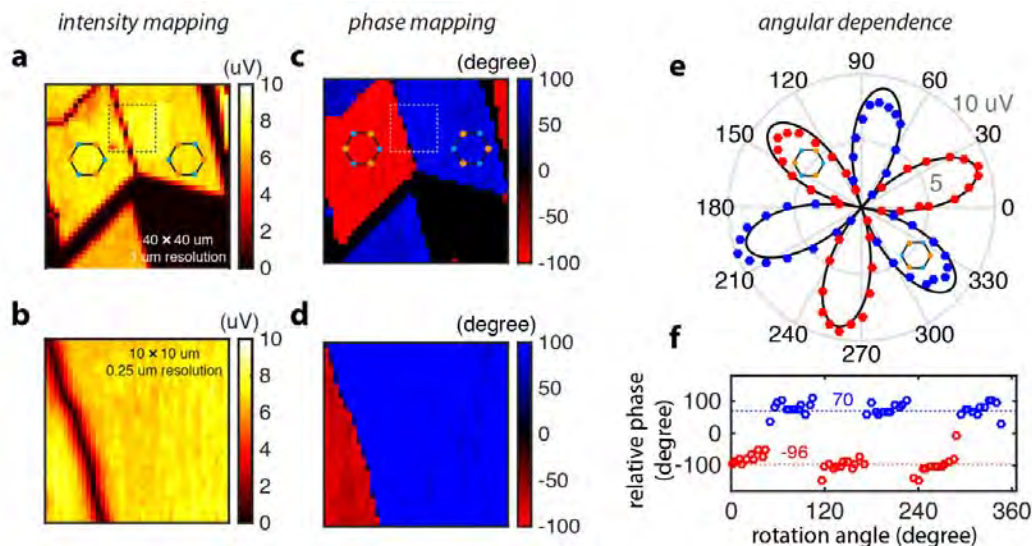


Figure 1. Phase-modulated OPA imaging of monolayer MoS<sub>2</sub>.

The new technique, known as phase-modulated optical parametric amplification imaging, or OPA imaging, is demonstrated in Fig. 1 (*to be published*). Whereas traditional SHG imaging techniques inform only on the squared magnitude of the second-order nonlinear susceptibility,  $|\chi^{(2)}|^2$ , OPA imaging also reveals the sign of  $\chi^{(2)}$  – or the absolute phase of the nonlinear signal. This additional information enables unambiguous determination of the absolute atomic arrangement in monolayer MoS<sub>2</sub> and reveals twin boundaries in CVD-grown samples that would otherwise be hidden from observation (Fig. 2).



**Figure 2.** Phase-modulated OPA imaging reveals absolute atomic arrangement and twin boundaries in CVD-grown MoS<sub>2</sub>.

### Recent Progress II: Nonequilibrium Dynamics in PbS Quantum Dot Solids

In Year 1 of the project we developed a novel method to synthesize highly monodisperse PbS quantum dots (QDs) over a broad size range, and to control the polydispersity by adjusting the Pb to S precursor ratio (*ACS Nano* 2014; *U.S. Patent* No. 9,481,582).<sup>4</sup> This new materials platform has enabled the investigation of a wide variety of mesoscale charge transport phenomena in disordered systems. Recently, we have used transient absorption spectroscopy to probe the nonequilibrium dynamics of photogenerated charge carriers in electrically conductive PbS QD solids (*Nano Letters* 2017; Fig. 3).<sup>5</sup> In addition to demonstrating that our most monodisperse ensembles of QDs are homogeneously broadened, we also made the surprising observation that spatial disorder – rather than energetic disorder – dominates transport behavior in more monodisperse arrays.

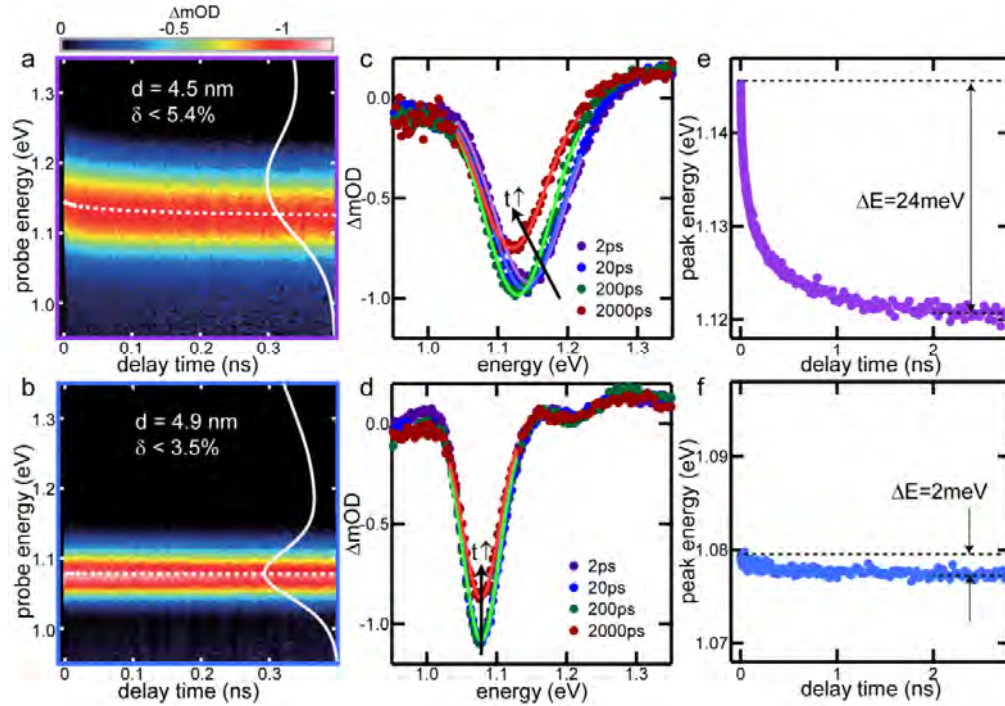


**Figure 3.** Transient absorption (TA) tracks the average energy of QDs containing excited charge carriers. (a, b) TA data collected from ethanethiol treated solids made from PbS QDs with polydispersity  $\delta < 5.4\%$  (a) and  $\delta < 3.5\%$  (b). Solid white lines are the ground state linear absorption spectra. Dashed lines show the TA bleach peak position as a function of time. (c, d) Spectral slices at selected times showing the redshift of bleach peak in the  $\delta < 5.4\%$  sample (c) but not in the  $\delta < 3.5\%$  sample (d). Dots represent data, and lines show Gaussian fits to the peaks. (e, f) Bleach peak energy as a function of time for the  $\delta < 5.4\%$  (e) and  $\delta < 3.5\%$  (f) samples. From Gilmore et al., *Nano Letters* (2017).<sup>5</sup>

### Recent Progress III: Origin of trap states in PbS Quantum Dot Solids

Over the past decade, deep electronic traps have emerged as the primary factor limiting the overall power conversion efficiency of QD solar cells. Traps reduce both the short circuit current and the open circuit voltage by limiting the minority carrier diffusion length and lowering the voltage at which charges are extracted from films. Through a series of unique experiments in which we directly photoexcited ground-state-to-trap-state transitions and observed subsequent upconversion of trapped charge carriers to the band edge (*to be published*), we have been able to conclude that these unwanted trap states do not arise from surface defects as assumed by many. Instead, we have evidence that suggests that these trap states originate from strongly-coupled QD dimers, which can form during the ligand exchange procedure.

### Future Plans

Now in the final year of the award, the major programmatic priority is publication of the many works-in-progress, including: demonstration of the phase-modulated OPA imaging technique, ultrafast dynamics at QD-TMD interfaces, origin of trap states in PbS QD solids, and temperature-dependent transport in QD solids.

CPIMS-Supported Publications (2015-2017)

1. A.J. Goodman & W.A. Tisdale; “Enhancement of Second-Order Nonlinear-Optical Signals by Optical Stimulation,” *Phys. Rev. Lett.* **114**, 183902 (2015).
2. P. Tyagi, S.M. Arveson, W.A. Tisdale; “Colloidal Organohalide Perovskite Nanoplatelets Exhibiting Quantum Confinement,” *J. Phys. Chem. Lett.* **6**, 1911-1916 (2015).
3. A.J. Goodman & W.A. Tisdale; “Reply to Comment on Enhancement of Second-Order Nonlinear-Optical Signals by Optical Stimulation,” *Phys. Rev. Lett.* **116**, 059402 (2016).
4. W.A. Tisdale, F. Prins, M.C. Weidman, M.E. Beck; “Nanocrystal Synthesis,” *U.S. Patent No.* 9,481,582 (2016).
5. R.H. Gilmore, E.M.Y. Lee, M.C. Weidman, A.P. Willard, W.A. Tisdale; “Charge Carrier Hopping Dynamics in Homogeneously Broadened PbS Quantum Dot Solids,” *Nano Letters* **17**, 893-901 (2017).

# Structural Dynamics in Complex Liquids Studied with Multidimensional Vibrational Spectroscopy

Andrei Tokmakoff

*Department of Chemistry, James Franck Institute, and Institute for Biophysical Dynamics  
The University of Chicago, Chicago, IL 60637  
E-mail: tokmakoff@uchicago.edu*

The ability of water to integrate charged species into its hydrogen bond (H-bond) network and the rapid transport of this charge, in particular the proton, has made aqueous systems attractive candidates for alternative energy sources such as fuel cells, water oxidation catalysis, and new battery technology. These unique properties of water are derived from its intricate H-bond network which results in strong intra- and intermolecular coupling that span many water molecules, leading to energy transport and dissipation on ultrafast timescales. It has been our aim to develop a molecular-level description of these collective, ultrafast processes in aqueous systems in order to gain a more fundamental understanding of how water stores, converts, and transports electrical, chemical, and thermal energy.

The research conducted over the past year has focused on understanding how the delocalized and mixed nature of water's vibrational modes give rise to ultrafast energy transport, and elucidating the ultrafast dynamical processes responsible for proton transport in aqueous acid solutions. As always, this work is driven by the development of new ultrafast broadband infrared laser sources for use in two-dimensional infrared spectroscopy (2D IR). Additionally we develop new theoretical methods in collaboration with Greg Voth (UChicago) to more accurately model and predict the spectroscopic behavior of water and proton transport in solution.

By expanding the capabilities of our spectrometer, we have been able to probe the dynamics of liquid water more deeply than was previously possible. In the 2D IR spectrum of the water HOH bend, we observe a broad excited state absorption that stretches from 1500–900  $\text{cm}^{-1}$  in the detection frequency. Given the initial excitation centered at 1650  $\text{cm}^{-1}$ , this corresponds to excited states ranging from 3150–3550  $\text{cm}^{-1}$ , which corresponds to excitations to the bend overtone and the OH stretch. The transition from one mode to another would be forbidden in the harmonic limit, but the anharmonicity induced by the H-bond network and the mixing resulting from the bend-stretch Fermi resonance facilitate this transition. The HOH bend relaxes on a rapid 180 fs timescale, and the ESA decays on a faster timescale of 110–150 fs, which indicates that the OH stretch can decay through channels other than the HOH bend such as librations. We also observe an 80 fs pump–probe anisotropy decay of the HOH bend, which is the timescale of the instrument response. The fast orientational randomization demonstrates that the excitation of the HOH bend is delocalized over multiple molecules, since the orientation decays an order of magnitude more quickly than physical reorientation of the molecule. The excitation energy dissipates into the “hot ground state,” a transient state with a weakened hydrogen bond network, and the hot ground state grows in on an 800 fs timescale. The timescale is identical when energy dissipates from the OH stretch, which provides another piece of evidence that both the stretch and the bend relax directly to low-frequency collective modes.

Our previous work on aqueous acids and the improved laser sources described above have opened up new avenues for directly measuring the structure and dynamics of proton solvation in water. We have collected 2D IR spectra of 2M HCl pumped at 6  $\mu\text{m}$ , directly exciting both the water bend at 1650  $\text{cm}^{-1}$  and the hydrated proton bend at 1760  $\text{cm}^{-1}$ . While the acid peak appears as a shoulder on the water bend peak in a linear FTIR spectrum, the acid peak appears distinct from the  $\text{H}_2\text{O}$  bend and with stronger intensity in

2D IR spectra. The acid bend peak is broad in both the excitation and detection axes, with no diagonal elongation visible, which means the breadth is dominated by fast homogeneous broadening. The lifetime of the acid bend vibration is less than 200 fs, however, the mode displays an unusually long-lived polarization anisotropy decay of about 2.5 ps. This is in stark contrast to the fast, instrument-limited anisotropy decays of the HOH bend (discussed above) and OH stretch in water. The slow orientational dynamics of the acid bend point to an acid species that is highly localized due to the strong defect induced in the water H-bond network by the excess proton. The 2.5 ps decay time is consistent with the H-bond switching dynamics measured in water, suggesting that the acid species does not lose its orientational memory until overall rearrangement of the surrounding H-bond network occurs. The 2.5 ps anisotropy decay places a new lower limit on the proton transfer process.

The improved bandwidth of our laser sources have now allowed us to investigate both the acid “continuum” spanning 1800–3000  $\text{cm}^{-1}$  and the broad feature at 1200  $\text{cm}^{-1}$ , referred to as the proton transfer mode (PTM). We have observed a strong orientational dependence of a cross peak generated at 1200  $\text{cm}^{-1}$  after pumping the acid bend. The cross peak is much stronger in the parallel ZZZZ pump–probe configuration compared to the perpendicular ZZZY arrangement. This suggests that the dipole moments between the acid bend and PTM are aligned. Moreover, the bleach is homogeneously broadened along the detection axis and closely resembles the lineshape seen in the linear FTIR spectrum. We also observe a strong homogeneous cross peak to the acid continuum, although no clear polarization dependence is observed. Both the PTM and continuum cross peaks are short-lived (<200 fs). These observations point to fast dephasing and spectral diffusion resulting from a wide distribution of structures caused by fluctuations in the H-bond network.

To further characterize the acid species, we have begun to pump the acid continuum region between 1800 and 3000  $\text{cm}^{-1}$ . These vibrations are thought to originate from acidic OH stretches in a wide distribution of local structures. Our initial data shows fast lived and homogeneously broadened features, much like those seen when pumping the acid bend. A strong cross peak to the acid bend is observed but, interestingly, no clear cross peak is observed to the PTM. This seems to suggest that the bending modes of the acid species can couple to both the continuum and PTM stretching vibrations, but that the continuum and PTM stretches are chemically distinct. We are currently working to capture the polarization-dependence and anisotropy decays of the continuum-pumped spectra, and will be working to shift our pump pulses down to 1200  $\text{cm}^{-1}$  in order to observe the spectral dynamics that arise from pumping the PTM.

To aid in the interpretation of the acid spectra and to better understand the vibrational spectral features that derive from different proton–water complexes, we have calculated the vibrational spectra for protonated water clusters extracted from reactive molecular dynamics trajectories using the latest multistate empirical valence bond (MS-EVB 3.2) proton model. We observe a broad distribution of structures ranging between the limiting Zundel and Eigen configurations. While there is much spectral overlap between the different sub-ensembles of structures, we observe a continuous frequency red-shift of the PTM while approaching Zundel-like configurations from Eigen solvation structures. The calculations also show that the continuum region mainly derives from distorted Eigen configurations. Most importantly, we have demonstrated that the different spectral features within the acid spectrum cannot simply be described by localized normal mode vibrations. Instead, the calculations indicate that there is strong mode mixing between the acid bend and acid stretches (continuum and PTM), and the PTM to both the bend and continuum.

## DOE Supported Publications 2015–2017

1. “Ultrafast 2D IR spectroscopy of the excess proton in liquid water,” M. Thämer, L. De Marco, K. Ramasesha, A. Mandal and A. Tokmakoff, *Science* **350**, 78–82 (2015).
2. “Vibrational dynamics of aqueous hydroxide solutions probed using broadband 2DIR spectroscopy,” A. Mandal and A. Tokmakoff, *J. Chem. Phys.* **143**, 194501 (2015).
3. “Role of presolvation and anharmonicity in aqueous phase hydrated proton solvation and transport,” R. Biswas, Y.-L. S. Tse, A. Tokmakoff and G. A. Voth, *J. Phys. Chem. B* **120**, 1793–1804 (2016).
4. “Differences in the vibrational dynamics of H<sub>2</sub>O and D<sub>2</sub>O: Observation of symmetric and antisymmetric stretching vibrations in heavy water,” L. De Marco, W. Carpenter, H. Liu, R. Biswas, J. M. Bowman and A. Tokmakoff, *J. Phys. Chem. Lett.* **7**, 1769–1774 (2016).
5. “Interplay of ion–water and water–water interactions within the hydration shells of nitrate and carbonate directly probed with 2D IR spectroscopy,” J. A. Fournier, W. Carpenter, L. De Marco and A. Tokmakoff, *J. Am. Chem. Soc.* **138**, 9634–9645 (2016).
6. “Anharmonic exciton dynamics and energy dissipation in liquid water from two-dimensional infrared spectroscopy,” L. De Marco, J. A. Fournier, M. Thämer, W. Carpenter and A. Tokmakoff, *J. Chem. Phys.* **145**, 094501 (2016).
7. “Molecular Modeling and Assignment of IR Spectra of the Hydrated Excess Proton in Isotopically Dilute Water,” Rajib Biswas, William Carpenter, Gregory Voth, and Andrei Tokmakoff, *Journal of Chemical Physics*, **145** (2016) 154504-1-12.
8. “IR spectral assignments for the hydrated excess proton in liquid water,” Rajib Biswas, William Carpenter, Joseph A. Fournier, Gregory Voth, and Andrei Tokmakoff, *Journal of Chemical Physics*, **146** (2017) 154507-1-11.
9. “Delocalization and Stretch-Bend Mixing of the HOH Bend in Liquid Water,” William B. Carpenter, Joseph A. Fournier, Rajib Biswas, Gregory A. Voth, and Andrei Tokmakoff, *Journal of Chemical Physics*, **147** (2017) 084503-1-10.

## Ab-initio analysis of molecular interactions in clusters and bulk systems

Marat Valiev

Environmental Molecular Sciences Laboratory, Pacific Northwest National Laboratory,  
P. O. Box 999, Richland, Washington 993521

### Abstract

The main focus of our project is to provide fundamental molecular level understanding of solvation processes that take place in clusters, interfacial and bulk molecular liquid systems. This is accomplished through development and application of advanced ab-initio simulation methods performed in close collaboration with experimental spectroscopy measurements. Our main objective is to identify common mechanisms and collective variables that account for electronic structure information and go beyond simple classical models. At the same time we would like to retain simple physically motivated driven description to allow insight into the overall behavior and properties of the complex solution system.

The underlying model that guides and defines our research activities is the view on solvation process as an interaction between three distinct components or subsystems - solute, interfacial region, and bulk solvent phase. Each of the components plays its own role in the solvation process and has unique requirements for its description. We believe such view provides good starting point to manage the inevitable complexity of our theoretical description.

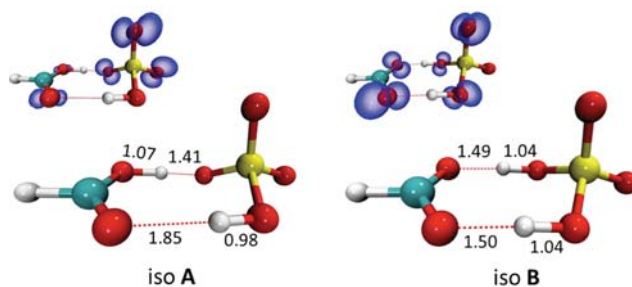


Fig.1 Structures of formic acid/bisulfate clusters

In the analysis solute part of the system we place a heavy emphasis on high-level electronic structure calculations. Solute, almost by construction, contains the least understood part of the system that often undergoes reactive changes, and whose description is particularly important to capture at highest levels to fidelity. The key component of our research efforts in this area is collaboration with experimental photoelectron spectroscopy efforts of Xuebin Wang's group at PNNL. Photoelectron spectroscopy provides a sensitive probe into electronic properties of the molecules and naturally integrates with ab-initio simulations as a required means to analyze and interpret the data.

Our current round of investigations in this area includes analysis of proton transfer processes in carboxylic acid and bisulfate clusters,  $(\text{RCOOH})(\text{HSO}_4)^-$ . It is commonly assumed that gas phase proton affinities provide a reliable metric for determining relative protonation state. This conventional wisdom is challenged in our recent studies of formic acid/bisulfate clusters, where temperature-dependent photoelectron spectroscopy and theoretical studies demonstrate the existence of  $(\text{HCOO}^-)(\text{H}_2\text{SO}_4)$  pair at the energy slightly below the conventional  $(\text{HCOOH})(\text{HSO}_4^-)$  structure (see Figure 1). Our analysis indicates that large proton affinity difference ( $\sim 36$  kcal/mol), favoring proton transfer to formate, is offset by the gain in inter-molecular interaction energy through the formation of two strong hydrogen bonds. However, this stabilization comes with severe entropic penalty, requiring the two species in the precise alignment. As a result, the population of  $(\text{HCOO}^-)(\text{H}_2\text{SO}_4)$  drops significantly at higher temperatures, rendering  $(\text{HCOOH})(\text{HSO}_4^-)$  to be the dominant species. We are currently extending our investigation to other types of carboxylic acids.

In addition to electronic structure driven analysis, we also interested in a more statistical mechanics based description solute-solvent descriptions in molecular liquids. The distinct feature of molecular liquid is the presence of two distinct correlations scales - strong short-ranged intra-molecular correlations that make up the molecular units and weak long-range inter-molecular correlations that render the overall system "liquid". Current approaches (e.g. RISM) apply the same level of approximations to both scales, which leads to significant errors. Our strategy is based on effective action theory enabling analytical treatment of intra-molecular interactions, and retaining conventional strategies for inter-molecular correlations.

#### **Project Publications:** (2016-present)

Valiev, M.; Deng, S. H. M.; Wang, X. B., How Anion Chaotrope Changes the Local Structure of Water: Insights from Photoelectron Spectroscopy and Theoretical Modeling of  $\text{SCN}^-$  Water Clusters. *J Phys. Chem. B* **2016**, *120* (8), 1518-1525.

Hou, G. L.; Valiev, M.; Wang, X. B., Deprotonated Dicarboxylic Acid Homodimers: Hydrogen Bonds and Atmospheric Implications. *J Phys Chem A* **2016**, *120* (15), 2342-2349.

Qin, Z. B.; Hou, G. L.; Yang, Z.; Valiev, M.; Wang, X. B., Negative ion photoelectron spectra of  $\text{ISO}_3^-$ ,  $\text{IS}_2\text{O}_3^-$ , and  $\text{IS}_2\text{O}_4^-$  intermediates formed in interfacial reactions of ozone and iodide/sulfite aqueous microdroplets. *J Chem Phys*, **2016**, *145* (21).

T. Pirojsirikul, M. Valiev, A. W. Götz, J. Weare, R. Walker, K. Kowalski, Combined Quantum-Mechanical Molecular Mechanics Calculations with NWChem and AMBER: Excited State Properties of Green Fluorescent Protein Chromophore Analogue in Aqueous Solution. *J. Comp. Chem.*, **2017**, *38*(18), 1631-1639

Hou, G.-L., Zhang, J., Valiev, M., Wang, X.-B., Structures and energetics of hydrated deprotonated cispinonic acid anion clusters and their atmospheric relevance *Phys. Chem. Chem. Phys.*, **2017**, *19*, 10676 - 10684

Hou, G.-L., Wang, X.-B., and Marat Valiev, Formation of  $(\text{HCOO}^-)(\text{H}_2\text{SO}_4)$  Anion Clusters: Violation of Gas-Phase Acidity Predictions, *J. Am. Chem. Soc.* **2017** *139* (33), 11321-11324

# Chemical Kinetics and Dynamics at Interfaces

## Cluster Model Investigation of Condensed Phase Phenomena

**Xue-Bin Wang**

Physical Sciences Division, Pacific Northwest National Laboratory, P.O. Box 999, MS K8-88, Richland, WA 99352. E-mail: [xuebin.wang@pnnl.gov](mailto:xuebin.wang@pnnl.gov)

Additional collaborators include: GL Hou, SH Deng, Zheng Yang, ZB Qin, J Zhang, ZR Sun, WT Borden, SR Kass, CC Cummins, SH Strauss, OV Boltalina, CEH Dessent, Paul G. Wenthold, SS Xantheas, K Kowalski, M Valiev

### Program Scope

We aim at obtaining a molecular-level understanding of solution chemistry and condensed phase phenomena using gas phase clusters as model systems. Clusters occupy an intermediate region between gas phase molecules and the condensed states of matter and play an important role in heterogeneous catalysis, aerosol chemistry, and biological processes. We use electrospray ionization (ESI) to generate a wide variety of molecular and ionic clusters to simulate key species involved in the condensed phase reactions and transformations, and characterize them using cryogenic negative ion photoelectron spectroscopy (NIPES) and high-resolution photoelectron imaging spectroscopy. Inter- and intra-molecular interactions and their variation as function of size and composition, important to understand complex chemical reactions and nucleation processes in condensed and interfacial phases can be directly obtained. Experiments and *ab initio* calculations are synergistically combined to

- Probe solute specific effects in hydrated anion and neutral clusters;
- Obtain a molecular-level understanding of the solvation and stabilization of Hofmeister anions important in condensed phases;
- Study temperature-dependent conformation changes and isomer populations of complex clusters;
- Investigate intrinsic electronic structures of environmentally and catalytically important species and reactive diradicals;
- Quantify thermodynamic driving forces resulting from hydrogen-bonded networks formed in aerosol nucleation processes and enzymatic catalytic reactions.
- Unravel new physics of photodetachment of multiply charged anions beyond the prevailing conventional model

The central goal of this research program lies at obtaining a fundamental understanding of environmental materials and solution chemistry important to many primary DOE missions, and enhances scientific synergies between experimental and theoretical studies towards achieving such goals.

### Recent Progress

**Developing High-resolution Cryogenic Photoelectron Imaging Spectroscopy, and Investigation of ECX<sup>-</sup> Anions (E = As, P, and N; X = S and O):** Recently, we have developed high resolution photoelectron imaging spectroscopy equipped with a cryogenic ion source and tunable laser systems, based on a new design of velocity-map imaging (VMI) electrostatic lens with wavenumber energy resolution. Employing this imaging spectrometer, we investigated three newly-synthesized [Na<sup>+</sup>(221-kryptofix)] salts containing AsCO<sup>-</sup>, PCO<sup>-</sup>, and PCS<sup>-</sup> anions. For each ECX<sup>-</sup> anion, a well-resolved NIPE spectrum was obtained, in which every major peak is split into a doublet. The splittings are attributed to spin-orbit coupling (SOC) in the ECX<sup>•</sup> radicals. Vibrational progressions in the NIPE spectra of ECX<sup>-</sup> were assigned to the symmetric and antisymmetric stretching modes in ECX<sup>•</sup> radicals. The electron affinities (EAs) and SOC splittings of ECX<sup>•</sup> are determined from the NIPE spectra to be: AsCO<sup>•</sup>: EA = 2.414 ± 0.002 eV, SOC splitting = 988 cm<sup>-1</sup>; PCO<sup>•</sup>: EA = 2.670 ± 0.005 eV, SOC splitting = 175 cm<sup>-1</sup>;

PCS<sup>-</sup>: EA = 2.850 ± 0.005 eV, SOC splitting = 300 cm<sup>-1</sup>. Calculations using the B3LYP, CASPT2, and CCSD(T) methods all predict linear geometries for both the anions and neutral radicals. The calculated EAs and SOC splittings for ECX<sup>-</sup> are in excellent agreement with the experimentally-measured values. The simulated NIPE spectra, based on the calculated Franck-Condon factors, and SOC splittings nicely reproduce all of the observed spectral peaks, thus allowing unambiguous spectral assignments. The finding that PCS has the greatest EA of the three triatomic molecules considered here is counterintuitive, based upon simple electronegativity considerations, but this finding is understandable in terms of the movement of electron density from phosphorus in the HOMO of PCO<sup>-</sup> to sulfur in the HOMO of PCS<sup>-</sup>. Comparisons of the EAs of PCO and PCS, with the previously measured EA values for NCO and NCS are made and discussed (*J. Am. Chem. Soc.* **2017**, *139*, 8922-8930).

**Cluster Model Studies of Anion and Molecular Specificities via Electrospray Ionization Photoelectron Spectroscopy.** Ion specificity, a widely observed macroscopic phenomenon in condensed phases and at interfaces, is a fundamental chemical physics issue. In a recent invited Feature Article (*J. Phys. Chem. A* **2017**, *121*, 1389-1401), we presented and summarized our recent studies of such effects using cluster models in an “atom-by-atom” and “molecule-by-molecule” fashion not possible with the condensed-phase methods, including topics on (1) anion specificity in hydrated clusters—cluster model insights on how kosmotrope and chaotrope anions guide the local solvation structure of water; (2) anion specificity in ion recognition and anion- $\pi$  complexes; (3) hydrogen bond network and its implications in anion recognition; and (4) cluster model studies on specific molecular effects in aerosol particle formation. We used ESI to generate molecular and ionic clusters to simulate key molecular entities involved in local binding regions, and characterized them employing NIPES. Inter- and intramolecular interactions and binding configurations are directly obtained as functions of the cluster size and composition, providing molecular-level descriptions and characterization over the local active sites that play crucial roles in determining the solution chemistry and condensed phase phenomena. The underlying insights obtained via these studies are relevant to research fields ranging from ion specific effects in electrolyte solutions, ion selectivity/recognition in normal functioning of life, to molecular specificity in aerosol particle formation, as well as in rational material design and synthesis. This Article was noted on the Cover, and awarded as ACS Editors’ Choice.

**Negative Ion Photoelectron Spectra of ISO<sub>3</sub><sup>-</sup>, IS<sub>2</sub>O<sub>3</sub><sup>-</sup>, and IS<sub>2</sub>O<sub>4</sub><sup>-</sup> Intermediates Formed in Interfacial Reactions of Ozone and Iodide/Sulfite Aqueous Microdroplets:** Three short-lived, anionic intermediates, ISO<sub>3</sub><sup>-</sup>, IS<sub>2</sub>O<sub>3</sub><sup>-</sup>, and IS<sub>2</sub>O<sub>4</sub><sup>-</sup>, were detected during reactions between ozone and aqueous iodine/sulfur oxides microdroplets. These species may play an important role in ozone-driven inorganic aerosol formation, however their chemical properties remain largely unknown. We addressed this issue in a recent work using NIPES and *ab initio* modeling. The NIPE spectra reveal that all of the three anionic species are characterized by high adiabatic detachment energies (ADEs) – 4.62 ± 0.10, 4.52 ± 0.10, and 4.60 ± 0.10 eV for ISO<sub>3</sub><sup>-</sup>, IS<sub>2</sub>O<sub>3</sub><sup>-</sup>, and IS<sub>2</sub>O<sub>4</sub><sup>-</sup>, respectively. Vibrational progressions with frequencies assigned to the S–O symmetric stretching modes are also discernable in the ground state transition features. Density functional theory (DFT) calculations show the presence of several low-lying isomers involving different bonding scenarios. Further analysis based on high level CCSD(T) calculations reveal that the lowest energy structures are characterized by formation of I–S and S–S bonds and can be structurally viewed as SO<sub>3</sub> linked with I, IS, and ISO for ISO<sub>3</sub><sup>-</sup>, IS<sub>2</sub>O<sub>3</sub><sup>-</sup>, and IS<sub>2</sub>O<sub>4</sub><sup>-</sup>, respectively. The calculated ADEs and vertical detachment energies (VDEs) are in excellent agreement with the experimental results, further supporting the identified minimum energy structures. The obtained intrinsic molecular properties of these anionic intermediates and neutral radicals should be useful to help understand their photochemical reactions in the atmosphere (*J. Chem. Phys.* **2016**, *145*, 214310).

### Future Directions

The main thrust of our BES program will continue to be on cluster model studies of condensed phase phenomena in the gas phase. The experimental capabilities that we have developed give us the

opportunity to attack a broad range of fundamental chemical physics problems pertinent to ionic solvation, solution chemistry, homogeneous / heterogeneous catalysis, aerosol chemistry, biological processes, and material synthesis. The ability to cool and control ion temperature and wavenumber energy resolution of VMI capability enable us to study different isomer populations and conformation changes of environmentally important hydrated clusters. Another major direction is to use gaseous clusters to model ion-specific interactions in solutions, ion transport, and ion-receptor interactions in biological systems, and initial nucleation processes relevant to atmospheric aerosol formation.

## References to Publications of DOE CPIMS Sponsored Research (2015 - present)

1. TT Clikeman, SHM Deng, AA Popov, XB Wang, SH Strauss and OV Boltalina. "Fullerene Cyanation does not Always Increase Electron Affinity: An Experimental and Theoretical Study". *Phys. Chem. Chem. Phys.* 17, 551-556 (2015).
2. J Zhang, B Zhou, ZR Sun, and XB Wang. "Photoelectron Spectroscopy and Theoretical Studies of Anion- $\pi$  Interactions: Binding Strength and Anion Specificity". *Phys. Chem. Chem. Phys.* 17, 3131-3141 (2015).
3. LK San, EV Bukovsky, BW Larson, JB Whitaker, SHM Deng, N Kopidakis, G Rumbles, AA Popov, YS Chen, XB Wang, OV Boltalina and SH Strauss. "A Faux Hawk Fullerene with PCBM-like Properties" *Chem. Sci.* 6, 1801-1815 (2015).
4. SHM Deng, XY Kong, and XB Wang. "Probing the Early Stages of Salt Nucleation – Experimental and Theoretical Investigations of Sodium/Potassium Thiocyanate Cluster Anions", *J. Chem. Phys.* 142, 024313-1-9 (2015).
5. J Zhang, ZR Sun, and XB Wang. "Examining the Critical Roles of Protons in Facilitating Oxidation of Chloride Ions by Permanganates: A Cluster Model Study", *J. Phys. Chem. A* 119, 6244-6251 (2015).
6. DA Hrovat, GL Hou, XB Wang, and WT Borden. "Negative Ion Photoelectron Spectroscopy Confirms the Prediction that 1,2,4,5-Tetraoxatetramethylenebenzene Has a Single Ground State", *J. Am. Chem. Soc.* 137, 9094-9099 (2015).
7. A Sen, GL Hou, XB Wang, C Dessent. "Electron Detachment as a Probe of Intrinsic Nucleobase Dynamics in Dianion-Nucleobase Clusters: Photoelectron Spectroscopy of the Platinum II Cyanide Dianion Bound to Uracil, Thymine, Cytosine and Adenine", *J. Phys. Chem. B.* 119, 11626-11631 (2015).
8. TT Clikeman, EV Bukovsky, XB Wang, YS Chen, G Rumbles, SH Strauss, OV Boltalina. "Core Perylene Diimide Designs via Direct Bay and Ortho (Poly)trifluoromethylation: Synthesis, Isolation, X-ray Structures, Optical and Electronic Properties", *Eur. J. Org. Chem.* 6641-6654 (2015).
9. WL Li, Y Li, CQ Xu, XB Wang, E Vorpapel, and J Li. "Periodicity, Electronic Structures, and Bonding of Gold Tetrahalides  $[\text{AuX}_4]^-$  (X = F, Cl, Br, I, At, Uus)", *Inorg. Chem.* 54, 11157-11167 (2015).
10. A Sen, EM. Matthews, GL Hou, XB Wang, and CEH Dessent. "Photoelectron Spectroscopy of Hexachloroplatinate-nucleobase Complexes: Nucleobase Excited State Decay Observed via Delayed Electron Emission", *J. Chem. Phys.* 143, 184307-1-8 (2015).
11. K Bhaskaran-Nair, M Valiev, SH Deng, WA Shelton, K Kowalski, and XB Wang. "Probing Microhydration Effect on the Electronic Structure of the GFP Chromophore Anion: Photoelectron Spectroscopy and Theoretical Investigations" *J. Chem. Phys.* 143, 224301-1-6, 2015 (**Featured on Cover, Dec. 14, 2015 Issue**).
12. M Valiev, SH Deng, and XB Wang. "How Anion Chaotrope Changes the Local Structure of Water: Insights from Photoelectron Spectroscopy and Theoretical Modeling of SCN – Water Clusters", *J. Phys. Chem. B.* 120, 1518-1525 (2016).
13. KC Rippey, EV Bukovsky, TT Clikeman, YS Chen, GL Hou, XB Wang, AA Popov, OV Boltalina, and SH Strauss. "Copper Causes Regiospecific Formation of  $\text{C}_4\text{F}_8$ -Containing Six-Membered Rings and their Defluorination/Aromatization to  $\text{C}_4\text{F}_4$ -Containing Rings in Triphenylene/1,4- $\text{C}_4\text{F}_8\text{I}_2$  Reactions" *Chem. Eur. J.* 22, 874-877 (2016).
14. KP Castro, TT Clikeman, NJ DeWeerd, EV Bukovsky, KC Rippey, IV Kuvychko, GL Hou, YS Chen, XB Wang, SH Strauss, and OV Boltalina. "Incremental Tuning Up of Fluorous Phenazine Acceptors" *Chem. Eur. J.* 22, 3930-3936 (2016).

15. DA Hrovat, GL Hou, B Chen, XB Wang, and WT Borden. "Negative Ion Photoelectron Spectroscopy Confirms the Prediction that  $D_{3h}$  Carbon Trioxide ( $\text{CO}_3$ ) Has a Singlet Ground State", *Chem. Sci.* 7, 1142-1150 (2016).
16. GL Hou, XT Kong, M Valiev, L Jiang and XB Wang, "Probing the Early Stages of Solvation of cis-Pinate Dianions by Water, Acetonitrile, and Methanol: a Photoelectron Spectroscopy and Theoretical Study" *Phys. Chem. Chem. Phys.* 18, 3628-3637 (2016).
17. A Shokri, XB Wang, Y Wang, GA O'Doherty, and SR Kass. "Flexible Acyclic Polyol-Chloride Anion Complexes and their Characterization by Photoelectron Spectroscopy and Variable Temperature Binding Constant Determinations", *J. Phys. Chem. A* 120, 1661-1668 (2016).
18. GL Hou, M Valiev, and XB Wang. "Deprotonated dicarboxylic acid homodimers: hydrogen bonds and atmospheric implications", *J. Phys. Chem. A* 120, 2342-2349 (2016).
19. GL Hou, B Chen, WJ Transue, DA Hrovat, CC Cummins, WT Borden, and XB Wang. "Negative Ion Photoelectron Spectroscopy of  $\text{P}_2\text{N}_3^-$ : Electron Affinity and Electronic Structures of  $\text{P}_2\text{N}_3^-$ ", *Chem. Sci.* 7, 4667-4675 (2016).
20. X Liu, GL Hou, XF Wang, and XB Wang. "Negative Ion Photoelectron Spectroscopy Reveals Remarkable Noninnocence of Ligands in Nickel Bis(dithiolene) Complexes  $[\text{Ni}(\text{dddt})_2]^-$  and  $[\text{Ni}(\text{edo})_2]^-$ ", *J. Phys. Chem. A* 120, 2854-2862 (2016).
21. WJ Transue, A Velian, M Nava, MA Martin-Drumel, CC Womack, J Jiang, GL Hou, XB Wang, MC McCarthy, RW Field, CC Cummins. "A Molecular Precursor to Phosphaethyne and Its Application in Synthesis of the Aromatic 1,2,3,4-Phosphatriazololate Anion." *J. Am. Chem. Soc.* 138, 6731-6734 (2016).
22. H Wen, GL Hou, YR Liu, XB Wang, W Huang. "Examining the Structural Evolution of Bicarbonate-Water Clusters: Insights from Photoelectron Spectroscopy, Basin-Hopping Structural Search, and Comparison with Available IR Spectral Studies." *Phys. Chem. Chem. Phys.* 18, 17470-17482 (2016).
23. GL Hou, LJ Li, SH Li, ZM Sun, X Gao, XB Wang. "Regioisomer-Specific Electron Affinities and Electronic Structures of  $\text{C}_{70}$  *para*-Adducts at Polar and Equatorial Positions with (Bromo)Benzyl Radicals: Photoelectron Spectroscopy and Theoretical Study." *Phys. Chem. Chem. Phys.* 18, 18683-18686 (2016).
24. GL Hou, B Chen, WJ Transue, DA Hrovat, CC Cummins, WT Borden, XB Wang. "A Joint Experimental and Computational Study of the Negative Ion Photoelectron Spectroscopy of the 1-Phospha-2,3,4-triazololate Anion,  $\text{HCPN}_3^-$ " *J. Phys. Chem. A* 120, 6228-6235 (2016).
25. Evgeny V. Beletskiy, Xue-Bin Wang, and Steven R. Kass. "Anion Binding of One-, Two-, and Three-Armed Thiourea Receptors Examined via Photoelectron Spectroscopy and Quantum Computations", *J. Phys. Chem. A* 120, 8309-8316 (2016).
26. Zhengbo Qin, Gao-Lei Hou, Zheng Yang, Marat Valiev, Xue-Bin Wang. "Negative ion photoelectron spectra of  $\text{ISO}_3^-$ ,  $\text{IS}_2\text{O}_3^-$ , and  $\text{IS}_2\text{O}_4^-$  intermediates formed in interfacial reactions of ozone and iodide/sulfite aqueous microdroplets", *J. Chem. Phys.* 145, 214310 (2016).
27. Xue-Bin Wang. "Cluster Model Studies of Anion and Molecular Specificities via Electrospray Ionization Photoelectron Spectroscopy", *J. Phys. Chem. A* 121, 1389-1401 (2017) (**Invited Feature Article, noted on the Cover, awarded as ACS Editors' Choice**).
28. Gao-Lei Hou, Jun Zhang, Marat Valiev, and Xue-Bin Wang. "Structure and energetics of hydrated deprotonated cis-pinonic acid anion clusters and their atmospheric relevance" *Phys. Chem. Chem. Phys.* 19, 10676-10684 (2017).
29. Gao-Lei Hou, Bo Chen, Wesley J. Transue, Zheng Yang, Hansjörg Grützmacher, Matthias Driess, Christopher C. Cummins, Weston Thatcher Borden, and Xue-Bin Wang. "Spectroscopic Characterization, Computational Investigation, and Comparisons of  $\text{ECX}^-$  (E = As, P, and N; X = S and O) Anions" *J. Am. Chem. Soc.* 139, 8922-8930 (2017).
30. Ekram Hossain, Shihu M. Deng, Samer Gozem, Anna I. Krylov, Xue-Bin Wang and Paul G. Wenthold. "Photoelectron Spectroscopy Study of Quinonimides" *J. Am. Chem. Soc.* 139, 11138-11148 (2017).
31. Gao-Lei Hou, Xue-Bin Wang, and Marat Valiev. "Formation of  $(\text{HCOO}^-)(\text{H}_2\text{SO}_4)$  Anion Clusters: Violation of Gas-Phase Acidity Predictions" *J. Am. Chem. Soc.* 139, 11321-11324 (2017) (communication).
32. Jonas Warneke, Gao-Lei Hou, Edoardo Aprà, Carsten Jenne, Zheng Yang, Zhengbo Qin, Karol Kowalski, Xue-Bin Wang, and Sotiris S. Xantheas. "Electronic Structure and Stability of  $[\text{B}_{12}\text{X}_{12}]^{2-}$  (X=F-At): A Combined Photoelectron Spectroscopic and Theoretical Study", *J. Am. Chem. Soc.* (2017, accepted).

## Nonequilibrium Properties of Driven Electrochemical Interfaces

PI: Adam P. Willard

Massachusetts Institute of Technology, Department of Chemistry

77 Massachusetts Ave., Cambridge, MA 02139

[awillard@mit.edu](mailto:awillard@mit.edu)

### Program Scope:

The influence of nanoscale disorder on individual electrochemical processes is an important and poorly understood problem. Active processes, such as interfacial electron transfer, influence both the static and dynamic properties of the interfacial environment, and ultimately drive the flux of reactive species across the electrochemical interface. Understanding and characterizing the nonequilibrium response of the interfacial environment is essential for predicting and quantifying these effects. The goal of this project is to investigate the dynamic properties of driven electrochemical interfaces, and to determine how these properties are affected by the presence of nanoscale disorder.

Our approach utilizes all-atom molecular simulation to explore the nonequilibrium response of electrolytes to changes in local electrostatic environment. These results will facilitate the development of new coarse-grained mesoscale models designed to simulating the dynamics of driven electrochemical interfaces. These general phenomenological models will provide the capability to explicitly evaluate the theoretical assumptions that underlie traditional electrochemical theories. Unlike traditional theoretical frameworks, such as those based on the developments of Gouy, Chapman, and Stern, our models do not rely on the assumption that the electrochemical environment is a rapidly relaxing homogeneous continuum. Instead, our models explicitly treat the spatial fluctuations of charged species that drive individual electrochemical processes.

Our models also include a stochastic model of interfacial charge transfer to simulate active model electrochemistry. This will allow us to explicitly evaluate the interplay between charge mobility within the electrolyte and charge creation/annihilation at the electrochemical interface. By exploring this interplay, and how it is affected by nanoscale disorder at the interface, we aim to reveal fundamental physical insight into the microscopic processes that determine the properties of driven electrochemical interfaces.

### Recent Progress:

During the first few months of this project (the start date of this project was July, 1 2017) we have begun to develop simulation tools that can be used to quantifying the nonequilibrium response of liquid electrolytes. These tools are designed to reveal the space- and time-dependent properties of the electrostatic environment. We base our analysis on the Madelung definition of the local electrostatic potential of particle  $i$ ,

$$U_i(t) = \frac{e}{4\pi\epsilon_0} \sum_{j \neq i} \frac{q_j(t)}{|r_{ij}(t)|},$$

where  $e$  is elementary unit of charge,  $\epsilon_0$  is the vacuum permittivity, the summation is taken over all other particles,  $q_j(t)$  denotes the value of charge on particle  $j$  at time  $t$ , and  $r_{ij}$  is the vector separating particles  $i$  and  $j$ . This definition of the potential provides an instantaneous and species specific snapshot of the electrostatic environment. Our simulation tools analyze the statistics of  $U_i(t)$ , for specific ions within an electrolyte solution, to report on the space- and time-dependent dynamics of the electrolyte solution. For instance, as illustrated in Fig. 1, the time dependence of  $U_i(t)$  can be used to investigate the local relaxation of an electrolyte following a nonequilibrium electrostatic perturbation.

### Future Plans:

Our ongoing efforts in this project will focus on two specific topics.

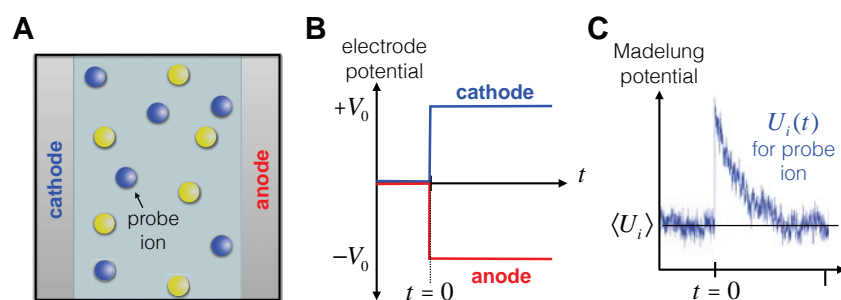


**Figure 1.** Using the Madelung potential to investigate electrolyte relaxation dynamics. (A) A schematic illustration of an electrochemical cell consisting of a liquid electrolyte confined between two constant potential electrodes. (B) Simulations are carried out with a time-dependent protocol for the electrode potentials. (C) The Madelung potential reports on the electrostatic environment and how it responds to this time-varying electrode potential.

*Investigating the effect of nanoscale disorder on the screening response of liquid electrolytes.* We will continue to development simulation tools for analyzing nonequilibrium electrolyte response. We will apply these tools to explore the dynamics of liquid electrolytes when they are placed out of equilibrium by the sudden application of an applied electrode potential, as illustrated in Fig. 2.

*Developing a model for simulating the microscopic flow of charge across the electrode-electrolyte interface.* We will develop a theoretical framework for simulating the dynamics of active electrochemical interfaces. This framework will explicitly describe both the effects of nanoscale disorder and the dynamic effects of interfacial charge transfer. An important feature of our model is that it will include the explicit effects of interfacial charge transfer processes and thus offer a realistic simulation of the driving forces that control the flow of current in an electrochemical cell. We will focus specifically on modeling the interfacial charge transfer processes that involve either the exchange of ionic species between the electrode and the electrolyte, as in the case of a battery, or the exchange of electrons between the electrode and specific chemical species with the electrolyte, as in the case of an electrochemical reactor. Our model will combine three basic ingredients: (1) a coarse-grained model of a constant potential electrode, (2) a coarse-grained model of an electrolyte, and (3) an empirical model of interfacial charge transfer. We will combine these three ingredients, as illustrated in Fig. 3, to simulate the flow of current in model electrochemical cells. Below we describe these ingredients, as they pertain to the model solid-polymer battery that is depicted in Fig. 3.

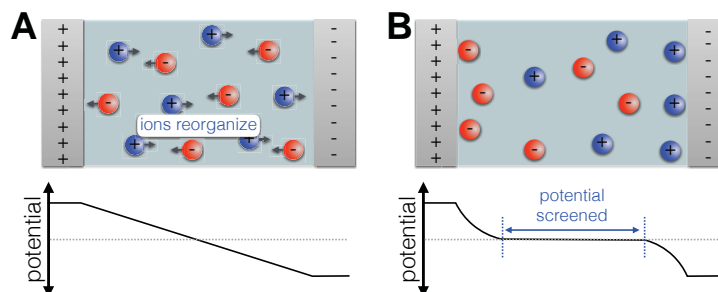


**Figure 2.** The screening response of an electrolyte confined between two constant potential electrodes. (A) When an applied electrode potential is introduced to an electrolyte that is initially at equilibrium, a linear potential gradient drives the flow of ions. (B) The equilibrium response of the electrolyte to an applied potential includes a buildup of excess ionic charge at each electrode compensates the electrode charges, screening the potential gradient in the regions away from the electrode surfaces.

(1) Constant potential electrodes: We will model constant potential electrodes following the formulation of Siepmann and Sprik, in which individual electrode atoms carry variable partial charges whose values are determined by a constant potential condition. To adapt this electrode model to our coarse-grained approach we will define effective coarse-grained electrode atoms whose size is selected to be commensurate with the length scale of the model ion-conducting polymer.

(2) Ion-conducting polymer: We will model the ion-conducting polymer using the dynamic bond percolation model that was developed by Mark Ratner more than 30 years ago. The original formulation is a lattice model in which ions diffuse randomly along three-dimensional lattice. In this model the polymer is represented by a set of slowly evolving constraints that prevent ionic occupation. The ion positions and kinetic polymer constraints evolve via a Metropolis Monte Carlo algorithm. This model has been demonstrated to provide useful physical insight into the equilibrium properties of bulk ion-conducting polymer. More recently, the Tom Miller's group has improved upon this model by including explicit energetic interactions and computing polymer dynamics directly from higher-level all-atom simulation. Building upon this success, we will utilize the Miller group's approach to parameterize our polymer model. We will begin with a model of poly(ethylene oxide) (PEO), which is perhaps the most widely used ion-conducting polymer.

(3) Interfacial charge transfer: We will model interfacial charge transfer with a stochastic model of electrode-electrolyte ion exchange. The model will be designed to simulate the discharge or intercalation of  $\text{Li}^+$  via the the creation and annihilation of cations at the surface of the electrode. The rate of these stochastic processes will be computed using a Marcus theory description of interfacial electron transfer. Specifically, we will derive an expression for the position dependent probability for ion creation or annihilation at the electrode interface. Like any standard model of condensed phase electron transfer, this expression will include a dependence of charge transfer probability on the donor-acceptor distance and the requirement of energy conservation between the initial and final state. This requirement includes a dependence on the Fermi function, and how it overlaps with the electronic energy levels of the donor or acceptor species. The electrode voltage determines the Fermi level and thus controls the charge transfer probability. In this way, electrodes with different potentials feature different characteristic charge transfer rates. In an electrochemical cell, these differences drive the flow of ions (and current) between the electrodes.

In our formulation, the probability for ion creation/annihilation depends on the details of configuration and is thus both spatially and temporally dependent. This means that different micro-environments can yield different rates of charge transfer, as illustrated in Fig. 4. Indeed, the importance of this effect has been recently highlighted by the Subotnik group, which incorporates a similar methodology for describing stochastic Marcus-like electron transfer in the context of all-atom molecular dynamics simulations. Our simulations will apply an analogous formalism to specifically analyze the effects of nanoscale disorder on the nonequilibrium dynamics of ions at the electrode interface.

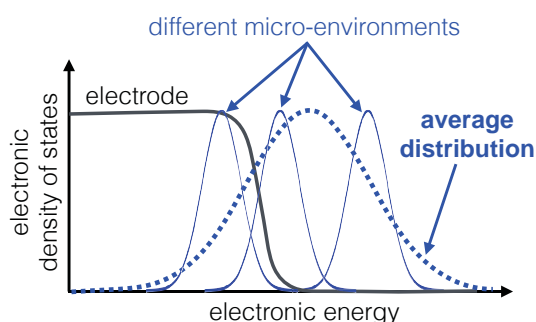


**Figure 4.** Variations in micro-environment lead to variations in charge transfer rates. This figure shows the distribution of electronic energy levels in the electrode (grey line) and the average over all Li-ions (dashed blue line). The distribution for individual ions (solid blue lines) can differ from the average distribution due to variations in micro-environment, for example arising from differences in local ionic coordination. Our methodology will treat these variations explicitly, so that local configuration directly influences charge transfer rates.

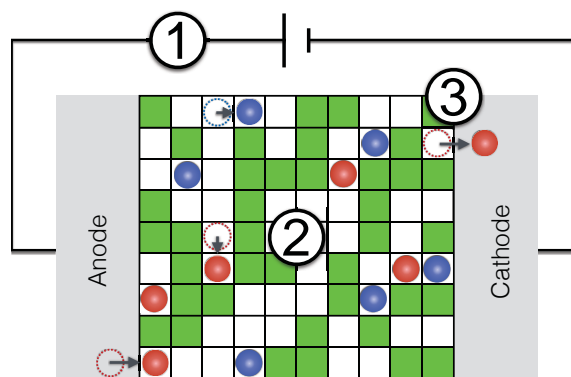


**Figure 3.** A schematic illustration of our coarse-grained model of a solid-polymer battery. This model will contain three specific ingredients: (1) constant potential electrodes, (2) a lattice model of an ion-conducting polymer, and (3) a stochastic model of interfacial charge transfer.

**Publications:**

Given the recent start date of this project, no publications have yet been produced under this award.

## Free Radical Reactions of Hydrocarbons at Aqueous Interfaces

Principal Investigator: Kevin R. Wilson

Lawrence Berkeley National Laboratory, 1 Cyclotron Road, MS 6R2100, Berkeley, CA 94720

Email: [krwilson@lbl.gov](mailto:krwilson@lbl.gov)

### Program Scope:

This Early Career Research project is focused on probing the surface chemistry of organic molecules residing on nanometer and micron-sized aqueous droplets exposed to gas phase hydroxyl radicals using atmospheric pressure surface sensitive mass spectrometry. This program aims to:

*Quantify the link between molecular structure, phase and surface reactivity at aqueous and organic interfaces using aerosols, nanoparticles and micron-sized droplets.*

This work broadly supports the Department of Energy's Basic Energy Sciences program to better assess, mitigate and control the efficiency, utilization, and environmental impacts of energy use. This work seeks a rigorous molecular understanding of how heterogeneous reaction pathways lead to either bulk solvation of a surface active organic molecule or its removal from the interface through decomposition into gas phase products. Understanding these fundamental processes are critical for predicting the chemical fate of hydrocarbon byproducts of energy use and consumption.

### Recent Progress:

**Multiphase Coupling of Free Radical and Acid/base Reaction Pathways.** We have completed a study on how free radical reactions pathways are altered by aqueous environments. The overall goal of this study is to quantitatively explain how networks of coupled free radical and acid base elementary reactions produce changes in properties of an aqueous interface (e.g. chemical erosion or water uptake). To do this we examined a long standing model system in my laboratory: the heterogeneous reaction of OH radicals with citric acid. This model system exhibits complex feedbacks between surface and bulk reactions and molecular diffusion. By combining experimental measurements of reaction rates and product distributions with detailed stochastic reaction diffusion simulations we were able to quantitatively explain how acid-base reactions, which occur concurrently with acyloxy radical formation and unimolecular decomposition of alkoxy radicals govern multiphase reaction pathways. Our analysis shows that free radical reactions mainly add functional groups to the carbon skeleton of neutral citric acid, since carboxylic acid moieties deactivate unimolecular fragmentation of alkoxy radicals. In contrast the presence of conjugate carboxylate groups originating from acid-base equilibria activate both acyloxy radical formation and carbon-carbon bond scission of alkoxy radicals, leading to the formation of low molecular weight, highly oxidized products such as oxalic and mesoxalic acid. It is the dynamic interplay between free radical, acid and conjugate base chemistry that controls the formation of gas phase reaction products and the onset of chemical erosion of the interface.

More generally our results suggest a new connection between how solution pH and water govern the balance of functionalization and fragmentation reactions in aqueous multiphase chemistry. Free radical oxidation promotes the formation of new carboxylic acid products, which in turn promotes water uptake and simultaneously acid-base reactions. This indicates that carboxylic acids play a dual role in oxidative aqueous phase chemistry. At early stages, these highly oxidized

species mainly contribute to increase in molecular weight and water uptake. When the character of the interface becomes aqueous, acid-base equilibria lead to an increase in carboxylate-mediated chemistry, which largely drives C-C bond scission reactions and chemical erosion of the interface.

**Spatial Reactivity at Interfaces.** Changes in the transport timescales of molecules to and from the interface can in turn induce complex feedbacks between the phase state (glass vs. well mixed solution) and reactivity, producing distinct locations (surface, subsurface, vs. bulk) where key reactions steps occur. To better understand this complex coupling, we also focused on studying the initial steps of a reactive collision between a gas phase species (hydroxyl and ozone) and a model organic interface. A key quantity is the depth below the interface that OH or O<sub>3</sub> can diffuse before reaction (e.g. the reacto-diffusive length). To measure these nanometer sized reacto-diffusive lengths we created core shell nanoparticles in the gas phase (i.e. aerosols). The dimensions of the core and shell can be precisely controlled with nanometer resolution using differential mobility analysis. Using a combination of reactive and unreactive shells and selecting a core material that is reactive to OH or ozone we quantified the transmission probability of OH and ozone as a function of shell thickness. Simple Fickian models of reaction + diffusion were used to interpret the data.

As expected, OH radicals are observed to react within a 1-3 nm region below the interface. Combining this OH depth profile with literature rate coefficients to simulate the cascade of subsequent free radical reactions, interfacial profiles of various intermediates are predicted. For example, the formation of alkyl radicals, the direct product of H abstraction by OH, is predicted to occur over a 6 nm region near the interface. Peroxy radicals (RO<sub>2</sub>) in comparison to OH are quite unreactive and diffuse well beyond the interface and into the bulk liquid. RO<sub>2</sub> + RO<sub>2</sub> reactions can form alkoxy radicals RO whose distribution closely resembles the RO<sub>2</sub> depth profile. These predictions, constrained by experiment, illustrate the complex interplay expected at real interfaces where elementary reaction pathways cannot in a simple way be isolated from molecular diffusion. For example, these measurements and associated simulations are for an “ideal” case where molecular diffusion to and from the interface is rapid compared to the OH reaction frequency (i.e. as in well-mixed droplet). However in more complex systems, it is easy to imagine how spatial distributions of reactivity could be significantly altered; for example at glassy or semisolid interfaces governed by strong diffusive confinement. We have obtained preliminary evidence that diffusive confinement can alter product distributions and enhance reaction pathways that would normally be too slow in well-mixed liquids or aqueous interfaces.

**Heterogeneous and Condensed Phase Reactions in Microdroplets.** We have developed a new branched quadrupole electrodynamic balance (BQT) designed to trap individual or “clouds” of micron-sized droplets for long periods of time (seconds to days). The ability to trap droplets over these long time scales (hours to days) allows us to access heterogeneous reaction conditions not previously possible. The device will allow new science questions to be addressed that center on how unimolecular peroxy radical reactions compete with bimolecular reactions at aqueous interfaces. We have also developed an interface in which we can simultaneously store 10-20 droplets for hours in the trap and then eject them on demand from the trap into an extractive electrospray ionization source obtain single droplet mass spectra.

The first experiments using the BQT focused on condensed phase reactions produced during a collision event between two droplets. This work seeks to understand why reactions in aqueous micro-compartments have been observed to occur significantly faster rates than those in the bulk;

often at rates that are a million times faster. The underlying mechanism for the observed enhancement remains unclear, but we suspect interfacial processes in small compartments may be key. The BQT allows for condensed phase chemical reactions to be initiated by colliding droplets with different reactants and levitating the merged droplet indefinitely. As a test, the reaction of ortho-phthalaldehyde (OPA) with alanine in the presence of dithiothreitol was measured using both fluorescence spectroscopy and single droplet paper spray (PS) mass spectrometry. The bimolecular rate constant for reaction of alanine with OPA is found to be  $84 \pm 10$  and  $67 \pm 6 \text{ M}^{-1} \text{ s}^{-1}$  in a  $30 \text{ }\mu\text{m}$  radius droplet and bulk solution, respectively, which demonstrates that bimolecular reaction rate coefficients can be quantified using merged microdroplets in the BQT. Reaction products were detected by real time single droplet paper spray mass spectrometry.

**Future Plans:** The end date for this ECRP award was June 2017.

#### **Publications Acknowledging Support of the DOE Office of Science Early Career Award:**

1. Jacobs, M., Davies, J.F., Lee, L., Davis, R.D. Wilson, K.R., Exploring chemistry in micro-compartments via the contactless manipulation and merging of droplets in a branched quadrupole trap. Submitted to *Analytical Chemistry*, 2017.
2. Preston, T.; Davies, J.; Wilson, K., The frequency-dependent response of single aerosol particles to vapour phase oscillations and its application in measuring diffusion coefficients. *Physical Chemistry Chemical Physics* 2017, 19, 3922-3931. DOI: 10.1039/C6CP07711K
3. Liu, M. J.; Wiegel, A. A.; Wilson, K. R.; Houle, F. A., Aerosol Fragmentation Driven by Coupling of Acid-Base and Free-Radical Chemistry in the Heterogeneous Oxidation of Aqueous Citric Acid by OH Radicals. *Journal of Physical Chemistry A* 2017, 121, (31), 5856-5870. DOI: 10.1021/acs.jpca.7b04892
4. Jacobs, M.; Kostko, O.; Ahmed, M.; Wilson, K., Low Energy Electron Attenuation Lengths in Core-Shell Nanoparticles. *Physical Chemistry Chemical Physics* 2017. DOI: 10.1039/C7CP00663B
5. Ruehl, C. R.; Davies, J. F.; Wilson, K. R., An interfacial mechanism for cloud droplet formation on organic aerosols. *Science* 2016, 351, (6280), 1447-1450. DOI: 10.1126/science.aad4889
6. Richards-Henderson, N. K.; Goldstein, A. H.; Wilson, K. R., Sulfur Dioxide Accelerates the Heterogeneous Oxidation Rate of Organic Aerosol by Hydroxyl Radicals. *Environmental science & technology* 2016, 50, (7), 3554-3561. DOI: 10.1021/acs.est.5b05369
7. Lee, L.; Wilson, K. R., The Reactive Diffusive Length of OH and Ozone in Model Organic Aerosols. *Journal of Physical Chemistry A* 2016. DOI 10.1021/acs.jpca.6b05285
8. Davies, J. F.; Wilson, K. R., Raman Spectroscopy of Isotopic Water Diffusion in Ultraviscous, Glassy, and Gel States in Aerosol by Use of Optical Tweezers. *Analytical chemistry* 2016, 88, (4), 2361-2366. DOI: 10.1021/acs.analchem.5b04315

9. Cheng, C. T.; Chan, M.; Kevin R., W., Importance of Unimolecular HO<sub>2</sub> Elimination in the Heterogeneous OH Reaction of Highly Oxygenated Tartaric Acid Aerosol. *Journal of Physical Chemistry A* 2016. DOI: 10.1021/acs.jpca.6b05289
10. Zhang, H.; Worton, D. R.; Shen, S.; Nah, T.; Isaacman-VanWertz, G.; Wilson, K. R.; Goldstein, A. H., Fundamental Time Scales Governing Organic Aerosol Multiphase Partitioning and Oxidative Aging. *Environmental Science & Technology* 2015, 49, (16), 9768-9777. DOI: 10.1021/acs.est.5b02115
11. Richards-Henderson, N. K.; Goldstein, A. H.; Wilson, K. R., Large enhancement in the heterogeneous oxidation rate of organic aerosols by hydroxyl radicals in the presence of nitric oxide. *Journal of Physical Chemistry Letters* 2015, 6, (22), 4451-4455. DOI: 10.1021/acs.jpcelett.5b02121

# Non-Empirical and Self-Interaction Corrections for DFTB: Towards Accurate Quantum Simulations for Large Mesoscale Systems

Bryan M. Wong

Department of Chemical & Environmental Engineering and Materials Science & Engineering Program, University of California-Riverside, Riverside, CA 92521

E-mail: [bryan.wong@ucr.edu](mailto:bryan.wong@ucr.edu), Web: <http://www.bmwong-group.com>

## 1. Program Scope

This project is comprised of two complementary (but parallel) thrusts: (1) implementing massively-parallelized computing hardware for calculating the electron structure and dynamics of large chemical systems, and (2) introducing self-interaction corrections for improving the accuracy of the density functional tight binding (DFTB) approach. While classical molecular dynamics can handle hundreds of thousands of atoms, it cannot provide a first-principles based description of mesoscale systems at the quantum level. At the other extreme, conventional Kohn-Sham DFT methods can probe the true quantum mechanical nature of chemical systems; however, these methods cannot tackle the large sizes relevant to mesoscale dynamics and length scales. The DFTB formalism utilized in this project provides a viable approach for probing these mesoscale systems at a quantum mechanical level of detail. However, to utilize the DFTB approach for accurate calculations of electronic properties, it is crucial to incorporate *quantum-based non-empirical corrections* in DFTB since exchange-correlation effects can still remain very strong in these large systems. At the same time, enhancing the computational efficiency of DFTB is also essential since optimal computational performance is required for addressing the large size scales associated with mesoscale systems. As such, the new non-empirical corrections and computing hardware enhancements implemented in this project will enable accurate *and* computationally efficient approaches to directly probe electronic properties in these large, complex systems.

## 2. Recent Progress

The start date of this project was 08/15/2016, and during the past year we have devoted half of our initial efforts to graphical processing unit (GPU) parallelization of electron dynamics and the other half of our focus to an in-house (i.e., from scratch) implementation of self-interaction corrections (SICs) in an all-electron DFT code. Both of these efforts and our progress in each of these initiatives are described further below.

The specific material systems we have chosen at the moment for GPU parallelization are large metallic nanoclusters systems and arrays. In particular, we are harnessing GPUs and implementing new computational routines to understand plasmonic interactions and collective many-body excitations in these metallic nanoparticles on an atomistic scale with DFTB. We have chosen metallic nanoparticles as an ideal system for GPU parallelization since our understanding of the detailed quantum-mechanical mechanisms in these collective excitations is severely limited due to the sheer size and complexity of plasmonic nanostructure-molecule interfaces. Specifically, while classical electrodynamics methods can handle metallic nanostructures at a continuum level, they cannot provide a first-principles based description of plasmonic systems at the quantum level, which is *absolutely crucial for describing electron tunneling processes at sub-nanometer gaps*. While conventional linear-response time-dependent methods can probe the quantum-mechanical dynamics of chemical systems, these (frequency-domain) methods cannot tackle the large sizes relevant to *collective excitations* in plasmonic materials. Recently, using real-time time-dependent

DFTB (TDDFTB), we have shown that collective plasmonic excitations produce large electric fields on metallic surfaces, leading to dramatic enhancements in the optical response. In particular, the largest electric field enhancements occur

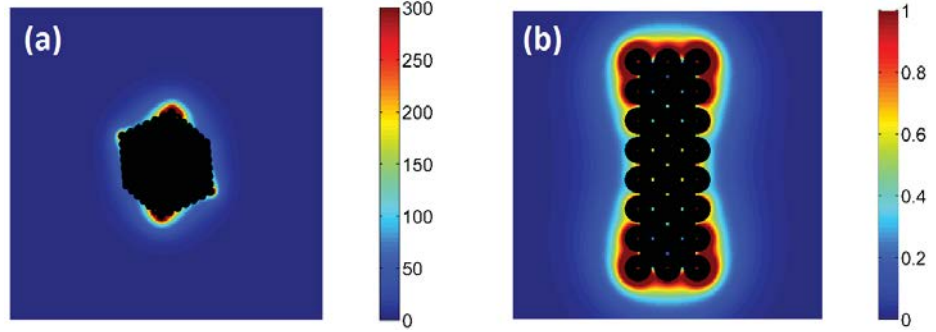


**Figure 1.** Electric field enhancement obtained from RT-TDDFTB for (a) an icosahedral-shaped sodium nanoparticle and (b) a rod-shaped sodium nanoparticle.

on regions of highest local curvature (i.e., at the corners of the structure), yielding “hot spots” on the surface of the metal nanoparticle (cf. **Figure 1**). As such, the development of GPU-enhanced electron dynamics methods that can resolve these features for large systems plays an important step in predicting and understanding the dynamics in these complex plasmonic systems.

To probe the dynamics of these large systems using massively-parallelized GPUs, we calculate the time evolution of the density matrix from a numerical integration of the Liouville-Von Neumann equation of motion. For extremely large systems, the memory requirements for storing the DFTB density matrices exceeds the GPU global memory, which severely limits the types of systems that can be studied. Currently, we are implementing and evaluating three custom algorithms for out-of-core matrix-matrix multiplication designed to address this problem for larger systems. Within these three different algorithms, we split the multiplicands into block matrices and perform the multiplication as follows:

$$[A][B] = \begin{bmatrix} A_1 \\ A_2 \end{bmatrix} [B_1 \ B_2] = \begin{bmatrix} A_1 B_1 & A_1 B_2 \\ A_2 B_1 & A_2 B_2 \end{bmatrix}. \quad (1)$$

In **Algorithm 1**, memory is allocated for one submatrix of the first multiplicand and one submatrix of the second. The single multiply is performed, and memory is copied back to the product matrix before moving on to the next computation. Of the three algorithms tested, this uses the least memory of the algorithms, but generates the most memory transfer operations as we split the matrix into more submatrices. In **Algorithm 2**, memory is allocated for one submatrix of the first multiplicand and the entire second multiplicand. Using this additional memory, we are able to launch all of the kernels for one row group at once. This allows for better performance at the cost of additional memory requirements. Finally, for **Algorithm 3**, we modified the first algorithm and pipelined it with CUDA streams, with each thread in the operation having a corresponding CUDA stream. This increases the performance of the first algorithm in most cases when the number of threads and streams is optimal for the number of submatrices and the size of the problem. A downside of this approach is that this algorithm uses more memory than the first on both the host and the GPU, because each thread or stream needs a context to work in.

Using these custom GPU algorithms, we have calculated the absorption spectrum of extremely large gold nanoparticles obtained from the Fourier transform of the time-dependent dipole moment after deconvolution of the applied electric field (cf. **Figure 2**). It is worth mentioning that it is computationally prohibitive to obtain these results with conventional Casida-type TDDFT methods due to the immense size of these systems, whereas the entire spectrum can be directly obtained with the RT-TDDFTB approach. Most importantly, as opposed to frequency-domain calculations common in linear-response TD-DFT, it is relatively straightforward to parallelize the time-propagation steps on GPUs. We are still evaluating the efficiencies in each of the three

different algorithms, and our preliminary assessment is as follows: Algorithm 3 serves as a pipelined version of Algorithm 1 which puts the amount of memory it uses on a sliding measure between algorithm 1 and 2. Accordingly, it exhibits the best performance of all three algorithms for all matrix sizes tested in this project. At the recent 2017 American Chemical Society (ACS) meeting in San Francisco, *the PI received an ACS COMP Open Eye Outstanding Junior Faculty Award for this DOE-acknowledged work on GPU parallelization.*

Within the second thrust of this project, we have focused on implementing unitarily-invariant self-interaction corrections (SICs) using Fermi Orbitals (FOs) as described by Pederson and coworkers (Pederson, M.R.; Ruzsinszky, A.; Perdew, J. P. *J. Chem. Phys.* **2014**, *140*, 121103). During the past year, we have concentrated our efforts on developing an in-house (i.e., from scratch) implementation of FO-SIC in NWChem. We have chosen to implement this first in an all-electron DFT code to both verify and understand all the subtle intricacies of the FO-SIC approach before proceeding to the more difficult task of modifying this new formalism for DFTB. The specific procedure for implementing the FO-SIC approach in our NWChem implementation is summarized in **Figure 3** and given as follows: (1) For a set of DFT orbitals,  $\{\psi_\alpha\}$ ,  $N$  centroid positions  $\{\mathbf{a}_1, \mathbf{a}_1, \dots, \mathbf{a}_N\}$  are found which provides a set of  $N$  normalized linearly independent (but not orthogonal) FOs,  $\{F_1, F_2, \dots, F_N\}$ . Within our NWChem implementation, we obtain initial guesses of these centroids via a Foster-Boys localization method. (2) Löwdin’s method of symmetric orthonormalization is then used to construct a set of localized orthonormal orbitals,  $\{\phi_1, \phi_2, \dots, \phi_N\}$  and construct the SIC-DFTB energy from the set of FOs; (3) the SIC-DFTB energy is minimized as a function of the DFTB orbitals and the FO centroids. Within our specific NWChem implementation, we have found that a Broyden-Fletcher-Goldfarb-Shanno (BFGS) algorithm gives enhanced (or, at the very least, comparable) convergence to the original conjugate gradient approach used previously. In addition, we have also re-formulated some of the original expressions in the FO-SIC description to take advantage of the underlying symmetries in the expressions for  $\Delta_{lk,m}^1$  and  $\Delta_{lk,m}^3$ , which should be instrumental when this approach is implemented in DFTB. Most importantly, the FO-SIC approach circumvents the original Perdew-Zunger localization equations which scale as  $O(N^6)$  and will also be of paramount importance when it is

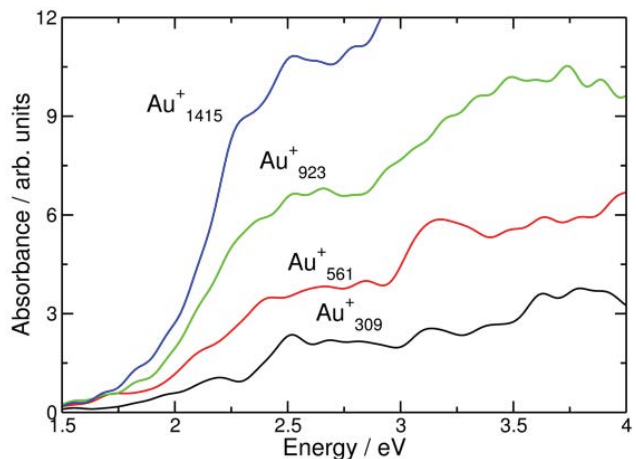


**Figure 2.** Absorption spectra of gold nanoparticles obtained from the GPU-enhanced RT-TDDFTB approach.

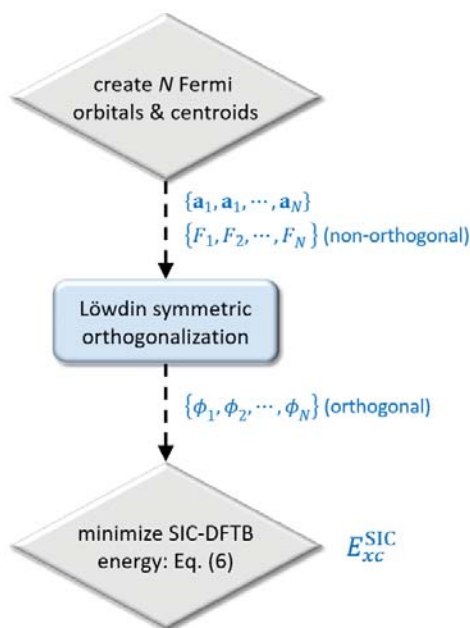


**Figure 3.** Simplified algorithmic flowchart for our NWChem implementation of FO-SIC. The computed outputs of each block are listed next to the dotted arrows, which are later used in subsequent blocks.

implemented in the DFTB formalism. To validate our FO-SIC implementation, we have carried out detailed comparisons between total electronic energies, atomization energies, and ionization potentials from a very recent arXiv publication by Perdew and co-workers (arXiv: 1703.10742v1 [physics.comp-ph]) as shown in Table 1. After several extensive benchmark comparisons between centroid positions, electronic energies atomization energies, and ionization potentials benchmarks provided by Dr. Zeng-hui Yang and Prof. Alan Jackson, we have confirmed that our FO-SIC approach is fully functional. With the DFTB FO-SIC approach properly benchmarked, we intend to couple this approach with the GPU enhancements mentioned previously to probe the electronic structure and dynamics of large systems within DFTB.

Table 1: Benchmark of total energies.

Molecule	Total(Hartree)			
	LSDA ref <sup>a</sup>	LDA NW <sup>b</sup>	FO-SIC ref <sup>a</sup>	FO-SIC NW <sup>b</sup>
N <sub>2</sub>	-108.692	-108.692	-109.842	-109.842
O <sub>2</sub>	-149.332	-149.331	-150.736	-150.737
CO	-112.471	-112.471	-113.635	-113.635
CO <sub>2</sub>	-187.273	-187.273	-189.096	-189.097
C <sub>2</sub> H <sub>2</sub>	-76.625	-76.624	-77.594	-77.593
LiF	-106.702	-106.702	-107.716	-107.716
H <sub>2</sub>	-1.1251	-1.1251	-1.1745	-1.1745
Li <sub>2</sub>	-14.724	-14.724	-15.050	-15.050
CH <sub>4</sub>	-40.109	-40.109	-40.667	-40.667
NH <sub>3</sub>	-56.107	-56.106	-56.761	-56.761
H <sub>2</sub> O	-75.909	-75.909	-76.665	-76.664
CH <sub>3</sub> OH	-114.84	-114.84	-116.13	-116.13

<sup>a</sup> Yang, Z. et. al. arXiv online.

<sup>b</sup> NWChem implementation.

### 3. Future Plans

With the FO-SIC all-electron DFT code fully-working and functional, we intend to focus all our effort into modifying this formalism in the DFTB approach during year 2 of this project. Two manuscripts detailing our all-electron FO-SIC approach and its accuracy compared with other SIC approaches are also in progress. This DOE Grant has partially supported 1 Postdoctoral Associate, 2 PhD students, and 2 MS students. The 2 MS theses will be completed by October 2017, and 1 of the PhD theses supported by this DOE grant will be completed in Spring 2018.

**Grant Number and Title:** DE-SC0016269: “Non-Empirical and Self-Interaction Corrections for DFTB: Towards Accurate Quantum Simulations for Large Mesoscale Systems”

### Publications acknowledging DOE grant DE-SC0016269 in the last 12 months:

- Alejandro Alvarez Barragan, Niranjana V. Ilawe, Lanlan Zhong, Bryan M. Wong, and Lorenzo Mangolini, “A Non-Thermal Plasma Route to Plasmonic TiN Nanoparticles.” *Journal of Physical Chemistry C*, **121**, 2316 (2017).
- Sangavi Pari, Inger A. Wang, Haizhou Liu, and Bryan M. Wong, “Sulfate Radical Oxidation of Aromatic Contaminants: A Detailed Assessment of Density Functional Theory and High-Level Quantum Chemical Methods.” *Environmental Science: Processes & Impacts*, **19**, 395 (2017). (Invited Paper)
  - Featured as the front cover for the March 2017 themed collection on [QSARs and Computational Chemistry Methods in Environmental Chemical Sciences of Environmental Science: Processes & Impacts \(Issue 3\)](#)
- Lindsey N. Anderson, M. Belén Oviedo, and Bryan M. Wong, “Accurate Electron Affinities and Orbital Energies of Anions from a Non-Empirically Tuned Range-Separated Density Functional Theory Approach.” *Journal of Chemical Theory and Computation*, **13**, 1656 (2017).
- Niranjana V. Ilawe, M. Belén Oviedo, and Bryan M. Wong, “Real-Time Quantum Dynamics of Long-Range Electronic Excitation Transfer in Plasmonic Nanoantennas.” *Journal of Chemical Theory and Computation*, **13**, 3442 (2017).



## Intermolecular Interactions in the Gas and the Condensed Phase

Sotiris S. Xantheas

Advanced Computing, Mathematics & Data Division,  
Pacific Northwest National Laboratory, PO Box 999, MS K1-83, Richland WA 99352  
[sotiris.xantheas@pnl.gov](mailto:sotiris.xantheas@pnl.gov)

**Program Scope:** The overarching themes of this research component of the Molecular Theory & Modeling Program are:

- establish accurate benchmarks for archetypal intermolecular interactions, aqueous clusters and guest – host interactions relevant to energy applications,
- incorporate the appropriate physics into models (classical or quantum) that explicitly account for the desired behavior,
- elucidate the molecular level factors that control complex behavior,
- understand the interplay between the molecular level information and the macroscopic properties of complex aqueous environments.

The ultimate goal of the program is *to develop accurate descriptions of intermolecular interactions for complex environments that include molecular level detail.*

**Recent Progress:** In current work, we have focused on the aqueous solvation of multi-valent metal ions by explicitly considering the low-lying electronic states and the reaction channels leading to water hydrolysis that they induce. These channels arise from the fact that the second ionization potential (I.P.) of most metals is larger than the ionization potential of water (12.62 eV). In particular, we considered the various electronic states arising from the sequential hydration of the  $\text{Ca}^{2+}$ ,  $\text{Mg}^{2+}$ ,  $\text{Al}^{3+}$ ,  $\text{Fe}^{2+}$  and  $\text{Fe}^{3+}$  ions with up to six water molecules. Our results offer insight into the shifting of electronic states and dissociation asymptotes with the degree of solvation, identify their complex interaction with other states arising from different dissociation channels, and shed light on the mechanism behind the energetic stabilization of the multi- charged hydrated  $\text{M}^{+q}(\text{H}_2\text{O})_n$  moieties observed in solution with respect to the water ionization products. A critical number of water molecules is necessary to create a stable  $\text{M}^{+k}(\text{H}_2\text{O})_n$  complex; for Mg this number is at least two, while for Al at least four.

A more complex system (see Figure 1) deals with the ground and low-lying electronically excited states of the  $[\text{Fe}(\text{H}_2\text{O})_6]^{2+}$  and  $[\text{Fe}(\text{H}_2\text{O})_6]^{3+}$  clusters as well as their aggregate. Both the second and third ionization potentials of Fe are larger than the one for water, so the ground-state products asymptotically correlate with dissociation channels that are repulsive in nature at large separations containing at least one  $\text{H}_2\text{O}^+$  fragment and a single positively charged

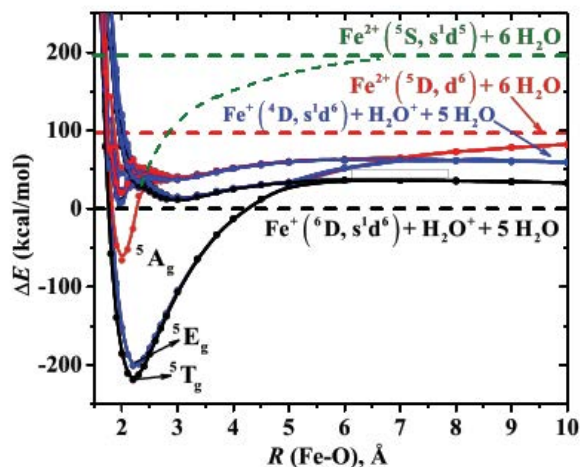


**Figure 1.** Potential energy curves of the quintet electronic states of  $[\text{Fe}(\text{H}_2\text{O})_6]^{2+}$ . Different colors correspond to different adiabatic fragments. The dashed green line traces the expected diabatic curve for the  ${}^5\text{A}_g$  state.

structures emanate from the channels consisting of the lowest electronic states of  $\text{Fe}^{2+}$  ( ${}^5\text{D}$ ;  $3d^6$ ) or  $\text{Fe}^{3+}$  ( ${}^6\text{S}$ ;  $3d^5$ ) and six neutral water molecules. Upon hydration, the ground state of  $\text{Fe}^{2+}(\text{H}_2\text{O})_6$  is a triply ( ${}^5\text{T}_g$ ) degenerate state, with the doubly ( ${}^5\text{E}_g$ ) degenerate state lying  $\sim 20$  kcal/mol higher in energy, while the  $[\text{Fe}(\text{H}_2\text{O})_6]^{3+}$  cluster has a ground state of  ${}^6\text{A}_g$  symmetry under  $T_h$  symmetry, which is well separated from the first excited state. Regarding their gas-phase interaction, for  $R(\text{Fe}-\text{Fe}) < 6.0 \text{ \AA}$ , the water molecules in the respective first solvation shells located between the two metal centers were found to interact via weak hydrogen bonds. We examined a total of 10 electronic states for this complex, including those corresponding to the electron transfer (ET) channel. A possible path via a quasi-symmetric transition state is suggested.

As a result of a joint experimental-theoretical effort, we have studied the formation of water clusters in helium droplets via the sequential capture of monomers. One or two Neon atoms are added to each droplet prior to the addition of water. The resulting infrared spectrum of the water cluster inside the droplet ensemble reveals several new bands, along with those previously assigned to the water monomer, dimer and larger cyclic clusters, up to the hexamer. The new features are assigned to be signatures of polar, water tetramer clusters having dipole moments between 2 and 3 Debye. Comparison with ab initio computations support the assignment of the cluster networks to non-cyclic “3+1” clusters, which are  $\sim 5.3$  kcal/mol less stable than the global minimum non-polar cyclic tetramer. The  $(\text{H}_2\text{O})_3\text{Ne} + \text{H}_2\text{O}$  ring insertion barrier is sufficiently large, such that evaporative helium cooling is capable of kinetically quenching the non-equilibrium tetramer system prior to its rearrangement to the lower energy cyclic species. To this end the reported process results in the formation of exotic water cluster networks that are either higher in energy than the most stable gas phase analogs or not even stable in the gas phase. The need to maximize the number of hydrogen bonds in the smaller clusters results in networks that do not resemble the connectivity found in liquid water. On the contrary, the formation of these exotic networks inside helium droplets does resemble the connectivity found in liquid water; to this end, these conditions allow for a “piece of liquid water” to be formed in a small cluster.

**Future Work:** We will investigate the interactions associated with the process of  $\text{CO}_2/\text{CH}_4$  exchange in a hydrate lattice, as well as the barrier and molecular mechanism corresponding to the diffusion of the guest species from one cage to the neighboring one. The latter must occur via the temporary breaking and reforming of hydrogen bonds in the lattice. We will attempt the first CCSD(T) calculation for the interaction of  $\text{H}_2$ ,  $\text{N}_2$ ,  $\text{CH}_4$ , and  $\text{CO}_2$  inside hollow  $(\text{H}_2\text{O})_{20}$  and  $(\text{H}_2\text{O})_{24}$  cages with a triple zeta quality set. Preliminary calculations at the MP2 and B3LYP+D levels will be performed. It should be remembered that at the DFT level the guest  $[\text{H}_2, \text{CH}_4] + \text{host} [(\text{H}_2\text{O})_{20}]$  system lies *above* the asymptote of the empty cage + the gas-phase molecule, whereas at the MP2 or CCSD(T) level it lies *below* the asymptote, i.e., it is more stable than the two isolated fragments. This finding further justifies the necessity of using high-level electronic structure calculations in order to quantify the relevant interactions in those systems. Additional

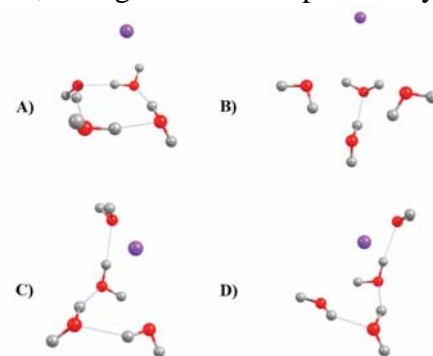


**Figure 2.** Optimized structures of  $(\text{H}_2\text{O})_4\text{-Ne}$  clusters. a) cyclic (udud)-Ne, b) cage-Ne, c) (3+1A)-Ne, d) (3+1B)-Ne.

calculations for the accommodation of CO<sub>2</sub> and CH<sub>4</sub> inside the small and large cages of the structure I (sI) hydrate lattice will focus on understanding their exchange mechanism between adjacent cages in the hydrate lattice by computing the barrier for that exchange between adjacent cages in the lattice.

Furthermore, we will extend our previous studies of weak  $\pi$ - $\pi$  interactions in an attempt to establish an accurate interaction energy for the Coronene dimer, a polyaromatic hydrocarbon (PAH) with 7 perifused benzene rings that has been used as a molecular model for the interactions between graphene sheets, at the MP2 and CCSD(T) levels of theory. Due to the technological applications of the electrical properties of graphene sheets and associated carbon-based functionalized nanomaterials, the magnitude of the interaction in the Coronene dimer has recently received a lot of attention. Most calculations have been performed to date using various density functionals, the accuracy of which is difficult to assess, since an accurate benchmark is currently not available. Following the same protocol we have established earlier for the benzene dimer, we expect that CCSD(T) single-point energy calculations with the cc-pVDZ and cc-pVTZ basis sets (1,775 basis functions) will provide an accurate binding energy for the Coronene dimer.

We will finally extend our work on weak intermolecular interactions to the C<sub>60</sub> dimers and trimers. To date, the interaction between two C<sub>60</sub> molecules as well as the simulation of their phase diagram has been reported using either classical potentials or various Density Functional Theory approaches and their variants. We will compute the interaction between two and three carbon nanoparticles up to C<sub>60</sub> at the MP2 and CCSD(T) levels of theory in order to obtain accurate dimer potential energy curves as well as the magnitude of the respective 3-body term. Of particular importance is the investigation of the long-range part of the interaction potential and the ability of MP2 to provide accurate 1/R behavior when compared to CCSD(T). For this purpose, we will also consider corrections to the c<sub>6</sub> coefficient at long range proposed by Head-Gordon. The ab initio potentials will be fitted to the simple PEFs developed during the past award period and will provide accurate pairwise additive and 3-body potentials that can be used to model the aggregation and phase diagram of those carbon nanoparticles. The nature of bonding both in and between those nanoparticles will be investigated using a recent analysis based on molecule-intrinsic quasi-atomic, bonding, and correlating orbitals. Subsequent studies will be extended to the interaction between carbon nanoparticles, starting from C<sub>24</sub> and extending all the way to C<sub>60</sub>.

### Publications Acknowledging this Grant in the last 3 years

1. J. C. Werhahn, E. Miliordos and S. S. Xantheas, "A new variation of the Buckingham exponential-6 potential with a tunable, singularity-free short-range repulsion and an adjustable long-range attraction", *Chemical Physics Letters* **619**, 133 (2015)
2. E. Miliordos and S. S. Xantheas, "On the validity of the basis set superposition error and complete basis set limit extrapolations for the binding energy of the formic acid dimer", *Journal of Chemical Physics* **142**, 094311 (2015)
3. E. Miliordos and S. S. Xantheas, "Ground and excited states of the [Fe(H<sub>2</sub>O)<sub>6</sub>]<sup>2+</sup> and [Fe(H<sub>2</sub>O)<sub>6</sub>]<sup>3+</sup> clusters: Insights into the electronic structure of the [Fe(H<sub>2</sub>O)<sub>6</sub>]<sup>2+</sup> - [Fe(H<sub>2</sub>O)<sub>6</sub>]<sup>3+</sup> complex", *Journal of Chemical Theory and Computation* **11**, 1549 (2015)

4. E. Miliordos and S. S. Xantheas, "An accurate and efficient computational protocol for obtaining the Complete Basis Set (CBS) limits of the binding energies of water clusters at the MP2 and CCSD(T) levels of theory: Application to  $(\text{H}_2\text{O})_m$ ,  $m = 2 - 6, 8, 11, 16$  and  $17$ ", *Journal of Chemical Physics* **142**, 234303 (2015)
5. S. Imoto, S. S. Xantheas and S. Saito, "Ultrafast dynamics of liquid water: Energy relaxation and transfer processes of the OH stretch and the HOH bend", B. Bagchi Special issue (invited), *Journal of Physical Chemistry B* **119**, 11068 (2015)
6. J. A. Fournier, C. T. Wolke, and M. A. Johnson, T. T. Odbadrakh and K. D. Jordan, S. M. Kathmann and S. S. Xantheas, "Snapshots of Proton Accommodation at a Microscopic Water Surface: Vibrational Spectral Signatures of the Charge Defect in Cryogenically Cooled  $\text{H}^+(\text{H}_2\text{O})_{n=2-28}$  Clusters", Feature Article (invited), *Journal of Physical Chemistry A* **119**, 9425 (2015). Journal cover
7. K. R. Brorsen, S. Y. Willow, S. S. Xantheas, and M. S. Gordon, "The melting temperature of liquid water with the effective fragment potential", *Journal of Physical Chemistry Letters* **6**, 3555 (2015)
8. J. S. Moore, S. S. Xantheas, J. W. Grate, T. W. Wietsma, E. Gratton, A. E. Vasdekis, "Modular Polymer Biosensors by Solvent Immersion Imprint Lithography", *Journal of Polymer Science, Part B: Polymer Physics* **54**, 98 (2016)
9. E. Miliordos and S. S. Xantheas, "The origin of the reactivity of the Criegee intermediate: implications for atmospheric particle growth", Communication to the Editor, *Angewandte Chemie International Edition* **55**, 1015 (2016). Hot paper
10. S. Yoo Willow, X. Cheng Zeng, S. S. Xantheas, K. S. Kim and S. Hirata, "Why is MP2-Water 'Cooler' and 'Denser' than DFT-Water?", *Journal of Physical Chemistry Letters* **7**, 680 (2016)
11. C. T. Wolke, J. A. Fournier, E. Miliordos, S. M. Kathmann, S. S. Xantheas, and M. A. Johnson, "Isotopomer-selective spectra of a single intact  $\text{H}_2\text{O}$  molecule in the  $\text{Cs}^+[(\text{D}_2\text{O})_5 \cdot \text{H}_2\text{O}]$  isotopologue: Going beyond pattern recognition to harvest the structural information encoded in vibrational spectra", *Journal of Chemical Physics* **144**, 074305 (2016)
12. S. Iwata, D. Akase, M. Aida and S. S. Xantheas, "Hydrogen-Bonded Networks in Polyhedral Water Clusters  $(\text{H}_2\text{O})_n$ ,  $n = 8, 20$  and  $24$ " *Physical Chemistry Chemical Physics* **18**, 19746 (2016)
13. E. Miliordos, E. Aprà and S. S. Xantheas, "A New, Dispersion - Driven Intermolecular Arrangement for the Benzene – Water Octamer Complex: Isomers and Analysis of their Vibrational Spectra", *Journal of Chemical Theory and Computation* **12**, 4004 (2016)
14. T.-M. Chang and S. S. Xantheas, A. E. Vasdekis, "Mesoscale Polymer Dissolution probed by Raman Spectroscopy and Molecular Simulations" *Journal of Physical Chemistry B* **120**, 10581 (2016)
15. S. S. Xantheas, "Spying on the neighbors' pool: Spectral signatures are obtained for the movement of protons in cold water clusters", invited Perspective, *Science* **354**, 1101 (2016)
16. G. E. Doublerly, R. E. Miller and S. S. Xantheas, "Formation of Exotic Networks of Water Clusters in Liquid Helium Droplets Facilitated by the Presence of Neon Atoms", *Journal of the American Chemical Society* **139**, 4152 (2017). Included in *Science* **355**, 1388 (2017) under *Research in Other Journals*
17. S. Yoo Willow and S. S. Xantheas, "A Molecular Level Insight of the Effect of Hofmeister Anions on the Interfacial Surface Tension of a Model Protein", *Journal of Physical Chemistry Letters* **8**, 1574 (2017)
18. T. B. Ward, E. Miliordos, P. D. Carnegie, S. S. Xantheas, M. A. Duncan, "Ortho-Para Interconversion in Cation-Water Complexes: The Case of  $\text{V}^+(\text{H}_2\text{O})$  and  $\text{Nb}^+(\text{H}_2\text{O})$  Clusters", *Journal of Chemical Physics* **146**, 224305 (2017)
19. P. Hamm, G. S. Fanourgakis, S. S. Xantheas, "A surprisingly simple correlation between the classical and quantum structural networks in liquid water", *Journal of Chemical Physics*, **147**, 064506 (2017)
20. J. Warneke, G.-L. Hou, E. Aprà, C. Jenne, Z. Yang, Z. Qin, K. Kowalski, X.-B. Wang and S. S. Xantheas, "Electronic Structure and Stability of  $(\text{B}_{12}\text{X}_{12})^{2-}$  ( $\text{X} = \text{F} - \text{At}$ ): A Combined Photoelectron Spectroscopic and Theoretical Study", *Journal of the American Chemical Society*, in press <http://pubs.acs.org/doi/abs/10.1021/jacs.7b08598> (2017)

***Abstracts  
(Solar Photochemistry  
Investigators)***



## FUNDAMENTAL ADVANCES IN RADIATION CHEMISTRY

Principal Investigators:

DM Bartels ([bartels.5@nd.edu](mailto:bartels.5@nd.edu)), I Carmichael, I Janik, JA LaVerne, S Ptasińska  
Notre Dame Radiation Laboratory, University of Notre Dame, Notre Dame, IN 46556

### SCOPE

- *Research in fundamental advances in radiation chemistry is organized around two themes. First, energy deposition and transport seeks to describe how energetic charged particles and photons interact with matter to produce tracks of highly reactive transients, whose recombination and escape ultimately determine the chemical effect of the impinging radiation. The work described in this part is focused on fundamental problems specific to the action of ionizing radiation. Particular projects include completion of a radiolysis model for high temperature water, experimental and theoretical investigation of the VUV spectra of liquids up to supercritical conditions, chemistry of highly excited states in spur and track recombination in aromatic hydrocarbon liquids, and quantitative characterization of a novel radiation source, the atmospheric pressure plasma jet. The second thrust deals with structure, properties and reactions of free radicals in condensed phases. Challenges being addressed include the experimental and theoretical investigation of solvated electron reaction rates, determination of the redox potentials of hyper-reduced transition metal ions, analysis of the structure and reactivity of aqueous halide ion oxidation products; and characterization of the structure and properties of the  $\text{CO}_2^-$  radical.*

### PROGRESS AND PLANS

In previous years it has been demonstrated that the equilibrium (1)  $\cdot\text{OH} + \text{H}_2 \rightleftharpoons \text{H}_2\text{O} + \text{H}^\bullet$  is the most critical in controlling the radiolytic production of corrosive oxidizing species in pressurized water cooled nuclear reactors, by the addition of excess  $\text{H}_2$  to the water. Quantitative modelling of the irradiated reactor water with a system of ca. 20 radical reactions proved elusive, and one point of uncertainty has been the magnitude of the backward reaction of  $\text{H}^\bullet$  atoms with water. In our previous modelling studies we realized that for very high continuous radiation dose rates, at temperatures similar to those found in power reactors, the steady state of  $\text{H}_2$  produced in neutral water is controlled entirely by the equilibrium (1). In the last year we have carried out an extensive series of experiments using high dose rates from 2.5MeV electrons, in the range 0.5 to 8 kGy/s, to measure the steady state  $\text{H}_2$  in neat water from room temperature to 350°C. The analysis is not yet complete. We certainly find the expected behavior above 200°C, and have a tentative value for the equilibrium constant ( $K_1$ ) at 300-350°C. However to our astonishment the steady state  $\text{H}_2$  produced between room temperature and 200°C is significantly larger than the accepted model of water radiolysis can account for. Nearly all of the reaction rates are measured up to 150°C, where the largest discrepancy is found. We expanded the scope of the experiment to include (room temperature) pH values 5, 9, and 11. The main source of uncertainty in the pure water radiolysis mechanism below 200°C involves the reduction and oxidation reactions of the  $\cdot\text{O}_2\text{H}/\cdot\text{O}_2^-$  radicals. Ab initio calculations for the reaction of  $\text{H}^\bullet$  atoms with  $\cdot\text{O}_2^-$  demonstrate that either reduction or oxidation may occur, in contradiction of the accepted model which assumes only a reduction of  $\cdot\text{O}_2^-$ . The oxidation can occur by production of a hydride ion intermediate,  $(\text{H}^-)_{\text{aq}}$ . This change in mechanism helps greatly to account for the neutral pH observations, but does not account for the very large  $\text{H}_2$  and  $\text{O}_2$  production found at pH 11. At this pH only the reaction of  $(e^-)_{\text{aq}}$  with  $\cdot\text{O}_2^-$  is both important and unmeasured. We tentatively conclude from our

modeling that an oxidation of  $\cdot\text{O}_2^-$  by  $(e^-)_{\text{aq}}$  is the only reaction that can explain our observations, i.e.  $(e^-)_{\text{aq}} + \cdot\text{O}_2^- \Rightarrow \text{O}_2 + \text{H}_2 + \text{OH}^-$ . Presumably a "dielectron" intermediate would be invoked to explain this process. Radiolysis experiments are in progress to measure both the reaction rate and the product of the reaction vs. temperature. We expect to report the results at the next CPIMS meeting.

Following our recent studies on vibrational characterization of  $\cdot\text{OH}$  radical adducts to halides and pseudohalides, we revisited the very important equilibrium formation of  $\text{ClOH}^\cdot$  in water. This equilibrium is foundational within the thermochemical network in the IUPAC compilation of inorganic radical standard electrode potentials. Even though the mechanism of OH-induced oxidation of chloride anions has long been explained by the formation of the OH adduct, we were not able to detect its existence using the time resolved resonance Raman (TRRR) method. Conditions of our previous experiments were based on the accepted literature values of the  $\text{Cl}^\cdot + \text{OH}^- \rightleftharpoons \text{ClOH}^\cdot$  equilibrium constant ( $K_{\text{eq}}$ ) and  $\text{ClOH}^\cdot$  extinction coefficient ( $\epsilon$ ). In re-examining this equilibrium we found that reported parameters are incorrect because they were determined with solutions of analytical grade sodium chloride containing minute amounts of  $\text{Br}^-$ . The presence of bromide ion caused formation of  $\text{ClBr}^\cdot$ , strongly absorbing light near 350 nm and obscuring the proper identification and characterization of  $\text{ClOH}^\cdot$ . We found that the equilibrium constant of  $\text{ClOH}^\cdot$  formation and the extinction coefficient of  $\text{ClOH}^\cdot$  are both almost 3 times lower than previously reported i.e.  $K_{\text{eq}} \sim 0.25 \text{ M}^{-1}$  and  $\epsilon \sim 1200 \text{ M}^{-1} \text{ cm}^{-1}$ , respectively. Linear dependence on  $K_{\text{eq}}$  and quadratic dependence on  $\epsilon$  of resonance Raman intensity will have resulted in almost 30 times smaller signal than expected, and may explain why we were not able to detect  $\text{ClOH}^\cdot$  with TRRR. The lower  $K_{\text{eq}}$  value also implies that the rate constant for  $\cdot\text{OH}$  addition to  $\text{Cl}^-$  has been previously underestimated by three times and should lie in the range of  $\sim 1.2 \times 10^{10} \text{ M}^{-1} \text{ s}^{-1}$ , similar to those of  $\cdot\text{OH}$  reaction with other halides and pseudohalides. In the temperature range 5-30°C formation of  $\text{ClOH}^\cdot$  is exothermic with enthalpy of  $-12.2 \text{ kJ mol}^{-1}$  and entropy  $-52.7 \text{ J mol}^{-1} \text{ K}^{-1}$ , respectively. Interestingly, above 30°C the Van't Hoff plot deviates from linearity, suggesting a temperature dependence of enthalpy and/or entropy of  $\text{ClOH}^\cdot$  formation. Re-evaluation of the thermodynamics of this equilibrium will require re-examination of the reduction potentials for many radicals and transient species, including  $\cdot\text{OH}$ ,  $\text{Cl}^\cdot$ ,  $\text{Cl}_2^\cdot$ ,  $\text{ClOH}^\cdot$ ,  $\text{SO}_4^\cdot$ ,  $\text{NO}_3^\cdot$ ,  $\text{ClO}_3^\cdot$ ,  $\text{Ti}^{3+}$ ,  $\text{Ti}^{2+}$ ,  $\text{TIOH}^+$ , and  $\text{TIOH}^{2+}$ .

Plasma effectiveness and formation of reactive species in a helium atmospheric pressure plasma jet (APPJ) were measured and characterized by molecular probes and optical emission spectroscopy, respectively. These features were studied as a function of several plasma source conditions such as applied voltage, frequency, and admixture of oxygen. Because a plasma species distribution varies at different positions along the discharge due to different gas-phase reactions involved, the relative emission intensities of various plasma species produced in several regions were examined, and possible reaction patterns were proposed. Based on the proposed chemical reactions, the plasma effectiveness for inducing damage to molecular probe was also explained. Moreover, a 2D numerical model that described the gas dynamics and the afterglow chemistry in an APPJ operating in helium with humid air impurity complemented this experimental work.

A high vacuum chamber for Stepwise Electron Spectroscopy (SWES) was recently constructed and successfully used to study radical formation from carbon tetrachloride ( $\text{CCl}_4$ ) at electron

kinetic energies close to 0 eV. At this incident electron energy, dissociative electron attachment (DEA) to CCl<sub>4</sub> leads to formation of only Cl<sup>-</sup> ions, while the other reaction product is presumed to be the trichloromethyl radical (CCl<sub>3</sub>•). Using the SWES technique we could choose a desired combination of the interaction- /acquisition time and the electron energy at each step. Moreover, we are also able to select during which step to perform the detection of specific ionic species. Therefore, by repeating the acquisition scheme for different energies, we measured the yield of CCl<sub>3</sub>• formed as a function of the incident electron energy scanned over the DEA resonance. To verify that CCl<sub>3</sub><sup>+</sup> yield observed in our mass spectra originated solely from the electron ionization of CCl<sub>3</sub>•, we repeated the acquisition scheme for different ionization energies. Based on the usual Wannier fit to the experimental data, the adiabatic ionization energy of CCl<sub>3</sub>• has been determined to be 8.1 ± 0.5 eV. This value appears to be in a very good agreement with previously reported experimentally determined values.

## PUBLICATIONS WITH BES SUPPORT SINCE 2015

- Kanjana K.; Walker J.A.; Bartels D.M. *J. Phys. Chem. A* **2015**, *119*, 1830-7. Hydroxymethyl radical self-recombination in high-temperature water.
- Rumbach P.; Bartels D.M.; Sankaran R.M.; Go D.B. *Nat Commun* **2015**, *6*, 7248. The solvation of electrons by an atmospheric-pressure plasma.
- Rumbach P.; Bartels D.M.; Sankaran R.M.; Go D.B. *J. Phys. D: Appl. Phys.* **2015**, *48*, 424001. The effect of air on solvated electron chemistry at a plasma/liquid interface.
- Kumar A., Walker J.A., Bartels D.M., Sevilla M.D. *J. Phys. Chem. A* **2015**, *119*, 9148-59. A simple *ab initio* model for the hydrated electron that matches experiment.
- Janik I., Marin T.W. *Rev Sci Instr.* **2015**, *86*, 015102. Design of an ultrashort optical transmission cell for vacuum ultraviolet spectroscopy of supercritical fluids.
- Arjunan K.P., Sharma V.K., Ptasińska S. *Int. J. Mol. Sci.* **2015**, *16*, 2971-3016. Effects of atmospheric pressure plasmas on isolated and cellular DNA – a review.
- Kanjana K.; Courtin B.; MacConnell A.; Bartels D.M. *J. Phys. Chem. A* **2015**, *119*, 11094-104. Reactions of hexa-aquo transition metal ions with the hydrated electron up to 300 degrees C.
- Dawley M.M.; Tanzer K.; Carmichael I.; Denifl S.; Ptasińska S. *J. Chem. Phys.* **2015**, *142*, 21501. Dissociative electron attachment to the gas-phase nucleobase hypoxanthine.
- Sterniczuk M.; Bartels D.M. *J. Phys. Chem. A* **2016**, *120*, 200-9. Source of molecular hydrogen in high-temperature water radiolysis.
- Sterniczuk M.; Yakabuskie P.A.; Wren J.C.; Jacob J.A.; Bartels D.M. *Radiat. Phys. Chem.* **2016**, *121*, 35-42. Low LET radiolysis escape yields for reducing radicals and H<sub>2</sub> in pressurized high temperature water.
- Walker J.A.; Mezyk S.P.; Roduner E.; Bartels D.M. *The Journal of Physical Chemistry B* **2016**, *120*, 1771-9. Isotope dependence and quantum effects on atomic hydrogen diffusion in liquid water.
- Janik I.; Tripathi G.N.R. *J. Chem. Phys.* **2016**, *144*, 154307-7. The nature of CO<sub>2</sub><sup>-</sup> radical anion in water.
- Huang W.; Ptasińska S. *Appl. Surf. Sci.* **2016**, *367*, 160-6. Functionalization of graphene by atmospheric pressure plasma jet in air or H<sub>2</sub>O<sub>2</sub> environments.
- Adhikari E.; Ptasińska S. *Eur. Phys. J. D* **2016**, *70*, 180-7. Correlation between plasma induced DNA damage level and helium atmospheric pressure plasma jet (APPJ) variables.
- Arjunan K.; Obrusnik A.; Jones B.; Zajickova L.; Ptasińska S. *Plasma Proc. and Polym.* **2016** *13*, 1089-105. Effect of additive oxygen on the reactive species profile and microbicidal property of a helium atmospheric pressure plasma jet.
- Marin T.M., Janik I., Bartels D.M., Chipman D.M., *Nat. Commun.* **2017**, *8*, 15435. Vacuum ultraviolet spectroscopy of the lowest-lying electronic state in subcritical and supercritical Water.

- Janik I., Carmichael I., Tripathi G.N.R., *J. Chem. Phys.*, **2017**, *146*, 214305. Transient Raman spectra, structure and thermochemistry of the thiocyanate dimer radical anion in water.
- Sargent, L., Sterniczuk, M., Bartels, D.M., *Radiat. Phys. Chem.* **2017**, *135*, 18-22. Reaction rate of H atoms with N<sub>2</sub>O in hot water.
- A Ribar, K Fink, Z Li, S Ptasińska, I Carmichael, L Feketeová, S Denifl. *Phys. Chem. Chem. Phys.* **2017**, *19*, 6406-6415. Stripping off hydrogens in imidazole triggered by the attachment of a single electron.
- Z. Li, A.R. Milosavljević, I. Carmichael, S. Ptasińska. *Phys. Rev. Lett.*, **2017**, *119*, 053402. Direct Observation and Characterization of Neutral Radicals from a Dissociative Electron Attachment Process.
- J. Gorfinkiel, S. Ptasińska. *Journal of Physics B: Atomic, Molecular, Optical Physics*, **2017**, *50*, 182001. Electron scattering from molecules and molecular aggregates of biological relevance.
- M. Ryszka, E. Alizadeh, Z. Li, S. Ptasińska. *J. Chem. Phys.* **2017**, *147*, 094303. Low-energy electron-induced dissociation in gas-phase nicotine, pyridine, and methyl-pyrrolidine.

## Pulse Radiolysis used to study conjugation, entropy, and charge escape

Principal Investigators: Andrew R. Cook, Matthew J. Bird and John R. Miller  
Department of Chemistry, Brookhaven National Laboratory, Upton, NY, 11973 USA  
acook@bnl.gov, mbird@bnl.gov, jrmiller@bnl.gov

### Program Scope:

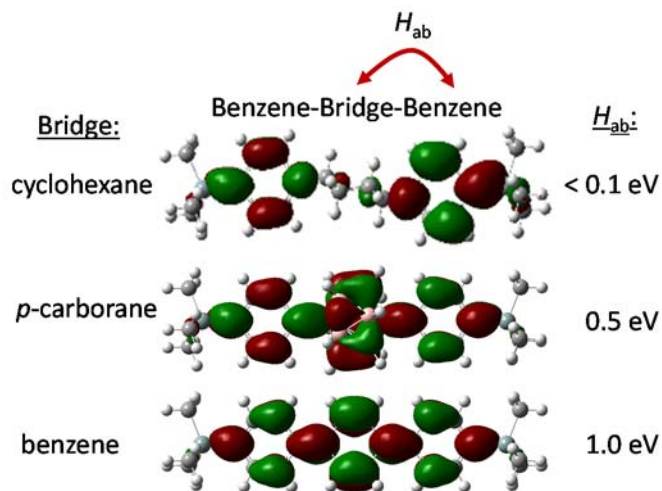
This program applies both photoexcitation and ionization by short pulses of fast electrons to investigate fundamental chemical problems relevant to the production and efficient use of energy and thus obtain unique insights not attainable with other techniques. These studies may play an important role in the development of safer, more effective, and environmentally beneficial processes for the chemical conversion of solar energy. Picosecond pulse radiolysis at the Laser Electron Accelerator Facility (LEAF) is employed to generate and study reactive chemical intermediates or other non-equilibrium states of matter in ways that are complementary to photolysis and electrochemistry and often uniquely accessible by radiolysis. This program also develops new tools for such investigations, applies them to chemical questions, and makes them available to the research community. Advanced experimental capabilities, such as Optical Fiber Single-Shot detection system (OFSS), allow us to work on fascinating systems with 5-10 ps time-resolution that were previously prohibitive for technical reasons.

### Recent Progress:

**Carborane Conjugation.** Carboranes are known for multicenter-multielectron bonding that leads to internal “3D aromaticity”. Despite this, the literature contains many reports where carboranes are incorporated into  $\pi$ -conjugated polymers where excited states are found not to delocalize onto or across them. A conclusion is that they are insulators, supported by being hard to oxidize or reduce. Previous experimental results determined spectra of radical anions of *p*-closo-carboranes ( $C_2B_{10}H_{12}$ , [12]) attached at the carbon termini to either phenyl-TMS ([6]) groups or other [12] units. We have analyzed this data in terms of Robinson-Day optical electron transfer (OET) absorption bands, allowing determination of both reorganization energies,  $\lambda$ , and electronic couplings,  $H_{ab}$ . Key findings follow:

1) In [6-12-6], the excess electron is *delocalized* across the entire molecule displaying a class III OET band. Such a transition through a carborane is unprecedented. It shows that carborane bridges are not simply electron withdrawing insulators, but rather have a radical anion energy similar to that of benzene<sup>-</sup>, are strongly bonded. Analysis of experimental results gives an electronic coupling,  $H_{ab}$ , between [12] and [6] units of  $\sim 0.5$  eV. We find similar coupling between two axially bonded [12] units.

Computations(B3LYP/D95\*/SCRF(THF)) furthermore place the magnitude of coupling midway between that for

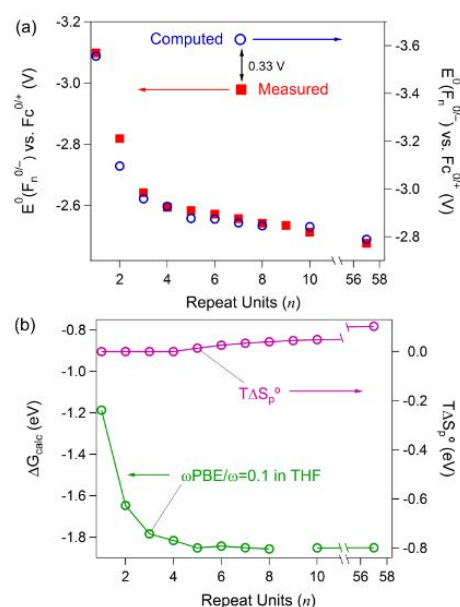


similarly sized fully saturated and  $\pi$ -conjugated spacers. The figure shows the corresponding computed delocalized HOMO orbitals.

2) When more than  $\sim 0.5$  of an excess electron is on a [12] unit, it distorts substantially, leading to class II OET bands. These distortions increase a single carbon-boron distance to  $\sim 2.4$  Å, to make an open or partially-nido structure. This does not change the strong  $H_{ab}$  determined, but results in a large reorganization energy for the optical transitions,  $> 2.5$  eV.

3) A clear conclusion is that for excess electrons, *p*-carborane can be an effective spacer for transmitting charge in molecular wires, in contrast to reports for excited states. Computational results suggest an *advantage* as well: because of the 5-fold axial symmetry of the HOMO in the carborane, there is *no loss* of electronic coupling when it rotates relative to the  $\pi$ -system, adding the ability to build some flexibility into molecules. By comparison,  $H_{ab}$  between the rings in poly-phenyl conjugated polymer radical anions drops rapidly as the rings become non-coplanar, and can drop to zero when the dihedral angle is 90 degrees.

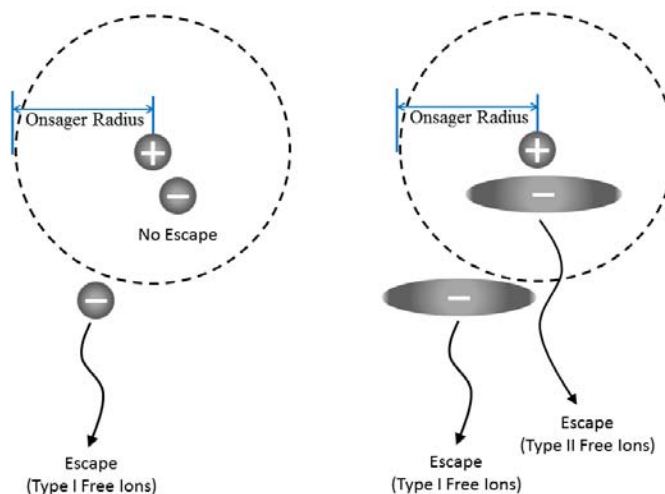
**Positional Entropy in Conjugated Molecules.**<sup>6</sup> Energetic properties of conjugated polymers are often “fit” with an empirical function of length, relating changing oligomer to ultimate polymer properties. Convergence at  $n$  repeat units is taken as a measure of polaron delocalization length,  $n_D$ . These functions were inspired by the description of a particle in a one dimensional box. Careful measurements of reduction potentials and triplet energies in our lab and others reveal that these properties do not stop shifting at some length, but continue to change as chains get longer. Redox potential determinations from our lab for oligo- and poly-fluorenes is shown in the figure, showing rapid changes at short length, but continued slow changes at long ones. This work explored and verified the hypothesis that entropy, predictable from the properties of the polarons, was responsible changes at long lengths. Results were compared to computations and a model of chain entropy, and are consistent with the idea that polaron energies do not change with lengths greater than  $n_D$ , but their free energies do. This constitutes a new picture that replaces a paradigm of empirical fits, without a clear physical origin. Now the physical origin is entropy described quantitatively by a simple model. Results further give a clear definition for  $n_D$ , also previously only inferred from when trends in properties appeared to stop shifting. Similar results were found for free energies for formation of triplet excited states obtained by equilibria; although triplet energies obtained by spectroscopy are expected to behave differently.



**Can charge delocalization enhance escape?** Many ions formed following pulse radiolysis are thermalized within the Onsager distance of each other. The fraction depends on the nature of the solvent and its dielectric constant. Most of these recombine, though this process is not fully understood. In ethers, and many other solvents, the initial radical cations fragment to produce solvated protons, which when they recombine with an anion, often neutralize the charge by proton transfer. Geminate recombination of 24 radical anions ( $M\bullet^-$ ) with solvated protons ( $RH_2^+$ ) was studied in tetrahydrofuran (THF) with pulse radiolysis. For all molecules protonated on O or N atom, the subsequent PT step is too fast ( $< 0.2$  ns) to measure, except for

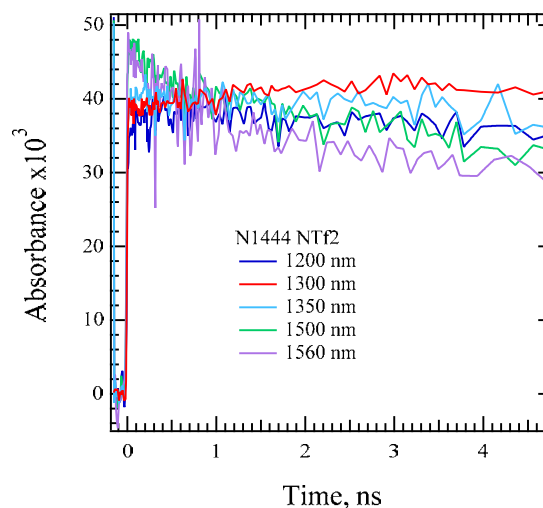
the anion of TCNE which did not undergo proton transfer. PT to C atoms was as slow as 70 ns and was always slow enough to be observable. While the free energy to protonate O, N, and C atoms is large, -1 to -2 eV, the difference in rate is understood in terms of a much larger reorganization energy required for the structural changes necessary to protonate a C atom compared to simply adding to the lone pairs of O or N.

For 21 of the 24 molecules studied here, a free ion yield of  $71.6 \pm 6.2$  nmol/J was formed. This yield of “Type I” free ions (figure, left side) is independent of the PT rate because it arises entirely by escape from the initial distribution of ion pair distances without forming intimate ion pairs. Three anions of oligo(9,9-dihexyl)fluorenes,  $\text{Fn}^{\bullet-}$  ( $n=2-4$ ) were able to escape from intimate ion-pairs to form additional yields “Type II” of free ions with escape rate constants near  $3 \times 10^6 \text{ s}^{-1}$ . Low charge density in the delocalized anions is essential for a substantial yield of these “Type II” free ions formed by escape from intimate pairs (figure, right side). The observed enhancement of escape of ion pairs to form free ions could be important an important principle in organic solar cells.



**OFSS:** The Optical Fiber Single-Shot detection system saw a major upgrade this year. This system provides a unique ability to study dynamics following pulse radiolysis at LEAF with a time resolution determined only by the electron pulse width ( $\sim 10$  ps). Full kinetic traces are collected in a single shot, enabling studies in samples that are available in only minute quantity, as well as those that cannot be flowed, for example solids and ionic liquids. InGaAs detectors were added as well as computer controlled focusing. The improved system can now probe samples throughout the visible to the NIR,  $\sim 1600$  nm. Note that this system, as well as others at LEAF, are available for use by outside collaborative users.

An early application of the new NIR capability was to begin to measure solvation dynamics of electrons ejected during pulse radiolysis in a wide range of structurally diverse viscous ionic liquids, in collaboration with Jim Wishart (please see his abstract). Preliminary results for one liquid are shown in the figure. The differences in the shape of the traces with wavelength result from a spectral shift as the excess electron solvates. Results inform on the different timescales for relaxation exhibited by the microscopically varied structures of different ionic liquids.



### Future Plans:

Previous work reported for the first time ultrafast (< 10ps) capture of holes following pulse radiolysis, which we have attributed to capture of holes before they are solvated. Work will seek to understand the mechanism by which this occurs. We will explore different media, spanning alkanes, ethers, nitriles, and possibly alcohols. Data suggest that pre-solvated hole capture may be possible in solids. This may provide a way to study charge transport on conjugated polymers in dilute solid matrices, and make comparisons to measurements in solution. Another question will focus on energetics – can capture of pre-solvated holes produce radical cations of solutes with higher IP than can diffusion of solvated holes? A consequence to be further explored is that capture of pre-solvated holes in certain cases appears to result in large amounts of both singlet and triplet solute excited states, produced following rapid recombination.

A relatively new program determines redox potentials without electrolyte by measuring equilibria among transiently created radical ions. This is important because redox potentials supply us energetic information for a variety of molecularly-based solar cells as well as for photosynthesis, but those energy converting systems do not contain the ~100 mM of electrolyte needed for electrochemical measurement of redox potentials. The electrolyte alters the potentials, but by how much. This question can be answered by creating radical ions with pulse radiolysis. A set of new experimental methods is underway.<sup>7</sup>

### Publications of DOE sponsored research that have appeared in the last 2 years:

1. Craig, P. R.; Havlas, Z.; Trujillo, M.; Rempala, P.; Kirby, J. P.; Miller, J. R.; Noll, B. C.; Michl, J. "Electronic Spectra of the Tetraphenylcyclobutadienecyclopentadienylnickel(II) Cation and Radical" *J. Phys. Chem. A* 2016, *120*, 3456-3462. doi:10.1021/acs.jpca.6b00648.
2. Hack, J.; Grills, D. C.; Miller, J. R.; Mani, T. "Identification of Ion-Pair Structures in Solution by Vibrational Stark Effects", *J. Phys. Chem. B* 2016, *120*, 1149-1157. doi:10.1021/acs.jpcc.5b11893.
3. Mezyk, S. P.; Horne, G. P.; Mincher, B. J.; Zalupski, P. R.; Cook, A. R.; Wishart, J. F. In *Atalante 2016 International Conference on Nuclear Chemistry for Sustainable Fuel Cycles*; Poinssot, C., Bourg, S., Eds.; Elsevier Science Bv: Amsterdam, 2016; Vol. 21, p 61-65. doi:10.1016/j.proche.2016.10.e09.
4. Wu, Q.; Zaikowski, L.; Kaur, P.; Asaoka, S.; Gelfond, C.; Miller, J. R. Multiply Reduced Oligofluorenes: Their Nature and Pairing with THF-Solvated Sodium Ions, *J. Phys. Chem. C* 2016, *120*, 16489-16499. doi:10.1021/acs.jpcc.6b05115.
5. Bird, M. J.; Bakalis, J.; Asaoka, S.; Siringhaus, H.; Miller, J. R. Fast Holes, Slow Electrons, and Medium Control of Polaron Size and Mobility in the DA Polymer F8BT, *J. Phys. Chem. C* 2017, *121*, 15597-15609. doi:10.1021/acs.jpcc.7b04602.
6. Chen, H. C.; Sreearunotha, P.; Cook, A. R.; Asaoka, S.; Wu, Q.; Miller, J. R. Chain Length Dependence of Energies of Electron and Triplet Polarons in Oligofluorenes, *J. Phys. Chem. C* 2017, *121*, 5959-5967. doi:10.1021/acs.jpcc.7b00099.
7. Matthew J Bird, Tomokazu Iyoda, Nicholas Bonura, Jin Bakalis, Abram Ledbetter, and John R Miller. "Effects of Electrolytes on Redox Potentials Through Ion Pairing", *Journal of Electroanalytical Chemistry* (accepted Sept 2017) Ms. No.: JELECHEM-D-17-00795R1.

## Radiation Chemical Impacts on Nuclear Power

Jay A. LaVerne and David M. Bartels

Notre Dame Radiation Laboratory, University of Notre Dame, Notre Dame, IN 46556

[laverne.1@nd.edu](mailto:laverne.1@nd.edu), [bartels.5@nd.edu](mailto:bartels.5@nd.edu)

### Program Scope

*A fundamental approach to the radiation chemistry associated with the nuclear power industry is being used to help maintain the present reactor fleet and to address concerns in the development of the next generation of nuclear power reactors. This program is an extension of studies on fundamental radiation chemical effects in homogeneous media that have been and continue to be a major effort at the NDRL. The extensive knowledge obtained for water, aqueous solutions, and organic liquids is being expanded to more directly address specific needs in the nuclear power industry. The program probes reactor water chemistry at operating conditions of BWR and PWR reactors, as well as the radiation chemistry at the molecular level occurring on interfaces. Development of newer separation systems that are more efficient and economic are being aided by fundamental studies on the organic separation media as well as the aqueous phases containing the high concentration of salts commonly associated with these systems. A variety of materials currently encountered in the storage of radioactive materials are being examined for their radiation stability and for their potential production of hazardous gaseous that may compromise the safety and security of these systems. As reflected in the publications, this program has evolved from that termed "Interfacial Radiation Sciences" which included contributions from Sylwia Ptasinska at the NDRL.*

### Recent Progress and Future Plans

Oxidation of reactor components by species produced in the radiolysis of the water coolant is the leading cause of their shortened lifetime and ultimate failure. While the OH radical is the more oxidizing species, H<sub>2</sub>O<sub>2</sub> is of more concern because of its mobility, longevity and ability to induce reactions at interfaces. The nuclear industry commonly employs the addition of H<sub>2</sub> in order to suppress the combination reactions of OH radicals to form H<sub>2</sub>O<sub>2</sub>. The presence of H<sub>2</sub> leads to a chain reaction that will eliminate all H<sub>2</sub>O<sub>2</sub> as long as there is an excess of H<sub>2</sub>. However, too much H<sub>2</sub> can cause embrittlement of reactor components and the values for excess H<sub>2</sub> are not known. Continuous radiolysis is found to lead to a steady-state concentration of H<sub>2</sub>O<sub>2</sub> that is proportional to its initial concentration, but there is no *a priori* method for estimating this steady-state concentration. Variation in dose rate has little effect on this steady state-value, which is surprising since models studies have long shown that the yield of H<sub>2</sub>O<sub>2</sub> should increase with increasing dose rate. The addition of H<sub>2</sub> to aqueous solutions of H<sub>2</sub>O<sub>2</sub> leads to a decrease in the high dose limiting concentration of H<sub>2</sub>O<sub>2</sub> that is linear with the initial H<sub>2</sub> concentration, but the amount of this decrease is not stoichiometric with respect to the amount of H<sub>2</sub> initially present. The variety of experiments that have been performed on this system have not lead to any clearer understanding of the complex chemistry responsible for the main chain reaction and all of the secondary reactions. More studies with selective radical scavengers will be employed to piece out their relative contributions and high LET radiolysis will be performed. An extensive deterministic modeling effort is currently underway to help elucidate the underlying mechanisms involved in these systems.

Systems for the separation of various metals from radioactive wastes are often mixed aqueous-organic phases in which the element of choice is dissolved in a concentrated nitric acid solution and then extracted into an organic liquid phase using selective ligands. Most of the systems were developed decades ago and they can be very expensive and often they are not very efficient. In order to facilitate the development of a variety of new ligands, an examination of the various components expected to be encountered in separation systems has been initiated. All separation systems begin by dissolving the metals of interest in aqueous solutions with very high (up to 6M) nitrate concentrations. Nitrites formed from the radiolytically induced dissociation of the nitrates have been suggested to interfere with many of the ligands currently in use and for several of those proposed for future use. A comprehensive examination of the formation of nitrites from nitrates has been undertaken. Radiolysis of nitrate solutions of 1 mM up to 1 M show that the production of nitrite is not linear with dose up to at least 1 kGy. At concentrations above 1 M nitrate the production of nitrite becomes linear with dose. Very little difference is observed for both aerated and deaerated solutions at very low or very high nitrate concentrations. The main reaction of nitrate is with the hydrated electron, and the competition of hydrated electrons with oxygen should be more effective than that with nitrate at the lower concentrations of the latter. Clearly there are a variety of competing reactions that are very dependent on nitrate concentration. At lower nitrate concentration the reactions of intermediates with OH radicals can occur leading to a steady state concentration of nitrite. At high nitrate concentrations the hydrated electron is quickly and completely scavenged so no further reactions of this species can occur. The exact mechanism is not understood, but stochastic track model calculations are currently underway. Further experiments will explore the results with high nitric acid concentrations and at high LET.

The recent accident at Fukushima has led to a renewed interest in the radiolysis of aqueous solutions of highly concentrated chlorides and bromides. The halides are found to thermally react with H<sub>2</sub>O<sub>2</sub> with chloride being more reactive than bromide. Radiolysis greatly increases the rate of loss of H<sub>2</sub>O<sub>2</sub> from such solutions. The reactions of OH radicals with chloride and bromide anions is well known to give an adduct that decomposes to yield the chlorine or bromine atom, respectively. Interestingly, the overall concentration of bromide does not change with increasing dose even though sufficient OH radicals have been formed to deplete the halide many times over. Presumably the hydrated electron is reducing any stable bromine species back to bromide. Aerated solutions show the same result, so the O<sub>2</sub><sup>-</sup> produced by the reaction of the hydrated electron with oxygen can also reduce bromine species to bromide. Further work will use other hydrated electron scavengers such as nitrous oxide to stop the back reduction process. The variation of other water products such as H<sub>2</sub> and H<sub>2</sub>O<sub>2</sub> will be examined as a function of halide concentration in order to better understand the mechanisms driving these systems.

#### **Publications with BES support (2015-2017)**

- J. Schofield, J. A. La Verne, D. Robertson, P. Collon and S. M. Pimblott (2017) "Material Dependence on the Mean Charge State of Light Ions in Titanium, Zirconium and copper", **Physical Chemistry Chemical Physics** *submitted*.
- S. C. Reiff and J. A. LaVerne (2017) "Radiolysis of water with aluminum oxide surfaces", **Radiation Physics and Chemistry** *131*, 46-50.
- D. Poster, M. Postek, A. Vldar, M. Driscoll, J. LaVerne, Z. Tsinas and M. Al-Sheikhly (2017) "Radiation Processing and its Potential in Advancing Biorefining and Nanocellulose Composite Materials Manufacturing", **Radiation Physics and Chemistry** *submitted*.

- J. A. LaVerne and S. R. Kleemola (2017) "Hydrogen Production in the Radiolysis of Dodecane and Hexane", **Solvent Extraction and Ion Exchange** 35, 210-220.
- J. A. La Verne, N. A. I. Tratnik and A. Sasgen (2017) "Gas Production in the Radiolysis of Poly(dimethylsiloxanes)", **Radiation Physics and Chemistry** *in press*.
- K. Iwamatsu and J. A. La Verne (2017) "Hydrogen Peroxide Kinetics in Water Radioysis", **Radiation Physics and Chemistry** *submitted*.
- G. P. Horne, S. M. Pimblott and J. A. LaVerne (2017) "Inhibition of Radiolytic Molecular Hydrogen Formation by Quenching of Excited State Water", **Journal of Physical Chemistry B** 121, 5385-5390.
- S. Feister, D. R. Austin, J. T. Morrison, K. D. Frische, C. Orban, G. Ngirmang, A. Handler, J. A. La Verne, E. A. Chowdhury and W. M. Roquemore (2017) "Relativistic Electron Acceleration by mJ-class kHz Lasers Normally Incident on Liquid Targets", **Optics Express** *in press*.
- X. Zhang and S. Ptasińska (2016) "Heterogeneous oxygen-containing species formed via oxygen or water dissociative adsorption onto a gallium phosphide surface", **Top. Catal.** 59, 564-573.
- X. Zhang and S. Ptasińska (2016) "High pressure induced pseudo-oxidation of copper surface by carbon monoxide", **ChemCatChem** 8, 1632-1635.
- X. Zhang and S. Ptasińska (2016) "Electronic and chemical structure of the H<sub>2</sub>O/GaN(0001) interface under ambient conditions", **Sci. Rep.** 6, 24848.
- J. Schofield, S. C. Reiff, S. M. Pimblott and J. A. La Verne (2016) "Radiolytic hydrogen generation at silicon carbide - water interfaces", **Journal of Nuclear Materials** 469, 43-50.
- T. X. T. Sayle, F. Caddeo, T. Sakthivel, S. Das, S. Seal, X. Zhang and S. Ptasińska (2016) "Structure-activity of ceria nanoparticles, nanocubes and mesoporous architectures", **Chem. Mater.** 28, 7287-7295.
- A. R. Milosavljevic, W. Huang, S. Sadhu and S. Ptasińska (2016) "Low-energy electron-induced degradation of organolead halide perovskite", **Angew. Chem. Int. Ed.** 55, 10083-10087.
- W. Huang, J. Manser, S. Sadhu, P. V. Kamat and S. Ptasińska (2016) "Direct observation of reversible transformation of CH<sub>3</sub>NH<sub>3</sub>PbI<sub>3</sub> and NH<sub>4</sub>PbI<sub>3</sub> induced by polar gaseous molecules", **J. Phys. Chem. Lett.** 7, 5068-5073.
- W. Huang, J. Manser, P. V. Kamat and S. Ptasińska (2016) "Evolution of chemical composition, morphology, and photovoltaic efficiency of CH<sub>3</sub>NH<sub>3</sub>PbI<sub>3</sub> perovskite under ambient conditions", **Chem. Mater.** 28, 303-311.
- X. Zhang and S. Ptasińska (2015) "Distinct and dramatic water dissociation on GaP (111) tracked by near ambient pressure XPS", **Phys. Chem. Chem. Phys.** 17, 3909-3918.
- X. Zhang and S. Ptasińska (2015) "Evolution of surface-assisted oxidation of GaAs (100) by gas-phase N<sub>2</sub>O, NO, and O<sub>2</sub> under near-ambient pressure conditions", **J. Phys. Chem. C** 119, 262-270.
- S. C. Reiff and J. A. La Verne (2015) "Radiation-Induced Chemical Changes to Iron Oxides", **Journal of Physical Chemistry B** 119, 7358-7365.
- S. C. Reiff and J. A. La Verne (2015) "Gamma and He Ion Radiolysis of Copper Oxides", **Journal of Physical Chemistry C** 119, 8821-8828.

- J. Ma, J. A. LaVerne and M. Mostafavi (2015) "Scavenging the Water Cation in Concentrated Acidic Solutions", **Journal of Physical Chemistry A** *119*, 10629-10636.
- L. Leay, W. Bower, G. Horne, P. Wady, A. Baidak, M. Pottinger, M. Nancekievill, A. D. Smith, S. Watson, P. R. Green, B. Lennox, J. A. LaVerne and S. M. Pimblott (2015) "Development of Irradiation Capabilities to Address the Challenges of the Nuclear Industry", **Nuclear Instruments & Methods in Physics Research Section B-Beam Interactions with Materials and Atoms** *343*, 62-69.

## Solution Reactivity and Mechanisms through Pulse Radiolysis

Sergei V. Lymar

Chemistry Department, Brookhaven National Laboratory, Upton, NY 11973-5000

e-mail: lymar@bnl.gov

### Scope

This program applies pulse radiolysis and complementary time-resolved techniques for investigating reactive intermediates and inorganic reaction mechanisms. The specific systems are selected based on their fundamental significance or importance in energy and environmental problems.

The first project investigates physical chemistry of nitrogen oxides and their congeneric oxoacids and oxoanions. These species play an essential role in environmental chemistry, particularly in the terrestrial nitrogen cycle, pollution, bioremediation, and ozone depletion. Nitrogen-oxygen intermediates are also central to the radiation-induced reactions that occur in nuclear fuel processing and within attendant nuclear waste. Equally important are the biochemical roles of nitrogen oxides. We apply time-resolved techniques for elucidation of the prospective reactions in terms of their thermodynamics, rates and mechanisms.

The second project deals with radiation chemistry in polar aprotic solvents. Due to their solubilizing properties, low nucleophilicity, and large electrochemical window, these solvents are widely used in mechanistic studies relevant to redox catalysis. Recently, we have shown that pulse radiolysis, particularly combined with time-resolved infrared detection (TRIR), is a powerful technique for gaining mechanistic insights into the dynamics of redox catalysis in polar aprotic solvents through probing normally inaccessible catalysts' oxidation states. However, this research is hampered by insufficient understanding of primary radiolysis species in these solvents and by the deficiency of methods for directing their reactivity toward generating strong reductants or oxidants that can be used for initiating useful redox chemistry. Our current work focuses on acetonitrile, which is our solvent of choice for a number of planned TRIR mechanistic studies.

The goal of the third project has been to gain mechanistic insight into proton coupled electron transfer (PCET). These reactions, which involve an overall transfer of a proton and an electron, play an important role in natural and artificial photosynthetic transformations providing low energy pathways in charge separation, charge transport and redox catalysis. In this project, we apply time-resolved techniques to investigate the reaction rates dependencies upon the driving force. When combined with the computational thermodynamic analysis, such an approach provides information that is critical for distinguishing between alternative stepwise and concerted PCET pathways and evaluating the influence of solvent properties on the PCET mechanisms.

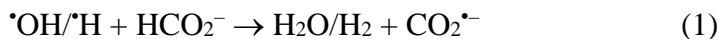
This abstract summarizes recent results from the last two projects; the first project was presented in detail at the 2014 CPIMS meeting.

Collaborators on these projects include M. Valiev (PNNL),<sup>1</sup> J. Hurst (WSU, emeritus),<sup>2-5</sup> D. Polyansky (BNL),<sup>4</sup> M. Ertem (BNL),<sup>6</sup> and D. Grills (BNL).<sup>7</sup>

### Recent progress

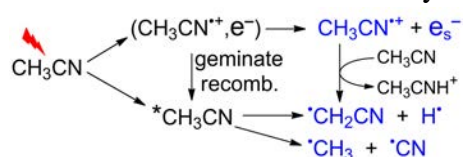
*CO<sub>2</sub><sup>•-</sup> Radical in Acetonitrile.* (with David C. Grills, BNL) Carbon dioxide radical anion (CO<sub>2</sub><sup>•-</sup>) is a powerful reductant ( $E^{\circ}(\text{CO}_2/\text{CO}_2^{\bullet-}) = -1.90 \text{ V vs NHE in H}_2\text{O}^{8-9}$ ). In aqueous pulse radiolysis, a common strategy to generate overall reducing conditions is to add formate anion

( $\text{HCO}_2^-$ ), resulting in the scavenging of  $\cdot\text{OH}$  and  $\cdot\text{H}$  radicals via H-atom transfer and the production of  $\text{CO}_2^{\cdot-}$ ; that is,



Recently, there has been increasing interest in organic solvents as media for pulse radiolysis. We are particularly interested in acetonitrile ( $\text{CH}_3\text{CN}$ ) as a solvent for mechanistic investigations of  $\text{CO}_2$  reduction catalysts using our recently-developed technique of pulse radiolysis combined with nanosecond time-resolved infrared spectroscopy (PR-TRIR).<sup>7</sup> Compared with water, much less is known about the identity and reactivity of the primary radiolysis products in  $\text{CH}_3\text{CN}$ .

However, product analysis studies<sup>10-11</sup> clearly identify fragmentation as the predominant radiation-induced process in MeCN, whereby a variety of solvent-derived radicals are produced as shown in the scheme to the left.



It was previously proposed<sup>12</sup> that the addition of  $\text{HCO}_2^-$  to  $\text{CH}_3\text{CN}$  results in the  $\text{CO}_2^{\cdot-}$  generation through H-atom abstraction from  $\text{HCO}_2^-$  by the radiolytically-generated  $\cdot\text{CH}_2\text{CN}$  radical; that is, a reaction analogous to eq 1



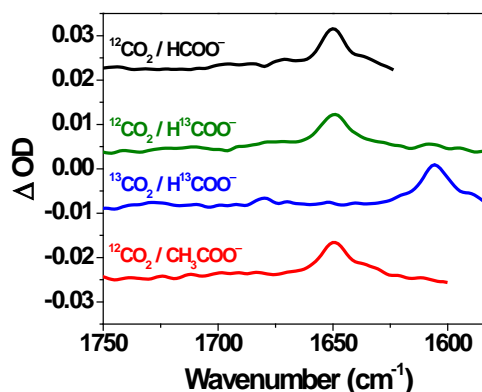
More recently we presented data that could be interpreted as a support for such reactivity.<sup>7</sup>

Another pathway for the radiolytic formation of  $\text{CO}_2^{\cdot-}$  in  $\text{CH}_3\text{CN}$ , which will be important in investigating  $\text{CO}_2$  reduction catalysts, is the direct reduction of dissolved  $\text{CO}_2$  by the solvated electrons; that is,



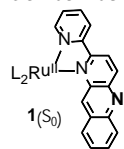
However, to the best of our knowledge, the  $\text{CO}_2^{\cdot-}$  radical has never been spectroscopically characterized or monitored in  $\text{CH}_3\text{CN}$  solution.

We have taken advantage of the structural specificity of the PR-TRIR technique to probe the generation of  $\text{CO}_2^{\cdot-}$  by both of the abovementioned pathways. The  $\text{CO}_2^{\cdot-}$  radical was found to absorb at  $1650\text{ cm}^{-1}$  (Figure to the right). Experiments with various combinations of unlabeled and  $^{13}\text{C}$ -labeled  $\text{CO}_2$  and  $\text{HCO}_2^-$  allowed us to unravel the contributions of the two pathways (eq. 2 and 3) into  $\text{CO}_2^{\cdot-}$  formation. Our results indicate that formate predominantly acts to boost the yield of  $\text{CO}_2^{\cdot-}$  from  $e_s^-$  (eq. 3). We conjecture that this occurs through  $\text{HCO}_2^-$  serving as a base that scavenges protons released during the solvent ionization, which helps to suppress the electron-proton geminate recombination thereby enhancing the  $e_s^-$  yield. The formation of  $\text{CO}_2^{\cdot-}$  from  $\text{HCO}_2^-$  through H-atom abstraction by solvent radicals is a minor pathway. From literature,<sup>8-9,13</sup> we estimate  $BDE(\text{H}-\text{CO}_2^-) \approx 92\text{ kcal/mol}$ . Because  $BDE(\text{H}-\text{CH}_2\text{CN})$  is  $\sim 97\text{ kcal/mol}$ , such a reaction is thermodynamically feasible, but its small driving force makes it rather slow and inefficient.

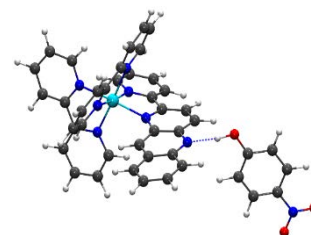


TRIR spectra recorded immediately after pulse radiolysis of  $\text{CD}_3\text{CN}$  containing various combinations of  $^{12}\text{CO}_2$ ,  $^{13}\text{CO}_2$ ,  $\text{HCO}_2^-$ ,  $\text{H}^{13}\text{CO}_2^-$ , and acetate.

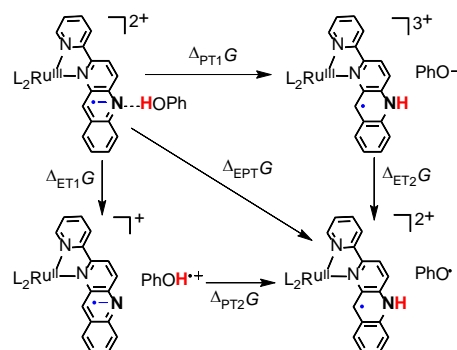
*Proton-Coupled Electron Transfer.*<sup>6</sup> (with Dmitry Polyansky and Mehmed Ertem, BNL) Photoexcitation of the polypyridine Ru(II) complex whose structure is shown to the left (L = bipyridine) leads to the triplet (T<sub>1</sub>) excited state, in which the electron is transferred from the Ru(II) center to the azaacridine ligand. This increases both the complex reduction potential (by 1.70 V) and Brønsted basicity of the ligand (by 4.5 pK<sub>a</sub> units). Through a combination of pulse radiolysis and flash photolysis experiments, we have shown that the complex in its T<sub>1</sub> is capable of oxidizing a variety of *para*-substituted phenols, that is,



Although formally this reaction amounts to hydrogen atom transfer, mechanistically it constitutes PCET because the electron goes to the Ru center and the proton is accepted by the ligand's N atom. This reaction exhibits negative activation energy, which is a clear indication that a precursor complex is formed between **1**(T<sub>1</sub>) and R-PhOH. Computational data strongly suggest that this complex is due to the hydrogen bonding interaction between the ligand's N atom and phenol's OH group, as shown to the right for *para*-nitrophenol. This result emphasizes the critical role that hydrogen bonding plays in PCET reactions in general.



To gain a deeper mechanistic insight into reaction 4, we have employed the in-depth energy analysis of the three possible PCET pathways shown in the Scheme below. Based on this analysis, we have concluded that the nature of a *para* substituent plays a decisive role in the partitioning of reactivity between these pathways. For phenols with more electron-donating substituents (*e.g.*, MeO- or Ph-), reaction 4 occurs entirely through the diagonal, one-step pathway in the Scheme which can be described as a concerted electron-proton transfer (EPT). In contrast, for phenols with electron-donating substituents (*e.g.*, NC- or O<sub>2</sub>N-), the two-step PT1-ET2 pathway consisting of proton transfer followed by electron transfer within the **1**(T<sub>1</sub>)-H/PhO<sup>-</sup> ion pair becomes dominant. The two-step ET1-PT2 pathway that begins with electron transfer does not play any role due to the prohibitively strong endothermicity of this step for all phenols.



MeO- or Ph-), reaction 4 occurs entirely through the diagonal, one-step pathway in the Scheme which can be described as a concerted electron-proton transfer (EPT). In contrast, for phenols with electron-donating substituents (*e.g.*, NC- or O<sub>2</sub>N-), the two-step PT1-ET2 pathway consisting of proton transfer followed by electron transfer within the **1**(T<sub>1</sub>)-H/PhO<sup>-</sup> ion pair becomes dominant. The two-step ET1-PT2 pathway that begins with electron transfer does not play any role due to the prohibitively strong endothermicity of this step for all phenols.

*Planned work will investigate:*

- Nature and radiation yields of primary acetonitrile radiolysis products.
- Techniques for directing primary radiolysis species toward generating strong reductants or oxidants in acetonitrile.
- Novel pathways for generating nitroxyl species (<sup>1</sup>HNO and <sup>3</sup>NO<sup>-</sup>) and their reactivity, including their self-decay and spin-forbidden ground state bond breaking/making reactions.
- Energetics and redox reactivity of trioxodinitrate (HN<sub>2</sub>O<sub>3</sub><sup>-</sup>/N<sub>2</sub>O<sub>3</sub><sup>2-</sup>) species, and their nitroxyl release mechanism.
- Redox and radical chemistry in the nitrite/nitrate system, including: formation pathways and thermodynamics of nitrate radical anion, NO<sub>3</sub><sup>2-</sup>; rates and mechanisms of its acid-catalyzed and redox reactions.
- Kinetic isotope effect and kinetic solvent effect in the PCET reactivity.

**References** (DOE sponsored publications in 2015-present are marked with asterisk)

- (1) Shaikh, N.; Valiev, M.; Lymar, S. V. *J. Inorg. Biochem.* **2014**, *141*, 28-35.
- (2) Cape, J. L.; Lymar, S. V.; Lightbody, T.; Hurst, J. K. *Inorg. Chem.* **2009**, *48*, 4400-4410.
- (3) Stull, J. A.; Britt, R. D.; McHale, J. L.; Knorr, F. J.; Lymar, S. V.; Hurst, J. K. *J. Am. Chem. Soc.* **2012**, *134*, 19973-19976.
- (4) Polyanskiy, D. E.; Hurst, J. K.; Lymar, S. V. *Eur. J. Inorg. Chem.* **2014**, 619-634.
- (5\*) Hurst, J. K.; Roemeling, M. D.; Lymar, S. V. "Mechanistic Insight into Peroxydisulfate Reactivity: Oxidation of the *cis,cis*-[Ru(bpy)<sub>2</sub>(OH<sub>2</sub>)<sub>2</sub>O]<sup>4+</sup> "Blue Dimer"" *J. Phys. Chem. B* **2015**, *119*, 7749-7760.
- (6\*) Polyanskiy, D. E.; Ertem, M.; Lymar, S. V. "Mechanistic Insights into Photoinduced Proton-Coupled Electron Transfer from Phenols to Polypyridine Ru(II) Complexes" *J. Am. Chem. Soc.* **2016**, submitted.
- (7) Grills, D. C.; Farrington, J. A.; Layne, B. H.; Lymar, S. V.; Mello, B. A.; Preses, J. M.; Wishart, J. F. *J. Am. Chem. Soc.* **2014**, *136*, 5563-5566.
- (8) Armstrong, D. A.; Huie, R. E.; Lymar, S.; Koppenol, W. H.; Merényi, G.; Neta, P.; Stanbury, D. M.; Steenken, S.; Wardman, P. *Bioinorg. React. Mech.* **2013**, *9*, 59-61.
- (9\*) Armstrong, D. A.; Huie, R. E.; Lymar, S.; Koppenol, W. H.; Merényi, G.; Neta, P.; Ruscic, B.; Stanbury, D. M.; Steenken, S.; Wardman, P. "Standard Electrode Potentials Involving Radicals in Aqueous Solution: Inorganic Radicals (IUPAC Technical Report)" *Pure Appl. Chem.* **2015**, *87*, 1139-1150.
- (10) Bradley, D.; Wilkinson, J. *J. Chem. Soc. A* **1967**, 531-537.
- (11) Ayscough, P. B.; Drawe, H.; Kohler, P. *Radiation Res.* **1968**, *33*, 263-273.
- (12) Burrows, H. D.; Kosower, E. M. *J. Phys. Chem.* **1974**, *78*, 112-117.
- (13) Wagman, D. D.; Evans, W. H.; Parker, V. B.; Schumm, R. H.; Halow, I.; Bailey, S. M.; Churney, K. L.; Nuttall, R. L. *J. Phys. Chem. Ref. Data* **1982**, *11*, Suppl. 2.

## Ionic Liquids: Radiation Chemistry, Solvation Dynamics and Reactivity Patterns

James F. Wishart

Chemistry Department, Brookhaven National Laboratory, Upton, NY 11973-5000

wishart@bnl.gov

### Program Definition

Ionic liquids (ILs) are a rapidly expanding family of condensed-phase media with important applications in energy production, storage and consumption, including advanced devices and processes and nuclear fuel and waste processing. ILs generally have low volatilities and are combustion-resistant, highly conductive, recyclable and capable of dissolving a wide variety of materials. They are finding new uses in dye-sensitized solar cells, chemical synthesis, catalysis, separations chemistry, batteries, supercapacitors and other areas. Ionic liquids have dramatically different properties compared to conventional molecular solvents, and they provide a new and unusual environment to test our theoretical understanding of primary radiation chemistry, charge transfer and other reactions. We are interested in how IL properties influence physical and dynamical processes that determine the stability and lifetimes of reactive intermediates and thereby affect the courses of reactions and product distributions. We study these issues by characterization of primary radiolysis products and measurements of their yields and reactivity, quantification of electron solvation dynamics and scavenging of electrons in different states of solvation. From this knowledge we wish to learn how to predict radiolytic mechanisms and control them or mitigate their effects on the properties of materials used in nuclear fuel processing, for example, and to apply IL radiation chemistry to answer questions about general chemical reactivity in ionic liquids that will aid in the development of applications listed above.

Soon after our radiolysis studies began it became evident that the slow solvation dynamics of the excess electron in ILs (which vary over a wide viscosity range) increase the importance of pre-solvated electron reactivity and consequently alter product distributions and subsequent chemistry. This difference from conventional solvents has profound effects on predicting and controlling radiolytic yields, which need to be quantified for the successful use under radiolytic conditions. We directly measure electron solvation dynamics in ILs by picosecond pulse radiolysis and compare them with other solvation processes (e.g. coumarin-153 dynamic emission Stokes shifts or benzophenone anion solvation) in the same ILs. Pre-solvated electron reactivity is measured using different scavengers to assess the competition with the solvation process and the differential reactivities of various pre-solvated states.

A second important aspect of our interest in ionic liquids is how their unusual sets of properties affect charge transfer and charge transport processes. This is important because of the many applications of ionic liquids in devices that operate on the basis of charge transport. While interest in understanding these processes in ionic liquids is growing, the field is still in an early stage of development. We are using donor-bridge-acceptor systems to study electron transfer reactions across variable distances in a series of ionic liquids with a range of structural motifs and whose dynamical time scales vary from moderately fast to extremely slow, and to compare them with conventional solvents.

**Methods.** Picosecond pulse radiolysis studies at BNL's Laser-Electron Accelerator Facility (LEAF) are used to identify reactive species in ionic liquids and measure their solvation and reaction rates. This work is aided greatly by the development of Optical Fiber Single-Shot (OFSS) detection at LEAF by A. Cook (DOI: 10.1063/1.3156048) and its recent extension into the NIR regime. LEAF's unique capability in mid-infrared transient absorption detection<sup>3</sup> allows precise identification of radiolytic intermediates and their reaction kinetics. IL solvation and rotational dynamics, and electron transfer reactions, are measured by TCSPC in the laboratory of E. W. Castner, Jr. at Rutgers Univ. Picosecond transient absorption measurements of excited state dynamics and electron transfer reactions are done in our lab at BNL. Diffusion rates of anions, cations and solutes are obtained by PGSE NMR in the S. Suarez and S.

Greenbaum labs at CUNY and by Castner's group at Rutgers. We have extensive collaborations with other major groups in ionic liquid synthesis, physical chemistry, simulations and radiation chemistry.

***Ionic liquid synthesis and characterization.*** Our work often involves novel ILs that we design to the requirements of our radiolysis and solvation dynamics studies and are not commercially available. We have developed robust in-house capabilities and long-standing collaborations (particularly with S. Lall-Ramnarine of Queensborough CC) to design, prepare and characterize ILs in support of our research objectives. Cation synthesis is done by several methods, including a CEM microwave reactor, resulting in higher yields of purer products in much shorter time than traditional methods. We have a diverse instrumentation cluster including DSC, TGA, viscometry, AC conductivity, Karl Fischer moisture determination, ion chromatography and ESI-mass spec (for purity analysis and radiolytic product identification). The cluster serves as a resource for a widespread network of collaborations. Our efforts are substantially augmented by internships from the BNL Office of Educational Programs, which brings collaborative faculty members and undergraduates into the lab for ten weeks each summer. Since 2003, a total of 51 undergrads, three graduate students, one pre-service teacher, two high school students and four junior faculty have worked on IL projects in our lab, many of them for more than one summer.

## Recent Progress

***A single carbon makes a huge difference.***<sup>1</sup> X-ray diffraction and molecular dynamics simulations were used to probe the structures of two families of ionic liquids containing oligoether tails on the cations.<sup>1</sup> Imidazolium and pyrrolidinium bis(trifluoromethylsulfonyl)amide ILs with side chains ranging from 4 to 10 atoms in length, including both linear alkyl and oligo-ethylene oxide tails, were prepared. Their physical properties, such as viscosity, conductivity and thermal profile, were measured and compared for systematic trends. As we reported earlier<sup>5</sup> the number of ether units in the pyrrolidinium ILs increases there is hardly any increase in the viscosity, in contrast to alkympyrrolidinium ILs where the viscosity increases steadily with chain length. Viscosities of imidazolium ether ILs increase with chain length but always remain well below their alkyl congeners. To complement the experimentally determined properties, molecular dynamics simulations were run on the two ILs with the longest ether chains. We obtained multiple lines of evidence pointing to ether chain curling and disruptive interaction with the polar parts of the IL, particularly the cations. Notably in the imidazolium case, an important fraction of these specific interactions are intramolecular and operate via the first and second oxygens in the ether chain, through favorable interactions in the case of O1 and hydrogen bonds in the case of O2. This happened to be the case because our ether chains are linked by ethylene groups that provide the conformational flexibility for the first oxygen to closely approach the H2 and H5 protons of the imidazolium ring, and also likely provide an optimal configuration for H-bonding of O2 with the same protons (Fig. 1). Other groups have done X-ray scattering and MD simulations on imidazolium ILs with methylene-linked oligoether tails that are sterically restricted from having such intramolecular interactions involving the first oxygen, and simulations showed that their structures are different on the molecular scale. They compared the methylene-linked imidazolium ether cations to scorpions because they curl their tails above their bodies. We think an apt comparison for the ethylene-linked imidazolium ether cations would be with lizards, since some species can curl their tails from side-to-side.

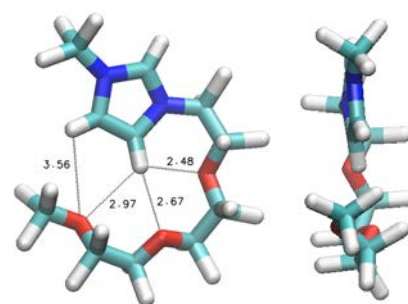


**Figure 1.** Two views of the structure of an EOEOEOMmim<sup>+</sup> cation selected from our MD simulation showing the ether chain conformation close to the plane of the imidazolium ring. Distances in Ångstroms.

## Future Plans

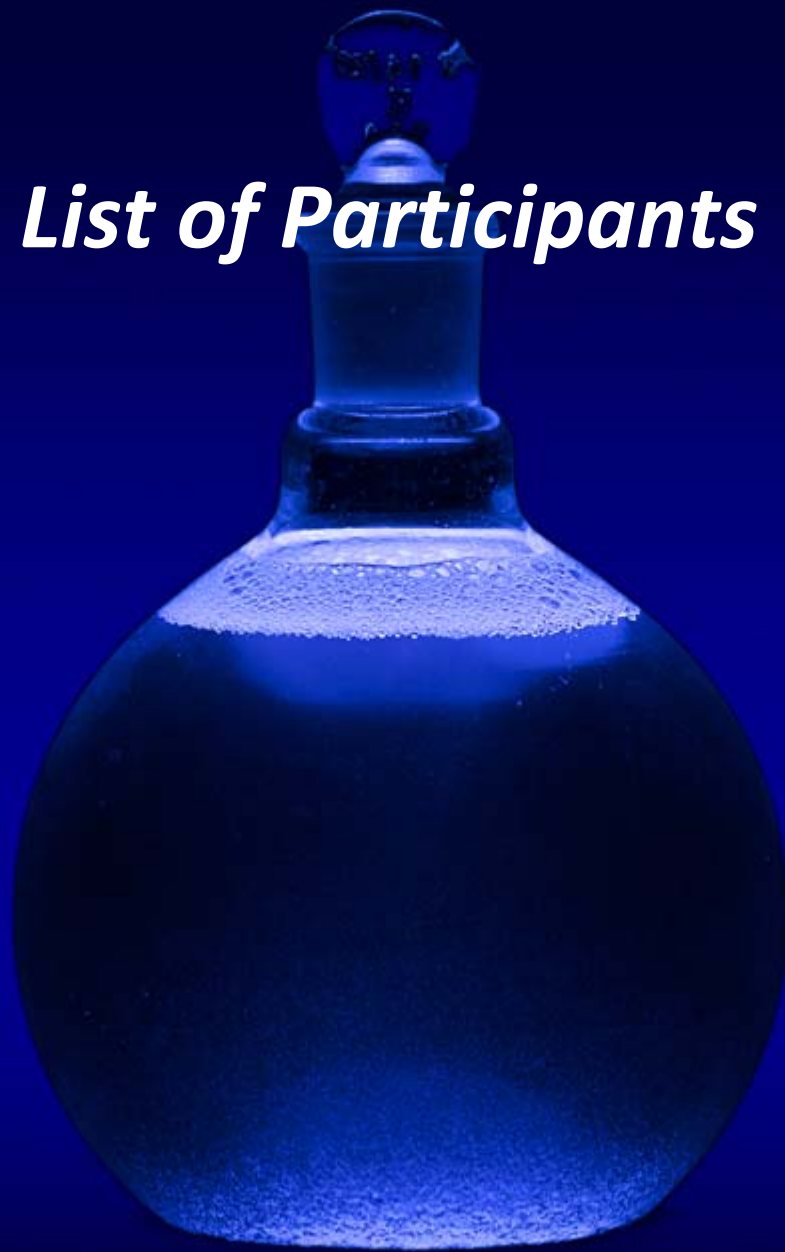
**Scavenging and solvation processes of pre-solvated electrons in ionic liquids.** Our work on the reactivity of excess electrons in ionic liquids showed that pre-solvated electron scavenging plays a more important role in determining the distributions of early radiolysis products and radiolytic damage accumulation in ILs than in conventional solvents. In addition, the slower relaxation dynamics of ILs, in combination with LEAF's OFSS picosecond detection capabilities, make them excellent media for the general study of fundamental radiolysis processes without the need to use cryogenic techniques. With the extension of the OFSS technique into the NIR, we can directly observe electron solvation dynamics as a blue shift (i.e., 1400 to 1100 nm) of the excess electron absorption band. The timescales of the electron solvation dynamics are then compared to the kinetics of electron scavenging by selected solutes, also measured by OFSS. (We say "timescales" because ILs are glassy materials that have heterogeneous dynamics.) Various scavengers (e.g., nitrate, benzophenone, CO<sub>2</sub>) show different reaction profiles towards the various precursor states to the solvated electron. These differences in reactivity are evident in the OFSS traces, and they carry implications about the nature of the pre-solvated states. The combination of extended IL dynamical time scales and the time resolution of the LEAF OFSS detection system, coupled with the fact that it uses only small amounts of samples that do not have to be flowed, as well as the ability of ILs to dissolve polar and nonpolar scavengers, provides a unique opportunity to characterize the fundamental reactivity of pre-solvated electron species and understand how the properties of scavengers control their reaction profiles. The knowledge gained in ILs can be applied to understanding these same processes in conventional solvents where the measurements are more difficult. In general, it will permit the design of better systems to control radiation-induced reactivity, for example in the processing of radioactive materials (whether in ionic liquids or not), in systems for radiation processing and sterilization, and during long-term exposure to space, for example. (with A. Cook, BNL)

## Publications

1. *Connecting Structural and Transport Properties of Ionic Liquids with Cationic Oligoether Chains*, S. I. Lall-Ramnarine, M. Zhao, C. Rodriguez, R. Fernandez, N. Zmich, E. D. Fernandez, S. B. Dhiman, E. W. Castner Jr., and J. F. Wishart, *J. Electrochem. Soc.*, **164**, H5247-H5262 (2017). DOI: 10.1149/2.0371708jes
2. *Exploring the use of ionic liquid mixtures to enhance the performance of dicationic ionic liquids*, S. I. Lall-Ramnarine, S. N. Suarez, E. D. Fernandez, C. Rodriguez, S. Wei, M. Gobet, J. R. P. Jayakody, S. B. Dhiman, and J. F. Wishart, *J. Electrochem. Soc.*, **164**, H5150-H5159 (2017). DOI: 10.1149/2.0271708jes
3. *Investigation of Dynamics in BMIM TFSA ionic liquid through variable temperature and pressure NMR relaxometry and diffusometry* K. Pilar, A. Rua, S. N. Suarez, C. Mallia, S. Lai, J. R. P. Jayakody, J. L. Hatcher, J. F. Wishart, and S. Greenbaum, *J. Electrochem. Soc.*, **164**, H5189-H5196 (2017). DOI: 10.1149/2.0301708jes, May 2017,
4. *In situ Probing of Ion Ordering at Electrified Ionic Liquid/Au Interface* W. Sitaputra, D. Stacchiola, J. F. Wishart, F. Wang, and J. T. Sadowski, *Advanced Materials*, **29**, 1606357 (2017). DOI: 10.1002/adma.201606357
5. *The Effect of Lengthening Cation Ether Tails on Ionic Liquid Properties* S. I. Lall-Ramnarine, C. Rodriguez, R. Fernandez, N. Zmich, E. D. Fernandez, S. B. Dhiman and J. F. Wishart *ECS Trans.*, **75**, 215-232 (2016). DOI: 10.1149/07515.0215ecst

6. *Transport Properties of Ionic Liquid Mixtures Containing Heterodications* S. I. Lall-Ramnarine, E. D. Fernandez, C. Rodriguez, S. Wei, S. B. Dhiman and J. F. Wishart *ECS Trans.*, **75**, 555-565 (2016). DOI: 10.1149/07515.0555ecst
7. *Improving the Radiation Hardness of Graphene Field Effect Transistors* K. Alexandrou, A. Masurkar, H. Edrees, J. F. Wishart, Y. Hao, N. Petrone, J. Hone, I. Kymissis, *Appl. Phys. Lett.*, **109**, 153108 (2016). DOI: 10.1063/1.4963782
8. *The Chemistry of Separations Ligand Degradation by Organic Radical Cations* S. P. Mezyk, G. P. Horne, B. J. Mincher, P. R. Zalupski, A. R. Cook and J. F. Wishart, *Procedia Chemistry*, **21**, 61-65 (2016). DOI: 10.1016/j.proche.2016.10.009

*List of Participants*



## LIST OF PARTICIPANTS

Dr. Musahid Ahmed  
Lawrence Berkeley National Laboratory  
<https://sites.google.com/site/musaswebcorner/home>

Professor Heather Allen  
Ohio State University  
<https://research.cbc.osu.edu/allen.697/>

Professor Abraham Badu-Tawiah  
Ohio State University  
<https://research.cbc.osu.edu/badu-tawiah.1/>

Professor L. Robert Baker  
Ohio State University  
<https://research.cbc.osu.edu/baker.2364/>

Dr. David Bartels  
Notre Dame Radiation Laboratory  
<http://rad.nd.edu/people/faculty/david-m-bartels/>

Dr. Matthew Beard  
National Renewable Energy Laboratory  
<https://www.nrel.gov/research/matt-beard.html>

Dr. Hendrik Bluhm  
Lawrence Berkeley National Laboratory  
<https://sites.google.com/a/lbl.gov/hendrik-bluhm/>

Professor Ian Carmichael  
Notre Dame Radiation Laboratory  
<http://rad.nd.edu/people/faculty/ian-carmichael/>

Professor Aurora Clark  
Washington State University  
<https://aclark.chem.wsu.edu/>

Dr. Andrew Cook  
Brookhaven National Laboratory  
<https://www.bnl.gov/chemistry/bio/CookAndrew.asp>

Professor Tanja Cuk  
Lawrence Berkeley National Laboratory  
<http://www.cchem.berkeley.edu/tkgrp/>

Dr. Liem Dang  
Pacific Northwest National Laboratory  
[http://www.pnl.gov/science/staff/staff\\_info.asp?staff\\_num=5604](http://www.pnl.gov/science/staff/staff_info.asp?staff_num=5604)

Professor Michael Fayer  
Stanford University  
<http://www.stanford.edu/group/fayer/>

Dr. Christopher Fecko  
DOE/Basic Energy Sciences  
<http://science.energy.gov/bes/csgb/about/staff/dr-christopher-fecko/>

Dr. Gregory Fiechtner  
DOE/Basic Energy Sciences  
<http://science.energy.gov/bes/csgb/about/staff/dr-gregory-i-fiechtner/>

Professor Miriam Freedman  
Pennsylvania State University  
<http://research.chem.psu.edu/mafgroup/People.html>

Mr. John Fulton  
Pacific Northwest National Laboratory  
[http://www.pnl.gov/science/staff/staff\\_info.asp?staff\\_num=5587](http://www.pnl.gov/science/staff/staff_info.asp?staff_num=5587)

Professor Etienne Garand  
University of Wisconsin  
<http://garand.chem.wisc.edu/>

Dr. Bruce Garrett  
DOE/Basic Energy Sciences  
<https://science.energy.gov/bes/csgb/about/staff/dr-bruce-garrett/>

Dr. Niranjan Govind  
Pacific Northwest National Laboratory  
[http://www.pnl.gov/science/staff/staff\\_info.asp?staff\\_num=8375](http://www.pnl.gov/science/staff/staff_info.asp?staff_num=8375)

Dr. Alexander Harris  
Brookhaven National Laboratory  
<http://www.bnl.gov/chemistry/bio/HarrisAlex.asp>

Professor Teresa Head-Gordon  
Lawrence Berkeley National Laboratory  
<http://thglab.berkeley.edu/>

Dr. Wayne Hess  
Pacific Northwest National Laboratory  
[http://www.pnl.gov/science/staff/staff\\_info.asp?staff\\_num=5505](http://www.pnl.gov/science/staff/staff_info.asp?staff_num=5505)

Dr. Ireneusz Janik  
Notre Dame Radiation Laboratory  
<http://rad.nd.edu/people/faculty/ireneusz-janik/>

Professor Caroline Chick Jarrold  
Indiana University  
<http://mypage.iu.edu/~ciarrold/index.htm>

Professor Mark Johnson  
Yale University  
<http://ilab.chem.yale.edu/>

Professor Kenneth Jordan  
University of Pittsburgh  
<http://www.pitt.edu/~jordan/>

Dr. Shawn Kathmann  
Pacific Northwest National Laboratory  
[http://www.pnl.gov/science/staff/staff\\_info.asp?staff\\_num=5601](http://www.pnl.gov/science/staff/staff_info.asp?staff_num=5601)

Dr. Bruce Kay  
Pacific Northwest National Laboratory  
[http://www.pnl.gov/science/staff/staff\\_info.asp?staff\\_num=5530](http://www.pnl.gov/science/staff/staff_info.asp?staff_num=5530)

Professor Munira Khalil  
University of Washington  
<https://sites.google.com/a/uw.edu/khalilgroup/>

Dr. Greg Kimmel  
Pacific Northwest National Laboratory  
[http://www.pnl.gov/science/staff/staff\\_info.asp?staff\\_num=5527](http://www.pnl.gov/science/staff/staff_info.asp?staff_num=5527)

Professor Amber Krummel  
Colorado State University  
<http://sites.chem.colostate.edu/krummellab/>

Dr. Jeffrey L. Krause  
DOE/Basic Energy Sciences  
<http://science.energy.gov/bes/csgb/about/staff/dr-jeffrey-l-krause/>

Professor Christy Landes  
Rice University  
<http://www.lrg.rice.edu/>

Dr. Jay LaVerne  
Notre Dame Radiation Laboratory  
<http://rad.nd.edu/people/faculty/jay-a-laverne/>

Professor Stephan Link

Rice University

<http://slink.rice.edu/>

Professor Xiaosong Li

University of Washington

<http://depts.washington.edu/ligroup/people/>

Dr. Sergei Lymar

Brookhaven National Laboratory

<https://www.bnl.gov/chemistry/bio/LymarSergei.asp>

Professor Kranthi Mandadapu

Lawrence Berkeley National Laboratory

<http://stage.cchem.berkeley.edu/~kranthi/>

Professor Thomas Markland

Stanford University

<https://web.stanford.edu/group/markland/group.html>

Diane Marceau

DOE/Basic Energy Sciences

<http://science.energy.gov/bes/csgb/about/staff/>

Dr. John Miller

Brookhaven National Laboratory

<https://www.bnl.gov/chemistry/bio/MillerJohn.asp>

Dr. Karl Mueller

Pacific Northwest National Laboratory

[http://www.pnnl.gov/science/staff/staff\\_info.asp?staff\\_num=8286](http://www.pnnl.gov/science/staff/staff_info.asp?staff_num=8286)

Dr. Christopher Mundy

Pacific Northwest National Laboratory

[http://www.pnl.gov/science/staff/staff\\_info.asp?staff\\_num=5981](http://www.pnl.gov/science/staff/staff_info.asp?staff_num=5981)

Dr. Mark Pederson

DOE/Basic Energy Sciences

<http://science.energy.gov/bes/csgb/about/staff/dr-mark-r-pederson/>

Professor Hrvoje Petek

University of Pittsburgh

<http://www.ultrafast.phyast.pitt.edu/Home.html>

Professor Sylwia Ptasinska

University of Notre Dame

<https://www3.nd.edu/~sptasins/people.html>

Professor Krishnan Raghavachari

Indiana University

<http://php.indiana.edu/~krgroup/>

Professor Neeraj Rai

Mississippi State University

<http://railab.che.msstate.edu/members.html>

Professor Geraldine Richmond

University of Oregon

<http://richmondscience.uoregon.edu/>

Dr. James Rustad

DOE/Basic Energy Sciences

<http://science.energy.gov/bes/csgb/about/staff/dr-james-rustad/>

Professor Sapna Sarupria

Clemson University

<http://www.clemson.edu/ces/molecularsimulations/>

Professor Richard Saykally

Lawrence Berkeley National Laboratory

<http://www.cchem.berkeley.edu/risgrp/>

Dr. Gregory Schenter

Pacific Northwest National Laboratory

[http://www.pnl.gov/science/staff/staff\\_info.asp?staff\\_num=5615](http://www.pnl.gov/science/staff/staff_info.asp?staff_num=5615)

Dr. Robert Schoenlein

SLAC National Accelerator Laboratory

<https://ultrafast.stanford.edu/people/robert-schoenlein>

Professor Benjamin Schwartz

University of California, Los Angeles

<http://www.chem.ucla.edu/dept/Faculty/schwartz/index.html>

Dr. Viviane Schwartz

DOE/Basic Energy Sciences

<http://science.energy.gov/bes/csgb/about/staff/dr-vivian-schwartz/>

Professor Charles Sykes

Tufts University

<http://ase.tufts.edu/chemistry/sykes/Sykes%20Lab%20Research%20Group.html>

Professor William Tisdale

Massachusetts Institute of Technology

<http://web.mit.edu/tisdalelab>

Professor Andrei Tokmakoff  
University of Chicago  
<http://tokmakofflab.uchicago.edu/>

Dr. Marat Valiev  
Pacific Northwest National Laboratory  
[http://www.pnl.gov/science/staff/staff\\_info.asp?staff\\_num=8349](http://www.pnl.gov/science/staff/staff_info.asp?staff_num=8349)

Dr. Jao Van de Lagemaat  
National Renewable Energy Laboratory  
<https://www.nrel.gov/research/jao-vandelagemaat.html>

Dr. Xue-Bin Wang  
Pacific Northwest National Laboratory  
[http://www.pnl.gov/science/staff/staff\\_info.asp?staff\\_num=7753](http://www.pnl.gov/science/staff/staff_info.asp?staff_num=7753)

Professor Adam Willard  
Massachusetts Institute of Technology  
[http://willardgroup.mit.edu/current\\_members.html](http://willardgroup.mit.edu/current_members.html)

Dr. Kevin R. Wilson  
Lawrence Berkeley National Laboratory  
<http://wilsonresearchgroup.lbl.gov/home>

Dr. James Wishart  
Brookhaven National Laboratory  
<http://www.chemistry.bnl.gov/SciandTech/PRC/wishart/wishart.html>

Professor Bryan Wong  
University of California, Riverside  
<http://www.bmwong-group.com/>

Dr. Sotiris Xantheas  
Pacific Northwest National Laboratory  
[http://www.pnl.gov/science/staff/staff\\_info.asp?staff\\_num=5610](http://www.pnl.gov/science/staff/staff_info.asp?staff_num=5610)